AERIAL PHENOTYPING TO IDENTIFY SUPERIOR SUGARCANE GENOTYPES

BY NATALIE HOFFMAN

Submitted in fulfilment of the academic requirements of the degree of

PHILOSOPHIAE DOCTOR

in Agriculture (Crop Science)

School of Agricultural, Earth and Environmental Sciences

University of KwaZulu-Natal

Pietermaritzburg

South Africa

August 2024

Supervisors:

Prof. Abraham Singels, University of KwaZulu-Natal, South Africa

Dr. Shailesh Joshi, University of KwaZulu-Natal, South Africa

ABSTRACT

Sugarcane is a globally important food and bioenergy crop which necessitates continual improvement through breeding to ensure its sustainable production under increasingly challenging environments. Compared to other major crops, yield gains in sugarcane have stagnated worldwide in recent years. This could be attributed to the resource-intensive and time-consuming nature of breeding a genetically complex crop with long growth cycles and large, diverse populations. The primary objective of sugarcane breeding is to develop superior genotypes with enhanced genetic gains, securing sustainable production for the future. Aerial phenotyping (AP) with high-throughput phenotyping sensor technologies and unmanned aerial vehicles (UAVs, commonly known as drones) could assist breeding by increasing selection efficiency and accuracy, uncovering genetic variation for yield-promoting traits, and expediting large-scale trial screening. Key physiological traits governing canopy development and water use, namely green canopy cover (GCC) and stomatal conductance (g_s), can be estimated from the aerially measured Normalized Difference Vegetation Index (NDVI) and canopy temperature (Tc), respectively. While promising, further research is required to evaluate the efficacy of AP in breeding.

The study aimed to develop and test an AP procedure for identifying superior genotypes in sugarcane breeding. The specific objectives were to: (1) determine the impacts of ground (GCC and g_s) and aerially measured traits (NDVI and Tc), on stalk dry mass yield (SDM) under well-watered (WW) and water deficit (WD) conditions; (2) develop an AP procedure for estimating g_s, GCC and SDM from Tc and NDVI; (3) determine the genetic variation and broad-sense heritability of ground and aerially measured traits; (4) evaluate the feasibility and potential benefit of implementing AP to identify superior genotypes in breeding. These aims and objectives were addressed in three experimental phases.

An unreplicated pilot trial with two genotypes grown under WW and WD conditions (~ 200 m^2 in total) was used to establish preliminary relationships between ground and aerially measured traits under varying canopy and moisture conditions. Key findings were that FIPAR (fractional interception of photosynthetically active radiation - a surrogate measure of GCC) measured on the ground could be reliably estimated from NDVI, though the relationship required further investigation at partial canopy cover. Tc could be used to distinguish differences in measured g_s between water treatments under moderate to severe

stress conditions only. Overall, the experiment was used to formulate a preliminary AP protocol, with recommendations for further improvement in the subsequent phase.

A replicated field trial with 54 genotypes, grown under WW and WD conditions (~ 3 ha in total) in plant and first ratoon crops, was used to assess trait correlations, genetic variation and broad-sense heritability of traits, and to refine the AP procedure. In line with previous research, the study confirmed FIPAR and g_s as influential traits for determining SDM. FIPAR, measured at 2-3 months after crop start, could be used to identify high- and low-yielding genotypes, and could be predicted well from NDVI, at partial canopy for well-watered crops. Breeding programs for irrigated environments could benefit from the early identification of superior genotypes if traits with high heritability, like FIPAR, can be accurately and rapidly phenotyped. Furthermore, results suggested that high g_s benefits well-watered crops, while relatively low g_s could be advantageous in dry environments, though this requires further validation. Phenotyping of g_s from Tc was mostly unreliable, and its practical application in breeding programs requires further evaluation on a larger, genetically diverse population with improved measurement procedures. It was concluded that NDVI and Tc, which both showed significant genotypic variation and moderate to high heritability, could be used to identify high- and low-yielding genotypes when measured early in the crop cycle in young, partially canopied, well-watered crops planted in multi-row plots. Novel results also showed potential for screening of drought tolerance using water treatment differences in Tc and SDM, which has not been reported previously for sugarcane. Overall, this research was used to establish an AP procedure for subsequent use in breeding trials.

Lastly, the AP procedure was implemented in two rainfed early-stage breeding trials, with 1770 to 2130 genotypes, planted in replicated single-row plots over ~3.5 – 6 ha. This validation phase was used to test the utility of AP for enhancing selection accuracy and efficiency and contribute to yield improvement. The limited number of flights in the first trial prevented adequate capture of temporal and genotypic variations in aerially measured traits, which are necessary for accurate yield prediction. In the second trial, early estimates of NDVI and Tc, measured approximately 1.5 to 3 months after crop start in partially canopied, well-watered crops, showed significant genotypic variation, moderate to high heritability, and significant correlation with yield. Tc was also significantly correlated with yield when measured shortly after canopy closure but before row overlap due to crop growth.

Despite these promising results, the AP procedure implemented in these early-stage breeding trials did not achieve the precision required for genotype selection. A comparison of direct (SDM-based) and indirect (based on aerially measured traits) selection approaches showed that the number of positive matches was mostly offset by a larger number of incorrectly identified genotypes using aerially measured traits. It was concluded that the effectiveness of AP in breeding is currently hindered by limitations in the precision of aerial measurements and challenges in breeding trial execution.

The findings from this study highlight the potential and limitations of AP for physiological breeding. AP holds great promise for identifying genetic variation in yield-promoting traits, which could be leveraged in breeding for the identification of superior genotypes in irrigated environments, however further research is required to fully realize this potential. It is recommended to modify the design of early-stage trials by increasing plot length, number of rows, and row-spacing to facilitate accurate estimation of aerially measured traits using the developed AP procedure. Further efforts are also needed to overcome challenges inherent in breeding trial execution, such as lengthy planting periods introducing biases in early vigour, and variability in field soil composition, which directly and indirectly affect the quality of ground and aerially measured data. Should these recommendations be implemented, early screening of trials using AP could lead to shorter breeding cycles, the discovery of novel genetic variations, and improved selection efficiency, ultimately reducing the resource-intensive nature of traditional methods through early elimination of inferior genotypes from the program.

In conclusion, this study demonstrates the potential of AP to enhance sugarcane breeding by facilitating the early detection of important yield-promoting traits, particularly in well-watered crops. While AP shows promise to enhance sugarcane breeding, further work in refining its application is essential to fully realize its benefits. These research findings provide a strong foundation for future efforts to develop innovative breeding strategies and precision agriculture technologies.

PREFACE

The experimental work described in this thesis was carried out as part of a research project with the South African Sugarcane Research Institute (SASRI), from October 2017 to December 2023, under the supervision of Prof. Abraham Singels and Dr. Shailesh Joshi.

These studies represent original work by the author and have not otherwise been submitted in any form for any degree or diploma to any tertiary institution. Where use has been made of the work of others it is duly acknowledged in the text.

DECLARATION 1 - PLAGIARISM

I, Natalie Hoffman, declare that:

1. The research reported in this thesis, except where otherwise indicated, is my original research.
2. This thesis has not been submitted for any degree or examination at any other university.
3. This thesis does not contain other persons' data, pictures, graphs or other information, unless specifically acknowledged as being sourced from other persons.
4. This thesis does not contain other persons' writing, unless specifically acknowledged as being sourced from other researchers. Where other written sources have been quoted, then:
    a. Their words have been re-written but the general information attributed to them has been referenced
    b. Where their exact words have been used, then their writing has been placed in italics and inside quotation marks, and referenced.
5. This thesis does not contain text, graphics or tables copied and pasted from the Internet, unless specifically acknowledged, and the source being detailed in the thesis and in the References sections.
6. As the candidate's Supervisor I agree/do not agree to the submission of this thesis.

Signed:

……

Natalie Hoffman (Ph.D. candidate)

……

Supervisor: Abraham Singels

Associate Professor: School of Agriculture, Earth and Environmental Sciences, UKZN

……

Supervisor: Shailesh Joshi

Honorary Lecturer: School of Life Sciences, College of Agriculture, Engineering and Science, UKZN

DECLARATION 2 - PUBLICATIONS

DETAILS OF CONTRIBUTION TO PUBLICATIONS that form part and/or include research presented in this thesis.

Peer-reviewed articles:

- Hoffman, N., Singels, A. & Joshi, S. 2024. Aerial phenotyping for sugarcane yield and drought tolerance. Field Crops Research, 308, 109275. https://doi.org/10.1016/j.fcr.2024.109275
- Hoffman, N., and Singels, A. 2019.Hoffman, N. and Singels, A. 2019. Evaluating the use of aerially captured spectral data for characterizing drought-tolerance traits in sugarcane. Proceedings of the Australian Society of Sugar Cane Technologists (ASSCT) 41: 187-192.

Conference short communications and oral presentations:

- Hoffman, N., Singels, A., Joshi, S. & Moodley, D. 2021. Can drone phenotyping aid plant breeding? Preliminary results. Proceedings of the South African Sugar Technologists Association.
- Hoffman, N., Singels, A. & Joshi, S. 2020. Remote sensing of physiological traits with drones to assist sugarcane breeding: preliminary results. Combined Congress of the South African Society for Crop Production, Soil Science Society of South Africa, Southern African Society for Horticultural Sciences and Southern African Weed Science Society held from 21-23 January 2020 in Bloemfontein.

Signed:

…….

Natalie Hoffman (Ph.D. candidate)

ACKNOWLEDGEMENTS

I would firstly like to express my sincerest gratitude to my supervisors, Prof. Abraham Singels and Dr. Shailesh Joshi, for your time, patience, encouragement and dedication. To Abraham especially, thank you for all of these years of working together. I will always consider myself blessed to have been your student.

Thank you to my fellow colleagues within the Agronomy, GIS, breeding and technical field support departments at the South African Sugarcane Research Institute (SASRI) for assisting with field trial execution, data collection and analysis. Your hard work, perseverance and commitment to the project has been invaluable. I would also like to express my gratitude to the National Research Foundation and SASRI for funding the project, to the service providers at Agri-Sense International for assisting with drone operations and image processing, and to Mr Willem Botes at Stellenbosch University for the use of their drone-mounted camera during the preliminary trial phase.

This study would not have been possible without my family. To my mum, dad and sister- you have all played such a pivotal role in preparing me for this. For all the sacrifices you've made, the late nights and long days you've stayed with me- I am profoundly grateful.

My husband Matthew- you have been my stronghold all these years. Thank you for carrying me through this process. You alone understand what it took for us to finish this together. This journey has allowed us to find our faith in God together, to follow uncertain paths with grace, and to draw strength and solace from Him in both the quiet and the chaos.

Lastly, to our dearest daughter Lilly- mamma wrote this book for you. While it may not be something I read to you at bedtime, I hope it shows you that we can do hard things. You arrived so very early and unexpectedly during this study, showing me just how brave and resilient we are. I hope you'll proudly share with your friends one day that your mummy is a doctor of plants. I also hope that you always remember that no matter what life brings, giving up is never an option, and that things worth doing, deserve your very best efforts.

TABLE OF CONTENTS

LIST OF FIGURES

LIST OF TABLES

LIST OF SYMBOLS / ABBREVIATIONS

k_c	Canopy extinction coefficient
σ_x	Phenotypic standard deviation of SDM
ΔDM	Biomass production (kg m^{-2} d^{-1})
ΔTc	Canopy temperature values expressed as the difference between water deficit and well-watered treatments (°C)
ΔTleaf	Leaf temperature values expressed as the difference between water deficit and well-watered treatments (°C)
A	Leaf-level photosynthesis rate: net carbon fixation rate per unit leaf area (µmol CO_2 m^{-2} s^{-1})
ADM	Above-ground dry biomass (kg m^{-2})
AP	Aerial phenotyping
ASWC	Plant available soil water capacity (mm)
ASWCmax	Maximum plant available soil water capacity (mm)
ASWCmin	Minimum plant available soil water capacity (mm)
BD	Bulk density (g cm^{-3})
C_a	Ambient CO_2 concentration
CCS	Commercial cane sugar (%)
C_i	CO_2 concentration in the leaf sub-stomatal cavity
Cigreen	Chlorophyll index green
CiRE	Chlorophyll index red-edge
CR_x	Correlated response: estimated genetic gain in SDM when using aerially measured traits
CR_x/R_x	Relative efficiency of indirect selection
CWSI	Crop water satisfaction index
DAH	Days after harvest
DAP	Days after planting
DM	Dry matter content (%)
DN	Digital number
DNch1, DNch2	Digital numbers of channels 1 or 2, for the Sentera camera
DVI	Difference vegetation index
E	Leaf-level transpiration rate (mmol H_2O m^{-2} s^{-1})

E	Error variance of traits
e_a	Water vapour pressure of ambient air surrounding the leaf (Pa)
Ecref	Sugarcane reference evapotranspiration rate
e_i	Water vapour pressure within the substomatal cavity (Pa)
ERD	Estimated rooting depth (m)
ET	Crop evapotranspiration (m^3 m^{-2} d^{-1})
EVI	Enhanced vegetation index
F.pr.	Probability associated with the F-statistic
FC	Field capacity (soil water holding characteristic)
FIPAR	Fractional interception of photosynthetically active radiation by the crop canopy (%)
fv/fm	Chlorophyll a fluorescence ratio
G	Genetic variance of traits
g_c	Canopy conductance (mol m^{-2} s^{-1})
GCC	Green canopy cover
GCP	Ground control point
GCV	Genetic coefficient of variation
GDVI	Green difference vegetation index
GIS	Geographic information systems
GL	Green leaf number per shoot
GL*	WD values of green leaf number expressed relative to WW values
GLAI	Green leaf area index
GNDVI	Green normalized Difference vegetation Index
g_s	Leaf-level stomatal conductance (mmol H20 m^{-2} s^{-1})
g_s*	WD values of stomatal conductance expressed relative to WW values
GxExM	Genotype x environment x management interactions
HSB	Broad-sense heritability
HTP	High-throughput phenotyping
h_x	Broad-sense heritability of SDM, used in the estimation of CRx

h_y	Broad-sense heritability of the aerially measured trait, used in the estimation of CRx
i	Selection intensity
k_{PAR}	Canopy extinction coefficient for photosynthetically active radiation
K_{SRAD}	Canopy extinction coefficient for solar radiation from the entire shortwave spectrum
LA	Average leaf size (m^{-2})
LAI	Leaf area index
LiDAR	Light Detection and Ranging
NDRE	Normalized difference red edge
NDVI	Normalized Difference Vegetation Index
$NDVI_r$	Normalized NDVI, used in the estimation of VPI
$NDVI_{ref}$	Values of NDVI expressed relative to that of reference genotype NCo376
NIR	Near infrared
P&D	Pest and disease
PAR	Photosynthetically active radiation (µmol m^{-2} s^{-1}, W m^{-2})
PARi	Incoming photosynthetically active radiation
PARr	Reflected photosynthetically active radiation
PARt	Transmitted photosynthetically active radiation
PWP	Permanent wilting point (soil water holding characteristic)
r	Selection accuracy
r	Phenotypic correlation: Pearson correlation coefficient
RASWC	Relative available soil water content
REML	Restricted (or residual) maximum likelihood analysis
r_g	Genetic correlation
RGB	Red, green and blue spectral bands
RH	Relative humidity (%)
RS	Remote sensing
R_t	Genetic gain
RUE	Radiation use efficiency
RUE_c	RUE at the crop level

RUE_L	RUE at the leaf level
$RUEo_c$	Maximum RUE at the crop level
$RUEo_L$	Maximum RUE at the leaf level
RVI	Ratio vegetation index
R_x	Direct response to selection: expected genetic gain in stalk yield when using SDM directly
SASRI	South African Sugarcane Research Institute
SAVI	Soil-adjusted vegetation index
SDM	Stalk dry mass yield (t ha^{-1}, kg m^{-2})
SDM*	WD values of stalk dry mass yield expressed relative to WW values
SDM_{MLR}	Stalk dry mass yield estimated from multiple linear regression analysis of aerially measured traits
SDM_{ref}	Values of stalk dry mass yield expressed relative to that of reference genotype NCo376
SFM	Stalk fresh mass yield (t ha^{-1})
SH	Stalk height
SH*	WD values of stalk height expressed relative to WW values
SM	Individual stalk fresh mass (kg $stalk^{-1}$)
SP	Stress point (soil water holding characteristic)
SPOP	Stalk population
SPOP*	WD values of stalk population expressed relative to WW values
SRAD	Solar radiation (W m^{-2} or MJ m^{-2} d^{-1})
SRPIb	Simple ratio pigment index
SUC	Sucrose yield (t ha^{-1})
SWC	Soil water content (%)
SWCg	Gravimetric soil water content (%)
SWS	Soil water status
T	Transpiration (m^3 m^{-2} d^{-1})
t	Time taken to complete a breeding cycle
Tc	Canopy temperature (°C)
Tc_{col}	Mean canopy temperature for each trial column (°C)

Tc_i	Canopy temperature index; estimated genotype effect on Tc (°C)
Tc_r	Normalized Tc, used in the estimation of VPI
Tc_{ref}	Values of canopy temperature expressed relative to that of reference genotype NCo376
TE	Transpiration efficiency (kg m^{-3})
TEC	TE coefficient at a VPD of 1 kPa (kg m^{-3} kPa^{-1})
TEi	Intrinsic transpiration efficiency (µmol CO_2 mmol H_2O)
TE_L	TE at the leaf level (µmol CO_2 mmol H_2O)
Tleaf	Leaf temperature (°C)
Tmax	Daily maximum temperature (°C)
Tmean	Daily mean temperature (°C)
Tmin	Daily minimum temperature (°C)
TT	Thermal time (°Cd)
UAV	Unmanned aerial vehicle
VI	Vegetation index
VPD	Vapour pressure deficit (kPa)
VPI	Vegetation productivity index
WD	Water deficit treatment
WUE	Water use efficiency (kg m^{-3})
WW	Well-watered treatment
σ_A	Genetic variation for a given trait
Ω	Stomatal uncoupling coefficient

1. INTRODUCTION

Sugarcane (*Saccharum* spp.) is a key agricultural crop grown worldwide, serving as an important food source and contributor to bioenergy production. In 2021, 1967 million tons of cane were harvested from 27.5 million ha of area globally (FAOSTAT, 2023). In South Africa, sugarcane production contributes greatly to the socio-economic environment, where approximately one million people depend on the industry directly and indirectly. In 2022/2023, the South African sugarcane industry harvested 17.9 million tons of cane from an estimated 345 607 ha, with an average yield of 75.7 t ha^{-1} (Sithole et al., 2023). This cultivation spans cane-producing areas representing diverse agroclimatic regions, which can be broadly classified as irrigated (approximately 35%), rainfed coastal, or high altitude, with crop growth periods ranging from 12-24 months (Olivier and Singels, 2015; Zhou, 2022, 2013).

The global impact of sugarcane necessitates continual crop improvement to enhance sustainability and increase crop production. The breeding programme at the South African Sugarcane Research Institute (SASRI) was established in 1925 with the primary objective to test and release high-yielding, disease-resistant varieties adapted to target growing regions (Zhou, 2013). The breeding process currently comprises four selection stages, where approximately 250 000 clones (generated from hybridization of selected parents) are assessed every year for direct (i.e. stalk and sucrose yield, pest and disease resistance) and indirect (i.e. stalk height, diameter and population) selection criteria. A new variety is released after a period of 11 (irrigated program) to 20 (inland rainfed program) years (Zhou, 2022, 2013), emphasizing the resource intensive and time-consuming nature of breeding practices.

In recent years, compared to other crops, sugarcane has shown slow rates in yield improvement, with trends suggesting a general plateau in yield globally, highlighting the challenges in enhancing productivity through breeding (Jackson, 2019; Wei and Jackson, 2017; Yadav et al., 2021, 2020). This sluggish progress in sugarcane varietal improvement can be attributed to several factors, including the complex polyploidy nature of sugarcane genetics, long breeding cycles, difficulties in phenotyping large populations, and the relatively limited genetic diversity available for breeding programs (Luo et al., 2023; Wei and Jackson, 2017; Yadav et al., 2020). These challenges hinder the achievement of genetic gains through traditional breeding methods, compared to cereal crops (maize, wheat, and rice) or sugar beet, which have more than doubled yields worldwide in the last six decades due to genetic

improvements, investments in breeding research, and advancements in agronomic practices (Jackson, 2019). This is of particular concern for several reasons. In a broader context, several studies have indicated that crop production needs to increase by 45% to 110% by 2050 to meet world food production demands for a growing population (FAOSTAT, 2023; Tilman et al., 2011; van Dijk et al., 2021). Climate change threatens current and future crop production, and the increasing incidence of extreme weather events is predicted to reduce crop productivity globally (Lobell et al., 2013, 2008; Meehl et al., 2007; Schulze and Kunz, 2010; Zhao and Li, 2015). These considerations are particularly pertinent to sugarcane, the largest crop by production quantity (FAOSTAT, 2023), as it faces predictions of more frequent and severe weather events leading to significant yield losses or crop failure (Christina et al., 2021; Gilbert et al., 2008; Inman-Bamber and Smith, 2005; Zhao and Li, 2015). Furthermore, sugarcane serves as a major source of biofuel, and demands for renewable energy production are likely to increase (Christina et al., 2021; Goldemberg et al., 2014).

Genetic improvement in sugarcane breeding can be achieved through various strategies. Direct selection for traits of interest, such as stalk and sucrose yield, is considered to be traditional / empirical breeding, while indirect selection for secondary traits associated with higher yield potential is known as analytical / physiological breeding (Araus et al., 2008). The challenges in advancing yield improvement stem from long breeding cycles, difficulties in accurately phenotyping large, genetically complex populations, and confounding genotype x environment x management interaction effects (Luo et al., 2023). These difficulties could be mitigated with novel, high-throughput technologies to reduce breeding cycle length, improve selection accuracy and identify new genotypic variation for yield-promoting traits in the early stages of selection. Recent advances in molecular marker-assisted selection have facilitated high-throughput genotyping, which has shown promise for advancing breeding efforts despite the complex genetic makeup of sugarcane (Aitken, 2022; Wang et al., 2022). However, the effectiveness of these technologies relies on coupling genomic data with accurately phenotyped, high-throughput data to build robust prediction models for clonal performance. Despite advances in phenomics over the past few decades, application of high-throughput phenotyping in sugarcane breeding is still in its infancy and remains a bottleneck limiting genetic gain (Araus et al., 2018; Furbank and Tester, 2011; Jung et al., 2018; Luo et al., 2023; Song et al., 2021; Yadav et al., 2020).

Direct use of physiological understanding in breeding has been largely unsuccessful (Jackson et al., 1996), despite extensive evidence supporting the importance of secondary physiological traits for enhancing yield improvement (Araus et al., 2008; Condon et al., 2004; Jackson et al., 1996; Natarajan et al., 2020; Olivares-Villegas et al., 2007; Potgieter et al., 2017; Reynolds and Langridge, 2016; Richards, 2006). Research has highlighted stomatal conductance (g_s) and green canopy cover (GCC) as key physiological traits determining crop productivity across various moisture conditions in sugarcane (Basnayake et al., 2015; Chapman et al., 2014; De Silva and De Costa, 2009; Duan et al., 2017; Eksteen et al., 2014; Ferreira et al., 2017; Jackson et al., 2016; Natarajan et al., 2020, 2019) and other crops (Belko et al., 2013; Caine et al., 2019; Chapman et al., 2014; Duan et al., 2017; Fischer et al., 1998; Rebetzke et al., 2004). While there is evidence to suggest that these traits have been indirectly selected for through yield pressure in breeding (Basnayake et al., 2015), integration of physiological understanding in breeding has faced several challenges. Physiological screening has been underutilized within large-scale active breeding programs due to the slow and cumbersome nature of measurements which are also prone to high error variation resulting from variable environmental conditions. Consequently, physiological research often focuses on small genetic populations under controlled conditions, rather than on developing proof of concept under realistic breeding conditions (Araus et al., 2018; Araus and Cairns, 2014; Jackson et al., 1996; Passioura and Angus, 2010; Pauli et al., 2016). Furthermore, recent attempts to implement physiological screening in sugarcane breeding have shown complex trait interactions, resulting in a wide range of reported genetic correlations with yield, including both positive and negative associations (Basnayake et al., 2015; Li et al., 2017). As a result of these challenges and complex trait interactions, knowledge of key physiological traits governing water use and yield within the context of breeding, including genotypic variation and heritability of traits, and their impacts on yield, remains limited.

Field-based high-throughput phenotyping (HTP), which utilizes sensor and imaging technologies to collect accurate, high-resolution data on crop phenotypic traits in large populations, offers a cost-effective and resource-efficient alternative to traditional breeding methods (Araus and Cairns, 2014; White et al., 2012). Aerial phenotyping (AP), a type of HTP employing unmanned aerial vehicles (UAVs, also known as drones), holds promise for enhancing breeding. AP measures crop reflectance and radiation emittance across different electromagnetic spectra, enabling the estimation of vegetation indices such as the Normalized

Difference Vegetation Index (NDVI, Rouse Jr et al., 1974), from which information about crop canopy characteristics such as leaf chlorophyll content and area can be inferred (Jones and Vaughan, 2010). Key ground measured traits, GCC and g_s, can be estimated from aerially measured NDVI and canopy temperature (Tc), respectively. Tc is linearly related to evaporative cooling from the canopy, while the rate of water loss is strongly influenced by g_s, and therefore g_s can be estimated from Tc (Jarvis and Mcnaughton, 1986). Likewise, GCC and its surrogate measurement, fractional interception of photosynthetically active radiation (FIPAR) by the crop canopy, can be estimated from reflectance data (Jones and Vaughan, 2010). AP can enhance breeding by: (1) increasing selection efficiency through rapid screening of larger trials; (2) refining selection accuracy with improved estimates of genetic trait values; (3) identifying new genotypic variation for important traits; and (4) reducing the time required for selection (Araus et al., 2018). This could aid targeted efforts to identify superior genotypes, thereby accelerating breeding efficiency and genetic gains under current and future climate conditions. While studies have explored using FIPAR and g_s as selection traits (Basnayake, 2016; Basnayake et al., 2015; Ferreira et al., 2017; Ghannoum, 2016; Li et al., 2017; Natarajan et al., 2019), further validation is needed to test the technique for use in breeding.

1.1 Hypothesis

The hypothesis of the study is that FIPAR and g_s can be accurately and rapidly estimated for a large number of sugarcane genotypes from aerially measured NDVI and Tc, respectively. AP could be used to identify superior sugarcane genotypes in the breeding program, thereby increasing breeding efficiency and contributing to yield improvement.

1.2 Aims and objectives

The main aim of the study was to develop and test an AP procedure for identifying superior genotypes in sugarcane breeding.

The specific objectives were to:

1. Determine the impacts of ground (FIPAR and g_s) and aerially measured (NDVI and Tc) traits on SDM under well-watered (WW) and water deficit (WD) conditions;
2. Develop an AP procedure for estimating g_s, FIPAR and SDM from Tc and NDVI;
3. Determine the genotypic variation and broad-sense heritability of ground and aerially measured traits;

4. Evaluate the feasibility and potential benefit of implementing AP to identify superior genotypes in breeding.

1.3 Dissertation outline

Chapter 1 introduces the sugarcane industry and describes the economic importance of sugarcane as a major agricultural crop both globally and in South Africa. The chapter introduces sugarcane breeding, and briefly reviews its progress in advancing genetic gains over the last two decades. This is placed within the context of global food production demands and climate change into the future, and the challenges faced by sugarcane breeding. The need to develop novel technologies to assist breeding for high-yielding, water use efficient varieties is highlighted. The study introduces the concept of key traits (g_s and FIPAR) governing yield formation and crop water use, and the potential for these traits to be measured through with aerial phenotyping (AP), through remotely sensed NDVI and Tc. The potential for AP to be used in breeding is discussed. Lastly, the hypothesis, aims and objectives are outlined.

Chapter 2 describes the key principles underpinning sugarcane growth and development. It also reviews the successes and challenges with traditional breeding approaches, and how physiological knowledge could be used to enhance crop improvement. Lastly, the study reviews aerial phenotyping technologies, and how these have been tested in sugarcane breeding to date. This review was used to identify research opportunities and knowledge gaps.

Chapter 3 provides details of a pilot study, conducted in a rain shelter facility where two genotypes were grown under well-watered and water deficit conditions. The study was used to establish preliminary relationships between aerial imagery and ground measured plant traits. These findings were used to refine aerial data capture and image processing procedures, used in the follow-on experimental phase.

Chapter 4 provides details of field trials, where 54 genotypes with two water treatments were monitored in the plant and first ratoon crops. The overall aim was to estimate key trait values for many genotypes to assess trait impacts on yield, evaluate the feasibility of estimating FIPAR and g_s with aerially captured spectral information, and determine the heritability of ground and aerially measured traits. The chapter describes the methodological approaches used, as well as the key findings and outcomes. This information was used to formulate an AP procedure to be tested in a breeding trial.

Chapter 5 describes the validation of the AP procedure in two early-stage breeding trials and outlines the successes and challenges of implementing AP in breeding.

Chapter 6 concludes the study and discusses recommendations for future work.

2. LITERATURE REVIEW

2.1 Introduction

The aim of this review was to gather and assess existing literature in three key areas:

1. Sugarcane growth and development, where the fundamental principles governing resource utilization and plant-water relations are discussed.
2. Sugarcane breeding, highlighting successes and challenges in conventional breeding and exploring the potential integration of physiological knowledge.
3. Remote sensing, with a particular focus on the methodologies and utilization of AP in sugarcane.

This was used to identify research opportunities and pinpoint knowledge gaps to guide the study forward.

2.2 Sugarcane growth and development

Sugarcane, a perennial grass cultivated in tropical and sub-tropical climates, is a C4 species well-suited to thrive in high temperatures (with optimal and base temperatures of 28 – 30 °C, and 10 – 19 °C, respectively; Carr and Knox, 2011; Inman-Bamber, 1994; Liu et al., 1998) and high radiation. Sugarcane relies on substantial water intake (1100 – 1800 mm per annum; Carr and Knox, 2011), particularly during critical stages of crop development.

Bonnett (2014) provided an overview of sugarcane growth phases. These phases can be summarised briefly as follows: (1) germination, during which underground buds sprout from planted setts (stalk segments) and emerge from the soil surface as primary shoots; (2) tillering, when the axillary buds of primary shoots sprout to produce secondary shoots or tillers, contributing to overall plant density and canopy development; (3) grand growth, characterised by rapid vegetative growth, canopy expansion and biomass accumulation; (4) maturation, when expansive growth decreases and rapid accumulation of sucrose in stem tissues takes place. These crop development phases govern resource capture, biomass accumulation and partitioning, which ultimately determine yield formation.

2.2.1 Radiation capture and conversion efficiency

Yield formation framework

Under non water- and nutrient-limiting conditions, biomass production (ΔDM) in sugarcane is driven by the amount of photosynthetically active radiation (PAR, 4—700 nm) absorbed by the green leaf canopy (the fraction of PAR intercepted by the green canopy, FIPAR) and the efficiency with which absorbed radiation is converted to biomass through carbon assimilation (radiation use efficiency, RUE; Robertson et al., 1996):

$$\Delta DM = FIPAR\,.\,RUE \quad \text{(Equation 1)}$$

This relationship may also be described in terms of solar radiation (SRAD) from the entire shortwave radiation spectrum (290 – 4000 nm) which is intercepted by the crop canopy.

Radiation capture

Overview

Canopy development is a key determinant of yield formation, as it governs the interception of solar radiation that drives photosynthesis and crop evaporation. Canopy development has been shown to be genetically controlled (Singels and Donaldson, 2000; Zhou et al., 2003), though the process is also affected by environmental factors such as temperature, crop water and nutrient status (Campbell et al., 1998; Inman-Bamber, 1994), as well as management factors such as planting time, row-spacing and planting density (Inman-Bamber, 1994; Singels et al., 2005; Singels and Smit, 2002).

Interception of PAR by the crop canopy can be described using Beer's law of radiation extinction:

$$FIPAR = 1 - \exp\left(-k_c.GLAI\right) \quad \text{(Equation 2)}$$

where k_c is the extinction coefficient for either PAR (k_{PAR}) or SRAD (k_{SRAD}), and GLAI is the green leaf area index, defined as the total area of green leaves per unit ground area. k_c governs how radiation is transmitted as it penetrates down into the crop canopy, and is affected by canopy architecture (leaf size, angle, density and distribution). Singels et al. (2021) cited a number of studies where k_{PAR} was shown to range from 0.31 to 0.86 (A. L.C. De Silva and De Costa, 2012; Dias et al., 2019; Inman-Bamber, 1991; Meki et al., 2015; Zhou et al., 2003), and k_{SRAD} from 0.31 to 0.41 (A. L.C. De Silva and De Costa, 2012; Muchow et al., 1994). At the same GLAI, higher k_c values are indicative of canopies with

horizontal leaves (low leaf angles) which intercept or absorb more radiation, as compared to erect leaves.

GLAI is determined by canopy components, including average leaf size (LA), number of green leaves per shoot (GL) and shoot population per unit ground area (SPOP):

$$GLAI = LA.GL.SPOP \quad \text{(Equation 3)}$$

These components are governed by several processes such as tillering and leaf appearance rate, and leaf and stalk elongation, which are driven by temperature and radiation in unstressed crops.

Impact of water availability on canopy development

In the absence of water or nutrient limitations, canopy development of unstressed crops is driven by temperature, where FIPAR shows a genotype-dependent non-linear relationship with cumulative thermal time (TT, the accumulation of heat units required for growth and development; Inman-Bamber, 1994; Singels and Donaldson, 2000). Under water limited conditions, water stress acts to reduce FIPAR through a reduction in GLAI, as a result of reduced growth rates (leaf appearance and expansion) and leaf senescence.

Genotypic variation and opportunities for yield improvement

Several studies have reported significant genotypic variation in canopy development and its associated processes, offering potential avenues for targeted yield improvement. However, the best methods for increasing yields through improved radiation capture remain unclear, given the dynamic and interactive nature of processes and low-level traits. Acreche, (2017) found that newer varieties (released around 2005) intercepted 63% more radiation as compared to older varieties from 1940. This increase was due to differences in canopy architecture, resulting in higher maximum interception and a shorter duration to achieve canopy closure.

Field-based studies have demonstrated significant genotypic differences in canopy development rates (or the TT taken for FIPAR to reach 50%) within diverse genetic populations, ranging in number from two to 40 genotypes (Basnayake et al., 2015; A. L.C. De Silva and De Costa, 2012; Dias et al., 2020; Donaldson et al., 2008; Inman-Bamber, 1994; Jones et al., 2019; Muchow et al., 1994; Robertson et al., 1996; Singels et al., 2005). Moreover, studies have also reported genotypic variation in the underlying canopy

development processes (tillering and leaf appearance rate, and leaf and stalk elongation) (Bonnett, 1998; Hoffman and Singels, 2019; Inman-Bamber, 1994; Jones et al., 2019; Karno, 2007; Singels, 2008; Zhou et al., 2003). Model-based studies by Sexton et al. (2017) and Hoffman (2016) used APSIM-Sugar and DSSAT-Canegro to evaluate the influence of various traits on simulated biomass and stalk yield. Sexton et al. (2017) found that of the ten traits considered, green leaf number and leaf area were ranked second and fourth respectively, while Hoffman (2016) showed that leaf appearance rate had little impact on simulated stalk yield.

Previous studies have also reported genotypic differences in canopy development in response to soil water deficit (Eksteen et al., 2014; Smit and Singels, 2006; Smith et al., 1999), achieved through stomatal sensitivity, leaf shedding and osmotic adjustments to maintain positive turgor potential for longer periods. These have been proposed as potential drought tolerance mechanisms, however information regarding these traits in diverse genetic populations remains limited.

Radiation conversion

Overview

Radiation use efficiency (RUE) is generally defined as the ratio of dry biomass produced per unit of absorbed radiation (Monteith, 1977). However, definitions vary depending on the scale and context under consideration. RUE can be expressed as a function of above ground or total biomass, and of PAR or SRAD (Bonhomme, 2000; Singels et al., 2021). RUE at the crop level (RUE_c) is genetically controlled, and also affected by environmental (crop water and nutrient status, temperature, atmospheric humidity and CO_2 concentration) and agronomic factors (such as growing season and row-spacing, Inman-Bamber, 1994; Singels et al., 2005). RUE at the leaf level (RUE_L) is defined as the carbon assimilated per unit of absorbed PAR, and is influenced by environmental factors (leaf water and nutrient status, temperature, CO_2, humidity and vapour pressure deficit, VPD).

Impact of water availability on RUE

Under non-water and nutrient limiting conditions, maximum RUE at the crop level ($RUEo_c$) is defined as the rate achievable for young healthy crops under optimal environmental

conditions. Similarly, the maximum leaf level RUE achievable ($RUEo_L$) is defined for young, fully expanded sunlit leaves under optimal conditions.

In water limited environments, crops mitigate water loss through stomatal closure (decreasing CO_2 diffusion) and reduced leaf area (through increased leaf rolling and senescence), which in turn reduces biomass accumulation (Robertson et al., 1999). De Silva and De Costa (2012) reported a 50% reduction in RUE for eight cultivars in response to water deficit.

Genotypic variation in RUE and opportunities for yield improvement

There is contrasting evidence in literature as to whether genotypic variation in $RUEo_c$ exists, and its correlation with yield also appears to be inconclusive, possibly stemming from the challenges associated with phenotyping this complex trait (Singels et al., 2021). Acreche (2017) found that mean $RUEo_c$ values had increased by 14% amongst varieties released after 1987 in comparison to earlier releases. De Silva and De Costa (2012) reported a range of 25% in $RUEo_c$ values for eight genotypes. Singels and Inman-Bamber (2011) reported a range of 30% in $RUEo_c$ values for four clones and recommended that genotype specific $RUEo_c$ values be considered for crop modelling studies. Crop modelling studies by Marin et al. (2011) and Coelho et al. (2019) modified the reference $RUEo_c$ value for NCo376 by ~25 – 50% when calibrating numerous varieties. By contrast, (Dias et al., 2020) opted not to modify $RUEo_c$ values when calibrating 27 varieties, suggesting no genotypic differences.

$RUEo_L$ can be estimated from measurements of net photosynthetic rate per unit leaf area (*A*), stomatal conductance (g_s) and chlorophyll a fluorescence ratio (fv/fm). Numerous studies have considered diverse genetic populations (8 – 81 genotypes) and reported genotypic variation for these traits, where the range of values (expressed relative to the mean trait value) varied from 16 – 108% for *A*, and 40 – 84% for g_s (De Silva and De Costa, 2009; Hoffman et al., 2018; Inman-Bamber et al., 2011; Irvine, 1975; Singels et al., 2021, 2010; Zhao et al., 2019, 2015). Furthermore, the relationships between $RUEo_c$ and $RUEo_L$ with yield are also widely debated. Inman-Bamber et al. (2009) demonstrated a strong relationship between biomass yield with $RUEo_c$ for four clones grown in a pot experiment. Sexton et al. (2017) and Hoffman (2016) showed through crop modelling approaches, that $RUEo_c$ was the most impactful trait in determining simulated biomass and yield. De Silva (2004) and De Silva and De Costa (2012) reported that $RUEo_c$ was highly correlated with

cane yield, biomass and total biomass for eight genotypes grown under well-watered and water deficit conditions, whereas Donaldson et al. (2008) and Jones et al. (2019) reported that $RUEo_c$ was not well correlated with total biomass or stalk yields.

Leaf level physiological traits to inform $RUEo_L$ also show contrasting relationships with yield. Irvine (1975) reported a weak relationship between yield and *A* for 20 clones. By contrast, Hoffman et al. (2018) and Zhao et al. (2015) showed that g_s was well correlated with stalk yield for eight and fourteen genotypes, respectively, while Basnayake et al. (2015) reported a wide range of positive and negative associations between g_s and yield.

This research emphasizes the complexity of RUE and its impact on yield. Understanding the genetic basis for RUE is crucial for developing effective breeding strategies to improve crop productivity.

2.2.2 Plant-water relations

Overview

Biomass accumulation relies on the establishment and size of a crop canopy, as well as the efficiency of CO_2 fixation within that canopy. These processes are impacted by crop water status, emphasising the importance of understanding plant-water relations within the context of advancing yield improvement in sugarcane.

Plant-water relations considers the movement of water flow through the soil-plant-atmosphere continuum. The cohesion-tension theory (Dixon and Joly, 1895) describes the continuous column of water within plant xylem which is driven by negative pressure gradients. This process is initiated by transpiration, which creates a negative water potential that facilitates water uptake from the soil to the roots and further to the leaves.

Water use efficiency (WUE) is closely linked to plant-water relations within the soil-plant-atmosphere continuum, as it quantifies how effectively a plant utilizes water for biomass production. WUE is a complex trait governed by several processes including transpiration, stomatal conductance, and transpiration efficiency. Therefore, WUE reflects the efficiency of water uptake, transport, and utilization by the plant, all of which are fundamental aspects of plant-water relations. Additionally, canopy conductance and temperature, which govern

the exchange of water vapour between the crop canopy and the atmosphere, are key components of plant-water relations that ultimately impact WUE.

Yield formation frameworks

Several yield formation frameworks have been described within the context of plant-water relations (Singels et al., 2021). At the crop level, biomass accumulation (ΔDM, kg m^{-2} d^{-1}) can be described within the context of crop water use (ET) and WUE:

$$\Delta DM = ET \,.\, WUE \quad \text{(Equation 4)}$$

where ET represents crop evapotranspiration over a given time period (m^3 m^{-2} d^{-1}), and WUE is dry matter produced per unit of water used (kg m^{-3}).

From a plant physiological perspective, ΔDM can also be expressed more accurately as the product of transpiration (T, the water lost by the crop through leaf stomata, m^3 m^{-2} d^{-1}) and transpiration efficiency (TE, dry biomass produced per unit of water transpired, kg m^{-3}) to facilitate the interpretation of yield variation in water-limited environments (based on Condon and Richards, 1993; Passioura, 1977; Richards et al., 2002):

$$\Delta DM = T.TE \quad \text{(Equation 5)}$$

TE has been shown to be influenced by VPD (kPa), and the concept was reformulated by Tanner and Sinclair (1983) as the ratio of TEC (TE at a reference VPD of 1 kPa, representing a measure of intrinsic WUE, kg m^{-3} kPa^{-1}) to VPD:

$$TE = \frac{TEC}{VPD} \quad \text{(Equation 6)}$$

TE at the leaf level (TE_L, µmol CO_2 mmol H_20) is defined as the ratio of carbon assimilated through photosynthesis (*A*, leaf CO_2 assimilation, µmol CO_2 m^{-2} s^{-1}) per unit of water lost through the stomata (E, mmol H_2O m^{-2} s^{-1}):

$$TE_L = \frac{A}{E} \quad \text{(Equation 7)}$$

TE_L contains a combination of plant characteristics and atmospheric influences, and is not ideal for evaluating genetic impacts. Intrinsic transpiration efficiency at the leaf level (TEi, µmol CO_2 mmol H_20) can be calculated as the ratio of *A* (µmol CO_2 m^{-2} s^{-1}) to g_s (mmol H_2O m^{-2} s^{-1}) (Condon et al., 2002; Farquhar et al., 1989; Gilbert et al., 2011):

$$TE_i = \frac{A}{g_s} \quad \text{(Equation 8)}$$

Genotypic variation in traits associated with plant-water relations and opportunities for yield improvement

High yields in well-watered environments can be achieved by maximizing water uptake through increased transpiration, root growth and rapid canopy development, facilitated by increased conductance. A number of studies have demonstrated this using field experiments and crop modelling approaches, for environments with little to no water stress (Basnayake et al., 2015; Eksteen et al., 2014; Hoffman N, 2016; Hoffman and Singels, 2019; Inman-Bamber et al., 2012; Olivier et al., 2016).

In environments with limited water availability, the importance of early vigour is less certain, and the impacts of increased transpiration through conductance need to be carefully considered (Singels et al., 2021). A number of studies have reported significant genotypic variation for stomatal sensitivity to water deficit (Eksteen et al., 2014; Hoffman and Singels, 2019; Inman-Bamber and De Jager, 1986; Smit and Singels, 2006). Zhao et al. (2017) suggested that low conductance may be advantageous in very dry environments, as genotypes with low transpiration rates could experience a delayed onset of water stress. Inman-Bamber et al. (2012) used a crop modelling approach to investigate the impacts of increased root growth (density and depth of root systems) and reduced conductance on yield. Increased root growth was beneficial in both well-watered and water-limited environments, and especially for shallow soils. Reduced conductance mostly resulted in negative yield responses, except in very dry environments with better (deep) soils, where yield increased as a result of the crop conserving water for use during dry periods. Similarly, Singels et al. (2016) found that early stomatal closure (sensitivity to water deficit) in environments with little to no water stress, resulted in negative yield responses through reduced transpiration and biomass accumulation, while yield responses in water-limited environments were variable.

Several studies have also demonstrated significant genotypic variation for TEi in water-limited environments (Basnayake et al., 2012; Jackson et al., 2016; Li et al., 2017), though its suitability as a selection trait for yield is complex. While *A* and g_s are generally closely positively correlated, the relationship is curvilinear, and the slope decreases as g_s increases (Gilbert et al., 2011). Thus, relatively high TEi for a given genotype may result from increased *A*, or decreased g_s associated with low transpiration and productivity. Increased TEi due to higher *A* at any level of conductance is expected to be of more agronomic value (Ghannoum, 2016). Yield improvement using TEi is further complicated due to the uncoupling between g_s and crop transpiration (Jarvis and Mcnaughton, 1986). In sparse or aerodynamically rough canopies, where leaves are exposed to high air movement, stomata control water loss to a large extent. However, in dense, humid canopies where air flow is minimised, stomata exert little control over water loss. The degree of control of stomata on transpiration is quantified by the stomatal uncoupling coefficient (Ω) (Jarvis and Mcnaughton, 1986; Meinzer and Grantz, 1990), which ranges from zero (complete stomatal control of transpiration) to 1 (no stomatal control of transpiration). As a result of these complications, negative covariance is frequently observed between whole-plant transpiration and TE (Blum, 2009; Condon et al., 2004; Sinclair, 2012; Vadez et al., 2014).

Furthermore, many studies in sugarcane have demonstrated significant genotypic variation in g_s, and generally positive correlations with yield, which can be exploited for yield improvement across a range of environments (De Silva and De Costa, 2009; Hoffman et al., 2018; Inman-Bamber et al., 2011; Irvine, 1975; Singels et al., 2021, 2010; Zhao et al., 2019, 2015). Basnayake et al. (2015) monitored multi-location trials with diverse genetic populations (131 clones) grown under different moisture conditions, and observed highly significant genotypic variation in g_s, with a wide range of positive and negative genetic correlations between g_s and yield. The study found that canopy conductance (g_c), estimated as the product of g_s and LAI, showed stronger genetic correlation with yield as compared to g_s. Tc serves as a proxy for g_c and has also shown potential for improving water productivity and yield across different moisture conditions (Araus and Cairns, 2014). (Basnayake, 2016) conducted multi-location field experiments across different moisture regimes and production environments with between 20 – 99 genotypes, and reported significant genotypic variation in Tc, and strong genetic correlation between Tc and biomass. Chapman et al. (2014) monitored a field experiment with 40 clones and varying moisture regimes and reported

genotypic variation in Tc for the partially irrigated water treatment. Though promising, Tc may be strongly influenced by environment and measurement conditions which obscure genotypic differences. Natarajan et al. (2019) evaluated Tc in a large breeding population (2134 genotypes) and reported mostly low to moderate genetic correlations between Tc and cane yield.

In conclusion, yield improvement in sugarcane can benefit from understanding and leveraging traits that influence biomass accumulation, water uptake and TE. High yields in well-watered environments are often achieved through traits that enhance water uptake, such as increased g_s and rapid canopy development. Conversely, in water-limited environments, low g_s combined with high TEi, can delay the onset of water stress, potentially leading to higher yields under severe water constraints.

Literature has shown significant genotypic variation in traits such as *A*, g_s and *E*, which is reflected in the significant variation observed for TEi. Additionally, g_c, which reflects both g_s and GCC, and Tc, a proxy for g_c, have also shown considerable variation. However, further research is needed to understand how these traits and their derived metrics are influenced by varying environmental conditions, and to refine their use as selection criteria.

Ultimately, the integration of physiological insights with practical breeding approaches could enhance water productivity and yield across diverse environments, leading to more productive sugarcane genotypes.

2.3 Sugarcane breeding

2.3.1 Overview

Sugarcane breeding, originating in Java and Barbados in 1885 to 1888 (Mangelsdorf, 1953; Stevenson, 1966), has significantly contributed to the global sugar industry's growth and profitability, despite the relatively short history of breeding compared to other major crops. Its pivotal role remains integral to the continued success, expansion and sustainability of sugarcane production worldwide. Broadly, sugarcane breeding aims to develop resilient, high-yielding varieties with desirable traits such as increased sugar content, enhanced disease and pest resistance, ratooning ability and adaptability to diverse environments (Jackson, 2005).

The breeding process relies on the generation of segregating-progeny populations, created through controlled crosses, followed by continuous recurrent selection of promising individuals (Hoarau et al., 2022; Mirajkar et al., 2019). Different breeding technologies (conventional and molecular) are used for increasing the selection efficiency in breeding programmes. Conventional methods involve field screening of offspring at different stages of the breeding cycle at multiple locations for desired traits (Zhou, 2013), while molecular breeding utilizes advanced genetic biotechnological tools to increase the efficiency of selections in early stages of the breeding cycle. It is also being used to improve traits of interest through gene editing technologies (Kumar et al., 2016).

Conventional breeding

Traditional breeding strategies differ worldwide according to their specific objectives and goals, although they share common elements (Falconer and Mackay, 1996). Typically, the traditional breeding sequence begins with seedling selection, often involving thousands of candidates, which are then clonally propagated. These selections undergo recurrent selection in several stages spanning multiple years (Gazaffi et al., 2014; Hoarau et al., 2022; Zhou, 2013). Table 1 outlines the structures of several sugarcane breeding programs worldwide, highlighting key differences in duration, population and trial sizes, selection intensities and screening traits.

Breeding cycle lengths range from 6 to 20 years, though a cycle length of 10 to 12 years is most common across the different programs. These cycles comprise 3-9 selection stages, with most programs typically using about 5-6 stages. The early stages (1-3) generally involve

single stools or seedlings, often planted in single-row, unreplicated plots ranging from 1 x 1 m to 1 x 6 m. Some programs also utilize family replication during these early stages. In the intermediate (4-6) and advanced (7-9) stages, there is an increase in plot size and replication as compared to the early stages, with multi-row plots ranging from 2 x 5 m to 6 x 10 m, and two to four replicates. Multi-location testing is common during these stages, with 3 to 10 locations used to improve the accuracy of trait estimates, to evaluate genotype performance under diverse conditions, and address environmental variability.

Selection rates vary widely between stages, generally increasing in stringency as programs progress. Early stages typically have selection rates from 20-30%, reaching up to 50% in some cases. Intermediate stages often range from 10-30%, but can vary from 2-50%, while advanced stages employ selection rates from 2-25%, with most around 10%.

Early-stage selection focuses on broad, easily measurable traits to exclude less promising genotypes. This includes visual assessments of growth and vigour, and basic traits for characterizing stalk appearance and pest and disease resistance. Some programs also consider more specific traits such as tillering and pithiness for early screening. In the intermediate and advanced stages, the focus shifts to rigorous assessments of complex traits such as yield, sucrose content, and resistance to pests and diseases. Final selection stages also consider practical aspects like ratoonability, mechanical harvestability, and environmental adaptability. Traits such as ethanol and fiber content, and adaptation to environmental stresses (e.g. typhoons, drought) are also considered in some cases. Overall, these selection strategies ensure that genotypes are both high-performing and commercially viable.

Despite these distinctions, all breeding programs share overarching objectives such as developing superior varieties with increased yields, enhanced pest and disease resistance, and broad adaptation to different environments (Cursi et al., 2022). Some programs have more specific target-driven goals, such as achieving predetermined yield thresholds, (e.g. >70-90 t ha^{-1} with ratooning frequency of 3-5 in Japan, or > 75-80 t ha^{-1} in Vietnam) (Cao and Doan, 2022; Terajima et al., 2022). Ultimately these differences in objectives influence the design of selection programs.

Table 2.1. Details of the structures of sugarcane breeding programs worldwide.

Region	Country / territory	Reference	Breeding cycle length	Total no. selection stages	Plot size / replication / locations	Selection rate	Selection criteria[1]
Africa	Egypt	(Mehareb et al., 2022)	8 years	7	• Stage 1: single stools / seedlings • Stage 2: 1x 3 m row, unreplicated • Stage 3: 1x 6 m row, unreplicated • Stage 4: 6x 7 m rows, 3 reps • Stage 5: 6x 7 m rows, 4 reps, 4 locations • Stage 6: 6x 7 m rows, 4 reps, 4 locations • Stage 7: 10x 7 m rows, widespread demonstration	Varies from 20-30% between stages	• Stage 1: stalk diameter, brix%, stalk weight and tillering • Stage 2-3: P&D resistance, tillering, pithiness, stalk diameter and height, brix% • Stage 4-7: Yield, brix%, sucrose content, P&D resistance, ratoonability
	Mauritius	(Santchurn et al., 2022)	12-15 years	6	• Stage 1: single stool / seedlings • Stage 2: 1x 3 m row, unreplicated • Stage 3: 1x 5 m row, unreplicated • Stage 4: 2x 5 m rows, 3 reps • Stage 5: 4x 10 m rows, 3 reps • Stage 6: 4x 10 m rows, 3 reps	Varies from 13-30% between stages	More than 20 traits evaluated, including morphological characteristics not commonly used, e.g. ease of thrashing
	South Africa	(Zhou, 2022)	11-20 years	5	• Stage 1: single stools, family replication, 5 locations • Stage 2: 1x 1 m, family replication, 5 locations • Stage 3: 1x 4-8 m row, 2 reps, 5 locations • Stage 4: 2x 8 m rows, 3 reps, 5 locations • Stage 5: 5x 8 m rows, 3 reps	Ranges from 10-70% between stages	• Stage 1: Visual assessment, P&D resistance • Stage 2 -5: Yield, sucrose, P&D resistance
Asia	China	(Qi et al., 2022)	10 years	5	• Stage 1: single stools / seedlings • Stage 2: 1x 6 m row, unreplicated • Stage 3: 4x 7 m rows, unreplicated • Stage 4: 6x 7 m rows or 5x 6 m rows, 3 reps • Stage 5: 5x 7-10 m, 3 reps, 10 locations	Varies from 2-10% between stages	Yield, sucrose content, P&D resistance, tillering, ratoonability

	Country / territory	Reference	Breeding cycle length	Total no. selection stages	Plot size / replication / locations	Selection rate	Selection criteria[1]
Asia	India	(Ram et al., 2022)	13 years	9	• Stages 1-3: Single stools / seedlings, then single rows • Stage 4-9: 2-row trials, then advanced multi-plot field trials	20-25%	• Stage 1-2: Brix%, tillering, flowering, cane yield characteristics • Stage 4-7: cane quality analysis, P&D resistance, yield, ethanol and fibre content
	Indonesia	(Widyasari et al., 2022)	10 years	5	• Not specified	Ranges from 10 – 50% between stages	Yield, morphological and agronomic characteristics, P&D resistance
	Japan	(Terajima et al., 2022)	Not specified	6	• Stage 1: single stool / seedlings • Stage 2: 1x 1.5 m row, unreplicated • Stage 3: 1x 3-8 m row, unreplicated • Stage 4: 1x 4 m rows or 3x 2 m row, 2 reps, 2-4 locations • Stage 5: 3x 3-4 m rows, 3 reps, 6 locations • Stage 6: 4x 10 m rows, 3 reps	Not specified	Cane yield, sugar content, P&D resistance, ratoonability, adaptability (e.g. tolerance of typhoons and drought)
	Mynamar	(Aung et al., 2022)	10 – 11 years	8	• Stages 1-4: Single lines of 5 – 10 m; unreplicated; 1 – 3 locations • Stages 5-8: Size not specified (large plots); replicated; 3-10 locations	Varies from 4% - 50% between stages	• Stages 1-4: Visual assessment of vigour, brix%, P&D resistance, yield, cane quality • Stages 5-8: Ratooning ability, P&D resistance, maturity testing
	Pakistan	(Afghan et al., 2022)	Unknown	6	• Stages 1-3: single lines of 1-3 m; unreplicated • Stages 4-6: 10 – 25 rows of 10/15 m each; 3 / 4 reps	10% in each stage	• Stages 1-2: General growth & vigour; stalk characteristics, P&D resistance; no side shooting, pithiness • Stages 3-6: Germination, tillering, yield, chemical resistance, cane quality
	Philippines	(Luzaran et al., 2022)	8-10 years	4	• Not specified; ranges from 1x 95 m row, to 3x 95 m rows	Not specified	P&D resistance, pithiness, stalk size, quality and growth characteristics
	Thailand	(Khumla et al., 2022)	12 years	6	• Stage 2: single stools / rows / family selection • Stage 3: 1x 5-8 m row • Stage 4: 2-4 8 m rows, 2-4 reps, 1-2 locations • Stage 5: plot size 48-72 m^2, 4 reps, 4-6 locations • Stage 6: plot size 72 m^2, 8m rows, 4 reps, 6-8 locations	Varies from 2 – 50% between stages	Cane yield, brix, stalk characteristics, ratooning ability, hairiness, pithiness, canopy type, P&D resistance, abiotic stress tolerance, farmer's adoption, adaptation to different environments
	Vietnam	(Cao and Doan, 2022)	6-8 years	4	• Stages 1-2: Single stools, 2-3 m lines, replication not specified • Stages 3-4: Small- and large-scale field trials	Not specified	• Stages 1-3: P&D resistance, flowering, stalk population, stalk characteristics, brix%, ratooning ability • Stage 4: Not specified, but tested under controlled environments

	Country / territory	Reference	Breeding cycle length	Total no. selection stages	Plot size / replication / locations	Selection rate	Selection criteria[1]
South America	Argentina	(Ostengo et al., 2022)	11 – 14 years	5	• Stage 1: Single stools / seedlings, 2 locations • Stage 2: 1x 3 m row, unreplicated • Stage 3: 3x 3 m rows, 2 reps • Stage 4: 3x 8 m rows, 3 reps • Stage 5: 3x 10 m rows, 3 reps	Varies from 10-25% between stages	• Stage 1: Visual assessment of vigour, P&D resistance, brix% • Stage 2-3: As above, as well as stalk population and weight, estimated sugar yield • Stage 4: As above, as well as cane yield Stage 5: As above, as well as fibre content, maturity curve monitoring and ratoonability
	Brazil	(Cursi et al., 2022)	10-12 years	4	• Stage 1: 2x 27 m rows, 3 locations • Stage 2: 1x 5 m row • Stage 3: 2x 5 m rows, 2 reps, 6 locations • Stage 4: 4x 12 m rows, 4 reps, 10 locations	Not specified	• Stage 1: Yield, brix%, P&D resistance • Stage 2: Morphology, P&D resistance, yield • Stage 3: As in stages 1-2, with ratoonability • Stage 4: As in stages 1-2, with ratoonability
	Ecuador	(Castillo and Silva Cifuentes, 2022)	12 years	5	• Stage 1: Size not specified for replicated families • Stage 2: 1 x 8 m row, unreplicated • Stage 3: 2 x 15 m rows, 2 reps, 3 locations • Stage 4: 2x 20 m rows, 3 reps, 6 locations • Stage 5: 6x 200 m rows, 3 reps, 3 locations	Not specified	• Stage 1-2: sucrose content, P&D resistance, flowering • Stages 3-5: sucrose content, yield, ratooning ability, P&D resistance, flowering, stalk characteristics
North America and Caribbean	Caribbean (Barbados, Belize, Guyana, Jamaica, Romana)	(Kennedy, 2022)	Not specified	6	• Not specified; generally single unreplicated rows up to stage 2, followed by replicated single rows in stage 3 and plots / strip trials in advanced stages	Not specified	P&D resistance; cane and sugar yield; early assessment of vigour; stalk population, ratoonability
	Central America (Mexico, Guatemala)	(Orozco and Queme, 2022)	12 years	5	• Stage 1: Single stools / seedlings (family selection) • Stage 2: 1x 3-5 m row, unreplicated • Stage 3: 2x 5 m rows, 3 reps • Stage 4: 5x 10 m rows, 4 reps Stage 5: 5 rows of unspecified length (commercial conditions), 3-4 reps	Varies from 1.5-25% between stages	• Stage 1-2: Visual inspection for vigour, stalk population, height and diameter, P&D resistance, sugar content • Stage 3: As above, as well as yield • Stage 4-5: As above, as well as purity assessments and suitability checks for mechanical harvesting

	Country / territory	Reference	Breeding cycle length	Total no. selection stages	Plot size / replication / locations	Selection rate	Selection criteria[1]
North America and Caribbean	USA	(Hale et al., 2022)	12 years	Site-specific, but generally four	Varies from 0.4 m single row to 2x 16 m rows; early stages generally not replicated	Not specified	P&D resistance; cane and sugar yield; early assessment of vigour; stalk population
Oceania	Australia	(Wei et al., 2022)	12 years	3	• Stage 1: single rows, family replication; 4 locations • Stage 2: 8-10 m single rows; partially replicated; 4 locations • Stage 3: 4x10 m rows; 4 locations	Ranges from 16 – 50% between stages	Stalk yield, CCS, fibre, appearance (flowering, lodging), P&D resistance
	Reunion	(Dumont et al., 2022)	14 years	5	• Stage 1: Partially replicated families • Stage 2: plot area of 4.5 m^2, unreplicated • Stage 3: plot area of 15 m^2, 2 reps • Stage 4: plot area of 45 m^2, 3 reps • Stage 5: plot area of 45 m^2, 4 reps; multi-environment trials	Varies from 7-21% between stages	• Stage 1: Family inspection, P&D resistance • Stage 2: Visual inspection, brix%, P&D resistance • Stage 3: Visual inspection, P&D resistance, yield & ratoonability • Stage 4: As in stage 3 above • Stage 5: As in stage 3 above

[1] Pest & disease (P&D); CCS (commercial cane sugar)

Successes and challenges in conventional breeding

Traditional breeding has been pivotal in enhancing crop yield and refining agronomic traits since its inception (Meena et al., 2022). This is evidenced by some of the reported successes. For instance, India has reported notable increases in commercial cane yield from 30.9 to 78.3 t ha^{-1} since the 1930s (Ram et al., 2022). Similarly, in the USA, commercial yields have increased from 44 to 75 t ha^{-1} since the 1890s (Hale et al., 2022), while Pakistan has nearly doubled its average commercial yields since the 1960s (Afghan et al., 2022). Moreover, Mauritius, Brazil and Central American countries have reported consistent progress in genetic gain for yield over time (Cursi et al., 2022; Orozco and Queme, 2022; Santchurn et al., 2022).

Advancing sugarcane breeding poses substantial challenges. These include long breeding cycles, complexities in accurately phenotyping large, genetically diverse populations, confounding effects of genotype x environment x management (GxExM) interactions, and the large and complex nature of the crop's genome (Luo et al., 2023). Consequently, the breeding process remains time consuming and resource intensive. Despite the reported successes in breeding, there is evidence to suggest that genetic gain in sugarcane yield and sucrose content has stagnated across many breeding programs worldwide (Cursi et al., 2022; Jackson, 2005; Kumar et al., 2016; Wei and Jackson, 2017; Yadav et al., 2020).

Genetic gain (R_t) serves as a fundamental metric in breeding, quantifying the increase in performance achieved through artificial selection (Xu et al., 2017). R_t is estimated using the breeder's equation (Falconer and Mackay, 1996), using the selection intensity (i) and accuracy (r), genotypic variation (σ_A), and time taken to complete a breeding cycle (t):

$$R_t = \frac{i\, r\, \sigma_A}{t} \qquad \text{(Equation 9)}$$

Within the framework of the breeder's equation, enhancing R_t can be achieved by increasing selection intensity through larger population sizes and improving selection accuracy for more precise estimates of genetic value (performance of a genotype for a given trait). This concept is closely related to broad-sense heritability, defined as the proportion of variation for a given trait which can be attributed to genetic factors rather than environmental

influences (Fehr, 1987). Lastly, R_t can be enhanced by reducing the time required to complete a breeding cycle.

Physiological breeding

There is growing recognition of the potential to integrating physiological knowledge into traditional breeding strategies, particularly for enhancing drought tolerance. This has been discussed extensively in cereal crops such as maize (Messina et al., 2015, 2011), wheat (Condon et al., 2004, 2002), rice (Caine et al., 2019), and other crops (De Souza et al., 2017). However, the literature remains limited for sugarcane.

Studies discussing the use of physiological knowledge in sugarcane breeding have primarily focused on leaf-level and whole-plant traits such as transpiration efficiency, stomatal conductance, photosynthesis, transpiration rate and internal CO_2 concentration, as potential indicators for selecting high-yielding genotypes (Basnayake, 2016; Basnayake et al., 2015; Ferreira et al., 2017; Ghannoum, 2016; Hoffman et al., 2024; Jackson et al., 2016, 1996; Leanasawat et al., 2021; Li et al., 2017; Mall et al., 2020; Tippayawat et al., 2023; Zhao et al., 2017). Jackson et al. (2016) and Li et al., (2017) have highlighted the potential of TEi as a screening trait. This poses challenges, as high TE may arise as the result of high photosynthetic capacity (associated with increased productivity and yield), or reduced conductance (associated with lower water use and yield) (Gilbert et al., 2011). Moreover, there is uncertainty about whether enhancements in TEi will translate into advantages at the whole plant or crop level, due to the extent of uncoupling of stomatal control over transpiration under different conditions. Despite these complexities, these studies reported significant genetic variation in TEi which could be exploited in breeding. Basnayake et al. (2015) reported significant genetic variation (under a wide range of moisture conditions) and moderate broad-sense heritability (under well-watered conditions) for g_s which, when combined with LAI for estimating g_c, mostly showed good genetic correlations with cane yield. Genetic variation for g_s in sugarcane which can be exploited in breeding has been reported previously (De Silva and De Costa, 2009; Hoffman et al., 2018; Li et al., 2017; P. Zhao et al., 2017). Basnayake et al. (2015) confirmed the potential of g_c as a potential screening criterion in early-stage breeding trials.

Most of these studies directly or indirectly suggest that current sugarcane breeding strategies do not employ physiological knowledge of traits in selection procedures because: (1)

measurements of physiological traits are time-consuming and highly variable within and across environments, and high-throughput screening methods require complex validation (Araus et al., 2018; Basnayake et al., 2015); (2) relationships between physiological traits and crop productivity are wide ranging and complex (Basnayake et al., 2015; Li et al., 2017). The prevailing notion within the literature seems to suggest that for the development and implementation of physiological breeding to be successful, a multidisciplinary approach is essential (Jackson et al., 1996). This necessitates collaborative efforts between specialists from diverse fields, including genetics, plant physiology, agronomy and data science. Aerial phenotyping integrates expertise across all of these fields and serves as a promising avenue for the development of physiological breeding methods.

2.4 Remote sensing (RS)

2.4.1 Overview

Remote sensing (RS) technologies for monitoring vegetation (Jones and Vaughan, 2010) characterise a rapidly expanding, multidisciplinary research domain. Beginning with the application of satellite imagery to classify crop types in the Midwestern US (Bauer et al., 1979), RS in agriculture has shown substantial growth and diversification in recent years, as evidenced by an exponential increase in published literature since 2013 (Weiss et al., 2020). Remote sensing enhances precision agriculture by enabling the monitoring of crop productivity at high spatial and temporal resolution, while simultaneously covering large areas as compared to ground-based assessments of crop health and environmental conditions (Blatchford et al., 2019; Sadras et al., 2015). Remote sensing technologies comprise platforms such as satellites (Nakalembe et al., 2021), manned aircraft, unmanned aerial vehicles such as drones (Kim et al., 2019), and ground vehicles (Gonzalez-de-Santos et al., 2020) coupled with sensors (optical, thermal, microwave, LiDAR, radar and sonar; Jones and Vaughan, 2010). These systems are complemented by geographic information systems (GIS) for data analysis, integration and visualisation. Recent developments in the Internet of Things, artificial intelligence and machine learning (Shahab et al., 2024) have further advanced the capabilities of RS technologies through enhanced data processing, predictive analytics and decision making. Continued innovation in RS, and particularly in the use of aerial phenotyping (AP) technologies, holds promise for advancements in agricultural sustainability and productivity.

2.4.2 Aerial phenotyping (AP) in sugarcane

Overview

Within the context of the study, AP is defined as the use of UAVs (specifically drones) to capture aerially measured data of crop spectral properties. AP relies on capturing radiation reflectance and emittance from the crop surface using spectral sensors integrated with drones, across different bands of the electromagnetic spectrum, to measure crop spectral properties. The subsequent image and data processing workflows include corrections for atmospheric distortions, radiometric calibration to adjust sensor responses, geometric adjustments for precise spatial alignment, and image classification to differentiate leaf and soil spectral properties. Following this, vegetation indices (VIs) are estimated from two or more spectral bands which are associated with the biophysical parameters of interest. These data are used in a wide range of applications (Amarasingam et al., 2022) including crop growth monitoring (Li et al., 2021; Natarajan et al., 2019; Sofonia et al., 2019), pest and disease detection (Moriya et al., 2017; Narmilan et al., 2022; Sanseechan et al., 2019), agronomic management (Shendryk et al., 2020; Wang, 2019; Xu et al., 2020), yield estimation (Barbosa Júnior et al., 2023; Khuimphukhieo et al., 2023; Som-ard et al., 2024) and mapping (de Oliveira et al., 2023; Huang et al., 2024; Luna and Lobo, 2016).

Components of AP: Vehicles, sensors and analysis tools

A number of studies have reviewed the use of UAVs in sugarcane precision agriculture (Barbedo, 2019; Barbosa Júnior et al., 2022; Cardoso et al., 2022; Guo et al., 2021; Sumesh et al., 2021). Their underlying components, including the choice of aerial vehicle platform, sensor for capturing crop spectral properties, and tools for image and data analysis, govern their suitability for specific applications. These elements are briefly reviewed within the scope of this research.

Unmanned aerial vehicles (UAVs)

UAVs can be classified according to their design, level of autonomy, size, mass and power supply (De Rango et al., 2019), and can be broadly described as fixed-wing, rotary-wing or hybrid UAVs (Amarasingam et al., 2022; Barbosa Júnior et al., 2022; Guo et al., 2021). Of the 31 studies that were considered by Amarasingam et al. (2022), 84% used rotary-wing UAVs, 13% used fixed-wing UAVs and 5% used hybrid UAVs.

Fixed-wing UAVs resemble airplanes and feature fixed wings that generate lift through forward motion. They are commonly employed in large surveys due to their high speeds, extended flight time (50-90 minutes) and efficient energy consumption. However, their dependence on runways for take-off and landing restricts operational flexibility. Fixed-wing UAVs have been used in Brazil and Nicaragua over areas of 9 to 100 ha, for mapping sugarcane gap density to inform replanting strategies and crop management (de Souza et al., 2017; Luna and Lobo, 2016), and for height estimation for yield prediction (de Souza et al., 2017)

Rotary-wing UAVs are mostly represented by multi-rotor drones which generate lift through rotating blades. They are well suited to small-scale surveys requiring close-range inspections and high precision. Their reduced flight time (25-35 minutes), limited coverage, and payload capabilities restrict their usage in large-scale surveys. Multi-rotor UAVs have demonstrated success in capturing high resolution (1 – 13 cm) images for diverse applications, including for estimation of ground cover estimates (Duan et al., 2017), assessing growth in response to variable nitrogen rates (Sofonia et al., 2019), mapping mosaic virus (Moriya et al., 2017), estimating yield and cane quality (Sumesh et al., 2021; Chea et al., 2020) and for clonal selection in breeding (Natarajan et al., 2019) in Brazil, Australia and Thailand.

Hybrid UAVs combine the range and payload capacity of fixed-wing UAVs, with the take-off and landing capabilities of multi-rotor UAVs (Aktas et al., 2016; Pircher et al., 2017). They offer versatility for various operations but are hindered by their complex design and operation, as well as higher costs, limiting their widespread use. Mahachi et al. (2022) designed a hybrid UAV for sugarcane pest monitoring with a range of 97 m (1.5 hours flight time), though the system was untested.

Sensors

The aerial sensors for capturing crop characteristics and environmental data vary in their imaging modalities, ranging in precision from limited discrete bands to detailed spectral coverage (Amarasingam et al., 2022; Barbosa Júnior et al., 2022; Guo et al., 2021; Maes and Steppe, 2019).

RGB cameras measure reflectance in the spectral bands representing visible light (red, green and blue). Their low cost, ease of use, high spatial resolution and simplicity in terms of data

processing, have been beneficial for general aerial observations, establishing digital terrain and surface models, and estimating lodging extent and canopy height in sugarcane (de Souza et al., 2017; Duan et al., 2017; Li et al., 2021; Luna and Lobo, 2016; Som-ard et al., 2018; Sumesh et al., 2021; Yu et al., 2020). However, their limited spectral resolution (Nijland et al., 2014) lacks the information needed to inform crop phenotypic information for physiological traits, or pest and disease detection (Yang et al., 2017).

Multispectral sensors measure reflectance across several (typically four to six) broad or narrow spectral bands, which usually include red, green and blue, as well as the near infrared and red edge bands which are sensitive to small changes in chlorophyll content (Yao et al., 2019). They are one of the most widely used sensors in AP (Amarasingam et al., 2022; Yao et al., 2019), presumably due to their high spatial and spectral resolution. In sugarcane, they have been used for identifying high yielding genotypes and for screening of drought tolerance (Hoffman et al., 2024). They have also been used for detection of pathogen infestations such as white leaf disease (Sanseechan et al., 2019), for estimation of nutrients such as leaf nitrogen (Shendryk et al., 2020), determination of growth vigour (Akbarian et al., 2022) and for yield prediction and cane quality management (Chea et al., 2018; Cholula et al., 2020).

Hyperspectral sensors measure reflectance across the full spectrum (usually 400 – 1000 nm) in hundreds of narrow contiguous spectral bands (between 5-10 nm each), resulting in high-resolution spectral data with a high degree of radiometric accuracy (Amarasingam et al., 2022). (Moriya et al. (2017) demonstrated the capabilities of hyperspectral data to identify and map mosaic virus with high accuracy in sugarcane. Poudyal et al. (2022) showed some success in the use of hyperspectral imaging for clonal selection in sugarcane breeding. Due to the high costs of sensors, fewer studies have utilized hyperspectral data in sugarcane as compared to other sensors.

LiDAR (Light Detection and Ranging) sensors use laser pulses to precisely measure distances to target surfaces, providing high-resolution data characterized by dense point clouds and high spatial accuracy (Yao et al., 2019). This information is used to create detailed 3D model structures of crop canopies. Sofonia et al. (2019) compared the performance of LiDAR and multispectral imagery for determining sugarcane canopy height

across the growing season, and found that both systems performed similarly. Sofonia et al. (2019) also compared the two systems and found that they performed similarly in their prediction of sugarcane biomass. Shendryk et al. (2020) demonstrated the potential of LiDAR for predicting sugarcane biomass and leaf nitrogen content. While promising, the widespread use of LiDAR is hindered by its high cost, and challenges in processing large amounts of complex data.

Lastly, thermal sensors measure radiation emitted by crop canopies with a microbolometer in the long-wave infrared spectrum. Their estimates of relative surface temperature are used to inform crop growth monitoring and water stress detection (Yang et al., 2017). Hoffman et al. (2024) demonstrated the use of aerially captured thermal imagery for identifying high- and low-yielding genotypes, as well as for screening of drought tolerance. Basnayake, (2016), Chapman et al. (2014) and Natarajan et al. (2019) evaluated the use of UAV-derived thermal imagery for clonal selection in breeding, with some success. The effectiveness of thermal sensing is influenced by several challenges (Gonzalez-Dugo et al., 2012; Kelly et al., 2019; Mesas-Carrascosa et al., 2018). Atmospheric interference, such as variations in air temperature and humidity, can cause refraction and absorption of infrared radiation, leading to inaccuracies in thermal readings. Thermal loading from direct sunlight, depending on the sun's position relative to the UAV, can cause drift in the sensor's baseline calibration, further affecting measurement accuracy. Reflections from the soil surface, especially in areas with sparse canopy cover, can lead to overestimation of canopy temperatures. The comparatively lower resolution of thermal sensors, when compared to other sensor types, further complicates the accurate measurement of canopy temperature. These challenges necessitate careful calibration techniques and consideration of environmental factors to improve the reliability of thermal imagery for assessing plant health and water stress.

Software for image processing and analysis

Geospatial and image analysis tools are integral for both pre- and post-processing of aerial imagery. These software packages perform a series of processing steps specific to the image type under investigation.

The workflow begins with the acquisition of raw images from UAV sensors, which are calibrated to correct for sensor-specific distortions and environmental influences. For thermal imagery, calibration often involves the use of ground targets with known

temperature to adjust for sensor biases, where multispectral imagery often requires calibration using spectral boards with known reflectance values. Following calibration, the images are georeferenced, orthorectified (to correct for distortions caused by the camera's angle and terrain variations). and stitched to form an orthomosaic. This process relies on advanced positioning systems integrated into the UAV, such as Global Positioning Systems (GPS) for basic accuracy, Real-Time Kinematic (RTK) for real-time centimeter-level precision, and Post-Processed Kinematic (PPK) for post-flight corrections, which enhance the accuracy of stitching and the creation of a precise orthomosaic.

Feature identification (e.g. soil, green and senesced leaves) follows, involving extraction of relevant plant characteristics from the stitched image. Finally, vegetation indices are extracted and interpreted. Table 2.2 provides a summary of commonly used software packages used in AP to carry out many of these steps (Amarasingam et al., 2022).

Table 2.2. Details of image processing and analysis software packages commonly used in aerial phenotyping (AP).

Process	Software package	Advantages / disadvantages	Reference
Image processing	Pix4D Mapper	Powerful tool for creating high-resolution orthomosaic maps; facilitates creation of 3D models enabling volumetric analysis; customisation of process parameters possible in most cases; compatibility with most drone and camera platforms. Software is more costly than most other packages used in AP.	(Chea et al., 2020; Natarajan et al., 2019; Sofonia et al., 2019)
	ArcGIS Pro	Useful for spatial and GIS-based analyses. Not developed for image stitching or creation of spatial models. Specialised skills required to perform some tasks. High initial and licensing costs.	(Sumesh et al., 2021)
	ENVI	Allows detailed spectral analysis and extraction of band reflectance values. Not developed for drone image stitching. Hindered by complexity of use.	(Henry et al., 2017)
	Global Mapper	Compatible with various geospatial data formats, enabling precise vegetation index estimations. Lacks some advanced analysis capabilities.	(Sanseechan et al., 2019)
	OpenDroneMap	Open-source photogrammetry software package where source code can be accessed and modified. Supports various file formats for processing drone imagery, e.g. orthophoto generation, point cloud creation and 3D modelling of vegetation. Requires technical expertise in photogrammetry and in programming.	(Gill et al., 2022)
	Agisoft Metashape	Capable of producing accurate photogrammetric outputs such as orthomosaics, digital surface and 3D models. Limited open-source support and high costs.	(de Oliveira et al., 2022)
Image analysis	ArcGIS	Extensive geospatial analysis capabilities for accurate computation of vegetation indices. Complexity and high costs.	(Som-ard et al., 2018)
	QGIS	Open-source, with comparatively low costs for more sophisticated versions of the software. Useful for spatial analysis and visualization, and its functionality is enhanced by a wide range of plugins for applications in AP. However, it lacks advanced image processing capabilities commonly used in AP, and additional programming skills may be required for more specialized scripting and custom analysis.	(Villareal and Tongco, 2020)
	MATLAB	Enables custom analysis and advanced computations through programming. Extensive scripting and programming skills needed.	(Chea et al., 2020)
	ENVI	Capable of detailed spectral analysis and band value extraction.	(Henry et al., 2017)

Vegetation indices (VIs)

Vegetation indices are numerical values derived from mathematical combinations of spectral bands, which provide valuable information about crop health and vigour (Jones and Vaughan, 2010). Some commonly used VIs, particularly in sugarcane, are reported in Table 2.3. Studies done in sugarcane have evaluated the use of various VIs for characterising early vigour, detecting diseases, predicting cane quality and yield, and enhancing breeding efforts. Hoffman et al., 2024 reported that NDVI could be used as an indicator of early vigour to identify high-yielding genotypes in well-watered crops. Sanseechan et al. (2019) considered the use of 18 VIs for detecting white leaf disease and reported that VIs using NIR and red edge bands (NDRE and GNDVI particularly) showed the greatest predictive capacity Chea et al. (2018) evaluated the use of six aerially measured VIs (GNDVI, NDVI, RVI, Cigreen, CiRE and a simple ratio pigment index, SRPIb) for predicting cane quality parameters. The study reported that CiRE showed the strongest correlations with quality parameters Pol and CCS, though all of the VIs showed relatively high correlations with cane quality except for SRPIb. Furthermore, Natarajan et al. (2019) found that NDVI could be used in combination with other aerially measured traits (canopy height and cover) for enhancing clonal selection.

Table 2.3. Description of commonly used vegetation indices (VIs) in agricultural remote sensing (adapted from Amarasingam et al., 2022; Jones and Vaughan, 2010; Singels et al., 2021; White et al., 2012).

Index name or method	Index formula [1]	Relevant crop traits	Advantages / disadvantages	References
Difference Vegetation Index (DVI)	DVI = NIR – R	Chlorophyll and nitrogen content	Used to distinguish between plant and soil	(Jordan, 1969) Sugarcane: (Akbarian et al., 2022; Alemán-Montes et al., 2023; Amarasingam et al., 2022; Reyes-Trujillo et al., 2021; Simões and Rios do Amaral, 2023)
Ratio Vegetation Index (RVI)	RVI = NIR/R	Biomass, water, nitrogen	Partially corrects for variation in reflectance due to soil backgrounds. Prone to saturation in dense canopies.	(Birth and McVey, 1968) Sugarcane: (Amarasingam et al., 2022; Chea et al., 2020; Dengia et al., 2023; Li et al., 2022; Simões et al., 2005)
Normalized Difference Vegetation Index (NDVI)	NDVI = (NIR – R)/(NIR + R)	Vegetation cover, density and photosynthetic activity; Plant health, biomass, stress levels	Widely used indicator of crop cover and health. Better suited for early-stage crops as NDVI saturates in dense canopies & becomes less sensitive to small changes in chlorophyll content.	(Rouse Jr et al., 1974) Sugarcane: (Amarasingam et al., 2022; Bégué and Simoes, 2013; Chea et al., 2020; Khuimphukhieo et al., 2023; Li et al., 2022; Natarajan et al., 2019; Shendryk et al., 2020; Vasconcelos et al., 2023; Zhao et al., 2016)
Green DVI (GDVI)	GDVI = NIR - G	Vegetation cover, biomass and plant vigour, chlorophyll and nitrogen content, stress detection	Suggested to be less affected by atmospheric conditions as compared to NDVI. Limited chlorophyll sensitivity and lower sensitivity to vegetation stress as compared to NDVI.	(Tucker, 1979) Sugarcane: (Akbarian et al., 2022; Amarasingam et al., 2022; Dengia et al., 2023)
Green NDVI (GNDVI)	GNDVI = (NIR-G) /(NIR+G)	Vegetation cover, chlorophyll content, photosynthetic activity, moisture and nitrogen content of leaves	Better at higher LAI due to the higher saturation point of GDNVI; more sensitive to changes in chlorophyll content as compared to NDVI.	(Gitelson et al., 1996) Sugarcane: (Akbarian et al., 2022; Amarasingam et al., 2022; Chea et al., 2020; Dengia et al., 2023; Shendryk et al., 2020; Simões and Rios do Amaral, 2023)
Normalized Difference Red Edge (NDRE)	NDRE = (NIR – RE)/(NIR + RE)	Chlorophyll: Plant health, nitrogen levels, photosynthetic activity	Improved sensitivity to chlorophyll content and vegetation stress, and less affected by soil background variations, as compared to NDVI. Susceptible to atmospheric interference, requires narrow-band measurements in specialised sensors, less intuitive and requires careful interpretation due to high sensitivity.	Gitelson & Merzlyak (1994) Sugarcane: (Akbarian et al., 2020; Amarasingam et al., 2022; Dengia et al., 2023; Shendryk et al., 2020; Simões and Rios do Amaral, 2023)

Index name or method	Index formula	Relevant crop traits	Advantages / disadvantages	References
Enhanced Vegetation Index (EVI)	EVI = 2.5*(NIR - R) / (NIR + 6*R - 7.5*B + 1)	Chlorophyll, biomass, nitrogen	EVI is less affected by atmospheric and background interference; reduced saturation effects in dense canopies as compared to NDVI. Requires more complex multispectral band measurements and deeper understanding of correction factors for interpretation. Less established benchmarking as compared to NDVI.	(Huete et al., 2002) Sugarcane: (Dengia et al., 2023; Shendryk et al., 2020)
Soil-Adjusted Vegetation Index (SAVI)	SAVI = (1 + L) (N – R) / N+R+L)	Vegetation cover, Chlorophyll, biomass, photosynthetic activity Health and stress detection	SAVI reduces the influence of soil brightness, facilitating more accurate assessment of crops with varying soil backgrounds. Requires an adjustment factor (L) which can be difficult to estimate. Interpretation is more complex as compared to NDVI, requires more specialised sensing.	(Huete, 1988) Sugarcane: (Dengia et al., 2023; Li et al., 2022; Simões et al., 2005)
Chlorophyll Index – green (Cigreen)	Cigreen = (NIR/G) – 1	Chlorophyll Plant health, photosynthetic activity, stress detection	Sensitive to small variations in chlorophyll content. Not as widely used as other VIs.	(Gitelson et al., 2003) Sugarcane: (Chea et al., 2020)
Chlorophyll Index – red-edge (CiRE)	CiRE = (NIR/RE) - 1	Chlorophyll Plant health, photosynthetic activity, stress detection	Sensitive to changes in chlorophyll and vegetation structure overall. Enhanced sensitivity to atmospheric and background noise.	(Gitelson et al., 2003) Sugarcane: (Chea et al., 2020)
Canopy temperature (Tc)	Derived from FIR (thermal band)	Instantaneous transpiration, crop water status, biomass growth	Good indicator of crop water status, growth and yield. Difficult to estimate Tc; greatly influenced by changing environmental conditions, prone to large spatial variability, limited by spatial resolution of measurements.	(Blum et al., 1982; Chaudhuri et al., 1986; Jackson et al., 1981; Wanjura et al., 1984). Sugarcane: (Basnayake, 2016; Chapman et al., 2014; Inman-Bamber and De Jager, 1986; Khera and Sandhu, 1986; Pereira et al., 2020; Sinclair et al., 2004)

[1] The spectral bands used for estimation of VIs are red (R), green (G), blue (B), near infrared (NIR) and red-edge (RE).

Use of AP in crop improvement

AP has demonstrated considerable potential for enhancing breeding efforts by: (1) rapidly and reliably estimating trait values for large populations, thereby enhancing selection intensity and accuracy; (2) accelerating breeding cycle times through expedited screening procedures; (3) identifying genotypic variation in traits to be exploited in breeding (Araus et al., 2018). Despite its potential, there remains a relatively limited number of studies investigating the use of AP in sugarcane breeding as compared to other crops.

Most recently, Khuimphukhieo et al. (2023) assessed the effectiveness of an AP system equipped with simple RGB camera for assessing sugarcane yield. While the study showed a good agreement between cane quality (pol%) and yield measured at harvest, with canopy cover, height and VIs derived from aerial images, the dataset was limited due to the small population (seven genotypes). Poudyal et al. (2022) evaluated the use of hyperspectral imaging for yield prediction and genotypic selection in final-stage sugarcane breeding trials (9-13 genotypes). Although the study reported high accuracy in predicting yield and sucrose content from aerially measured data, only two out of five superior genotypes were correctly identified with AP, which is likely insufficient for breeding purposes. Natarajan et al. (2019) evaluated an AP system for screening canopy cover, height, NDVI and Tc in larger populations (40 – 2134 genotypes) than those previously reported. The study showed promising results for breeding applications, demonstrating high heritability and strong genetic correlations for aerially measured traits with yield. Basnayake, (2016) evaluated thermal sensing for predicting yield in a breeding population of 40 genotypes. While the study showed promise for the use of AP in breeding, Tc was found to be highly variable and influenced by environmental factors. Lastly, Chapman et al. (2014) implemented thermal sensing of 40 clones using AP, observing little variation in Tc amongst clones, across drought and irrigated treatments.

Overall, these studies highlight the potential of AP for breeding applications, but also allude to several key constraints hindering its widespread implementation. Rigorous testing of AP systems in breeding trials is needed to address the controlled nature and limited genetic diversity of most experiments, and to consider realistic GxExM interactions. Additionally, there is a need to enhance understanding of the breeding target, such as drought tolerance in sugarcane, and to identify candidate traits with sufficient genetic variability and heritability

(Jackson et al., 1996). Further advancements are also needed in sensor and platform technology, particularly regarding thermal imaging, where camera resolution remains a challenge (Basnayake, 2016; Chapman et al., 2014; Natarajan et al., 2019). Lastly, big data management and interpretation remains a challenge.

2.5 Knowledge gaps and research opportunities

One of the major challenges in conventional sugarcane breeding is the low broad-sense heritability of cane yield observed in early-stage selection trials with large populations. This low heritability suggests that the variation in cane yield is not predominantly genetically driven, and that the performance of genotypes in early-stage trials is not strongly predictive of their future performance. A better understanding of the underlying causes of this variation, particularly in yield-promoting traits such as g_s and FIPAR, is crucial. These traits are important contributors to yield under varying water regimes, and their influence on yield must be better understood to improve selection accuracy. The challenge lies in the accurate measurement of these traits across different developmental stages, which is particularly difficult in large populations. UAV-assisted phenotyping of indirect traits offers a promising approach for enhancing genetic gain through more precise indirect selection, provided that these traits are influential in determining yield. Further research, however, is required to fully realize this potential.

The physiological mechanisms governing radiation capture and conversion efficiency, and plant-water relations, have been extensively described in literature. Despite this, some uncertainties exist regarding genotypic variation and trait links with yield, particularly for RUE. Difficulties in measuring whole-plant photosynthesis and RUE are well documented. The underlying traits, FIPAR and g_s, show significant genotypic variation and strong links with yield in most cases, which holds promise for crop improvement. Remote sensing measurements of crop reflectance and radiation emittance offer potential for early identification of promising genotypes in sugarcane, yet research in this area remains limited.

UAV-assisted measurement of physiological traits that are reliable predictors of crop development, growth and water use could be more effective than direct measurement of final yield in the early breeding stages. For investigating the use of AP in breeding, multi-rotor and hybrid UAVs coupled with RGB cameras, multispectral and thermal sensors

emerge as feasible options for large-scale phenotyping in breeding trials, offering precision, relative ease of use and valuable insights regarding crop vigour and water use. There is also opportunity for hyperspectral and LiDAR sensing to enhance breeding, though their relative cost and data processing challenges should be considered.

Despite the potential for physiological screening in crop improvement, a clear strategy for integrating these traits in breeding remains unclear. There is need to establish relationships between ground and aerial measurements under breeding conditions, in order to identify the optimal conditions under which genetic control of these traits correlates strongly with yield. This will elucidate information regarding genotypic variation and heritability of traits in large breeding populations. Furthermore, there is need to report on the practical considerations or challenges associated with implementing AP in breeding, as this is not documented in literature.

3. PILOT STUDY: DEVELOPMENT OF AERIAL PHENOTYPING PROCEDURE

3.1 Introduction

The first experimental phase of the study comprised a pilot trial conducted in a rain shelter facility, where two genotypes were gown under well-watered (WW) and water deficit (WD) conditions. The aim of this trial was to develop preliminary correlations between vegetation spectral information from aerial imagery, and ground measurements of plant physiological parameters.

The specific objectives were to:

1. Assess whether aerially measured traits, Normalized Difference Vegetation Index (NDVI) and canopy temperature (Tc), could be used to infer genotypic differences in ground measured traits, green canopy cover (FIPAR) and stomatal conductance (g_s) under WW and WD conditions.
2. Develop preliminary aerial phenotyping (AP) procedures for estimating FIPAR and g_s from NDVI and Tc, respectively.

3.2 Methodology

3.2.1 Trial design and operations

The study was conducted at the SASRI Mount Edgecombe rain shelter facility (29°42’40”S, 31°02’35”E). Commercial sugarcane varieties NCo376 and N19 were chosen as they have shown significant varietal differences in g_s under well-watered conditions (Hoffman, 2016). Varieties were planted on 13 October 2017, within a trial comprising four unreplicated plots of six rows each, 7.7 m in length with 1.25 m row-spacing, with one plot per variety x water treatment (Figure 3.1, Figure 3.2). The trial was monitored for approximately eight months until harvest on 27 June 2018.

Fertiliser was applied according to standard recommendations to ensure nutrient sufficiency. Water was applied through a sub-surface drip irrigation system (emitters delivering 1.55 mm h^{-1}, spaced at 1.25 m x 0.6 m). Soil water status (SWS) was estimated with Aquacheck capacitance probes and used to inform irrigation scheduling. All plots (WW and WD) were well-watered and received the same irrigation amounts during the early stages of crop growth (up until 130 days after planting, DAP) to ensure stress free growth. Thereafter, mostly daily irrigation amounts of between 2 mm and 6 mm were applied in WW plots as required to

maintain SWS above stress point (SP, taken as 50% of the difference between field capacity, FC, and permanent wilting point, PWP). Water deficit was imposed in WD plots by withholding irrigation during two periods of four and eleven weeks respectively, with a recovery period of three weeks in between, during which irrigation was applied. During stress periods, water deficit was achieved with the rain shelter (shown in Figure 3.2) which was driven by cables pulled by rotors on either end. Movement was automatically activated by moisture sensors, causing the facility to close immediately when rainfall was detected.

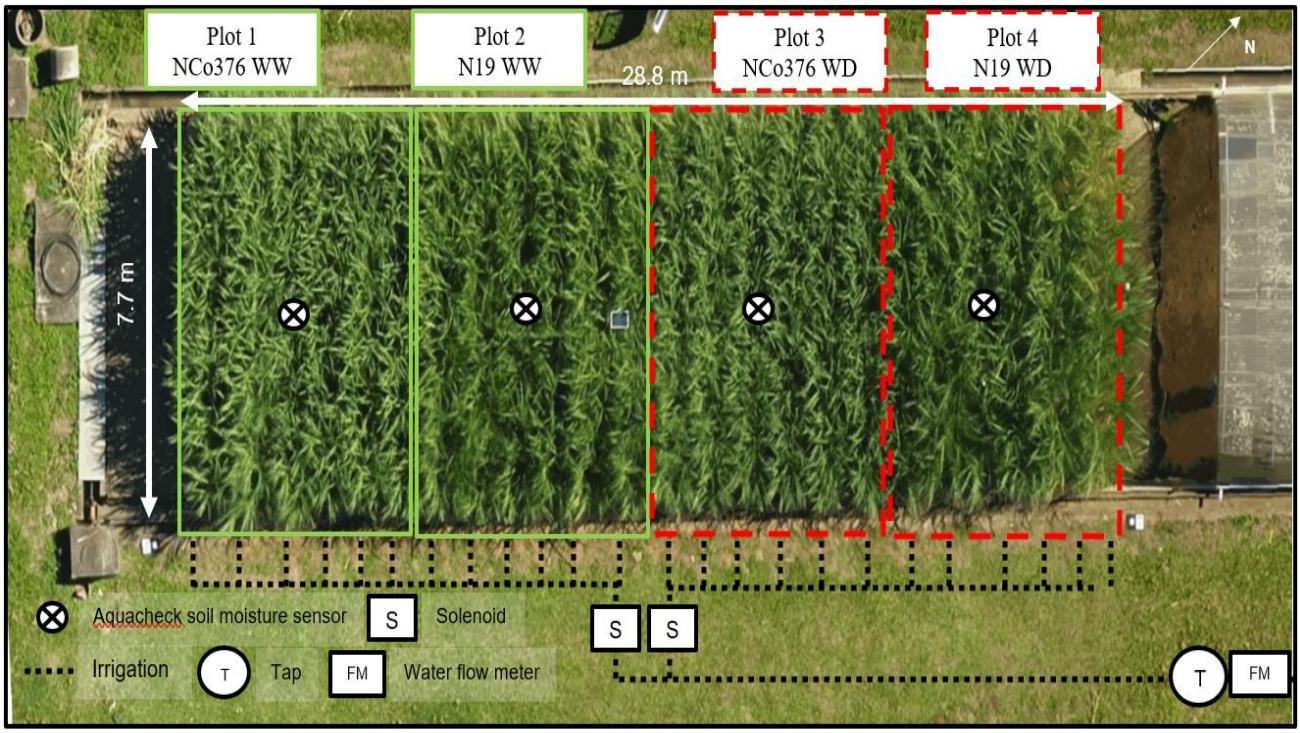

Figure 3.1. Rain shelter pilot trial comprising four treatments, consisting of two varieties (NCo376 and N19) grown under well-watered (WW, plots 1 and 2) and water deficit (WD, plots 3 and 4) conditions. The image was captured on 8 May 2018, at a crop age of seven months.

Figure 3.2. Rain shelter trial before (above) and after (below) the imposition of water stress in the water deficit treatment plots. The images were captured at a crop age of four and eight months, respectively.

Soil characterisation

The soil in the rain shelter was described previously by Eksteen et al. (2014). Briefly, it comprises soil originating from an A horizon of a Rhodic ferrasol (Micheli et al., 2006) or Oxisol (USDA, Soil Survey Staff, 1999). The soil was packed to a depth of 1 m atop plastic sheeting which lined the bottom of the rain shelter facility. Soil textural properties (clay, silt and sand of 10.7%, 4.8% and 85%, respectively) were taken as those reported by Ngxaliwe, (2014), which were determined following the method of Bouyoucos, (1962).

3.2.2 Ground measurements

Weather data

Daily average solar radiation (SRAD, W m^{-2}), temperature (°C), relative humidity (RH, %), rainfall (mm), wind speed (m s^{-1}) and vapour pressure deficit (VPD, kPa) were recorded from samples taken at ten second intervals using an automatic weather station located approximately 20 m from the trial site. Daily sugarcane reference evapotranspiration data (Ecref, mm d^{-1}) were calculated from hourly weather data using the Penman-Monteith equation (McGlinchey and Inman-Bamber, 1996).

Soil water content

SWS index was measured with Aquacheck capacitance-based continuous logging probes (model S/S 800mm HD, Aquacheck (Pty) Ltd, Durbanville, South Africa), installed vertically, 15 cm adjacent to drip emitters situated in the middle of the third row of each plot.

The probe readings, measured at 10 cm increments down to 80 cm depth, were calibrated against gravimetrically determined volumetric soil water content (SWC, %) (R^2 = 0.89, shown in Figure 3.3). SWC was measured at various intervals throughout the crop cycle, from 3 to 8 months of crop age. Soil samples were taken 30 cm from the probes at 20 cm depth increments, to the lowest depth possible with the manual auger, and weighed for wet and dry mass before and after drying, until constant dry mass was reached. Gravimetric (SWCg, %) and volumetric SWC were calculated as:

$$SWCg = \frac{Mass\ of\ wet\ soil - mass\ of\ dry\ soil}{Mass\ of\ dry\ soil} * 100 \quad \text{(Equation 10)}$$

$$SWC = SWCg * BD \quad \text{(Equation 11)}$$

where bulk density (BD, g cm^{-3}) was determined from the dry mass of core soil samples with known volume.

FC was taken as the SWC a day after thorough wetting of the soil, and PWP as the SWC in WD plots after all available water was extracted, respectively. FC and PWP for the WD plots were taken as 33 and 22.5%, respectively, and SP as 27.8%.

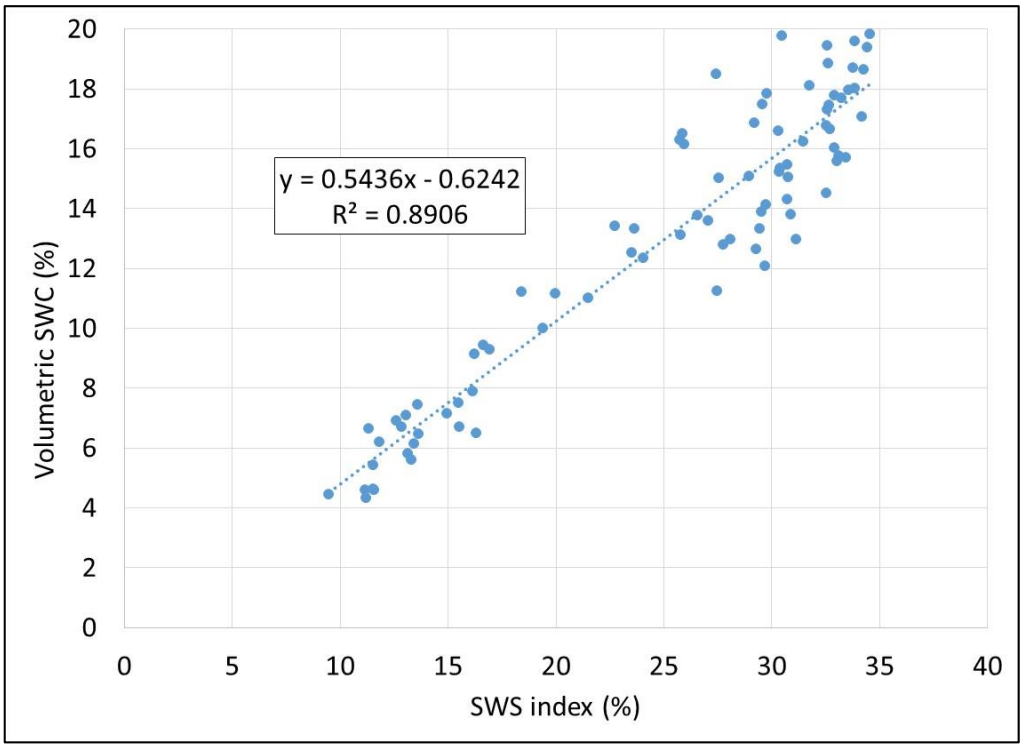

Figure 3.3. Relationship between volumetric soil water content (SWC, determined gravimetrically) and soil water status (SWS) index, determined from Aquacheck capacitance probes used in the rain shelter trial.

Phenology

Phenology measurements were used as a non-destructive measurement of water stress effects on crop growth and development. Green leaf number (GL), stalk population (SPOP) and stalk height (SH, up to the top visible dewlap) were measured approximately every two weeks on 20 tillers in the third and fourth rows of each plot, starting at a crop age of three months.

Radiation interception

The extent of green canopy cover (defined as the fraction of ground area covered by green leaves) was estimated from measurements of fractional interception of photosynthetic active radiation (PAR) by the canopy (FIPAR). A ceptometer (AccuPAR model LP-80, Decagon devices, Washington, USA) was used to measure the amount of PAR intercepted by the green leaf canopy every two weeks, starting at a crop age of three months. Incoming photosynthetically active radiation (PARi) was measured once outside each plot. Ten measurements of reflected PAR (PARr) and transmitted PAR (PARt) were taken above and

below the green canopy, respectively. FIPAR was estimated as described by Singels et al. (2018):

$$\text{FIPAR} = \frac{\text{PARi} - \text{PARt} - \text{PARr}}{\text{PARi}} \quad \text{(Equation 12)}$$

Leaf level traits

Leaf level g_s was measured approximately every two weeks starting at a crop age of four months, and on UAV flight dates to coincide with aerial measurements of crop reflectance. Measurements were carried out between 10:00 and 13:00 on three well-lit topmost leaves in rows three and four of each plot, using the CIRAS-3 photosynthesis system (PP systems, Hitchin, Herts, UK). Data were filtered to exclude negative intercellular CO_2 concentration readings, and relative humidity readings lower than 40 and exceeding 90%. Leaf temperature (Tleaf) was also measured concurrently with the handheld infrared thermometer (Optris MS plus, SRP Control Systems Ltd).

Yield components

Destructive sampling of biomass components was carried out at harvest on 27 June 2018. Stalks from rows three and four of each plot were manually harvested and weighed to determine stalk fresh mass yield (SFM, kg m^{-2}). A sub-sample of 12 stalks was collected from each plot and analysed by the SASRI mill-room for stalk composition (fibre, sucrose and non-sucrose contents) and for dry matter content (DM, %) according to established methods. Sub-samples were weighed for fresh mass, shredded in a blender, filtered, and juice samples assessed with a polarimeter and refractometer to determine pol and brix% respectively (Schoonees-Muir BM et al., 2009), before being dried in an oven at 80°C to constant mass and weighed again for dry weight to determine DM. SDM (kg m^{-2}) was calculated as the product of SFM and DM.

Stalks from a 2 m section of rows two and five were cut at the base and total above-ground fresh biomass (kg m^{-2}) and stalk population was recorded. Each sample was divided into green and senesced leaves, millable stalk and meristem, and weighed for fresh mass prior to being dried in an oven at 80°C to constant mass, and weighed again for dry weight to determine DM of the respective components.

Additionally, three stalks from rows two and five were used to measure green leaf area (with LI-3000C scanning head coupled to the LI-3050C desktop accessory), used to GLAI as the product of green leaf area per stalk, and stalk population.

3.2.3 Aerial imaging

Crop reflectance in the visible (RGB), near infrared (NIR) and thermal bands were captured on six measurement days (Table 3.1): (1) once prior to the onset of water stress; (2) twice during the first stress event; (3) once during the recovery period; (4) twice during the second stress event. The weather conditions for these dates are given in the Appendix (Table 8.1 and Table 8.2).

Prior to each measurement date, the trial was marked with four highly visible ground control points (GCPs) located at the corners of the trial. In two separate flights per measurement date, a single image of the trial was captured with a DJI Phantom 4 drone with (1) standard FC330 RGB camera and Sentera Precision NDVI single sensor (Sentera, Minneapolis, MN, USA); (2) FLIR Vue Pro thermal camera (336, 35° x 27° FOV, 9 mm, 9 Hz; FLIR Systems, Inc., Wilsonville, USA).

The crop canopy and water status on flight measurement days were quantified in terms of FIPAR and a crop water satisfaction index (CWSI). This was done to evaluate the trial data for different stages of crop development and water status. CWSI was calculated from relative available soil water content (RASWC) for each treatment plot, following the soil water deficit factor used in Ceres models (Jones and Kiniry, 1986):

$$RASWC = \frac{SWC-PWP}{FC-PWP} \quad \text{(Equation 13)}$$

$$CWSI = 2\,RASWC \quad \text{(Equation 14)}$$

Flights were categorised according to the CWSI as high (H, CWSI $\geq$ 0.8), medium (M, 0.4< CWSI < 0.8) or low (L, CWSI $\leq$ 0.4) (corresponding to low, medium and high levels of stress, respectively). Similarly, flights were categorised as having partial (FIPAR < 0.8) or full (FIPAR $\geq$ 0.8) canopy cover.

Table 3.1. Details of drone flights carried out in the rain shelter trial to capture visual (RGB), near infrared (NIR) and thermal imagery. Six flights were carried out over the course of the crop cycle (days after planting, DAP). For each flight, the average canopy cover (FIPAR) values were categorized as partial (P) or full (F), and the crop water satisfaction index (CWSI) values were categorized as low (L), medium (M) or high (H). For each flight, the time of capture and spatial resolution of images are given.

Flight	**Date (DAP)**	**FIPAR**				**CWSI**				**Time of flight**			**Spatial resolution (cm)**		
	Treatment:	NCo376 WW	N19 WW	NCo376 WD	N19 WD	NCo376 WW	N19 WW	NCo376 WD	N19 WD	RGB	NIR	Thermal	RGB	NIR	Thermal
1	12 Feb 18 (122)	0.74 (P)	0.68 (P)	0.81 (F)	0.76 (P)	1.00 (H)	1.00 (H)	1.00 (H)	1.00 (H)	10:47	10:47	13:23	3.1	6.8	14.7
2	9 Mar 18 (147)	0.86 (F)	0.73 (P)	0.85 (F)	0.82 (F)	1.00 (H)	1.00 (H)	1.00 (H)	0.80 (H)	10:44	10:44	13:41	1.9	4.3	15.1
3	19 Mar 18 (157)	0.88 (F)	0.84 (F)	0.87 (F)	0.83 (F)	1.00 (H)	1.00 (H)	0.80 (H)	0.41 (M)	11:03	11:03	12:56	2.3	4.6	15.0
4	12 Apr 18 (181)	0.90 (F)	0.89 (F)	0.88 (F)	0.84 (F)	1.00 (H)	1.00 (H)	1.00 (H)	1.00 (H)	10:16	10:16	13:08	2.1	3.1	14.5
5	8 May 18 (207)	0.91 (F)	0.91 (F)	0.89 (F)	0.87 (F)	1.00 (H)	1.00 (H)	0.98 (H)	0.73 (M)	10:55	10:55	13:50	2.1	4.6	15.1
6	1 Jun 18 (231)	0.91 (F)	0.91 (F)	0.87 (F)	0.84 (F)	1.00 (H)	1.00 (H)	0.27 (L)	0.08 (L)	11:44	11:44	13:49	2.1	4.6	14.5
	Seasonal average	0.87	0.85	0.86	0.83	1.95	2.11	1.22	1.02	-	-	-	-	-	-

Image processing and data analysis

Visual (RGB) and NIR imagery

The Sentera NIR imagery were pre-processed to isolate reflectance data within specific spectral bands, following recommended procedures (Sentera Documentation, 2017). Briefly, the camera measures reflectance in two overlapping channels: (1) both the red (575-675 nm) and NIR (800-875 nm) regions; (2) NIR region only. Using the QGIS software package (v2.18.1; Free Software Inc, Boston, MA, USA), NIR and red band isolation was done to mitigate the effects of overlapping (crosstalk) measurement of spectral response in both bands:

$$\text{Red} = 1.0 * \text{DNch1} - 1.012 * \text{DNch2} \quad \text{(Equation 15)}$$

$$\text{NIR} = 6.403 * DNch2 - 0.412 * DNch1 \quad \text{(Equation 16)}$$

where DNch1 and DNch2 are the digital numbers of channels 1 and 2, respectively.

Spectral response data was also corrected for unequal irradiance in the RED and NIR bands, where the irradiance of the red band was assumed to be 1.5x larger than that of the NIR band:

$$\text{NIR} = 1.5 * (6.403 * DNch2 - 0.412 * DNch1) \quad \text{(Equation 17)}$$

All RGB and NIR images were geo-rectified in the ArcGIS® (v10.1; ESRI, Redlands, CA, USA) software package using the GCPs (georeferenced using Trimble R4 PPK GNSS system, with vertical accuracy of < 15 mm and horizontal accuracy of < 8 mm).

For computation of the Normalized Difference Vegetation Index (NDVI, Rouse Jr et al., 1974), images were first digitised to exclude edge effects in plots (two outer cane rows and 1 m from the edges of rows). Plot average NDVI values were calculated using the zonal statistics function in the ArcGIS software package.

$$\text{NDVI} = \frac{\text{NIR}-\text{RED}}{\text{NIR}+\text{RED}} \quad \text{(Equation 18)}$$

Thermal imagery

The FLIR Vue Pro camera images provided raw DN (digital number) values as the camera is not radiometrically calibrated. To estimate surface temperature values from thermal imagery, a patch of bare soil and a body of water next to the trial were used as reference points (Figure 3.4). Ground readings of surface temperature were taken with a handheld infrared thermometer (Optris MS, SRP Control Systems Ltd.) for the bare soil and water bath were compared to the mean DN value for the two objects, and used to derive flight-specific calibration functions (Table 3.2) in a similar approach to that of Kelly et al. (2019).

Aerially measured Tc was estimated from pixels within the net plot area (Figure 3.4). The mean Tc value minus one standard deviation (equating to the 16th percentile of a normal distribution) was used to calculate a representative Tc value for each plot. This was done to exclude soil pixels from the analysis, which were expected to be hotter than green leaf material. Tc values were expressed as the difference between WD and WW treatments (ΔTc).

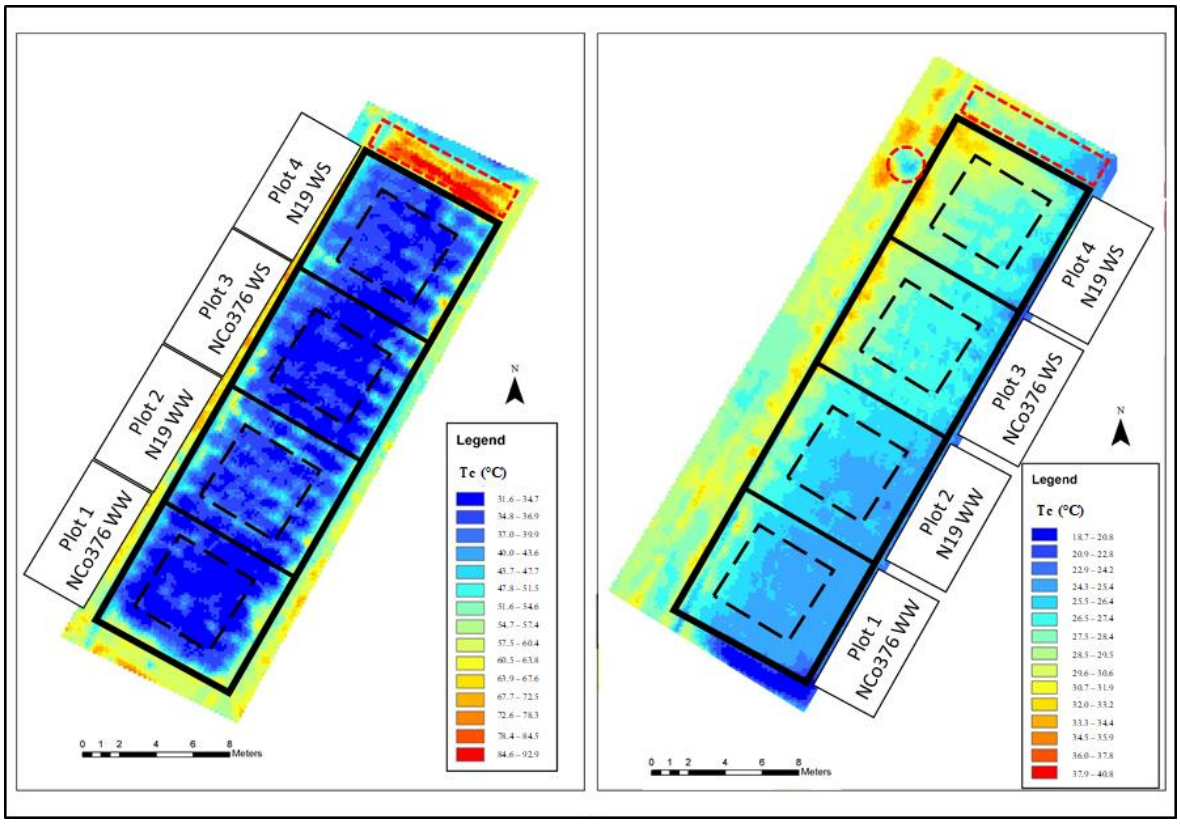

Figure 3.4. Thermal images of the rain shelter trial captured during the first (left) and sixth (right) flights. The trial area is demarcated by the solid black line while the net sample areas for calculating plot statistics for the different treatments are indicated by dashed lines. Reference bare soil (both images) and water bath (right only) were used as temperature targets (indicated by a red rectangle and circle, respectively) for calibration.

Table 3.2. Temperature (˚C) of a soil and water bath reference measured with a handheld infrared thermometer, as compared to soil and water bath digital number (DN) measured with an aerial thermal camera. Air temperature at the time of the flight, as well as flight-specific equations used to convert digital numbers (DN) to temperature values, are shown.

Flight	Soil temp	Soil DN	Water bath temp	Water bath DN	Air temp	Slope	Intercept	R^2
1	58.9	9214.2	-	-	26.6	-	-	-
2	55.5	8879.0	25.6	8517.8	25.9	0.083	679.4	-
3	52.5	8628.8	29.5	8474.8	27.8	0.149	1236.4	-
4	30.6	8365.2	26.5	8290.6	23.4	0.055	428.9	-
5	31.0	8587.7	27.8	8508.2	26.4	0.040	314.7	-
6	30.2	8400.0	26.9	8294.8	27.5	0.031	232.2	-
Pooled dataset	-	-	-	-		0.041	-311.4	0.75

3.2.4 Statistical analyses

Datasets for individual traits were tested for normality using the Shapiro-Wilk test. Statistical significance between varieties or water treatments could not be tested due to lack of replication within the trial design.

3.2.5 Trait correlations

Trial data were used to calculate the phenotypic (Pearson correlation coefficient, r) correlations between the following traits for individual measurement days: (1) FIPAR vs. NDVI; (2) g_s vs. Tleaf and Tc; (3) g_s expressed as the ratio between WD and WW values for each genotype (g_s*), vs. Tleaf and Tc expressed as the difference between WD and WW values for each genotype (ΔTleaf and ΔTc, respectively).

3.3 Results

3.3.1 Weather data

Weather data for the trial period are shown in Figure 3.5. Briefly, Tmax and Tmin ranged from 18.1 to 34.8 °C, and 9.3 to 22.7 °C respectively, and the average Tmin value of 17.4 °C was above the base temperature required for phenological development (Singels et al., 2018). Average SRAD showed a general decline over time, from the pre-stress period (18.1 MJ m^{-2} d^{-1}) to the end of the second stress event (10.8 MJ m^{-2} d^{-1}).

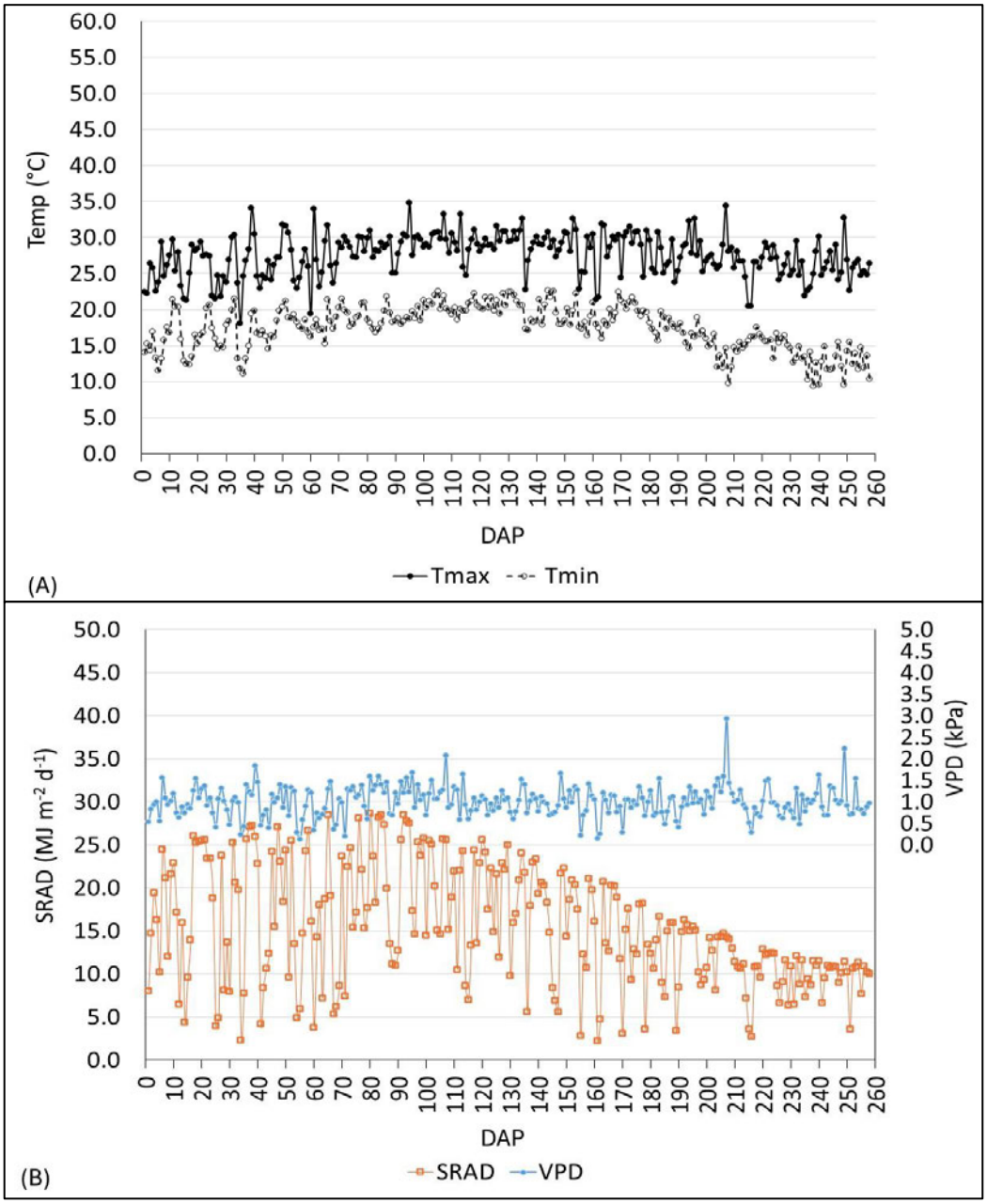

Figure 3.5. (A) Daily maximum (Tmax) and minimum (Tmin) air temperatures; (B) Daily solar radiation (SRAD) and daily vapour pressure deficit (VPD), measured over time (days after planting, DAP) in the rain shelter trial.

3.3.2 Crop water use

Profile average SWC for the four treatment plots is shown in Figure 3.6. All plots were well-watered and received the same irrigation amounts up until 130 DAP to ensure stress free growth during the early stages of crop development. Thereafter, the WW plots were kept well irrigated and maintained SWC above 80% of plant available water content. Irrigation was withheld in WD plots throughout the first stress event at 130 to 160 DAP, during which N19 used approximately 31% more water than NCo376. By the end of the stress phase, NCo376 and N19 reached medium CWSI levels of 0.79 and 0.56, respectively. Water stress was alleviated thereafter with irrigation applied during the recovery period from 161 to 180 DAP. In the second stress event lasting until harvest at 257 DAP, the difference in soil water extraction between the two WD plots was less pronounced compared to the initial stress event, when N19 extracted 10% more water than NCo376. Both varieties reached low CWSI levels of 0.26 and 0.15 for NCo376 and N19, respectively.

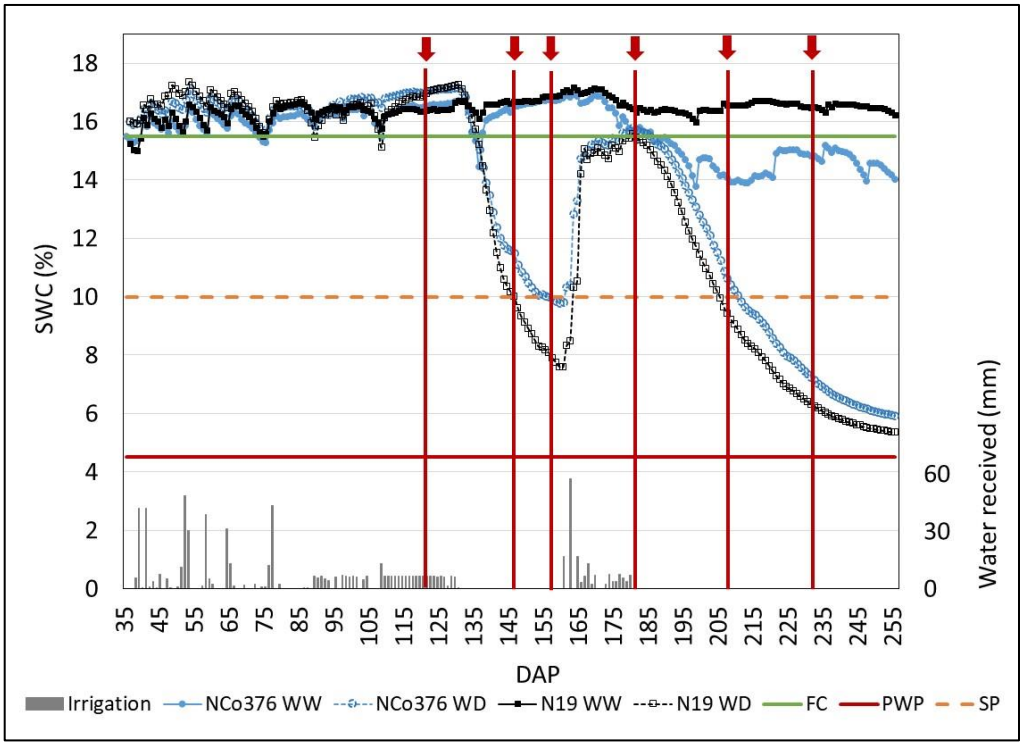

Figure 3.6. Profile average volumetric soil water content (SWC) measured over time (days after planting, DAP) with Aquacheck capacitance probes for varieties NCo376 and N19, which were grown under well-watered (WW) and water deficit (WD) conditions. The secondary axis shows water received via irrigation in WD plots. Green, orange and red lines represent field capacity (FC), stress point (SP) and permanent wilting point (PWP), respectively. Red arrows and vertical lines represent dates on which drone flights were conducted.

3.3.3 Crop growth

Phenology

Crop phenology (GL, SH and SPOP) data over time are shown in the Appendix (Figure 8.1, Figure 8.2 and Figure 8.3). Initially, both WD treatments showed similar GL prior to the imposition of stress. Thereafter, NCo376 appeared to cope better with water stress during the first event as it showed a smaller decrease (21%) in GL as compared to N19 (43%). SH appeared unaffected by initial water stress, but severe stress in the second stress period led to a more pronounced reduction in SH for N19 (10%) as compared to NCo376 (< 2%). Throughout the trial, SPOP appeared not to be affected by water stress. Furthermore, both WD treatments showed no visible green leaves at harvest.

Yield components

Biomass components data measured at harvest are shown in the Appendix (Table 8.3). Water stress reduced above-ground dry biomass (ADM) and SDM in N19 by 41 and 35%, respectively, while no reduction was found for NCo376. Both varieties showed a reduction in GLAI of approximately 76% in response to stress.

3.3.4 Trait correlations

FIPAR from NDVI

FIPAR and NDVI measured over time is shown in Figure 3.7. Initially, NCo376 WW showed approximately 25% higher FIPAR compared to N19 WW until 145 DAP. Thereafter, both WW treatments showed similar FIPAR. Similarly, NCo376 WW also maintained slightly higher NDVI (~5%) than N19 up until 147 DAP, after which no marked difference was observed between the two treatments.

For the WD treatments, similar FIPAR was observed in both varieties before the onset of water stress. Throughout the first stress period, recovery phase and second stress event, NCo376 WD maintained slightly higher FIPAR (~5%) compared to N19, with NDVI also showing a similar trend.

FIPAR and NDVI correlated significantly under partial and full canopy, for well-watered and mild stress conditions (Figure 3.8). However, the range in NDVI and FIPAR values was

limited, and can be improved with earlier measurements to reveal more about early vigour. Moreover, the relationship breaks down when considering the two outlying points corresponding to the WD treatments of the last flight, when CWSI was low.

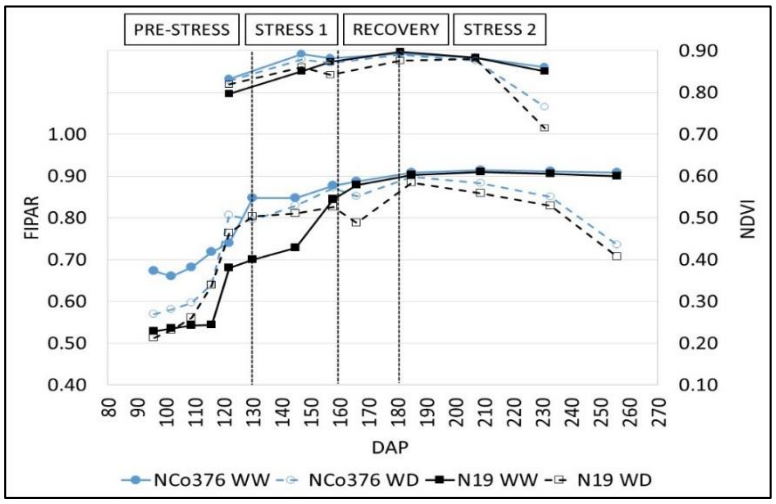

Figure 3.7. Fractional interception of photosynthetically active radiation (FIPAR, round markers) and Normalized Difference Vegetation Index (NDVI, square markers) measured over time (days after planting, DAP) for two varieties (NCo376 and N19) grown under well-watered (WW) and water deficit (WD) conditions. Stress and recovery events indicate periods during which irrigation was withheld and re-applied in WD plots, respectively.

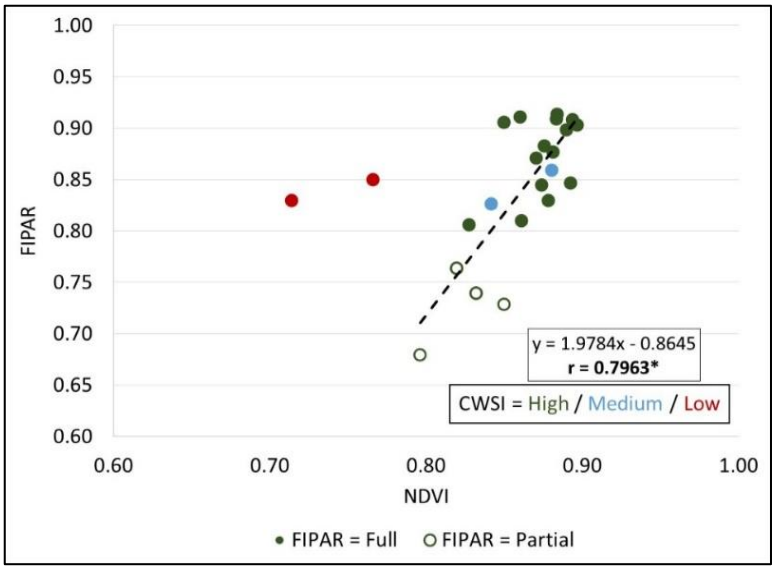

Figure 3.8. Relationship between fractional interception of PAR (FIPAR) and normalized difference vegetation index (NDVI) measured over several flights in the rain shelter trial. The data were categorised according to crop canopy cover (partial or full) and a crop water satisfaction index (high, medium or low). The significant correlation (at p = 0.05, shown in bold and indicated with an asterisk) is for partial and fully canopied crops under high and medium CWSI.

Leaf traits from canopy temperature

Measurements of g_s, Tleaf and Tc, as well as their relative values (g_s* ΔTleaf and ΔTc) over time, are shown in Figure 3.9 and Figure 3.10. NCo376 generally appeared to cope better with water stress than N19, maintaining higher g_s (25%) and g_s* (30%) during the initial stress period. Under these mild water stress conditions, Tleaf and Tc both showed small temperature differences (~ 0.4 °C) between NCo376 WD and N19 WD. As stress progressed during the second stress event, Tleaf and Tc showed larger temperature differences between water treatments (up to 4 °C, and 2 °C, respectively) rather than between varieties, as the varieties showed similar g_s under severe stress conditions.

When considering the relationships between ground and aerially measured traits, the data showed that g_s* and ΔTc correlated significantly, although obvious outliers are present (Figure 3.11). Closer investigation reveals statistically non-significant correlations between g_s and Tc, and between Tleaf and Tc for flights 1, 2 and 4 (Table 3.3). This suggests that Tc could not accurately distinguish small treatment differences in g_s and Tleaf when the crop was well-watered. This may in part be due to unsuccessful elimination of soil and senesced-leaf pixels from the statistical analysis. When data for these flights were excluded from the analysis, the relationships between g_s* with ΔTc improved marginally, while the correlation of g_s and Tleaf with Tc improved markedly (Table 3.3).

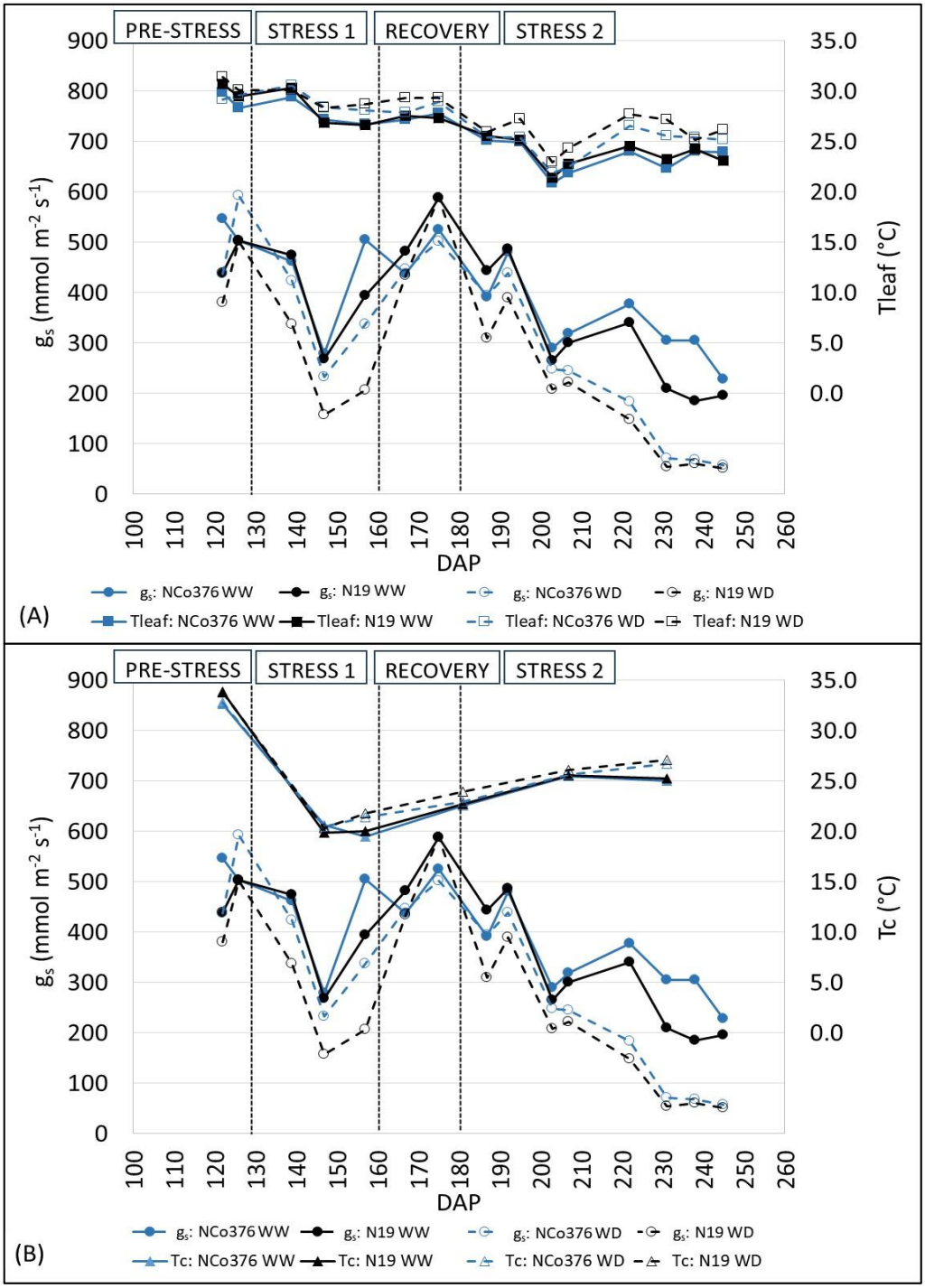

Figure 3.9. Measurements of (A) Stomatal conductance (g_s) and leaf temperature (Tleaf), and (B) g_s and canopy temperature (Tc), conducted over time (days after planting, DAP) for varieties NCo376 and N19, grown under well-watered (WW) and water deficit (WD) conditions. Stress and recovery events indicate periods during which irrigation was withheld and re-applied in WD plots, respectively.

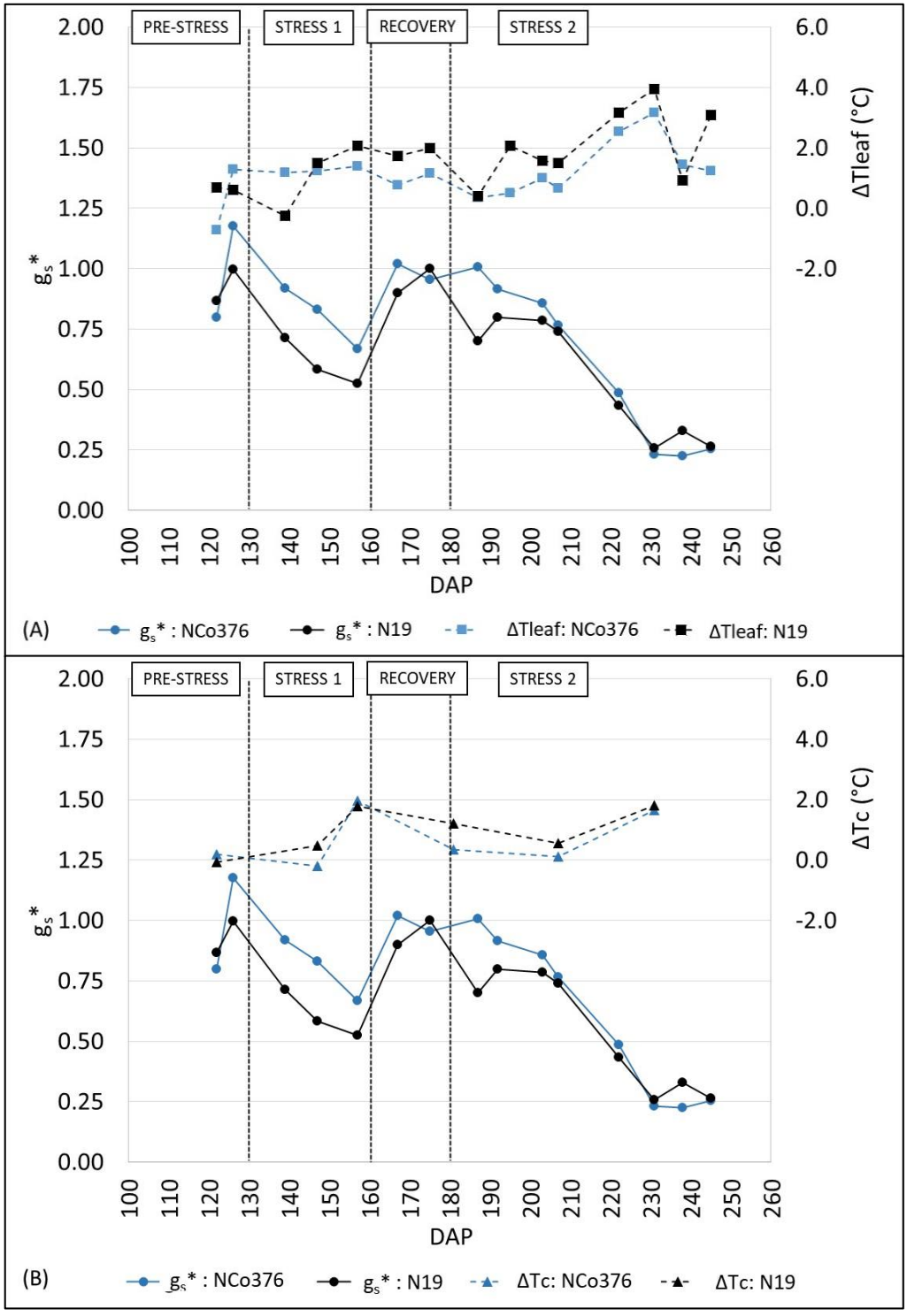

Figure 3.10. (A) Stomatal conductance, expressed as the ratio between water deficit (WD) and well-watered (WW) treatments (g_s*) and leaf temperature, expressed as the difference between WD and WW treatments (ΔTleaf); (B) g_s* and canopy temperature, expressed as the difference between WD and WW treatments (ΔTc), measured over time (days after planting, DAP) for varieties NCo376 and N19. Stress and recovery events indicate periods during which irrigation was withheld and re-applied in WD plots, respectively.

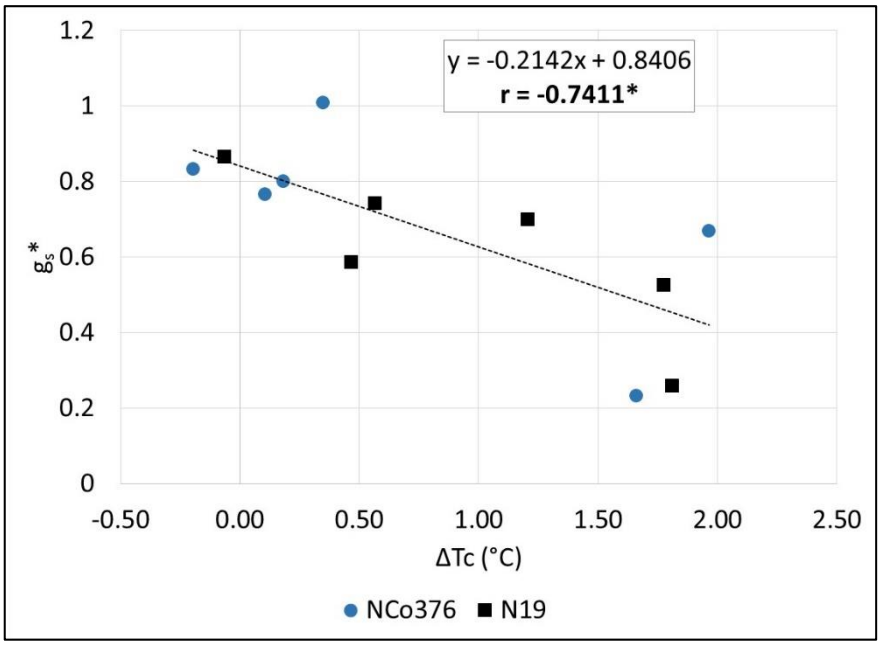

Figure 3.11. Relationship between stomatal conductance, expressed as the ratio between water deficit (WD) and well-watered (WW) treatments (g_s*), and canopy temperature, expressed as the difference between WD and WW values (ΔTc) for two varieties (NCo376 and N19).

Table 3.3. Regression coefficients for the relationships between stomatal conductance (g_s) and leaf temperature (Tleaf) with canopy temperature (Tc), estimated from data captured within individual flights, and for the pooled data (across flights) (all data), and for a limited dataset (flights 3, 5 and 6 only). Significance at p = 0.05 is indicated in bold with an asterisk.

Flight	g_s vs. Tc			Tleaf vs. Tc		
	Slope	Intercept	r	Slope	Intercept	r
1	-79.9	3110.8	-0.73	1.29	-12.9	0.85
2	-5.76	351.7	0.00	0.92	8.97	0.39
3	-103.9	2511.1	**-0.93***	0.89	9.11	**0.97***
4	35.1	-257.7	0.5	1.21	0.61	0.79
5	-133.9	3713.8	-0.82	3.50	-67.2	**0.94***
6	-113.5	3116.2	**-0.97***	2.11	-30.4	**0.98***
All data	3.97	239.8	0.01	0.14	23.3	0.24
3, 5 & 6	36.1	1135.7	**-0.74***	2.39	-38.3	**0.93***

3.4 Concluding discussion

The study aimed to address the following research questions:

Question 1: *Can NDVI and Tc effectively distinguish genotypic differences in FIPAR and g_s under WW and WD conditions?*

The study showed that FIPAR could be estimated from NDVI, though the relationship could be further improved using measurements of early vigour, captured at partial canopy cover. Findings from the study showed that Tc was not sensitive enough to detect varietal differences in g_s observed under well-watered and mild stress conditions. Rather, Tc proved effective in distinguishing water treatment differences in g_s under moderate to severe stress conditions.

Question 2: *Can the preliminary AP procedures used in this study reliably estimate NDVI and Tc, and what improvements can be implemented?*

The findings identified both successes and challenges in formulating effective AP procedures. For improved crop reflectance measurements, future studies at SASRI should utilize cameras with narrow and discrete bandwidths (e.g. Parrot Sequoia, Micasense RedEdge) to reduce spectral crosstalk between overlapping bands which affect estimates of NDVI. The use of radiometrically calibrated thermal cameras (e.g. FLIR Vue Pro R, FLIR Tau 2) in the second experimental phase of the study can enhance Tc estimation, with additional ground temperature target testing recommended for enhanced accuracy. Further refinement is also needed to enhance the filtering of soil and senesced leaf pixels within the follow-on phases of this study.

Overall, the study successfully developed preliminary correlations between vegetation spectral information and plant physiological parameters. Further evaluation of the relationship between NDVI and FIPAR at early vigour is needed to enhance the accuracy of using NDVI to infer genotypic differences. The use of Tc also requires refinement to better capture varietal differences in g_s, particularly under well-watered and mild stress conditions. Further refinement in AP methodologies will be crucial for improving the reliability of phenotyping genotypic differences in traits.

4. PHENOTYPING TRIALS: TRAIT-BASED ASSESSMENT OF YIELD AND DROUGHT TOLERANCE

4.1 Introduction

Findings from the pilot trial highlighted the need for refined ground and aerial measurement techniques, such as the monitoring of green canopy cover for early vigour and improving aerial image analyses to enhance accuracy of canopy temperature measurements. These recommendations were applied in the second experimental phase, which comprised a field trial where 54 genotypes (commercial South African and foreign varieties, and unreleased breeding lines) were grown under well-watered (WW) and water deficit (WD) conditions in plant and first ratoon crops.

The specific objectives were to:

1. Assess the impacts of ground measured traits, green canopy cover (FIPAR) and stomatal conductance (g_s), on stalk dry mass yield (SDM) under WW and WD conditions.
2. Assess the feasibility of estimating FIPAR and g_s from aerially measured traits, Normalized Difference Vegetation Index (NDVI) and canopy temperature (Tc), respectively.
3. Evaluate the potential for predicting SDM from NDVI and Tc.
4. Formulate best aerial phenotyping (AP) procedures.

4.2 Methodology

4.2.1 Trial design and operations

The study was conducted at the SASRI Komati research farm (25°33’08” S, 31°57’13” E). Fifty-four genotypes were selected to represent a wide range of genetic diversity that included commercial South African and foreign varieties, as well as unreleased breeding lines. These were planted between 22 - 26 October 2018. The plant and ratoon crops were monitored for 12 months until harvest on 4th October 2019, and 5-13 October 2020, respectively. The trial area (~3 ha) comprised three replicate blocks (~ 1 ha each), spaced apart, with each block divided into two water treatments (well-watered, WW, and water deficit, WD) (Figure 4.1). Each water treatment contained one plot per genotype, with each plot comprising of six rows, 8 m in length and at a row-spacing of 1.5 m. Alpha lattice design was used for each WW and WD treatment with three replications, and the position of the water treatments was also randomized within each replicate block.

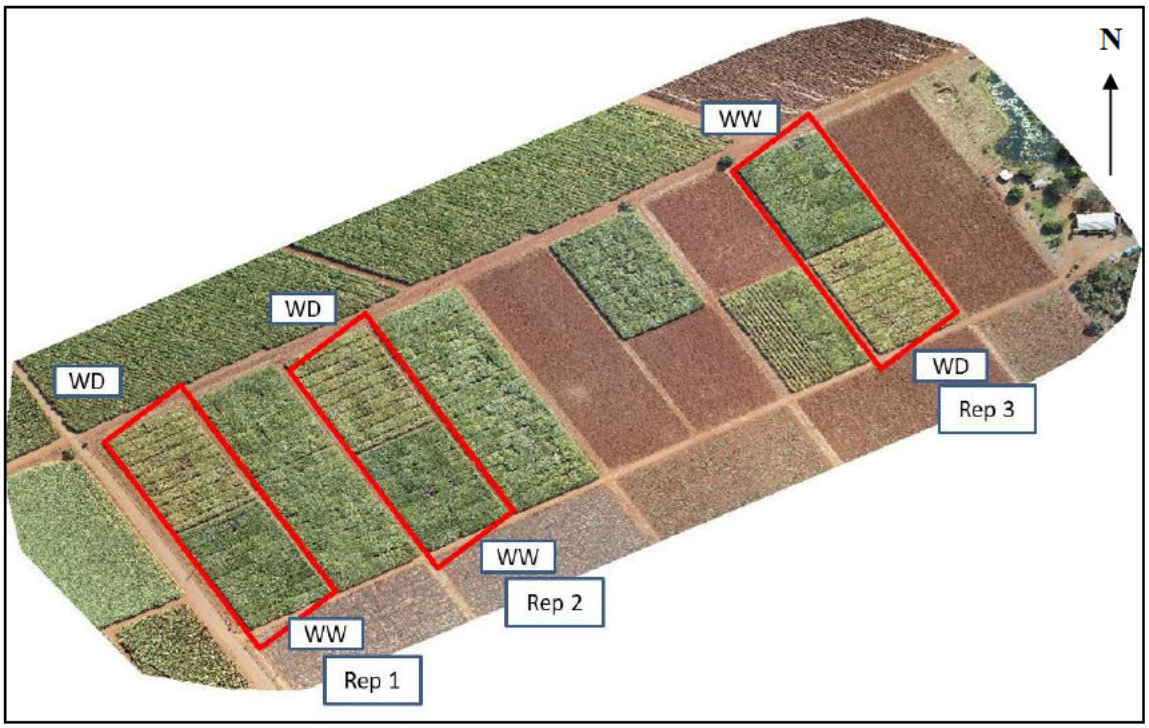

Figure 4.1. Komati field trial comprising 54 genotypes grown under well-watered (WW) and water deficit (WD) conditions, in three replicate blocks.

Fertiliser was applied according to standard recommendations to ensure nutrient sufficiency. Water was applied through a sub-surface drip irrigation system (emitters delivering 1.87 mm h^{-1}, spaced at 1.5 m x 0.6 m). SWS was estimated with Aquacheck capacitance probes and used to inform irrigation scheduling. All plots (WW and WD) were well-watered and received the same irrigation amounts during the early stages of crop growth (approximately 4-5 months) to ensure stress free growth. Thereafter, irrigation was continued in WW plots to maintain SWS above stress point (SP, taken as 50% of the difference between field capacity, FC, and permanent wilting point, PWP). These irrigation amounts generally varied between 22 to 48 mm, applied uniformly across the WW treatments mostly twice per week. Water deficit was imposed in WD plots by withholding irrigation during several stress periods, beginning from 160 DAP in the plant crop, and from 117 days after harvest (DAH) in the ratoon crop. These intermittent periods of stress were alleviated by rainfall only.

Genotype selection

The selection comprised released and foreign genotypes, as well as unreleased breeding lines, which represented a wide range of genetic diversity (shown in the Appendix, Table 8.4). This included (1) genotypes suited to rainfed and irrigated areas; (2) genotypes with

known differences in g_s and photosynthetic capacity under a range of moisture conditions (Eksteen et al., 2014; Hoffman et al., 2018; Smit and Singels, 2006); (3) drought tolerant and sensitive genotypes, based on expert breeding evidence in SASRI genotype sheets. The unreleased breeding lines were selected based on average yields under rainfed and irrigated conditions, where they represented 10 high- and low-ranking genotypes.

Soil characterisation

The field trial soil can be described as a shallow, red sandy clay loam, and has been previously classified as a Glenrosa soil form (Olivier and Singels, 2003; Rossler, 2013; Soil Classification Working Group, 1991), which is broadly equivalent to Leptic Cambisols (IUSS Working Group WRB, 2015). Visual assessment of soil pits in each block showed an Orthic A horizon to depths of 15 cm (rep 3), 40 cm (rep 1) and 50 cm (rep 2), and a Lithocutanic B horizon to depths of 40 cm (rep 3) and 60 cm (reps 1 and 2). The last layer consisted of unconsolidated material changing into the basalt parent material.

Soil sampling was conducted in selected plots at depths of 0-30, 30-60, 60-90 and 90-120 cm where possible, and analysed for textural (clay and silt %) properties (shown in the Appendix, Figure 8.5 and Table 8.5). Soil water retention properties FC and PWP, were estimated from clay content as described in van Antwerpen et al. (1994). Profile average clay content ranged from 36 to 48% across the trial replicates. Plant available soil water capacity (ASWCmax, mm) was on average 88.5 mm (± 24.4 mm) and was calculated as the product of the average difference between FC and PWP, multiplied by estimated rooting depth (ERD, m), determined by augering. ERD varied slightly within the trial areas, where samples taken in rep 1 suggest a gradient where the profile is slightly deeper at the southerly end (~ 0.9 m), and shallower at the northerly end (~ 0.6 m).

4.2.2 Ground measurements

Weather data

Weather data variables (SRAD, temperature, RH, rainfall, wind speed and VPD) were recorded from samples taken at five second intervals using an automatic weather station located approximately 120 m, 440 m and 580 m from the three replicate blocks, respectively. Daily Ecref was calculated from hourly weather data using the Penman-Monteith equation (McGlinchey and Inman-Bamber, 1996).

Soil water content

SWS index was measured with Aquacheck capacitance-based continuous logging probes (model S/S 800 mm HD) installed vertically, 15 cm adjacent to drip emitters situated in the middle of the third or fourth row of all plots containing variety NCo376, in each of the replicates and water treatments.

The probe readings were calibrated against gravimetrically determined volumetric SWC (R^2 = 0.62, shown in Figure 4.2), as previously described in Section 3.2.2. FC was taken as the SWC a day after thorough wetting of the soil, and PWP as the SWC in WD plots after all available water was extracted, respectively. FC and PWP for the WD plots were taken as 33 and 22.5%, respectively, and SP as 27.8%.

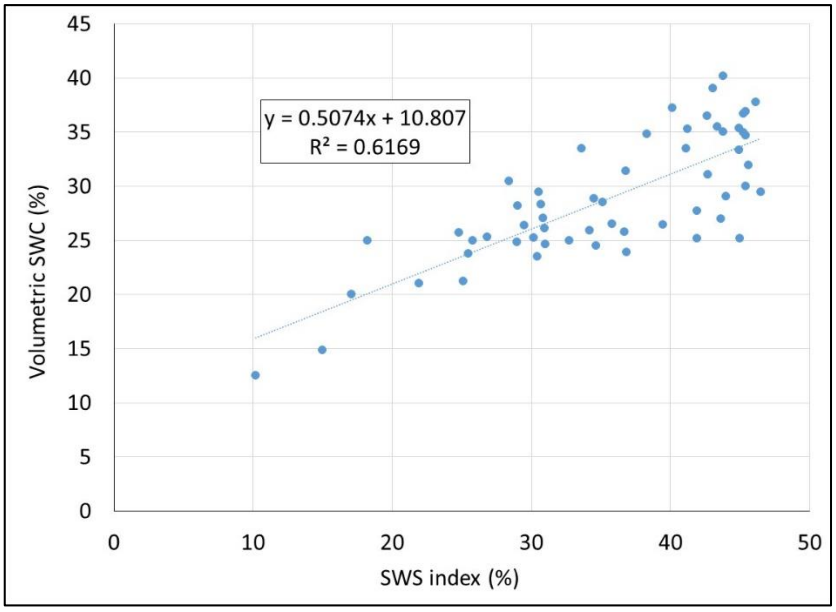

Figure 4.2. Relationship between volumetric soil water content (SWC, determined gravimetrically) and soil water status (SWS) index, determined from Aquacheck capacitance probes used in the Komati field trial.

Phenology

Phenology measurements were carried out in ten selected varieties (N12, N14, N19, N31, N36, N41, N51, N61, NCo376 and R570) in all replications and for both water treatments (60 plots in total). The data were used: (1) to relate crop development phase to aerial imagery; (2) as a non-destructive measure of water stress effect on crop growth and development. SPOP was measured by counting the number of stalks in 6 m sections of the third and fourth rows of each plot. In these two rows, ten tillers were marked and used for measurements of GL and SH once per month. Final GL, SPOP and SH at harvest were expressed as the ratio of WD to WW treatments for each genotype (GL*, SPOP* and SH*, respectively).

Radiation interception

A ceptometer (AccuPAR model LP-80, Decagon devices, Washington, USA) was used to measure FIPAR within a 6 m section of rows three and four of each plot, between 08:00 and 11:00 on cloudless days, as described previously in Section 3.2.2. This was done approximately every two weeks and coinciding with drone flights, for the ten selected varieties (60 plots in total). The ten varieties represented a wide range of genetic diversity, with known differences in canopy development, as described in the SASRI variety sheets.

Stomatal conductance

Leaf level g_s was measured on UAV flight dates to coincide with aerial measurements of crop reflectance, as described previously in Section 3.2.2. Two Decagon SC-1 porometers were used to measure g_s between 10:00 and 13:00 on three young sunlit leaves within plots representing the ten reference genotypes, in blocks one and three for both water treatments (40 plots in total). The ten selected varieties represented a broad genetic diversity, with previous studies demonstrating significant variation in g_s amongst these varieties under different moisture conditions (Eksteen et al., 2014; Hoffman et al., 2018; Smit and Singels, 2006).

Stalk yield

Stalks from rows three and four of each plot were manually harvested and weighed using a mechanical grab to determine SFM. DM was estimated from sub-samples comprising 12 stalks from each plot, which were weighed for fresh mass before being dried in an oven at

80°C to constant mass and weighed once again for dry weight. SDM was calculated as the product of SFM and DM.

4.2.3 Aerial imaging

Crop reflectance and emittance in the visible, NIR and thermal bands were captured on seven measurement days in the plant crop, and on four days in the ratoon crop (Table 4.1). The weather conditions for these dates are given in the Appendix (Table 8.7 and Table 8.8).

Prior to each measurement date, the trial was marked with 14 highly visible GCPs located at the corners of each replicate block and midway between replicates one and two. In three separate flights per measurement date, a DJI Phantom 4 drone was flown with (1) standard DJI FC330 RGB camera, (2) Sentera Precision NIR single sensor, and (3) FLIR Vue Pro R (336, 35° x 27° FOV, 9 mm, 9 Hz). The flights were carried out at approximate flight speeds of 3 (NIR and thermal) or 8 m s^{-1} (RGB), to cover forward/side overlap of images of 70/75% (RGB), 85/80% (NIR) and 90/75% (thermal).

Measurements were categorized in terms of soil water status, as well as canopy cover. This was done to group data for classes of crop water status and crop development. Flights were categorised according to the average CWSI of each water treatment into high, medium or low categories, and similarly, according to the average FIPAR of each water treatment into partial or full canopy cover categories, as described previously in Section 3.2.3.

Table 4.1. Details of drone flights to capture visual (RGB), near infrared (NIR) and thermal imagery in the Komati plant and ratoon crops. Several flights were carried out over the course of the two crops (days after planting, DAP, or days after harvest, DAH). For each flight, the average canopy cover (FIPAR) values were categorized as partial (P) or full (F), and the crop water satisfaction index (CWSI) values were categorized as low (L), medium (M) or high (H). For each flight, the time of capture and spatial resolution of images are given.

Crop	Flight	Date (DAP / DAH)	FIPAR		CWSI		Time of flight			Spatial resolution (cm)		
		Water treatment:	WW	WD	WW	WD	RGB	NIR	Thermal	RGB	NIR	Thermal
Plant	1	20 Feb 19 (118)	0.71 (M)	0.70 (M)	1.00 (H)	1.00 (H)	11:22	10:57	10:58	3.0	6.5	15.6
	2	12 Mar 19 (138)	0.75 (M)	0.73 (M)	1.00 (H)	1.00 (H)	11:18	11:22	11:20	2.9	6.8	14.5
	3	4 Apr 19 (161)	0.87 (H)	0.77 (M)	1.00 (H)	1.00 (H)	10:34	8:44	11:30	2.9	6.0	16.6
	4	2 May 19 (189)	0.81 (H)	0.78 (M)	1.00 (H)	0.68 (M)	10:41	10:55	10:55	2.8	6.1	14.1
	5	30 May 19 (217)	0.86 (H)	0.85 (H)	1.00 (H)	0.54 (M)	10:30	11:05	11:05	2.8	6.2	15.0
	6	17 July 19 (265)	0.87 (H)	0.86 (H)	1.00 (H)	0.40 (L)	10:46	11:54	12:30	2.9	6.1	15.3
	7	26 Sep 19 (336)	0.89 (H)	0.89 (H)	1.00 (H)	0.34 (L)	12:34	12:46	13:23	2.8	6.2	15.4
Ratoon	1	4 Feb 2020 (467 / 123)	0.83 (H)	0.82 (H)	1.00 (H)	1.00 (H)	11:22	10:57	09:00	3.0	6.5	15.6
	2	5 Mar 2020 (497 / 153)	0.87 (H)	0.86 (H)	1.00 (H)	1.00 (H)	11:18	11:22	14:00	2.9	6.8	14.5
	3	19 Mar 2020 (511 / 167)	0.88 (H)	0.87 (H)	1.00 (H)	0.65 (M)	10:34	8:44	12:00	2.9	6.0	16.6
	4	9 Sep 2020 (685 / 341)	0.92 (H)	0.91 (H)	1.00 (H)	1.00 (H)	10:41	-	12:00	2.8	-	14.1

Image processing & data analysis

The image processing pipelines for RGB, NIR and thermal imagery are shown graphically in the Appendix (Figure 8.6).

Visual (RGB) and NIR imagery

The Sentera NIR imagery were pre-processed to isolate reflectance data in the spectral bands, as described previously in Section 3.2.3. The RGB and NIR images were triangulated using the structure from motion algorithm, geo-rectified using the GCPs (georeferenced using Trimble R4 PPK GNSS system), and orthomosaicked in the Pix4D Mapper® photogrammetry software (v4.5.6; Pix4D, Lausanne, Switzerland). The orthomosaic images were then processed in the ArcGIS® (v10.1; ESRI, Redlands, CA, USA) software package. Individual plot boundaries were manually digitized to include the net plot area only (by excluding the two outer cane rows and 1 m from the edges of rows). Plot average NDVI values were then computed from pixels within the net plot area.

Thermal imagery

Pre-processing

Thermal imagery required two pre-processing steps. These included: (1) geotagging of images using corresponding RGB image coordinates captured simultaneously; (2) radiometric correction to account for ambient conditions at the time of the flight, using the FLIR Thermal Studio package (v1.1.69).

Processing of orthomosaics

The images were triangulated and orthomosaicked with Pix4D Mapper®. To obtain accurate estimates of Tc, soil and senesced leaf pixels were filtered from thermal orthomosaics using ArcGIS®. Four methods were developed and tested for this purpose, using the orthomosaic images from flights 1 and 4 (representing partial and full canopies). Briefly, the four methods were: (1) threshold application of thermal image (adapted from Jones, 2002; Meron et al., 2013); (2) supervised classification of thermal image (adapted from Ghebrezgabher et al., 2016; Haghighattalab et al., 2016); (3) supervised classification of RGB image (adapted from Ghebrezgabher et al. (2016) and Haghighattalab et al. (2016)); (4) unsupervised classification of thermal image (adapted from Haghighattalab et al., 2016). Method 3 was found to be the most accurate for masking soil and senesced leaf pixels. Briefly, the method

involved supervised classification of the RGB orthomosaic into three classes: green and senesced foliage, and soil. The RGB and thermal orthomosaics were superimposed, and the pixels classified as green foliage in the RGB image were used to extract corresponding pixels from the thermal image using the Maximum Likelihood classification tool. The extracted pixels were then used to compute plot average Tc values within net plot areas.

Processing of Tc estimates

For radiometric calibration of Tc estimates, values obtained with the FLIR Vue Pro R infrared camera were compared to the surface temperature of ground targets (wet soil, dry hot soil and a white car roof) measured with the Optris MS plus handheld infrared thermometer ($R^2 = 0.82$).

Tc for a given plot is determined by atmospheric conditions on the day of image capture (T_{aveF}), soil and crop conditions in the given replicate block (T_R), the effect of the water treatment (T_W), the effect of the spatial trend (T_S) and the effect of the genotype (T_G). This can be represented by the following mathematical model:

$$Tc = T_{aveF} + T_R + T_W + T_S + T_G \quad \text{(Equation 19)}$$

Additionally, random variation in Tc estimates could have resulted from camera drift effects, caused by internal heating of uncooled components and external thermal loading from the sun (Gonzalez-Dugo et al., 2012; Kelly et al., 2019; Mesas-Carrascosa et al., 2018).

Evaluation of Tc data measured in the plant crop revealed significant differences due to spatial variation within the field, rather than due to genotypic differences, against expectation. The data showed strong spatial trends in the east-west direction in all three reps for most flights, irrespective of whether the drone was flown across columns or rows. Tc values showed a strong relationship with column number (numbered from east to west), and no significant relationship with row number (number from south to north) (example shown in Figure 4.3). It is surmised that the observed variations could be attributed to a combination of soil heterogeneity within the field, and possibly gradients in irrigation application. Notably, the observed spatial variation persisted across different flight paths, suggesting that these trends were likely driven by the underlying soil and irrigation patterns. By contrast, the ratoon crop data showed less spatial trends in the east-west direction and could not be related to column number.

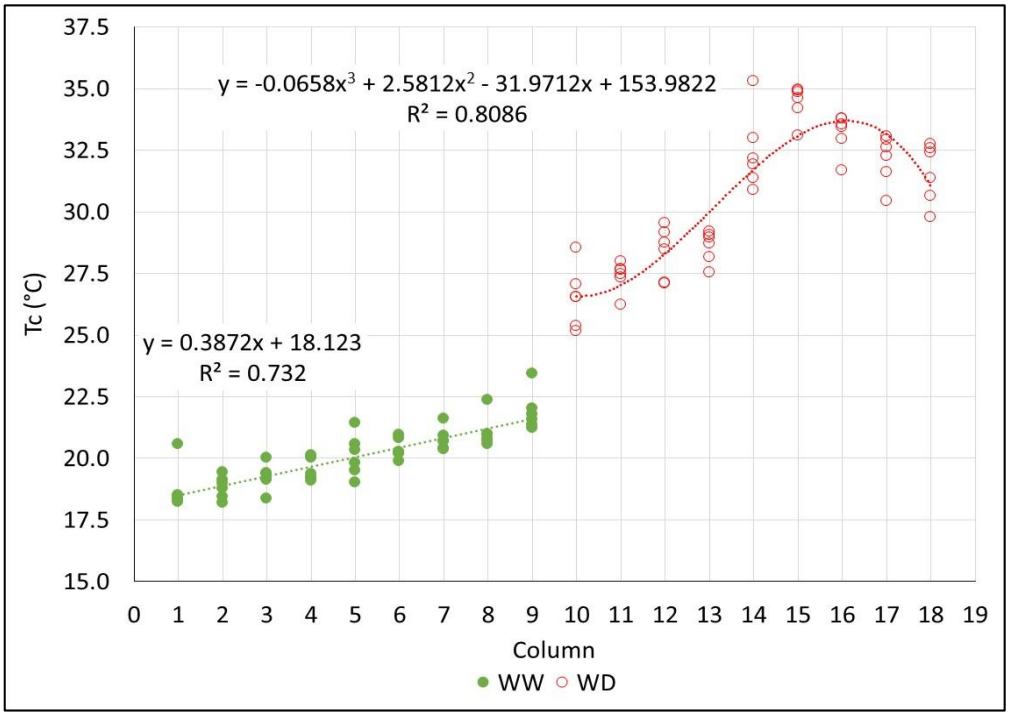

Figure 4.3. Relationship between canopy temperature (Tc) and plot column number for the well-watered (WW, green) and water deficit (WD, red) treatments, shown for rep 1 captured in the fourth flight of the Komati plant crop. Plot column number indicates the position of the plot in the replicate in the east (1) – west (19) direction.

To account for this spatial variation, and to ultimately isolate the G and W effects, Tc values were adjusted using a regression model to develop a canopy temperature index. Treatment specific regression equations were fitted for each flight, replicate and water treatment (shown in the Appendix, Table 8.6), and used to estimate mean Tc for each trial column (Tc_{col}). The estimated genotype effect on canopy temperature (Tc_i, referred to as the canopy temperature index) for the WW plots in each replication and for a given flight was calculated as:

$$Tc_i = (Tc - Tc_{col}) \quad \text{(Equation 20)}$$

where Tc is the average value for a given plot, and Tc_{col} is the average" Tc value for the relevant column as estimated through regression analysis of the spatial trend.

For WD plots the combined genotype and water deficit effect was calculated using the difference in Tc between the WW and WD treatments (Tc_{WW} and Tc_{WD}, taken as the average values for a given replicate block), as:

$$Tc_i = (\overline{Tc}_{WD} - \overline{Tc}_{WW}) + (Tc - Tc_{col}) \quad \text{(Equation 21)}$$

4.2.4 Statistical analyses

Datasets for individual traits were tested for normality using the Shapiro-Wilk test. Statistical significance (at p = 0.05), variance and covariance of traits for individual flight dates were estimated using REML analysis (Fixed model: Genotype; Random model: Rep/Block + Genotype) in the SAS software package (The SAS institute, Cary, NC, USA). The REML analyses were then repeated for data within categories of CWSI, using amended REML models (Fixed model: Genotype; Random model: Rep/Block + Flight + Genotype).

The genetic coefficient of variation (GCV, %) for individual traits was calculated using the square root of genetic variance (σ_g) and the mean value ($\bar{x}$) for a given trait:

$$GCV = \frac{\sigma_g}{\bar{x}} * 100 \quad \text{(Equation 22)}$$

Broad-sense heritability (HSB, Fehr, (1987)) for a given trait was estimated based on genotype means, using genetic (σ_g^2) and error (σ_e^2) variances, and the number of replications (n_r):

$$HSB = \frac{\sigma_g^2}{\sigma_g^2 + \frac{\sigma_e^2}{n_r}} \quad \text{(Equation 23)}$$

Genetic correlations (r_g, Kempthorne, 1957) between traits *x* and *y* were estimated using the genetic covariance between the two traits ($Cov_{g(xy)}$), as well as the respective individual genetic variances (σ_{gx}^2 and σ_{gy}^2):

$$r_g = \frac{Cov_{g(xy)}}{\sqrt{\sigma_{gx}^2} \times \sqrt{\sigma_{gy}^2}} \quad \text{(Equation 24)}$$

The data were analysed for individual measurement days, across measurement days, over the season, as well as for different CWSI categories.

4.2.5 Trait correlations

The study considered the phenotypic (r) and genetic (r_g) correlations between traits for individual measurement days, across the season and for categories of CWSI, where appropriate. Genetic correlations are an important consideration for quantitative genetics and breeding (Falconer and Mackay, 1996), as they describe the genetic effects between two traits, where high correlations suggest that the genes governing the traits may be co-inherited (Walsh B and Lynch M, 1998). Phenotypic correlations by comparison, do not distinguish between variation due to correlated genetic effects and experimental error.

The study considered the following relationships: (1) SDM vs. ground (FIPAR, g_s) and aerially measured (NDVI, Tc) traits; (2) FIPAR vs. NDVI and g_s, vs. Tc; (3) SDM and Tc, expressed as the ratio (SDM*) or difference (ΔTc) between WD and WW values for a given genotype.

4.3 Results

4.3.1 Weather data

Weather data for the trial period are shown in Figure 4.4. Briefly, both crops showed similar trends in daily Tmax (26.2 to 35.0 °C), Tmin (6.0 to 21.0 °C) and SRAD (12.4 to 22.3 MJ m^{-2} d^{-1}), where values peaked in approximately December-February during summer when rainfall is also highest and declined thereafter. Overall, the ratoon accumulated higher thermal time (estimated as the cumulative average daily temperature above a base temperature of 10 °C), and experienced more rainfall, as compared to the plant crop (4520 vs. 4467 °Cd, and 742 vs. 658 mm, respectively).

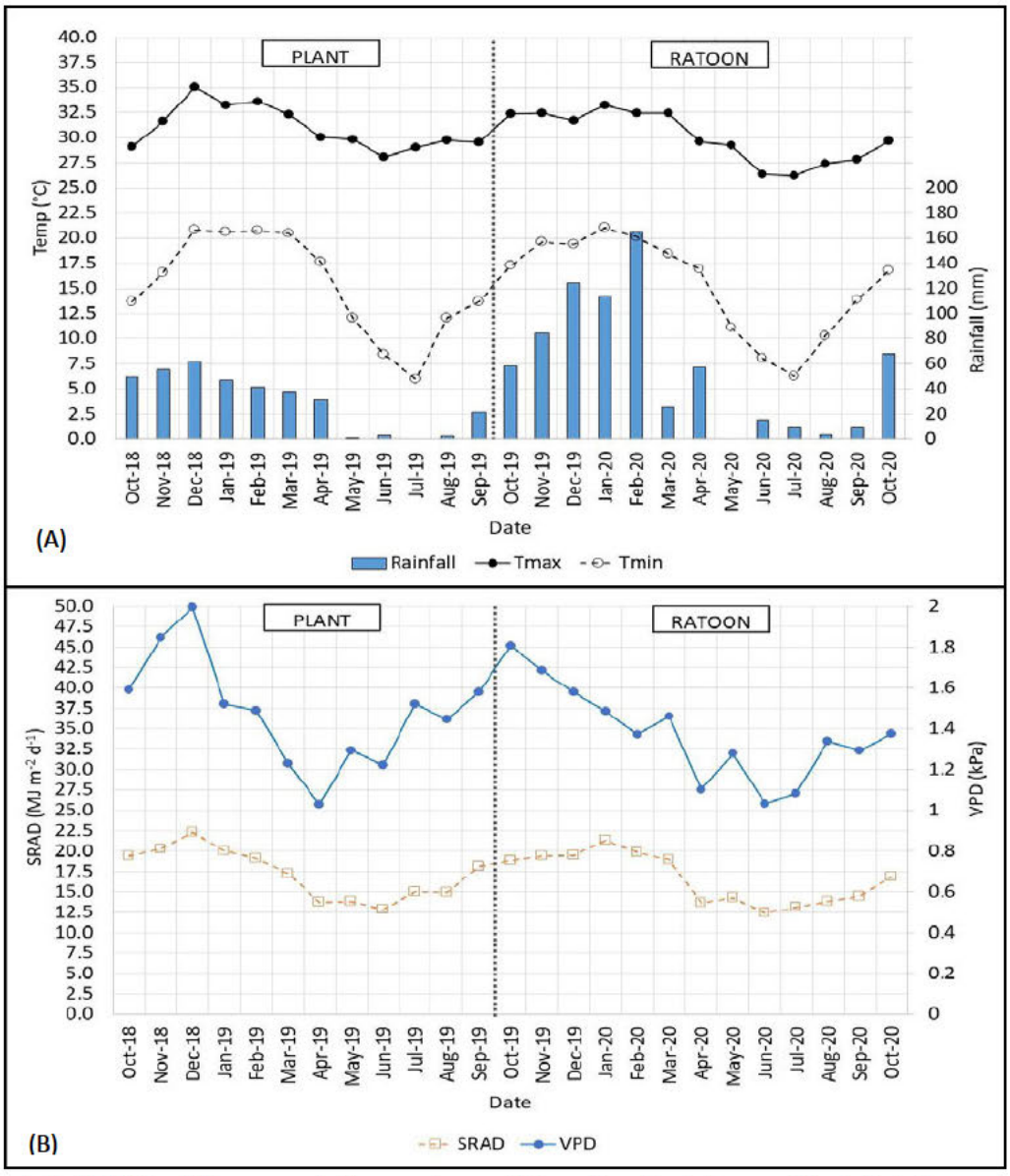

Figure 4.4. (A) Monthly mean daily maximum (Tmax) and minimum (Tmin) air temperatures and monthly rainfall; (B) daily solar radiation (SRAD) and daily vapour pressure deficit (VPD), for the plant and ratoon crops.

4.3.2 Crop water use

Profile average SWC for all plots measured in both crops is shown in Figure 4.5. Overall, the WW plots were kept well irrigated and mostly maintained SWC above 80% of FC in both crops. The WD treatment of the plant crop was kept well-watered during the early growth stages, and received 68% (321 mm) of the total rainfall experienced by the crop up to 160 DAP. Thereafter, little rainfall was experienced, and water deficit was imposed by withholding irrigation during eight stress periods that lasted between 9 and 29 days each. Similarly, the WD treatment of the ratoon crop was well-watered until 117 DAH (461 DAP). The first intended stress event was interrupted by rainfall (127 mm) experienced between 125 – 130 DAH (469 - 474 DAP). Thereafter, the WD treatment experienced the longest period of water stress from 150 - 175 DAH (494 – 519 DAP). Several stress events occurred thereafter, lasting no more than 14 days each. Overall, the ratoon crop experienced less severe water stress, and for shorter periods of time, as compared to the plant crop, due largely to high and more frequent rainfall events.

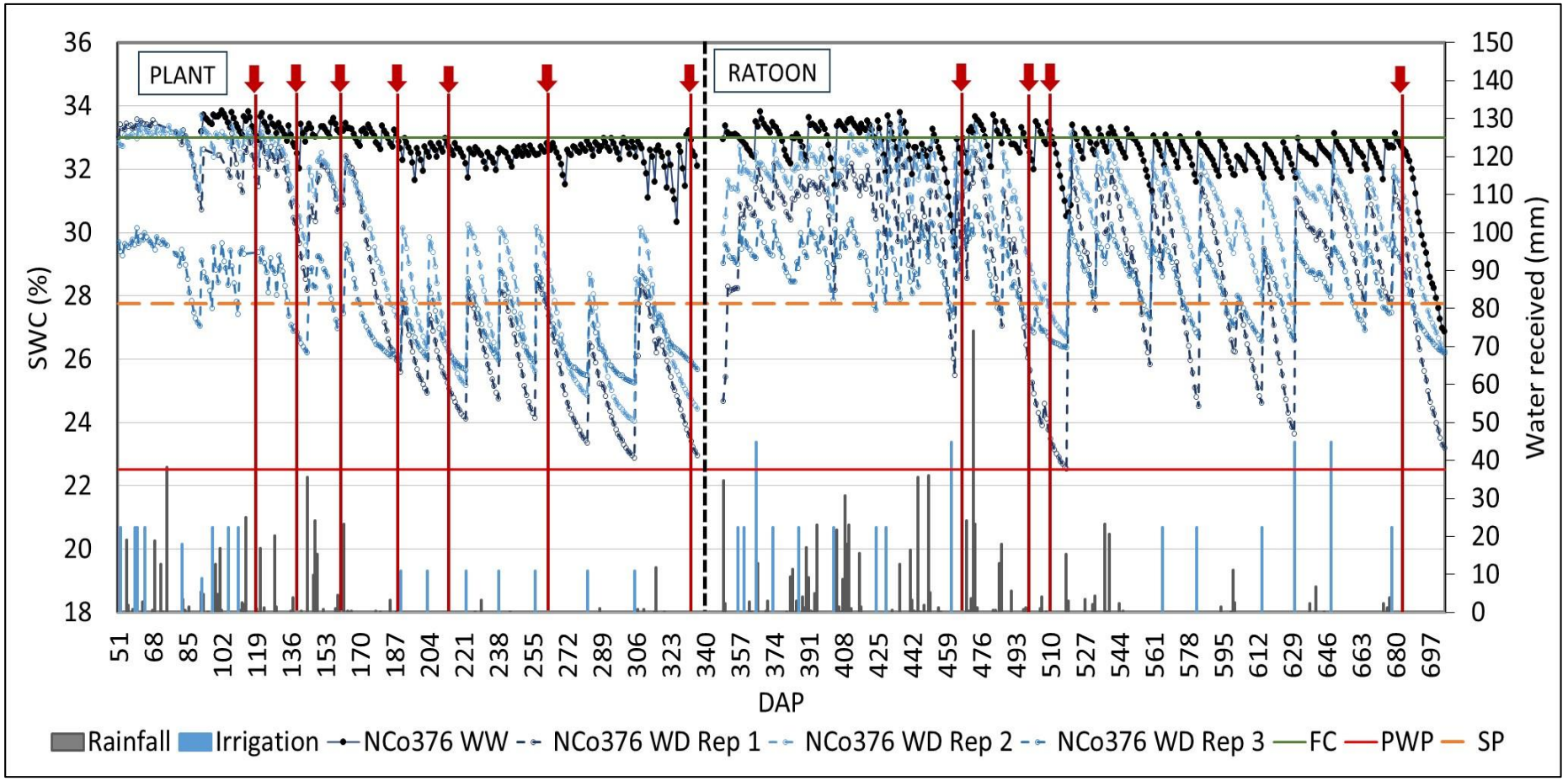

Figure 4.5. Profile average volumetric soil water content (SWC) measured over time (days after planting, DAP) in plant and ratoon crops, measured with Aquacheck capacitance probes in well-watered (WW) and water deficit (WD) plots. The secondary axis shows water received in the WD treatments (rainfall and irrigation). Green, orange and red lines represent field capacity (FC), stress point (SP) and permanent wilting point (PWP), respectively. Red arrows and vertical lines represent dates on which drone flights were conducted.

4.3.3 Crop growth

Ground measurements

Phenology

Crop phenology (GL, SH and SPOP) data collected shortly before harvest for both plant and ratoon crops, are shown in the Appendix (Table 8.9). Briefly, the lower degree of stress experienced by the ratoon crop as compared to the plant crop, was evident in the average GL of the WD treatment, expressed relative to that of the WW treatment (GL*), for the two crops (0.80 vs. 0.41), respectively. Final SPOP was not significantly reduced by water stress in either of the crops, and average SPOP* was 0.99 and 1.0 for the plant and ratoon crops respectively. Final SH was reduced by 23 and 13% due to crop water stress in the plant and ratoon crops, respectively.

Stomatal conductance

Measurements of g_s did not differ significantly between genotypes for any of the individual measurement days for either crop (Table 4.3). This could have been attributed to the relatively limited genetic diversity within the small population measured in the trial.

Radiation interception

Statistical analysis of FIPAR showed significant genotypic differences and high HSB (0.76 – 0.86) for both water treatments at partial canopy in the plant crop at 98 and 109 DAP, and in the ratoon crop at 422 DAP (78 DAH), after which no significant genotypic differences were observed as canopy closure occurred (Table 4.2, and shown graphically in the Appendix, Figure 8.7) . Furthermore, water deficit did not significantly reduce canopy cover for any of the genotypes on any measurement date for either of the two crops.

Table 4.2. Statistical analysis of green canopy cover (FIPAR) in the well-watered (WW) and water deficit (WD) treatments of the plant and ratoon crops. Standard deviation values are indicated in brackets. Values of F. probability (F.pr.) due to genotypic differences, genetic (G) and error (E) variance, genetic coefficient of variation (GCV, %) and broad-sense heritability (HSB) are shown. Values in bold with an asterisk indicate statistical significance at p = 0.05.

Crop	Plant													
Water treatment	WW							WD						
DAP / DAH	Mean	F.pr.	G	E	HSB	GCV	n	Mean	F.pr.	G	E	HSB	GCV	n
54	0.10 (0.04)	0.74	0.30	0.002	0.27	14.3	30	0.12 (0.06)	0.77	-	0.002	-	-	30
88	0.54 (0.14)	0.66	0.005	0.009	0.64	13.6	30	0.51 (0.14)	0.96	-	0.02	-	-	30
98	0.56 (0.07)	**0.02***	0.001	0.0009	0.77	5.70	30	0.56 (0.06)	**0.04***	0.001	0.001	0.76	5.69	30
109	0.68 (0.06)	**0.04***	0.002	0.0009	0.86	6.34	30	0.66 (0.06)	**0.03***	0.002	0.002	0.81	7.13	30
124	0.78 (0.08)	0.52	0.0009	0.003	0.50	4.04	30	0.73 (0.07)	0.22	0.0007	0.001	0.65	3.65	30
146	0.77 (0.06)	0.06	0.002	0.002	0.80	6.09	30	0.74 (0.05)	0.07	0.0005	0.002	0.39	2.88	30
161	0.87 (0.02)	0.32	0.0002	0.0002	0.76	1.80	30	0.77 (0.04)	0.06	0.0002	0.001	0.35	1.86	30
181	0.77 (0.06)	0.23	0.0006	0.002	0.49	3.10	30	0.74 (0.05)	0.85	0.00006	0.003	0.06	1.01	30
203	0.87 (0.02)	0.47	-	0.0004	-	-	30	0.85 (0.04)	0.09	0.0001	0.002	0.18	1.39	30
218	0.86 (0.02)	0.38	0.00004	0.0005	0.22	0.77	30	0.85 (0.03)	0.12	0.00006	0.0005	0.24	0.88	30
242	0.90 (0.01)	0.85	0.00002	0.00009	0.40	0.46	30	0.86 (0.02)	0.99	-	0.0002	-	-	30
293	0.90 (0.02)	0.06	0.00008	0.0002	0.51	1.02	30	0.90 (0.02)	0.89	-	0.0001	-	-	30
337	0.89 (0.03)	0.56	-	0.0005	-	-	23	0.89 (0.03)	0.18	0.00009	0.0006	0.32	1.08	30
	Ratoon													
386	0.59 (0.10)	0.07	0.002	0.003	0.65	7.30	30	0.57 (0.10)	0.10	0.001	0.002	0.74	7.56	30
400	0.65 (0.06)	0.18	0.00009	0.0006	0.32	1.48	30	0.60 (0.08)	0.24	0.002	0.004	0.61	7.45	30
422	0.82 (0.04)	**0.01***	0.001	0.0005	0.88	4.23	30	0.80 (0.04)	0.06	0.0008	0.001	0.69	3.62	28
445	0.83 (0.05)	0.25	0.0006	0.0006	0.76	3.00	30	0.82 (0.05)	0.12	0.001	0.0009	0.80	4.11	30
462	0.85 (0.03)	0.16	0.0003	0.0003	0.78	2.15	30	0.85 (0.03)	0.05	0.0004	0.0004	0.76	2.47	30
483	0.92 (0.04)	0.98	-	0.00005	-	-	23	0.91 (0.02)	0.10	0.00001	0.0002	0.18	0.37	26
498	0.92 (0.05)	0.99	-	0.00	-	-	15	0.88 (0.01)	0.76	0.00001	0.00003	0.6	0.41	24
512	0.92 (0.02)	0.91	-	0.0008	-	-	20	0.90 (0.01)	0.23	0.000001	0.00003	0.15	0.15	25
534	0.92 (0.01)	0.99	-	0.00001	-	-	22	0.94 (0.04)	0.87	-	0.000006	-	-	24
608	0.94 (0.03)	0.90	-	0.00003	-	-	25	0.92 (0.02)	0.88	0.00007	-	-	-	24

Table 4.3. Statistical analysis of stomatal conductance (g_s, mmol m^{-2} s^{-1}), estimated on measurement days which coincided with drone flights in the well-watered (WW) and water deficit (WD) treatments of the plant and ratoon crops. Standard deviation values are indicated in brackets. Values of F. probability (F.pr.) due to genotypic differences, genetic (G) and error (E) variance, genetic coefficient of variation (GCV, %) and broad-sense heritability (HSB) are shown.

Crop	Plant													
Water treatment	WW							WD						
Flight	Mean	F.pr.	G	E	HSB	GCV	n	Mean	F.pr.	G	E	HSB	GCV	n
1	264.0 (65.9)	0.49	-	897.2	-	-	20	262.7 (45.4)	0.80	-	2063.9	-	-	20
2	325.0 (102.6)	0.70	-	2005.8	-	-	20	290.9 (106.3)	0.35	4702.5	6573.3	0.59	23.6	20
3	273.9 (67.6)	0.73	-	2522.0	-	-	20	295.8 (83.3)	0.27	-	4289.1	-	-	20
4	232.1 (100.8)	0.71	-	6632.9	-	-	20	179.0 (101.1)	0.66	-	8042.8	-	-	20
5	218.8 (93.9)	0.98	-	1813.4	-	-	18	177.5 (119.2)	0.49	-	6303.2	-	-	20
6	132.1 (39.7)	-	-	-	-	-	8	109.7 (44.0)	0.34	-	1827.3	-	-	20
7	126.6 (30.2)	-	-		-	-	12	88.1 (53.8)	-	-	-	-	-	8
	Ratoon													
1	184.6 (35.0)	0.95	-	955.1	-	-	20	222.7 (48.8)	0.94	-	2204.0	-	-	20
2	189.4 (27.3)	0.20	35.1	525.4	0.12	3.13	20	229.3 (102.2)	0.97	-	1616.6	-	-	20
3	240.1 (64.5)	0.82	-	4158.0	-	-	20	140.0 (21.1)	0.71	-	275.0	-	-	20
4	149.3 (24.9)	0.67	-	379.4	-	-	20	160.0 (26.5)	0.57	-	554.3	-	-	20

Stalk yield

Statistical analysis of SDM showed significant genotypic differences for both water treatments of the plant and ratoon crops (Table 4.4), with moderate to high HSB for the WW (0.68 – 0.71) and WD (0.34 – 0.72) treatments, respectively. SDM for the WW and WD treatments were on average, 39% and 108% higher in the ratoon compared to that of the plant crop, respectively, indicating less water stress in the former. Average SDM* values for the ratoon crop ranged from 0.6 to 1.1, which was higher compared to that of the plant crop, where values ranged from 0.4 to 0.8 (data shown in the Appendix, Figure 8.9). Rankings of SDM* between the plant and ratoon crops were not consistent and were not significantly correlated, presumably because of the different stress conditions experienced by the two

crops. Overall, the heritability of the WW and WD treatments across both crops were high (0.74) and moderate (0.60), respectively.

The MyCanesim® crop model was used to investigate climatic, water status and crop class effects on yields. The model simulated higher potential yields for the ratoon crop as compared to the plant crop because of environmental factors (radiation and rainfall) and crop class factors (faster germination, and higher interception of radiation in early summer due to faster canopy development in the ratoon crop). Simulated SDM for the WW and WD treatments were 11 and 120% higher in the ratoon as compared to the plant crop, and SDM* was 0.27 and 0.65 for the two crops, respectively.

Table 4.4. Statistical analysis of stalk dry mass (SDM, t ha^{-1}) yield measured at harvest for the well-watered (WW) and water deficit (WD) treatments of the plant and ratoon crops. Standard deviation values are indicated in brackets. The statistics shown include: values of F. probability (F.pr.) due to genotypic (G), crop (C) and genotypic x crop (G x C) differences; genetic (G) and error (E) variances; broad-sense heritability (HSB) and the genetic coefficient of variation (GCV, %). Values in bold with an asterisk indicate statistical significance at p = 0.05.

Crop	Treatment	Mean	F.pr.			G	E	HSB	GCV	n
			G	C	G x C					
Plant	WW	33.3 (5.3)	**<0.0001***	-	-	12.6	12.1	0.68	10.7	159
	WD	18.9 (3.0)	**0.0002***	-	-	3.02	5.82	0.34	9.2	159
Ratoon	WW	46.2 (8.3)	**<0.0001***	-	-	25.0	29.9	0.71	10.8	159
	WD	39.3 (6.5)	**<0.0001***	-	-	17.6	20.4	0.72	10.7	159
Plant + Ratoon	WW	39.7 (9.5)	**<0.0001***	**<0.0001***	0.54	14.4	30.5	0.74	9.6	318
	WD	29.1 (11.4)	**<0.0001***	**<0.0001***	**<0.0001***	2.85	11.25	0.60	5.8	318
	WW + WD	34.4 (11.8)	**<0.0001***	**<0.0001***	0.55	2.79	46.7	0.26	4.9	636

Aerial imaging

NDVI

Statistical analysis of NDVI for each measurement day and water treatment, and across categories of CWSI, are shown in Table 4.5 and Table 4.6, respectively. NDVI differed significantly between genotypes for all flights conducted in both crops, with moderate to high HSB estimates for the WW (0.54 – 0.90) and WD (0.70 - 0.86) treatments. NDVI also differed significantly between genotypes for all categories of CWSI in both crops, with moderate to high heritability in the WW (0.58 – 0.69) and WD (0.45 – 0.80) treatments.

Table 4.5. Statistical analysis of normalised difference vegetation index (NDVI) estimated from aerial imagery, captured in several flights for the well-watered (WW) and water deficit (WD) treatments of the plant and ratoon crops. Standard deviation values are indicated in brackets. Values of F. probability (F.pr.) due to genotypic differences, genetic (G) and error (E) variance, genetic coefficient of variation (GCV, %) and broad-sense heritability (HSB) are shown. Values with an asterisk indicate statistical significance at p = 0.05.

Water treatment		WW						WD						
Crop	Flight	Mean	F.pr.	G	E	HSB	GCV	Mean	F.pr.	G	E	HSB	GCV	n
Plant	1	0.72 (0.05)	**0.0006***	0.00051	0.00097	0.61	3.1	0.73 (0.04)	**<0.0001***	0.0006	0.0004	0.80	3.3	159
	2	0.81 (0.02)	**<0.0001***	0.0002	0.0001	0.83	1.9	0.81 (0.02)	**<0.0001***	0.0002	0.0001	0.83	1.5	159
	3	0.83 (0.02)	**<0.0001***	0.0001	0.00007	0.89	1.6	0.82 (0.02)	**<0.0001***	0.0001	0.00007	0.86	1.4	159
	4	0.82 (0.02)	**<0.0001***	0.0002	0.0001	0.86	1.9	0.73 (0.04)	**<0.0001***	0.0005	0.0004	0.78	2.9	159
	5	0.81 (0.02)	**<0.0001***	0.0003	0.0002	0.83	2.3	0.64 (0.05)	**<0.0001***	0.0009	0.0007	0.79	4.7	159
	6	0.77 (0.03)	**<0.0001***	0.0006	0.0002	0.90	3.1	0.58 (0.05)	**<0.0001***	0.0005	0.0003	0.84	3.7	159
	7	0.75 (0.05)	**<0.0001***	0.001	0.0005	0.90	5.1	0.45 (0.04)	**<0.0001***	0.0003	0.0002	0.79	3.8	159
Ratoon	1	0.84 (0.02)	**<0.0001***	0.00022	0.00018	0.79	1.8	0.83 (0.03)	**<0.0001***	0.0002	0.0002	0.79	1.9	159
	2	0.89 (0.01)	**0.005***	0.00004	0.00009	0.54	0.7	0.87 (0.02)	**0.008***	0.0001	0.0002	0.70	1.3	159
	3	0.88 (0.02)	**<0.0001***	0.00021	0.00014	0.82	1.7	0.77 (0.05)	**<0.0001***	0.0011	0.00084	0.80	4.4	159

Table 4.6. Statistical analysis of normalised difference vegetation index (NDVI) estimated from aerial imagery across multiple flights for the well-watered (WW) and water deficit (WD) treatments of the plant and ratoon crops. Data were categorised by crop water satisfaction (high, medium or low, H / M / L, and combinations thereof). Standard deviation values are shown in brackets. F. probabilities (F.pr.) due to genotypic differences (indicated as significant with an asterisk) are shown along with corresponding genetic (G) and error (E) variances, genetic coefficient of variation (GCV, %) and broad-sense heritability (HSB) values for the respective categories. The number of datapoints analysed (n) is also shown.

Crop	Water treatment	Crop water satisfaction category	Mean	F.pr.	G	E	HSB	GCV	n
Plant	WW	H	0.79 (0.05)	**<0.0001***	0.00028	0.00061	0.58	2.11	1113
	WD	H	0.79 (0.05)	**<0.0001***	0.00021	0.00031	0.67	1.85	477
		M	0.69 (0.06)	**<0.0001***	0.00069	0.00058	0.80	3.81	318
		L	0.51 (0.08)	**<0.0001***	0.00031	0.00047	0.66	3.44	318
		H+M	0.75 (0.07)	**<0.0001***	0.00025	0.00074	0.51	2.13	795
		M+L	0.60 (0.11)	**<0.0001***	0.00045	0.00071	0.66	3.54	636
		H+M+L	0.68 (0.13)	**<0.0001***	0.00024	0.00086	0.45	2.25	1113
Ratoon	WW	H	0.87 (0.03)	**<0.0001***	0.00013	0.00018	0.69	1.33	477
	WD	H	0.85 (0.03)	**<0.0001***	0.00019	0.00018	0.76	1.64	318
		H+M	0.82 (0.05)	**<0.0001***	0.00042	0.00058	0.69	2.51	477

Canopy temperature

Statistical analysis of Tc for each measurement day and water treatment, and across categories of CWSI, are shown in Table 4.7 and Table 4.8, respectively. In the plant crop, Tc differed significantly between genotypes for the WW and WD treatments during the first two flights only, with moderate to moderately high HSB estimates (0.52 – 0.67). These Tc data showed generally weaker correlations with column number (described previously in Section 4.2.3) and thus less spatial variation in the east-west direction as compared to the later flights. For flights 3-7, HSB estimates were generally poor otherwise (0.09 – 0.57), presumably due to spatial variation which obscured any genotypic variation in Tc (an example is shown in the Appendix, Figure 8.10).

By contrast, the ratoon crop data showed less spatial trends in the east-west direction and could not be related to column number. These data showed significant genotypic differences in Tc for both treatments of flight 3, and for the WW treatment of flight 4, with moderate to high HSB estimates (0.62 – 0.75) (Table 4.7).

The study found statistically non-significant genotypic differences in Tc across most categories of CWSI for either crop (Table 4.8), except when CWSI was high in the WD treatment. This could be attributed to the effects of spatial variation on Tc estimates, and significant genotype x date interactions in some cases.

To account for this spatial variation, and to ultimately isolate the G and W effects, Tc values were adjusted using a regression model to develop a canopy temperature index (Tc_i) as described in Section 4.2.3. Statistical analysis of Tc_i values (shown in the Appendix, Table 8.10 and Table 8.11) showed significant genotypic differences for most of the flights conducted later on in the crop cycle, with slightly improved HSB estimates for the WW (0.37 – 0.51) and WD (0.43 – 0.53) treatments as compared to measured Tc values. Overall, HSB estimates declined slightly with crop age and with water stress. When considering categories of CWSI, Tc_i differed significantly between genotypes only when CWSI was high, though HSB estimates were low (0.18 and 0.19) presumably due to significant genotype x measurement date interactions.

Table 4.7. Statistical analysis of canopy temperature (Tc, °C) estimated from aerial imagery, captured in several flights for the well-watered (WW) and water deficit (WD) treatments of the plant and ratoon crops. Standard deviation values are indicated in brackets. Values of F. probability (F.pr.) due to genotypic differences, genetic (G) and error (E) variance, genetic coefficient of variation (GCV, %) and broad-sense heritability (HSB) are shown. Values with an asterisk indicate statistical significance at p = 0.05.

Water treatment		WW						WD						
Crop	Flight	Mean	F.pr.	G	E	HSB	GCV	Mean	F.pr.	G	E	HSB	GCV	n
Plant	1	28.9 (2.44)	**0.0003***	2.17	3.64	0.64	5.1	27.2 (2.39)	**<0.0001***	1.44	2.14	0.67	4.4	159
	2	20.4 (1.45)	**0.006***	0.30	0.81	0.52	2.7	22.0 (1.29)	**0.0001***	0.26	0.48	0.62	2.3	159
	3	22.9 (0.96)	0.05	0.15	0.34	0.57	1.7	26.1 (2.73)	0.8	-	5.88	-	-	159
	4	21.3 (2.59)	0.09	0.12	0.88	0.29	1.6	29.7 (2.61)	0.63	-	0.65	-	-	159
	5	17.7 (2.57)	0.26	0.18	5.44	0.09	2.4	21.2 (2.91)	0.14	0.46	3.4	0.29	3.2	159
	6	17.7 (1.03)	0.35	0.03	0.99	0.09	1.1	20.3 (1.88)	0.39	-	2.69	-	-	159
	7	14.3 (2.56)	0.26	0.24	1.99	0.27	3.5	18.7 (2.17)	0.81	-	4.67	-	-	159
Ratoon	1	36.4 (1.18)	0.50	0.0043	1.37	0.01	0.18	36.0 (3.14)	0.35	0.12	0.16	0.24	1.0	159
	2	30.5 (1.60)	0.16	0.042	0.38	0.26	0.7	31.8 (2.18)	0.19	0.14	1.00	0.29	1.2	159
	3	31.4 (2.36)	**<0.0001***	0.28	0.53	0.62	1.7	35.5 (2.21)	**<0.0001***	0.37	0.38	0.75	1.7	159
	4	31.2 (1.77)	**<0.0001***	1.09	1.46	0.69	3.4	33.3 (2.31)	0.68	-	2.85	0.16	6.9	159

Table 4.8. Statistical analysis of canopy temperature (Tc, °C) estimated from aerial imagery, captured in several flights for the well-watered (WW) and water deficit (WD) treatments of the plant and ratoon crops. The data were grouped for different categories of crop water satisfaction (high (H), medium (M) and low (L)), and combinations thereof. Standard deviation values are indicated in brackets. Values of F. probability (F.pr.) due to genotypic differences, genetic (G) and error (E) variance, genetic coefficient of variation (GCV, %) and broad-sense heritability (HSB) are shown. Values in bold with an asterisk indicate statistical significance at p = 0.05.

Crop	Water treatment	Crop water satisfaction category	Mean	F.pr.	G	E	HSB	GCV	n
Plant	WW	H	20.5 (4.78)	0.26	0.058	3.62	0.05	1.18	1113
	WD	H	25.1 (3.14)	**0.0009***	0.41	3.88	0.24	2.56	477
		M	25.5 (5.11)	0.07	0.52	5.84	0.21	2.82	318
		L	19.5 (2.18)	0.99	-	4.03	-	-	318
		H+M	25.3 (4.04)	0.08	0.52	5.48	0.22	2.87	795
		M+L	22.5 (4.93)	0.22	0.082	5.38	0.04	1.27	636
		H+M+L	23.6 (4.45)	0.67	0.30	5.18	0.15	2.31	1113
Ratoon	WW	H	32.4 (2.95)	0.33	0.04	2.92	0.04	0.62	636
	WD	H	33.7 (3.10)	0.98	-	4.17	-	-	477
		H+M	34.1 (3.01)	0.91	-	3.68	-	-	636

4.3.4 Trait correlations

A summary of the phenotypic (r) and genetic (r_g) correlations between ground and aerially measured traits measured on different dates and for the season as a whole, are shown for both crops in Table 4.9 and Table 4.10, respectively, and shown graphically in the Appendix (Figure 8.11). The data were also considered for different categories of CWSI, as shown for both crops in Table 4.11. These will be discussed in depth in the following sections.

Table 4.9. Phenotypic correlations (r) estimated in the plant and ratoon crops between stalk yield (SDM) with green canopy cover (FIPAR) and stomatal conductance (g_s); FIPAR and normalized difference vegetation index (NDVI); g_s and canopy temperature (Tc) and SDM with NDVI and Tc, for the well-watered (WW) and water deficit (WD) treatments measured for different flights (carried out on specified days after planting, DAP, or days after harvest, DAH) and for the season. For each flight and treatment, average canopy cover (FIPAR) values were categorized as partial (P) or full (F) canopy, and crop water satisfaction index (CWSI) values categorized as low (L), medium (M) or high (H). Values in bold with an asterisk indicate statistical significance at p = 0.05.

Crop	Flight	DAP / DAH	FIPAR		CWSI		SDM vs. FIPAR		SDM vs. g_s		FIPAR vs. NDVI		g_s vs. Tc		SDM vs. NDVI		SDM vs. Tc	
		Water treatment:	WW	WD	WW	WD	WW	WD	WW	WD	WW	WD	WW	WD	WW	WD	WW	WD
Plant	1	118	P	P	H	H	0.46	-0.35	**0.91***	**-0.81***	**0.87***	**0.71***	-0.55	-0.40	**0.64***	**0.36***	**-0.59***	**-0.48***
	2	138	P	P	H	H	0.50	-0.48	**0.75***	0.27	**0.70***	0.41	-0.57	-0.11	**0.56***	**0.32***	**-0.56***	**-0.40***
	3	161	F	P	H	H	0.38	-0.03	0.06	0.22	**0.67***	0.39	-0.36	0.12	**0.53***	**0.28***	**-0.24***	-0.00
	4	189	F	P	H	M	0.31	0.16	**0.84***	**0.77***	**0.73***	0.34	0.08	0.18	**0.54***	**0.53***	-0.00	-0.20
	5	217	F	F	H	M	0.42	0.24	**0.78***	0.05	0.39	0.22	-0.22	0.63	**0.40***	**0.29***	-0.17	-0.19
	6	265	F	F	H	L	0.28	0.13	-	0.57	0.06	0.20	-	0.40	**0.45***	0.22	0.00	0.00
	7	336	F	F	H	L	0.27	0.49	0.57	-	0.15	0.19	-0.32	-	**0.32***	**0.37***	-0.20	-0.20
		Seasonal ave	-	-	-	-	0.54	0.15	**0.88***	0.38	**0.69***	0.00	**-0.32***	0.21	**0.65***	**0.47***	**-0.54***	**-0.46***
Ratoon	1	467 / 123	F	F	H	H	0.36	-0.42	0.10	0.45	0.39	**0.84***	0.00	-0.45	**0.45***	**0.55***	**-0.32***	**-0.33***
	2	497 / 153	F	F	H	H	0.48	-0.20	0.14	0.22	0.31	0.51	-0.30	-0.56	**0.32***	**0.62***	**-0.37***	**-0.36***
	3	511 / 167	F	F	H	M	0.30	-0.05	0.14	0.53	0.31	0.18	-0.17	0.00	**0.65***	**0.57***	**-0.48***	**-0.32***
	4	685 / 341	F	F	H	H	-	-	**0.75***	0.36	-	-	-0.22	0.00	-	-	**-0.44***	**-0.33***
		Seasonal ave	-	-	-	-	0.56	-0.20	0.17	0.00	0.61	**0.72***	**-0.41***	-0.26	**0.75***	**0.62***	**-0.57***	**-0.44***

Table 4.10. Genetic correlations (r_g) estimated in the plant and ratoon crops between stalk yield (SDM) with green canopy cover (FIPAR) and stomatal conductance (g_s); FIPAR and normalized difference vegetation index (NDVI); g_s and canopy temperature (Tc); SDM with NDVI and Tc, for the well-watered (WW) and water deficit (WD) treatments measured for different flights (carried out on specified days after planting, DAP, or days after harvest, DAH) and for the season. Values in bold with an asterisk indicate statistical significance at p = 0.05.

Crop	**Flight**	**DAP / DAH**	**SDM vs. FIPAR**		**SDM vs. g_s**		**FIPAR vs. NDVI**		**g_s vs. Tc**		**SDM vs. NDVI**		**SDM vs. Tc**	
		Water treatment:	WW	WD	WW	WD	WW	WD	WW	WD	WW	WD	WW	WD
Plant	1	118	0.23	-0.26	0.97	-0.90	0.49	0.63	-0.34	-0.02	0.50	0.32	-0.40	-0.16
	2	138	0.27	-0.34	0.50	0.18	0.69	0.51	-0.05	0.55	0.54	0.36	-0.32	-0.19
	3	161	0.51	-0.19	0.29	0.22	0.61	0.18	-0.01	-0.05	0.47	0.26	0.10	-0.07
	4	189	0.17	0.12	0.09	0.05	0.02	-0.23	-0.67	0.65	0.41	0.34	0.10	-0.19
	5	217	0.09	-0.23	-0.24	-0.26	0.03	-0.15	-0.30	0.78	0.40	0.29	-0.01	-0.21
	6	265	-0.21	-0.10	-	-0.73	0.05	-0.19	-	-0.06	0.37	0.22	-0.05	0.04
	7	336	0.11	0.17	0.31	-	0.04	0.08	-0.20	-	0.27	0.32	0.04	-0.19
		Seasonal ave	0.39	0.10	0.62	0.19	0.39	-0.49	-0.25	0.15	0.24	0.08	-0.03	-0.07
Ratoon	1	467 / 123	0.36	-0.39	0.70	-0.39	0.36	0.57	-0.28	0.26	0.25	0.55	-0.29	-0.36
	2	497 / 153	0.34	-0.10	0.57	0.10	0.30	0.67	-0.50	-0.70	0.19	0.60	-0.48	-0.15
	3	511 / 167	0.21	-0.01	0.41	0.39	0.33	0.41	-0.02	0.46	0.42	0.59	-0.15	-0.30
	4	685 / 341	-	-	0.71	0.44	-	-	-0.34	0.12	-	-	-0.17	-0.15
		Seasonal ave	0.35	-0.12	0.50	0.19	0.63	0.71	-0.30	-0.10	0.22	0.39	-0.11	-0.26

Table 4.11. Phenotypic (r) and genetic correlations (r_g) estimated in the plant and ratoon crops between stalk yield (SDM) with stomatal conductance (g_s); g_s and canopy temperature (Tc); SDM with normalized difference vegetation index (NDVI) and Tc. Data were considered for two water treatments (well-watered, WW and water deficit, WD), and for different categories of crop water satisfaction (high, H; medium, M; and low, L), and combinations thereof.

		Variable	SDM vs. g_s		g_s vs. Tc		SDM vs. NDVI		SDM vs. Tc	
Crop	Water treatment	Crop water satisfaction category	r	r_g	r	r_g	r	r_g	r	r_g
Plant	WW	H	**0.88***	0.62	**-0.32***	-0.25	**0.65***	0.24	**-0.55***	-0.03
	WD	H	**0.73***	-0.45	**-0.50***	0.20	**0.43***	0.16	**-0.40***	-0.09
		M	**0.83***	0.02	0.14	0.62	**0.40***	0.21	**-0.49***	-0.11
		L	0.32	-0.73	-0.10	-0.06	0.30	0.15	**-0.52***	-0.08
		H+M	0.33	-0.10	0.00	0.45	**0.48***	0.13	**-0.48***	-0.10
		M+L	**0.85***	-0.34	0.22	0.32	**0.37***	0.11	**-0.53***	-0.07
		H+M+L	0.26	0.19	0.26	0.15	**0.47***	0.08	**-0.55***	-0.07
Ratoon	WW	H	0.17	0.50	**-0.41***	-0.30	**0.75***	0.22	**-0.57***	-0.11
	WD	H+M	0.38	0.19	0.21	-0.10	**0.62***	0.39	**-0.49***	-0.26

Trait impacts on stalk yield

SDM and FIPAR

Phenotypic (r) and genetic (r_g) correlations between SDM and FIPAR are shown for flight days in Table 4.9 and Table 4.10 respectively, and shown fully for all measurement days in the Appendix (Figure 8.11). Correlations between SDM and FIPAR for the WW treatment of the plant crop were strongest and significant at partial canopy at 98 (r = 0.73*) and 109 DAP (r = 0.66*) when FIPAR differed significantly between genotypes (Table 4.2, Figure 8.11). FIPAR values could be combined for these two measurement dates (F.pr. = 0.59), and the overall correlation was also significant (r = 0.71*). The relationship was also significant at 422 DAP (78 DAH) in the WW treatment of the ratoon crop, when FIPAR differed significantly between genotypes (Table 4.2, Table 4.9). The relationship was not significant for the WD treatment, presumably because water stress caused yield loss without affecting FIPAR. Furthermore, the genetic correlations between SDM and FIPAR were moderate for the WW treatments of the plant (r_g of 0.38 and 0.50 at 98 and 109 DAP, respectively) and ratoon crops (r_g of 0.49 at 422 DAP) when FIPAR differed significantly between genotypes (Table 4.10).

SDM and g_s

SDM and gs correlated significantly in the plant crop for all measurement dates (r = 0.75* – 0.91*) except at 161 and 336 DAP, across the season for the WW treatment (r = 0.88*) (Table 4.9). By comparison, the relationship for the WD treatment varied over time, where SDM and g_s showed a strong negative correlation in the pre-stress period at 118 DAP (r = -0.81*), and a significant positive correlation (r = 0.77*) shortly after the imposition of mild water stress at 189 DAP (shown graphically in Figure 4.6). Against expectation, the ratoon crop results showed mostly statistically non-significant phenotypic correlations, and generally poor genetic correlations, between SDM and g_s for individual measurement dates, over the season, and for categories of CWSI. The limited number of measurements conducted (particularly early in the crop cycle), coupled with the high error variance associated with g_s data, may have contributed to the mostly statistically non-significant correlations observed. Data collection in the ratoon crop was hindered by COVID-19 lockdown restrictions, impacting the number of measurements taken.

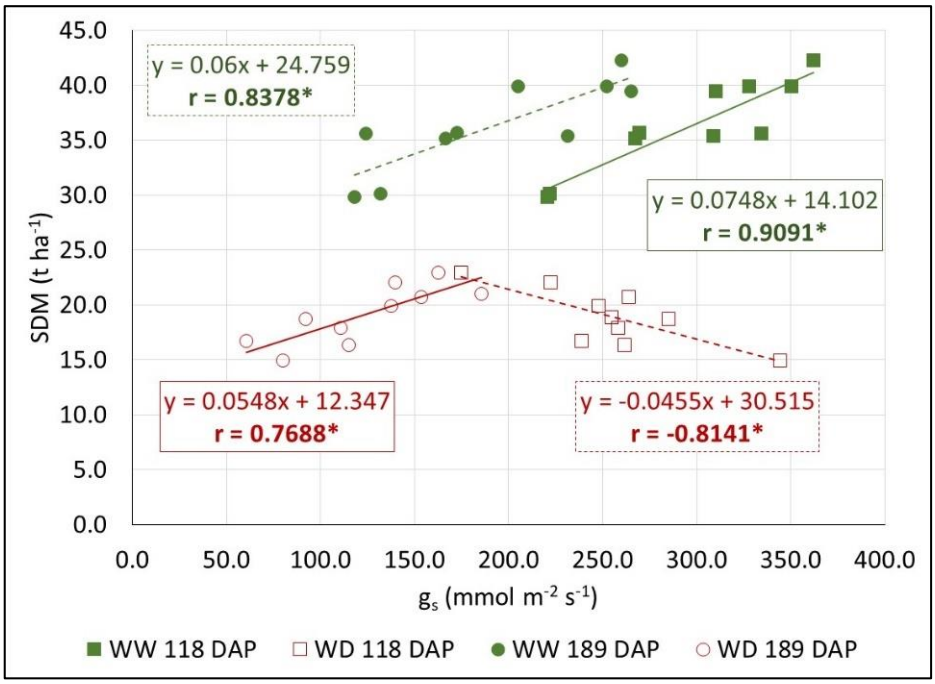

Figure 4.6. Relationship between stalk dry mass (SDM) and stomatal conductance (g_s) measured at 118 (pre-stress) and 189 (mild stress) days after planting (DAP) for the well-watered (WW) and water deficit (WD) treatments of the plant crop. Statistical significance at p = 0.05 is indicated with an asterisk.

Trait phenotyping from aerial imagery

FIPAR from NDVI

FIPAR and NDVI correlated well (r = 0.73*) for both water treatments and crops under conditions of partial canopy cover and high CWSI (Figure 4.7). This pooled dataset also showed a strong genetic correlation (r_g = 0.81) between FIPAR and NDVI. Water stress significantly reduced NDVI in the WD treatment of the plant crop under full canopy cover, although this was not observed in ground measurements of FIPAR. As such, the relationship deteriorated with water stress and with crop age.

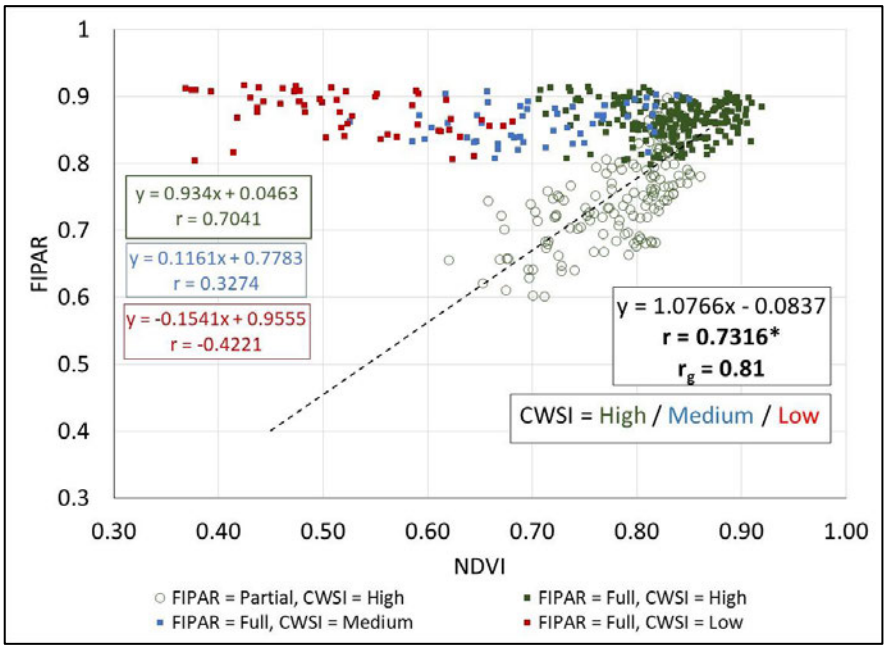

Figure 4.7. Relationship between fractional interception of PAR (FIPAR) and normalized difference vegetation index (NDVI) measured over several flights in the plant and ratoon crops. Data were categorised by canopy cover (partial: open markers; full: coloured markers) and a crop water satisfaction index (high: green; medium: blue; low:, red). Significant phenotypic (r, p = 0.05, with an asterisk) and genetic (r_g) correlations are shown for stress-free crops with partial canopy cover.

g_s from Tc

Data measured in the plant and ratoon crops showed that g_s and Tc were not significantly correlated for individual measurement dates for either water treatment (Table 4.8). However, g_s correlated significantly with Tc when considered across the season for the WW treatment (r = -0.32* and -0.41*, respectively) (Table 4.9). The strength of these correlations may have been impacted by variability in trait estimates due to environmental conditions and the limited genetic diversity of the population that was studied. Consequently, there were no significant genotypic differences in g_s for individual measurement dates (Table 4.3), and spatial variation in Tc obscured genotypic effects in some cases (Table 4.7), confounding the relationships between g_s and Tc.

Yield phenotyping from aerial imagery

SDM from NDVI

SDM and NDVI were mostly significantly correlated for both crops and water treatments throughout and across the season (r = 0.32* to 0.75* and 0.22 to 0.62* for WW and WD conditions, respectively) (Table 4.9). The phenotypic and genetic correlations for the WW treatment declined slightly with crop age and with water stress in the plant crop and were mostly stronger than that of the WD treatment. When the data were considered for categories of CWSI (Table 4.11), phenotypic correlations were significant (r = 0.37* to 0.75*) except when CWSI was low, and genetic correlations were better for the WW treatments (r_g = 0.22 to 0.24) as compared to when stress was imposed.

SDM from Tc

The relationship between SDM and Tc is shown in Figure 4.8. Tc data in the plant crop ranged from approximately 22 to 28 °C during the first two flights, when the mean ambient temperature was 25 °C, mean relative humidity ranged from 75 to 83%, and Ecref ranged from 3.3 to 6.1 mm d^{-1} (Table 8.8). In contrast, Tc data in the ratoon crop showed higher values as compared to the plant crop, ranging from 31 to 35 °C, presumably due to higher Ecref values (4.3 to 8.0 mm d^{-1}) influenced by ambient temperature, low relative humidity, and wind speeds. SDM and Tc were significantly correlated in the plant crop under non-water stressed conditions for the earlier flights (r = -0.24* to -0.59*), as well as for individual measurement days and across the season for the ratoon crop (r = -0.32* to -0.57*), when the spatial variation did not affect Tc estimates (Table 4.9, Figure 4.8). Genetic correlations were also highest for the first two flights of the plant (r_g = -0.16 to -0.40) and ratoon (r_g = -0.15 to -0.48) crops respectively, prior to water stress being imposed. Phenotypic correlations were significant for all categories of CWSI (Table 4.11), though these estimates were considered unreliable given the impact of spatial variation in the data and its influence on Tc estimates. These data also showed poor genetic correlations (r_g = -0.03 to -0.26), presumably due to the impact of spatial variation. The study also considered the relationship between SDM and Tc_i, though the results were not greatly improved compared to that of Tc itself. Phenotypic correlations between SDM and Tc_i were found to only be significant for the first four flights for the two water treatments (r = -0.39* to -0.55*) and when CWSI was high (r = -0.48* to -0.66*), and genetic correlations were also not generally strong (r_g = -0.09 to -0.43).

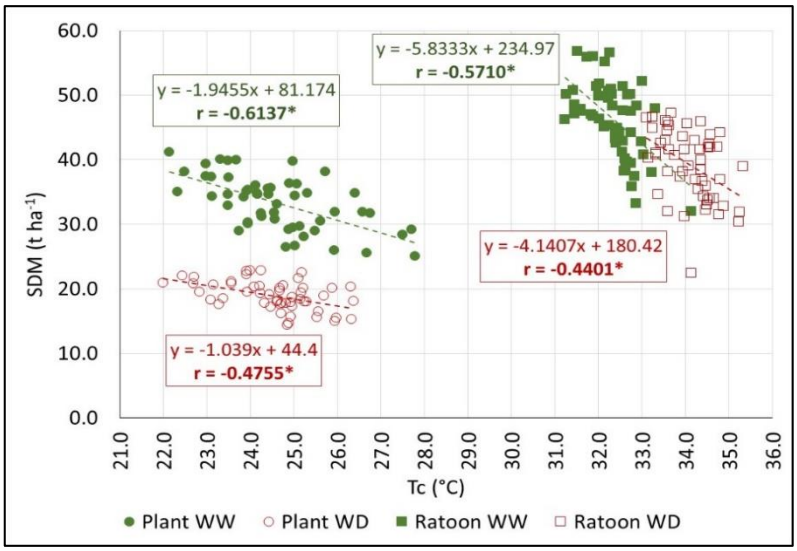

Figure 4.8. Relationship between stalk dry mass (SDM) yield and canopy temperature (Tc), taken as the average value for the first two flights for the respective well-watered (WW) and water deficit (WD) treatments of the plant crop (round series), and as the average over the season for the ratoon (square series) crops, when spatial variation did not significantly affect Tc estimates.

Drought tolerance phenotyping

Interestingly, the study found a significant correlation between SDM* and ΔTc for the initial flights of the plant crop when Tc differed significantly between genotypes (r = -0.55*), and over the season for the ratoon crop (r = -0.56*) (Figure 4.9).

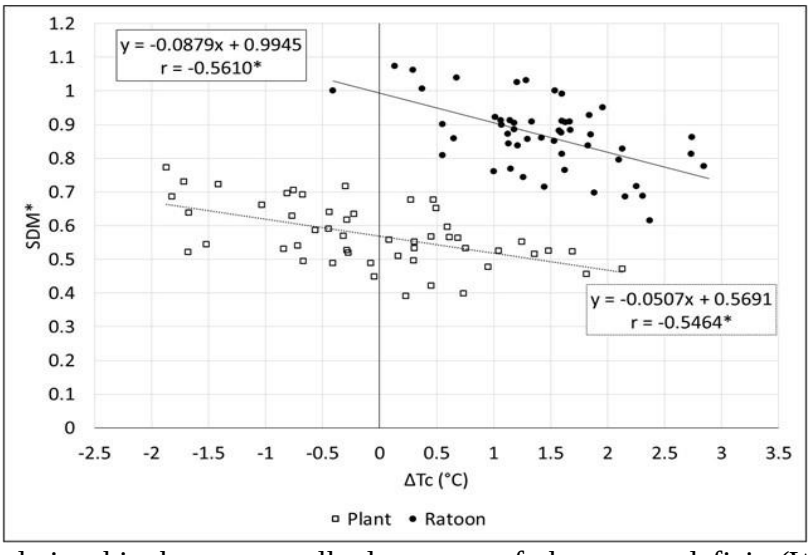

Figure 4.9. Relationship between stalk dry mass of the water deficit (WD) treatment expressed relative to the corresponding well-watered (WW) values (SDM*), and differences in canopy temperature between the WD and WW treatments, taken as the average value per genotype. Results from both the plant and ratoon crops are shown.

4.4 Concluding discussion

The study aimed to address the following research questions:

Question 1: *Is SDM influenced significantly by FIPAR and g_s, and if so, how much genotypic variation exists and how heritable are these key traits?*

The study confirmed both FIPAR and g_s as influential traits for determining SDM. FIPAR could be used as an indicator of early vigour to identify high- and low-yielding genotypes in well-watered crops, as early as 98 and 78 DAP in plant and ratoon crops, respectively. FIPAR also showed significant genotypic variation and high heritability when measured early in the crop cycle under well-watered conditions, confirming previous research which also reported significant genotypic variation in canopy development rates within diverse genetic populations (Basnayake et al., 2015; Dias et al., 2020; Donaldson et al., 2008; Evensen et al., 1997; Inman-Bamber, 1994; Jones et al., 2019; Robertson et al., 1996; Singels et al., 2005). By contrast, g_s showed limited genotypic variation, likely due to the limited genetic diversity within the trial population and practical constraints in the measurement protocol, resulting in low heritability for this trait.

SDM could also be predicted from g_s in well-watered crops, aligning with previous research which showed generally positive correlations between g_s and stalk yield under well-watered or mildly water stressed sugarcane crops (Basnayake et al., 2015; Hoffman et al., 2018; Li et al., 2017; D. Zhao et al., 2017). Furthermore, the interesting preliminary finding that high g_s is desirable only in stress-free environments, and that relatively low g_s may be advantageous in environments where water deficit is likely, requires further investigation. Understanding and selecting for optimal g_s in sugarcane could be crucial in developing resilient varieties that can maintain productivity under the predicted future increase in water deficit conditions due to climate change (Lobell et al., 2013, 2008; Meehl et al., 2007; Schulze and Kunz, 2010; Zhao and Li, 2015). A previous study by Inman-Bamber et al. (2012) showed, through a crop modelling approach, that yield increased (approximately 3 – 5%) in response to reduced conductance in very dry environments with better (deep) soils only, due to the crop conserving water for use during dry periods. The use of process-based crop modelling with long-term simulations could be used to evaluate the potential benefit of selecting for increased or reduced conductance for specific target environments in breeding. Additional work is also needed to demonstrate significant genotypic variation and high

heritability in g_s, as this was not found in the current due to the limited dataset that was considered.

Question 2: *Can FIPAR and g_s be phenotyped reliably through aerially measured NDVI and Tc?*

FIPAR could be reliably estimated from NDVI for well-watered crops at partial canopy, with the relationship showing strong phenotypic and genetic correlations. The relationship was found to deteriorate with water stress and with crop age, aligning well with previous research (Begue et al., 2010; Morel et al., 2014; Muller et al., 2020). Further experimental validation is needed to confirm that earlier measurements of NDVI effectively capture genotypic differences in FIPAR and early vigour in breeding populations.

Furthermore, the results suggest that g_s could be more reliably estimated from Tc for well-watered crops, though the strength of correlations may be too weak for effective enhancement of breeding. These results highlighted the complexities in measuring both g_s and Tc, which possess an inherently complex relationship that is further confounded by the variability in trait estimates due to environmental conditions. For example, genotypic differences in Tc were obscured by noise in the data and by spatial variation, particularly in the latter flights of the plant crop. The noise and spatial variations in Tc could be due to a combination of factors, including soil heterogeneity within the field, variability in irrigation application, and drift effects from the thermal camera, attributable to internal heat from uncooled microbolometers and external thermal loading from the sun (Gonzalez-Dugo et al., 2012; Kelly et al., 2019; Mesas-Carrascosa et al., 2018). Further work to improve this relationship for effective use in breeding on a routine basis will require extensive measurements of g_s carried out on a genetically diverse population, with improved data acquisition and image processing procedures which account for spatial variation in Tc. Attempts to statistically correct for spatial variation in Tc were largely unsuccessful in the current study.

Question 3: *Can high yielding and/or drought tolerant genotypes be identified through UAV captured NDVI and Tc?*

Encouragingly, the data presented in this study show promise for the use of NDVI and Tc to identify high- and low-yielding genotypes earlier on in well-watered crops, which could

bode well for application in breeding. These traits mostly showed significant genotypic variation, significant phenotypic and genetic correlations with yield, as well as moderate to high broad-sense heritability, which bodes well for application in breeding. Zhao et al., (2016) also demonstrated the potential of using NDVI measured at the early growth stages as a screening tool for yield in early-stage breeding trials in Florida. However, this study made use of proximal sensing close to the crop canopy, where the multispectral sensor was mounted on a pole. Begue et al. (2010), Ueno et al. (2005) and Almeida et al. (2006) suggested that sugarcane yield is reliably predicted from NDVI about two months prior to harvest (or crop age of ~8-10 months), under a range of moisture conditions, although these studies considered NDVI derived from satellite imagery for commercial conditions. A more recent study by Khuimphukhieo et al. (2023) reported significant correlations between aerially measured NDVI and yield at between 155-323 DAP, and while this was deemed promising for use in breeding, the study only considered a limited number of genotypes (seven). Other studies have reported significant relationships between yield and Tc for sugarcane (Basnayake, 2016; Basnayake et al., 2015; Chapman et al., 2014) demonstrating its potential as a screening tool. Natarajan et al. (2019) showed promising results for the use of aerial screening of NDVI and Tc in large breeding populations (40-2134 genotypes) using a selection index approach. While this approach is not currently used for sugarcane breeding in South Africa, the trait information presented in this study could be used in the development of selection indices for genotype selection in future work.

Furthermore, novel results showed that canopy temperature differences between water treatments could be used to identify drought tolerant genotypes, a finding which has not been reported previously for sugarcane. However, the inconsistent performance of SDM across different water environments highlights the challenge of selecting widely adapted genotypes, particularly for rainfed environments. This limitation emphasizes the need for additional research to refine UAV-based screening across different water regimes.

Question 4: *How can the AP procedure developed in this study be improved?*

The study highlighted a few areas that require improvement in AP procedures to improve its reliability for identifying superior genotypes. Estimation of NDVI could be improved in future by using a more sophisticated discrete narrow-band multispectral camera (e.g. Micasense RedEdge-MX; MicaSense, Inc., USA), enabling the investigation of other vegetation indices more sensitive to small changes in biomass and yield, as compared to NDVI. The AP procedure for estimating Tc could also be improved with the use of: (1) a more sophisticated thermal camera, such as the FLIR TAU2 640 (as in Natarajan et al., 2019) or Micasense Altum-PT; (2) using more ground calibration points; (3) correcting for thermal drift by using an integrated UAV capture board suited to the thermal camera (as in Natarajan et al. (2019); TeAx ThermalCapture, Germany); (4) more accurately masking soil and senesced leaf pixels using alternate approaches possible with higher resolution thermal images (Jones and Sirault, 2014). Despite these limitations in the AP procedures used, the study was still able to detect significant genotypic differences in aerially measured traits over the season, for different stages of canopy development and under a range of moisture conditions.

Overall, the study highlighted FIPAR and g_s as impactful traits for determining SDM. FIPAR was identified as an early indicator of vigour, distinguishing high- and low-yielding genotypes under well-watered conditions. While g_s was also impactful for determining SDM in well-watered crops, its limited genotypic variation in this study suggests that future research should expand the genetic population to enhance the understanding and application of g_s in breeding. The study demonstrated the effectiveness of NDVI in estimating FIPAR for well-watered crops with partial canopy cover, while also underscoring the complexities of accurately phenotyping g_s through Tc. This emphasizes the need for refined measurement and data processing techniques to enhance their application in breeding. Encouragingly, the results suggest that NDVI and Tc could be valuable tools for the early identification of high-yielding and drought-tolerant genotypes, with further validation needed for broader application in breeding programs. The study also provided valuable insights into the improvements required in AP procedures to enhance their reliability for identifying superior genotypes in future studies.

5. BREEDING TRIALS: VALIDATION OF AERIAL PHENOTYPING PROCEDURE

5.1 Introduction

The aerial phenotyping (AP) procedure described in Chapters 3 and 4 was implemented in two early-stage (single-row plot) breeding trials. The aim of this work was to assess the ability of AP to discern clonal performance in breeding populations. The current conventional breeding approach is resource-intensive and time-consuming, constrained by long breeding cycles, large trial sizes and complex phenotyping of large populations. This experimental phase was used to test whether AP could streamline these procedures and improve the efficiency of screening and selection within large populations, ultimately contributing to yield improvement.

The specific objectives were to:

1. Assess the genotypic variation and broad-sense heritability of ground and aerially measured traits, and determine their correlations with stalk dry mass yield (SDM).
2. Determine the accuracy of selecting high-yielding genotypes using direct (SDM-based) vs. indirect (based on aerially measured traits) approaches.
3. Evaluate the feasibility and potential benefit of implementing AP in the breeding program.

5.2 Methodology

5.2.1 Trial design and operations

The early-stage single-row field trials, established by the breeding department as part of stage 2 of the selection program, were conducted at the SASRI Empangeni research farm (28°43’33.0”S, 31°53’51.0”E), which is a selection site for the coastal short cycle (12 months) rainfed breeding programme.

Both field trial areas at this site comprised a red clay soil, classified as a Shortlands soil form (Soil Classification Working Group, 1991), broadly equivalent to Rhodic Nitisols (Micheli et al., 2006), with between 35 - 55% clay in the B horizon. Visual assessment of soil pits showed an Orthic A horizon to depths of 15 - 30 cm, and a red structured B horizon to depth of 65 – 90 cm. Average estimated rooting depth is approximately 1.0 m. Soil profiles of selected banks are shown in the Appendix (Table 8.12).

Breeding trial 1: SR 19-20

The SR 19-20 breeding trial (plant crop) comprised of 2008 genotypes and 15 controls (released varieties), which were replicated twice within the trial (4240 single-row plots).The trial was planted using an alpha lattice design across 11 parts. Each part comprised several (6-8) banks. A bank is defined as a column of single-row plots that extends the length of the field. Each single-row plot measured 4 m in length with 1.2 m row-spacing. Of the 15 control varieties, only five were planted within every part of SR 19-20 (NCo376, N41, N55, N56 and N58). These varieties, with known relative performance and genetic potential, served as benchmarks to account for trial heterogeneity and to facilitate evaluation of genotype performance within each part. The trial spanned three fields (Field 31 A and B, and Field 32D), covering approximately 3.5 ha (Figure 5.1). Planting took place from 5 - 27 March 2019, starting sequentially with Part A, and ending with Part J. Part K was planted approximately three months after Parts A-J due to lack of seedcane, and was therefore excluded from the analysis. The cropping cycle for coastal rainfed areas is typically 12 months, however due to operational delays (due to COVID-19 lockdown), harvesting was carried out at a crop age of 17 months, from 31 August - 8 September 2020.

Breeding trial 2: SR 21-22

The SR 21-22 breeding trial (ratoon crop) comprised of 1771 genotypes and 15 controls, which were replicated twice (3860 single-row plots). The trial was planted using an alpha lattice design across 11 parts, each comprising 2-9 banks each, with single-row plots measuring 6 m in length with 1.2 m row-spacing. Of the 15 control varieties, only seven were planted within every part of SR 21-22 (NCo376, N19, N31, N41, N51, N55 and N58). The trial was located adjacent to that of SR 19-20 and spanned two fields (Fields 63 and 64), covering approximately 6 ha (Figure 5.2). Planting took place between 24 March and 26 May 2020, with disruptions caused by the COVID-19 pandemic, and the plant crop was harvested from 4 - 19 October 2021. This study monitored the ratoon crop, which was grown from 20 October 2021 until harvest, between 17 - 31 October 2022.

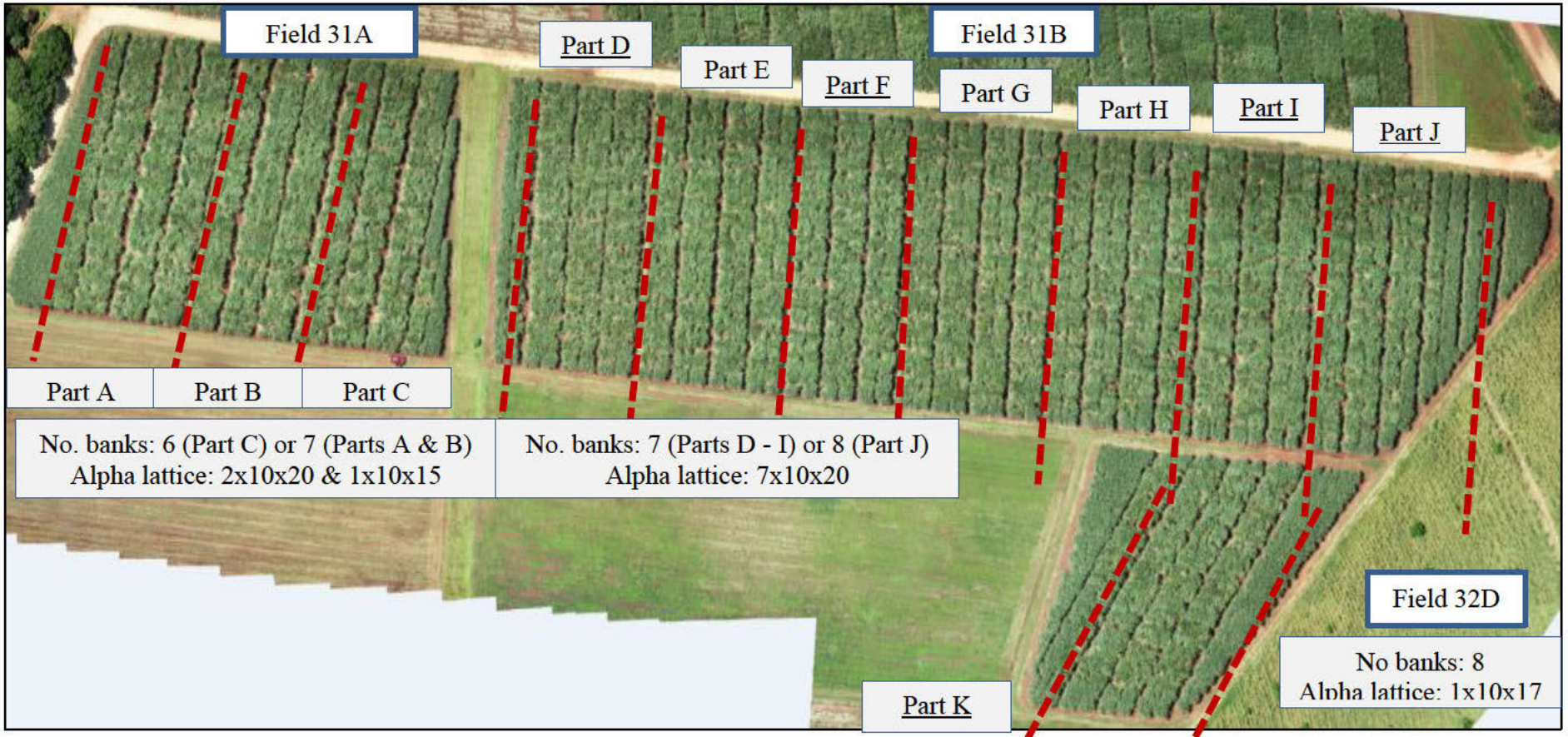

Figure 5.1. Aerial image of the first Empangeni single-row breeding trial (SR 19-20) comprising 2008 genotypes and 15 control varieties, with two replicates (total of 4240 single-row plots). Fields 31A, B and 32D include several trial parts, with 6-8 banks (columns of single-row plots extending the length of the field) in each, planted as an alpha lattice design. The image was captured on 16 January 2020, at a crop age of approximately 11 months.

Figure 5.2. Aerial image of the second Empangeni single-row breeding trial (SR 21-22) comprising 1771 genotypes and 15 control varieties, with two replicates (total of 3860 single-row plots). Fields 63 and 64 include several trial parts, with 2-9 banks (columns of single-row plots extending the length of the field) in each, planted as an alpha lattice design. The image was captured on 10 January 2022, at a crop age of approximately 3 months.

5.2.2 Ground measurements

Weather

Daily solar radiation (SRAD, MJ m^{-2} d^{-1}), temperature (°C), relative humidity (RH, %), rainfall (mm) wind speed (m s^{-1}) and vapour pressure deficit (VPD, kPa) were recorded using an automatic weather station located ~500m from the trial sites. Daily sugarcane reference evapotranspiration data (Ecref, mm d^{-1}) (McGlinchey and Inman-Bamber, 1996) were calculated from hourly weather data.

Soil water status

Soil water status (SWS) index was measured with Aquacheck capacitance-based continuous logging probes, installed vertically down to 80 cm into the soil profile.

The SR 19-20 trial was monitored for SWS using four probes that were installed in single-row plots of NCo376 in Banks 1 (Part A), 11 (Part B), 39 (Part F) and 65 (Part J). The SR 21-22 trial was also monitored for SWS with four probes, installed in Banks 11 (Part B) and 44 (Part F) of Field 63, and in Banks 57 (Part G) and 75 (Part J) of Field 64.

The MyCanesim® crop model was used to investigate climatic and water status effects on yield. To compare observed SWS with simulated crop water status, SWS was compared to the user specified ASWC. The highest and lowest SWS values were compared to ASWCmax and ASWCmin values, taken as 130 mm and 0 mm in the SR 19-20 trial respectively, and 122 mm and 0 mm in the SR 21-22 trial, respectively. Parameters used in the MyCanesim® simulations are shown in Table 5.1.

Table 5.1. MyCanesim® parameters used to simulate the SR 19-20 and SR 21-22 trials.

Trial	SR 19-20	SR 21-22
Crop start / harvest date	6 Mar 2019 – 31 Aug 2020	20 Oct 2021 – 10 Oct 2022[1]
Crop type	Plant	Ratoon
Variety	NCo376	NCo376
Row-spacing	1.2m	1.2m
Soil parameters	• Clay loam • Rooting depth of 100 cm • Clay content: 39% • Silt content: 10% • ASWCmax: 130 mm	• Clay loam • Rooting depth of 100 cm • Clay content: 47% • Silt content: 6% • ASWCmax: 122 mm
Initial ASWC	Full profile at the start of simulation[2]	Full profile at the start of simulation[3]

[1] The start date of the ratoon crop was taken as the day following the completion of the plant crop harvest.

[2] Assumed full profile at the start of the simulation, given the total rainfall experienced by the crop in the month preceding, and month of, planting (190 mm, including one rainfall event of 86 mm two weeks prior to planting).

[3] Assumed full profile at the start of the simulation, given the total rainfall experienced by the crop in the month preceding, and month of, crop start (139 mm, with 53 mm occurring two weeks prior to crop start).

Stalk yield

Manual harvesting of all single-row plots was carried out from 31 August - 8 September 2020 in trial SR 19-20, and 17 – 31 October 2022 in trial SR 21-22, respectively. Yield components, namely stalk population (SPOP, number of stalks per plot), stalk height (SH, of 3 stalks per plot) and diameter (SD, at the centre of 3 stalks per plot), were recorded. A sub-sample of 12 stalks from each plot was used to estimate dry matter content using mill-room analysis, as described previously in Section 3.2.2.

Stalk fresh mass yield (SFM, kg m^{-1}) was calculated using two methods: (1) SFM_1, using the product of stalk fresh mass per stalk (SM, determined from mill-room sub-samples, kg $stalk^{-1}$) and SPOP (stalks m^{-1}); (2) SFM_2, using stalk radius (SR, cm), stalk height (SH, cm) and SPOP (stalks m^{-1}) (De Sousa-Vieira and Milligan, 1999), assuming a specific gravity of 1.0 g cm^{-3} for a perfect cylinder (Gravois et al., 1991):

$$SFM_1 = SM * SPOP \quad \text{(Equation 25)}$$

$$SFM_2 = \frac{\pi SR^2 SH * SPOP}{1000} \quad \text{(Equation 26)}$$

There was a good relationship between the two methods (Figure 5.3) in both breeding trials, though method one showed slightly less variation presumably due to the lower error associated with fewer variables. Method one was therefore used to estimate SFM. SDM was calculated as the product of SFM and dry matter content.

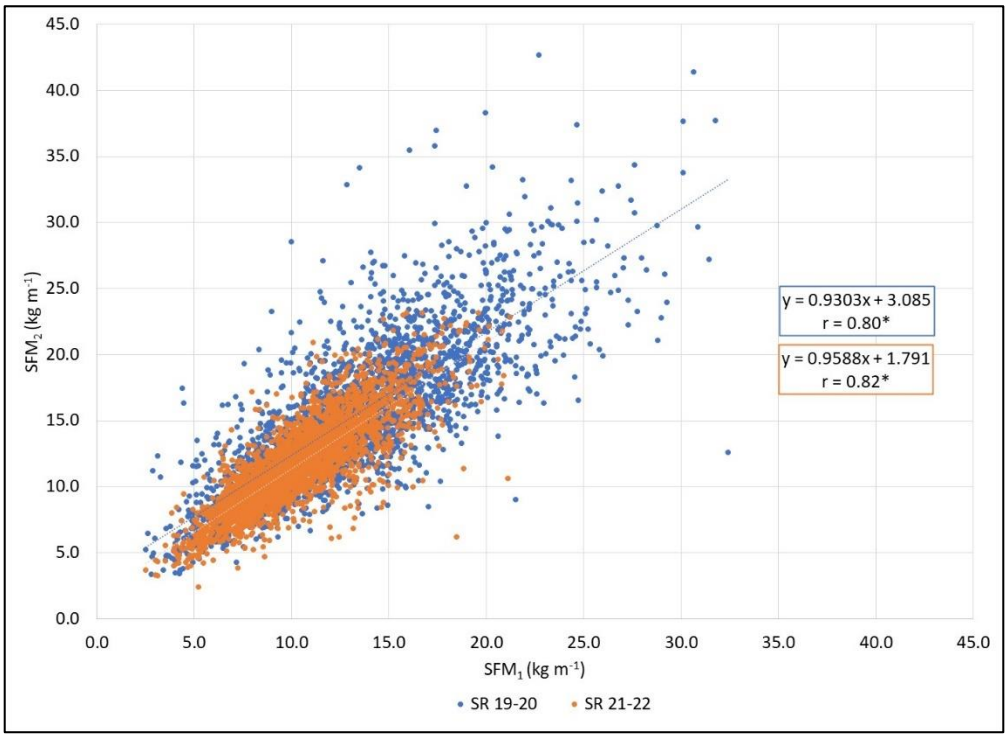

Figure 5.3. Comparison of two methods to estimate stalk fresh mass yield (SFM) in two breeding trials (SR 19-20 and SR 21-22). Method 1 (SFM_1) was calculated as the product of stalk fresh mass per stalk and stalk population, while method 2 (SFM_2) used stalk radius, height and population. Statistical significance at p = 0.05 is indicated with an asterisk (n = 2644 and 2555 for SR 19-20 and SR 21-22, respectively).

5.2.3 Aerial imaging

Section 4.2.3 describes the aerial data acquisition procedures that were followed. Crop reflectance and emittance in the respective bands were captured on three measurement days in the SR 19-20 trial, at 317, 331 and 385 DAP, when the crop canopy was fully developed and CWSI was medium (flights 1 and 2, respectively) and high (flight 3) (Table 5.2). The weather conditions for these dates are given in the Appendix (Table 8.15 and Table 8.16).

Drone flights were carried out on five measurement days in the SR 21-22 trial, between 51 – 245 DAH. The first two flights were performed under partial canopy conditions, when

CWSI was high. For the third flight, the crop was considered fully canopied based on MyCanesim® simulation data and visual assessment of the RGB, and CWSI was high. NIR and thermal imagery could not be captured on the second and third flights respectively, due to technical difficulties with AP equipment and in-field instrument breakdown. The fourth and fifth flights were conducted under full canopy conditions with high CWSI. The weather conditions for these dates are given in the Appendix (Table 8.20 and Table 8.21).

To categorise flights according to the extent of canopy cover, FIPAR was estimated from the average NDVI measured in each flight, using the regression developed in Section 4.3.4. It was not feasible to conduct measurements of FIPAR in the breeding trials given the large number of treatments and trial design (single lines). Flights were also categorized according to soil water status, as described in Section 4.2.3.

Table 5.2. Details of drone flights to capture visual (RGB), near infrared (NIR) and thermal imagery in the Empangeni breeding trials. Several flights were carried out over the course of the two crops (days after planting, DAP, or days after harvest, DAH). For each flight, the average canopy cover (FIPAR) values were categorized as partial (P) or full (F), and the crop water satisfaction index (CWSI) values were categorized as low (L), medium (M) or high (H). For each flight, the time of capture and spatial resolution of images are given.

Trial	**Flight**	**Date (DAP / DAH)**	**NDVI**	**FIPAR**	**CWSI**	**Time of flight**			**Spatial resolution (cm)**		
						RGB	NIR	Thermal	RGB	NIR	Thermal
SR 19 – 20	1	16 Jan 20 (317)	0.82	0.80 (F)	0.66 (M)	13:40	10:45	11:05	2.0	6.1	17.2
	2	30 Jan 20 (331)	0.85	0.83 (F)	0.67 (M)	12:45	9:15	11:55	1.9	4.8	14.1
	3	24 Mar 20 (385)	0.90	0.89 (F)	1.00 (H)	11:25	9:45	9:25	1.9	5.0	12.9
SR 21 - 22	1	9 Dec 21 (51)	0.73	0.70 (P)	1.00 (H)	10:00	10:10	12:15	2.5	6.4	15.5
	2	10 Jan 22 (83)	0.79	0.76 (P)	1.00 (H)	09:45	11:40	-	2.2	6.9	-
	3	3 Mar 22 (135)	-	-	0.76 (M)	10:20	-	11:45	2.9	-	16.1
	4	18 May 22 (211)	0.82	0.80 (F)	1.00 (H)	09:00	09:55	13:30	2.1	5.9	17.5
	5	21 June 22 (245)	0.81	0.80 (F)	1.00 (H)	10:50	11:15	11:50	2.2	5.6	17.9

Image processing & data analysis

Visual (RGB), NIR and thermal imagery

Section 4.2.3 describes the hardware and image processing procedures used for RGB, NIR and thermal imagery. This is also shown graphically in the Appendix (Figure 8.6). In contrast to these methodologies described previously, RGB images from both breeding trials were digitised for analysis of individual plots. Additionally, crop reflectance measurements in the SR 21-22 trial were obtained using a discrete narrow-band multispectral camera (e.g. Micasense RedEdge-MX; MicaSense, Inc., USA), representing an advancement in hardware technology compared to the earlier phases of the study. RGB and NIR images were triangulated and mosaicked using the structure from motion algorithm, and geo-rectified using nine GCPs, in the Pix4D Mapper® photogrammetry software package (v4.5.6; Pix4D, Lausanne, Switzerland) according to recommended procedures. Average NDVI values were computed from pixels within individual plots.

Thermal image acquisition procedures were also refined with additional geotagging hardware (FLIR Vue Pro GPS Geotagger, Drone Base Inc., Italy), which facilitated accurate spatial referencing of captured imagery. Average Tc values were computed from leaf pixels extracted from individual plots. The Tc data did not show strong spatial trends with column or row number as described previously in Section 4.2.3, and therefore did not require statistical correction.

5.2.4 Statistical analyses

Initial assessment of ground measured data (i.e. SPOP, SH, SD and SM) collected at harvest in the SR 19-20 trial showed high variability (where data were often outside of accepted bounds), missing data, and inconsistencies between ground and aerial measurements (e.g. plots recorded as not having germinated, but growth visible on the RGB imagery). Gound and aerially measured data that were collected in the breeding trials were filtered using exclusion criteria to remove suspect data (Table 5.3).

Table 5.3. Exclusion criteria applied to ground and aerially measured data captured in the Empangeni breeding trials.

Exclusion criteria	Range / condition
Stalk height	Blank / zero values, > 3.5 m
Stalk diameter	< 10 and > 60 mm
Stalk population	< 12 and > 95 stalks per plot
Cane dry matter content	<20 and > 35 %
Individual stalk mass	< 0.2 and > 2.5 kg
Aerial imagery	Exclude plots which could not clearly be delineated due to overlapping growth of the cane
Replication	Genotypes with fewer than two replications after exclusion criteria applied
Reference genotype	Exclude trial parts where NCo376 did not meet criteria

Datasets were analysed in the SAS software package (The SAS institute, Cary, NC, USA). REML analysis was used to test for statistical significance (at $p = 0.05$) of genotypic differences (Fixed model: Genotype; Random model: Rep/Block + Genotype) for the respective ground (SPOP, SH, SD and SDM) and aerially measured (NDVI and Tc) traits. This was done separately for each trial part, measured within individual flights. REML analysis was then repeated for the pooled datasets, for categories of CWSI using amended REML models (Fixed model: Genotype; Random model: Rep/Block + Flight + Genotype).

Furthermore, the genetic coefficient of variation (GCV), broad-sense heritability (HSB), and genetic correlations (r_g) between ground and aerially measured traits were estimated using trait variance and covariance components from REML analysis, as described in Section 4.2.4.

5.2.5 Trait correlations

The phenotypic and genetic correlations between SDM with NDVI and Tc were assessed for categories of CWSI in the SR 19-20 trial. The data were pooled across flights, given that the crop showed similar developmental conditions (full canopy and levels of crop water stress) at the time of aerial measurements. The correlations were also investigated for the respective

traits when values were expressed relative to that of the reference genotype NCo376 (SDM_{ref}, $NDVI_{ref}$ and Tc_{ref}).

Initial assessment of phenotypic correlations using mean trait values for individual genotypes were consistently non-significant (data not shown). To reduce noise in the data, genotype average SDM values within each trial part were ranked from high to low, and partitioned into 10 classes of equal increments based on SDM values. Class average SDM values were then compared to class average NDVI and Tc values. The study therefore reports on the phenotypic correlations for the stratified data. Stratified data could not be used for REML analysis, or for estimating variance components. Genetic correlations using variance components were therefore done based on genotype means, as described in Section 4.2.4.

Correlations between the respective traits were evaluated separately for each trial part measured within individual flights, as well as for categories of CWSI, in the SR 21-22 trial.

5.2.6 Genotype selection

The SASRI breeding program selects superior genotypes from single-row trials by considering stalk yields, pest and disease data and visual assessment of genotype performance in the field (Zhou, 2013). Variability in trait values is typically high due to the high genetic variability, short plot lengths, inter-plot competition dynamics, large trial sizes and spatial variation in soil. Stalk yield data are therefore expressed relative to that of the highest-yielding control (commercial variety) in each trial part, and a given genotype is selected if it outperforms the control. Of the 15 controls planted in each trial, five were consistently planted in every block/part of SR 19-20, and seven were planted throughout SR 21-22. NCo376 was consistently planted across all parts in both trials and was therefore used as the reference variety in both cases. A given genotype was chosen using direct selection (SDM-based) when its average SDM exceeded that of NCo376. A given genotype was chosen using indirect selection (with aerially measured traits) when NDVI and Tc were higher and lower than NCo376, respectively.

Furthermore, the potential for combining the effects of NDVI and Tc to estimate SDM was investigated using two approaches: (1) a vegetation productivity index (VPI); (2) SDM estimated from multiple linear regression analysis of aerially measured traits (SDM_{MLR}).

This was done to enable selection of genotypes with the highest overall performance for aerially measured traits.

VPI was calculated as the product of Normalized NDVI ($NDVI_r$) and Tc (Tc_r):

$$VPI = NDVI_r * Tc_r \quad \text{(Equation 27)}$$

$$NDVI_r = \frac{(NDVI_g - NDVI_{avg})}{NDVI_{max} - NDVI_{min}} \quad \text{(Equation 28)}$$

$$Tc_r = 1 - \frac{(T_g - T_{avg})}{T_{max} - T_{min}} \quad \text{(Equation 29)}$$

where *g* denotes the average trait value for a given genotype; *avg*, *max* and *min* denote the average, maximum and minimum trait values for a given trial part.

For NDVIr and Tcr to carry equal weighting in the estimation of VPI, the respective values measured for a given trial part and measurement day were partitioned into 10 classes and assigned values from 0.1 (corresponding to low productivity) to 1.0 (corresponding to high productivity). VPI was then estimated as the product of these assigned values.

SDM_{MLR} was estimated through equations derived from multiple linear regression analysis of NDVI and Tc, as shown in the Appendix (Table 8.13 and Table 8.14). This analysis assumes linearity between independent (NDVI and Tc) and dependent (SDM_{MLR}) variables. It also assumes that the independent variables are not correlated with one another. This could not be done for flights 2 and 3 in the SR 21-22 trial, as Tc data were not captured in flight 2, and NDVI were not captured in flight 3, respectively.

Selection accuracy

The accuracy of indirect selection (based on aerially measured traits NDVI, Tc, VPI and SDM_{MLR}) was evaluated with the following criteria: (1) the number of positive matches (common genotypes selection by both SDM and the respective aerially measured trait); (2) misses (genotypes selected using SDM, but not with the respective aerially measured trait); (3) false positives (genotypes selected with the aerially measured trait but not with SDM). This was done for the pooled data (categories of CWSI) in the SR 19-20 trial, and for each flight in the SR 21-22 trial.

Selection response

The efficiency of indirect selection was compared to that of direct selection (as described by Falconer and Mackay, 1996). The direct response to selection (R_x) was first estimated, which in this case, describes the expected genetic gain in stalk yield when using SDM directly:

$$R_x = h_x^2 \, \sigma_x \quad \text{(Equation 30)}$$

where h^2_x and σ_x is the broad-sense heritability and phenotypic standard deviation for SDM, respectively. Subsequently, the correlated response (CR_x) described the estimated genetic gain in SDM when using aerially measured traits:

$$CR_x = h_x \, h_y \, r_g \, \sigma_x \quad \text{(Equation 31)}$$

where h_x represents the broad-sense heritability of SDM, and h_y represents the broad-sense heritability of the aerially measured trait being considered (i.e. NDVI, Tc, VPI or SDM_{MLR}); r_g is the genetic correlation between the traits x and y, and σ_x is the phenotypic standard deviation of SDM. The relative efficiency of indirect selection (CR_x/R_x) was then estimated:

$$\frac{CR_x}{R_x} = \frac{h_y \, r_{gxy}}{h_x} \quad \text{(Equation 32)}$$

5.3 Results

5.3.1 Breeding trial 1: SR 19-20

Weather data

Tmax and Tmin averaged over the respective months ranged from 24.9 to 32.5 °C, and from 11.2 to 20.9 °C, respectively (Figure 5.4). The average Tmin value of 16 °C measured over the trial period, was above the base temperature required for phenological development (Singels et al., 2018). The crop experienced a total of 1165 mm of rainfall during the trial period of 18 months. Overall, the seasonal global solar radiation available for the crop was 8855 MJ m^{-2}, with a daily mean of 16.2 MJ m^{-2} d^{-1}.

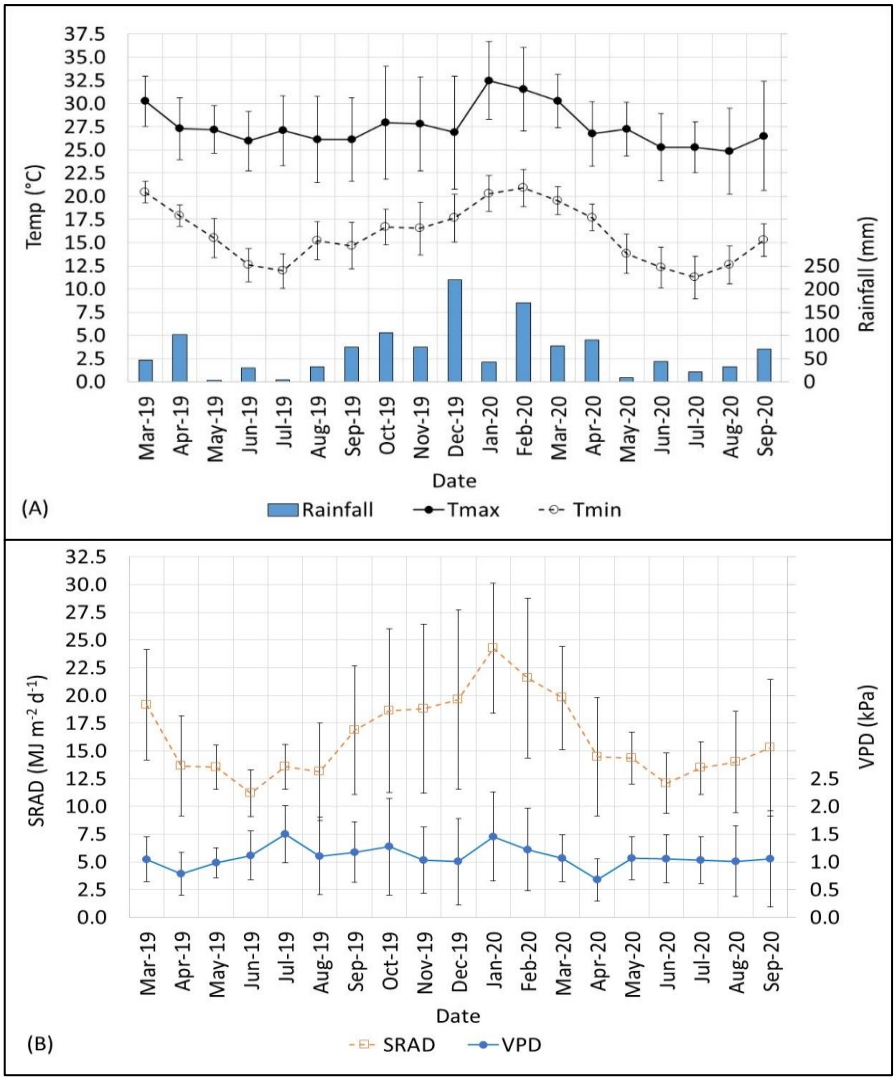

Figure 5.4 (A) Monthly mean daily maximum (Tmax) and minimum (Tmin) air temperatures and monthly rainfall; (B) monthly mean daily solar radiation (SRAD) and vapour pressure deficit (VPD), for the Empangeni SR 19-20 breeding trial. Vertical bars represent standard deviation values.

Crop water use and growth

Crop water use

Measured and simulated crop water use, growth and development are shown for the trial period in Figure 5.5 and Figure 5.6. The simulation results suggest that the crop received sufficient rainfall to maintain ASWC above SP from planting up to approximately 80 DAP, when the crop had reached full canopy (simulated FIPAR exceeded 80%). There was a prolonged period of water stress from 85 to 275 DAP, during which simulated ASWC dropped below SP, and CWSI dropped from 0.90 to 0.19. Water stress was relieved with rainfall which occurred between 275 and 305 DAP. Thereafter, both simulated and measured ASWC showed that the crop experienced further intermittent periods of stress up until harvest at 545 DAP.

The model predicted SDM at harvest of 26.8 t ha^{-1} for NCo376, which was within the range of observed SDM values (22.6 – 49.7 t ha^{-1}). A simulation of the crop under fully irrigated conditions (data not shown) showed a potential SDM of 51.6 t ha^{-1}, which suggests that SDM may have been reduced by approximately 50% due to water stress.

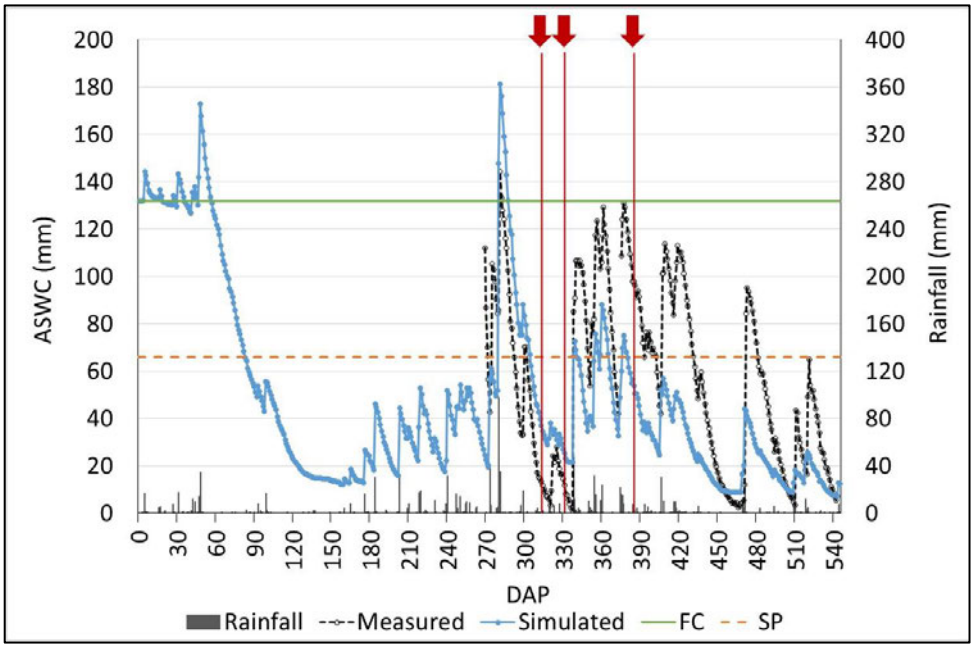

Figure 5.5. Plant available soil water content (ASWC) shown over time (days after planting, DAP) for the SR 19-20 breeding trial. ASWC was measured across the trial using capacitance probes and simulated using the MyCanesim® model. The secondary axis shows rainfall received. Green and orange lines represent field capacity (FC) and stress point (SP), respectively. Vertical red lines and arrows indicate three occasions on which aerial imagery was captured.

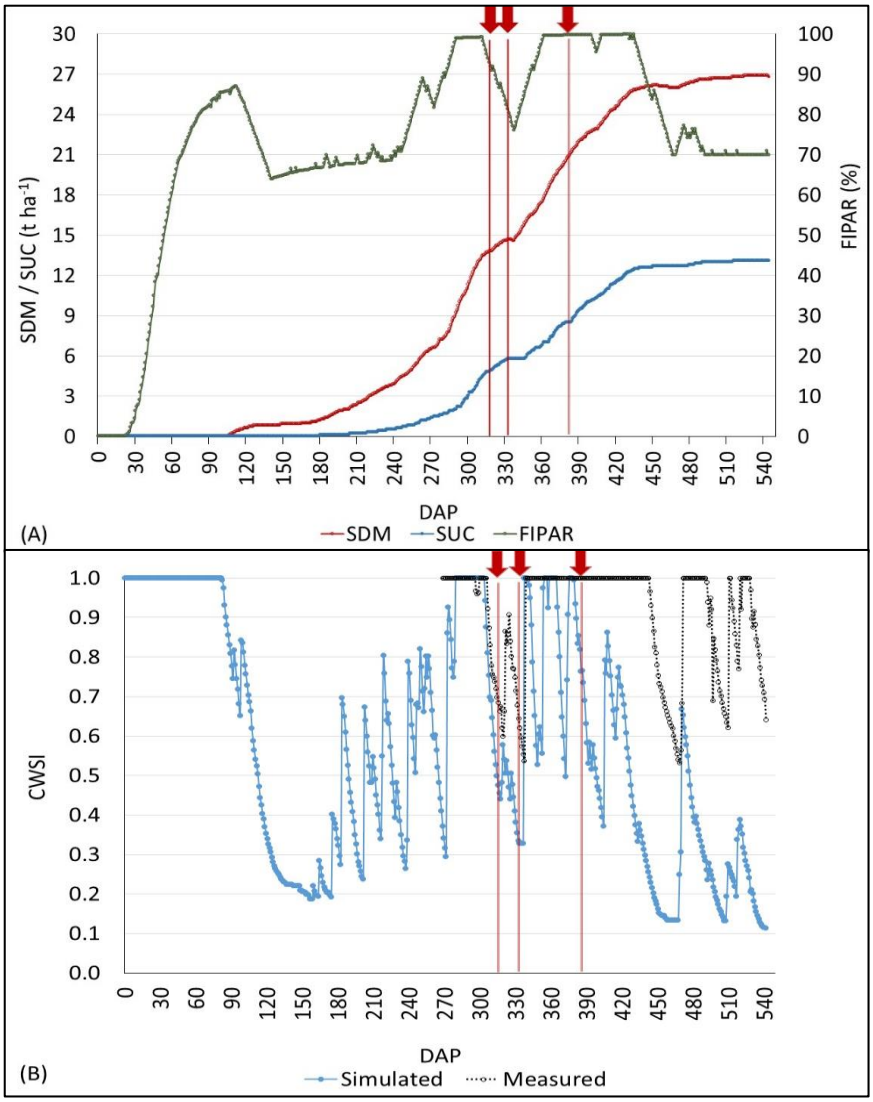

Figure 5.6. (A) Fractional interception of photosynthetic active radiation (FIPAR) and yield (stalk dry mass, SDM and sucrose yield, SUC), and (B) crop water satisfaction index (CWSI) as calculated from simulated and measured soil water status over time (days after planting, DAP) for the SR 19-20 breeding trial. Vertical red lines and arrows indicate three occasions on which aerial imagery was captured.

Crop growth

Ground measurements

Statistical analysis of ground measured traits for trial SR 19-20 at harvest are shown in Table 5.4. SDM differed significantly between genotypes and showed high broad-sense heritability estimates (0.78 - 0.91) in the trial parts that were considered. SH, SD and SPOP also differed significantly between genotypes in all trial parts, and generally showed moderate to high heritability estimates (0.30 - 0.85).

Table 5.4. Statistical analysis of stalk dry mass yield (SDM, kg m^{-1}), stalk height (SH, m), diameter (SD, mm) and population (SPOP, stalks per plot) measured at harvest within each part of the SR 19-20 trial. Standard deviation values are shown in brackets. F. probabilities (F.pr.) due to genotypic differences (indicated as significant at p = 0.05 with an asterisk) are shown along with corresponding genetic (G) and error (E) variances, genetic coefficient of variation (GCV, %) and broad-sense heritability (HSB) values. The number of datapoints analysed (n) is also shown.

Variable	SDM						SH						SD						SPOP						
Trial part [1]	Mean	F.pr.	G	E	GCV	HSB	Mean	F.pr.	G	E	GCV	HSB	Mean	F.pr.	G	E	GCV	HSB	Mean	F.pr.	G	E	GCV	HSB	n
A	3.96 (1.20)	**<0.0001***	1.12	0.33	26.7	0.87	2.02 (0.23)	**0.04***	0.008	0.039	4.5	0.30	25.1 (2.88)	**0.0004***	3.44	3.65	7.4	0.65	61.4 (12.6)	**<0.0001***	80.3	71.7	14.6	0.69	414
B	3.73 (1.02)	**<0.0001***	0.68	0.38	22.0	0.78	2.00 (0.25)	**0.04***	0.015	0.045	6.1	0.40	24.5 (2.75)	**0.01***	3.53	3.54	7.7	0.67	62.0 (11.9)	**0.05***	42.4	99.5	10.5	0.46	318
C	3.78 (1.44)	**<0.0001***	1.77	0.34	35.2	0.91	1.95 (0.29)	**0.02***	0.031	0.034	9.0	0.65	24.3 (2.85)	**0.03***	3.98	4.10	8.2	0.66	63.3 (13.4)	**0.01***	83.8	97.3	14.5	0.63	222
F	3.67 (1.03)	**<0.0001***	0.72	0.35	23.1	0.80	2.01 (0.26)	**<0.0001***	0.039	0.029	9.8	0.73	24.8 (3.22)	**<0.0001***	7.40	2.67	11.0	0.85	60.0 (13.3)	**<0.0001***	93.6	84.4	16.7	0.69	522
J	4.42 (1.46)	**<0.0001***	1.69	0.44	29.4	0.88	2.36 (0.30)	**0.008***	0.036	0.053	8.0	0.57	25.3 (2.87)	**<0.0001***	4.83	3.40	8.7	0.74	53.5 (14.0)	**<0.0001***	130.8	65.5	21.4	0.80	360

[1] Trial parts D, E, G, H and I were excluded from the analysis as the reference variety NCo376 did not meet the exclusion criteria for reliable data.

Aerial imaging

Statistical analysis of aerially measured trait data is shown in Table 5.5. NDVI and Tc showed statistically non-significant differences between genotypes, and consequently low heritability (0.03 - 0.51), in most cases. For the few instances where NDVI and Tc showed significant genotypic variation, the data showed low to moderate HSB estimates (0.36 - 0.63). NDVI and Tc did not show significant genotypic differences when the data were combined across flights for categories of CWSI (shown in the Appendix, Table 8.17).

Table 5.5. Statistical analysis of normalised difference vegetation index (NDVI) and canopy temperature (Tc, °C) estimated from aerial imagery, captured during three drone flights per trial part in the SR 19-20 trial. Standard deviation values are indicated in brackets. F. probabilities (F.pr.) due to genotypic differences (indicated as significant at p = 0.05 with an asterisk) are shown along with corresponding genetic (G) and error (E) variances, genetic coefficient of variation (GCV, %) and broad-sense heritability (HSB) values.

Variable		NDVI						Tc						
Flight	Trial part	Mean	F.pr.	G	E	GCV	HSB	Mean	F.pr.	G	E	GCV	HSB	n
1	A	0.74 (0.033)	0.34	0.000023	0.00058	0.64	0.07	37.2 (1.30)	0.57	NS	0.89	NS	NS	138
	B	0.76 (0.022)	0.16	0.00010	0.00029	1.32	0.41	37.4 (1.23)	**0.003***	0.46	0.53	1.81	0.63	106
	C	0.73 (0.038)	0.12	0.00024	0.00050	2.13	0.49	39.0 (1.56)	0.86	NS	1.15	NS	NS	74
	F	0.71 (0.028)	0.44	NS	0.00060	NS	NS	39.6 (1.23)	0.87	NS	0.76	NS	NS	174
	J	0.74 (0.033)	0.32	0.00002	0.00047	0.60	0.08	39.2 (1.19)	0.48	0.066	0.71	0.66	0.16	120
2	A	0.78 (0.039)	0.23	0.000013	0.00084	0.47	0.03	42.7 (1.27)	0.24	NS	0.68	NS	NS	138
	B	0.80 (0.029)	0.09	0.00027	0.00051	2.05	0.51	41.6 (1.07)	**0.02***	0.24	0.36	1.18	0.58	106
	C	0.76 (0.047)	0.25	0.00035	0.00071	2.46	0.50	42.7 (0.87)	0.83	NS	0.47	NS	NS	74
	F	0.73 (0.041)	0.11	0.00013	0.0013	1.53	0.16	43.4 (1.27)	0.74	NS	0.76	NS	NS	174
	J	0.78 (0.035)	0.64	NS	0.00072	NS	NS	41.2 (1.05)	0.46	NS	0.66	NS	NS	120
3	A	0.82 (0.050)	**0.03***	0.00061	0.0019	3.02	0.39	21.1 (1.08)	0.11	0.11	0.42	1.57	0.34	138
	B	0.82 (0.051)	0.07	0.00052	0.0021	2.77	0.34	20.5 (1.25)	0.11	0.096	0.42	1.51	0.31	106
	C	0.82 (0.052)	**0.047***	0.00058	0.0021	2.9	0.36	20.0 (1.29)	0.15	0.24	0.39	2.4	0.55	74
	F	0.83 (0.045)	0.28	0.00018	0.0018	1.6	0.16	27.2 (0.80)	0.51	NS	0.25	NS	NS	174
	J	0.84 (0.046)	0.44	0.00018	0.0018	1.60	0.16	31.2 (0.91)	**0.03***	0.071	0.15	0.86	0.48	120

NS Variance components and HSB could not be calculated due to statistically non-significant genotypic differences.

Trait correlations

Trait correlations were evaluated by pooling data for categories of CWSI, as shown in Table 5.6. NDVI and Tc showed mostly statistically non-significant correlations with SDM (r = 0.00 to 0.74*, and 0.00 to -0.79*, respectively) for the respective trial parts and categories of CWSI. Genetic correlations were also consistently weak (r_g = -0.16 to 0.26, and -0.22 to 0.03 for NDVI and Tc, respectively), due to low genetic variance (i.e. limited genetic variability) in both aerial traits. Furthermore, the data showed no improvement in the strength of correlations when expressing values relative to that of NCo376 (shown in the Appendix, Table 8.18).

Table 5.6. Phenotypic (r) and genetic (r_g) correlations between stalk dry mass (SDM) yield measured at harvest within each part of the SR 19-20 trial, with normalized difference vegetation index (NDVI) and canopy temperature (Tc) estimated from aerial imagery. Data were categorised by crop water satisfaction (high or medium, H / M, and combinations thereof). The number of datapoints (n) is shown, and statistical significance at p = 0.05 is indicated with an asterisk.

	Variable	SDM vs. NDVI				SDM vs. Tc			
Trial part	Crop water satisfaction category	r	n	r_g	n	r	n	r_g	n
A	M	**0.70***	10	0.13	136	-0.49	10	-0.04	136
	H	0.35	10	0.04	136	-0.61	10	-0.22	136
	M+H	**0.66***	10	0.08	136	-0.60	10	-0.02	136
B	M	**0.74***	10	0.15	105	**-0.79***	10	-0.03	105
	H	0.00	10	-0.07	105	-0.14	10	-0.18	105
	M+H	0.59	10	0.04	105	-0.62	10	-0.01	105
C	M	0.59	10	0.26	73	-0.14	10	-0.03	73
	H	0.00	10	-0.16	73	-0.32	10	-0.20	73
	M+H	0.56	10	0.10	73	0.57	10	-0.01	73
F	M	0.48	10	0.06	173	-0.10	10	-0.02	173
	H	0.58	10	0.13	173	-0.10	10	0.03	173
	M+H	0.57	10	0.05	173	-0.09	10	0.00	173
J	M	0.42	10	0.04	120	0.00	10	0.02	120
	H	0.10	10	0.06	120	-0.26	10	-0.13	120
	M+H	0.40	10	0.04	120	-0.19	10	0.00	120

Genotype selection

Selection accuracy

Direct and indirect genotype selection methods were compared within trial parts (shown in the Appendix, Table 8.19), as well as across the entire trial (Table 5.7), for the respective CWSI categories. Indirect selection using NDVI, Tc, or a combination of both traits (VPI or SDM_{MLR}) consistently resulted in a higher number of misses or false positives compared to positive matches within trial parts (Table 8.19), as well as across the trial (Table 5.7). The results showed that positive matches outnumbered misses or false positives in only one instance, which occurred when Tc and SDM_{MLR} were used in Part J under conditions of high CWSI (Table 8.19).

Table 5.7. Comparison of direct (SDM-based) and indirect (based on aerially measured traits, i.e. NDVI, Tc, VPI and SDM_{MLR}) genotype selection methods across all parts of the SR 19-20 breeding trial. The analysis included a subset of genotypes after exclusion criteria were applied. Data were categorised by crop water satisfaction (high or medium, H / M, and combinations thereof). Selection methods were compared by considering: (1) the number of genotypes that were selected with the respective traits; (2) the number of positive matches (genotypes selected by both SDM and the respective aerially measured trait); (3) misses (genotypes selected with SDM but not with the respective aerially measured trait) and false positives (genotypes selected with the aerially measured trait but not with SDM).

	CWSI	**M**																
Genotypes planted	**Genotypes considered after exclusion criteria applied**	**Genotypes selected**					**Positive Matches**				**Misses**				**False positives**			
	Selection trait	**SDM**	**NDVI**	**Tc**	**VPI**	**SDM_{MLR}**	**NDVI**	**Tc**	**VPI**	**SDM_{MLR}**	**NDVI**	**Tc**	**VPI**	**SDM_{MLR}**	**NDVI**	**Tc**	**VPI**	**SDM_{MLR}**
950	309 (33%)	127 (41%)	105 (34%)	80 (26%)	84 (27%)	94 (30%)	41 (32%)	26 (33%)	36 (43%)	40 (43%)	86 (68%)	101 (80%)	91 (72%)	87 (69%)	64 (61%)	54 (68%)	48 (57%)	54 (57%)
		H																
950	309 (33%)	127 (41%)	113 (37%)	113 (37%)	121 (39%)	153 (50%)	57 (50%)	64 (57%)	64 (53%)	76 (50%)	70 (55%)	63 (50%)	63 (50%)	51 (40%)	56 (50%)	49 (43%)	57 (47%)	77 (50%)
		M + H																
950	309 (33%)	127 (41%)	120 (39%)	73 (24%)	74 (24%)	105 (34%)	57 (45%)	31 (24%)	36 (28%)	55 (43%)	70 (55%)	96 (76%)	91 (72%)	72 (57%)	63 (53%)	42 (58%)	38 (51%)	50 (48%)

Note: The percentages indicate: (1) The number of genotypes selected with the respective trait, were expressed relative to the number of genotypes considered after exclusion criteria were applied (n = 309); (2) Positive matches were expressed relative to the number of genotypes selected, with the respective trait; (3) Misses were expressed relative to the number of genotypes selected with SDM; (4) False positives were expressed relative to the number of genotypes selected with the respective trait.

Selection response

The relative efficiency (CR_x/R_x) of indirect selection is shown in Table 5.8. The aerially measured traits generally showed poor correlated responses to selection within trial parts, due to low heritability of aerially measured traits and poor genetic correlation with stalk yield. Tc could not be considered in the analysis, as heritability could not be calculated when the data showed statistically non-significant differences between genotypes. The relative efficiency of indirect selection within trial parts varied from 0.06 - 0.18 for all aerially measured traits. This suggests that at best, NDVI was 18% as effective as direct selection for SDM, specifically in trial part C only.

Table 5.8. Metrics of direct response to selection (R_x) for stalk dry mass yield (SDM); the correlated selection response (CR_x) using indirect selection (i.e. aerially measured traits, normalized difference vegetation index, NDVI; vegetation productivity index, VPI; SDM estimated from multiple linear regression analysis, SDM_{MLR}); and the relative efficiency of indirect selection (CR_x/R_x), for different trial parts measured across three flights.

Trial part	Trait	R_x	CR_x	CR_x/R_x
A	SDM	1.04	-	-
	NDVI	-	0.06	0.06
	VPI	-	0.09	0.09
	SDM_{MLR}	-	0.14	0.14
B	SDM	0.80	-	-
	NDVI	-	0.07	0.08
	VPI	-	0.12	0.15
	SDM_{MLR}	-	0.12	0.15
C	SDM	1.31	-	-
	NDVI	-	0.23	0.18
	VPI	-	0.14	0.11
	SDM_{MLR}	-	0.15	0.11
F	SDM	0.82	-	-
	NDVI	-	0.03	0.04
	VPI	-	0.02	0.03
	SDM_{MLR}	-	0.06	0.08
J	SDM	0.91	-	-
	NDVI	-	0.01	0.02
	VPI	-	0.01	0.01
	SDM_{MLR}	-	0.07	0.08

5.3.2 Breeding trial 1: SR 21-22

Weather data

Weather data for the trial period are shown in Figure 5.7. Tmax and Tmin averaged over the respective months ranged from 24.0 to 31.4 °C, and from 11.8 to 21.1 °C, respectively, and the average Tmin value for the year was 17.1 °C. The crop experienced a total of 1217 mm of rainfall during the trial period of 12 months. Overall, the seasonal global solar radiation available for the crop was 6026 MJ m^{-2}, with a daily mean of 16.6 MJ m^{-2} d^{-1}.

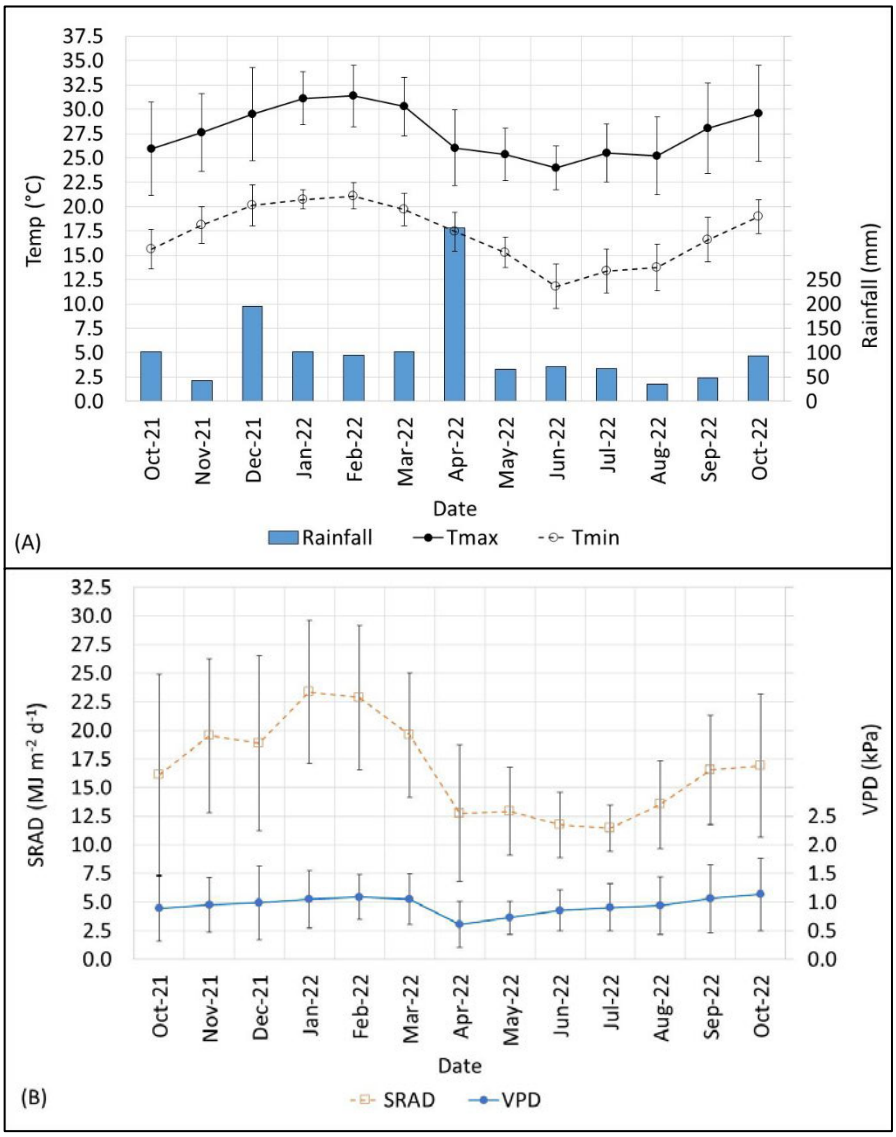

Figure 5.7. (A) Monthly mean daily maximum (Tmax) and minimum (Tmin) air temperatures and monthly rainfall; (B) mean daily solar radiation (SRAD) and vapour pressure deficit (VPD), for the Empangeni SR 21-22 breeding trial. Vertical bars represent standard deviation values.

Crop water use and growth

Crop water use

Measured and simulated crop water use, growth and development are shown for the trial period in Figure 5.8 and Figure 5.9. Both simulated and measured ASWC data showed that the crop received adequate rainfall to maintain ASWC above SP (with CWSI of between 0.8 and 1.0) during the initial stages of crop growth, up until approximately 105 DAH when the crop canopy had fully developed (simulated FIPAR of 95%). The crop then experienced intermittent water stress during two periods lasting 5 and 20 days respectively, up until 165 DAH. Both simulated and measured ASWC data showed that the crop was well-watered from 165 to 265 DAH, followed by a prolonged period of water stress up until 360 DAH when harvest took place.

The model predicted SDM at harvest of 29.1 t ha^{-1} for NCo376, which was within the range of observed SDM values (21.1 – 34.4 t ha^{-1}). A simulation of the crop under fully irrigated conditions (data not shown) showed a potential SDM of 51.6 t ha^{-1}, which suggests that SDM may have been reduced by approximately 44% due to water stress.

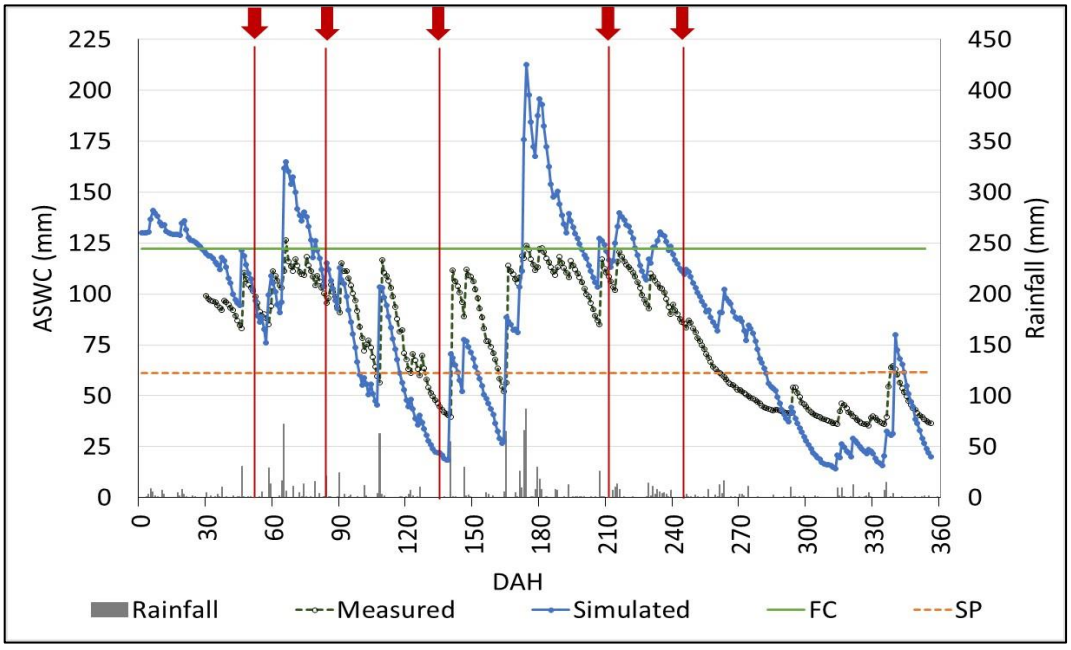

Figure 5.8. Plant available soil water content (ASWC) shown over time (days after harvest, DAH) for the SR 21-22 breeding trial. ASWC was measured across the trial using capacitance probes and simulated using the MyCanesim® model. The secondary axis shows rainfall received. Green and orange lines represent field capacity (FC) and stress point (SP), respectively. Vertical red lines and arrows indicate five occasions on which aerial imagery was captured.

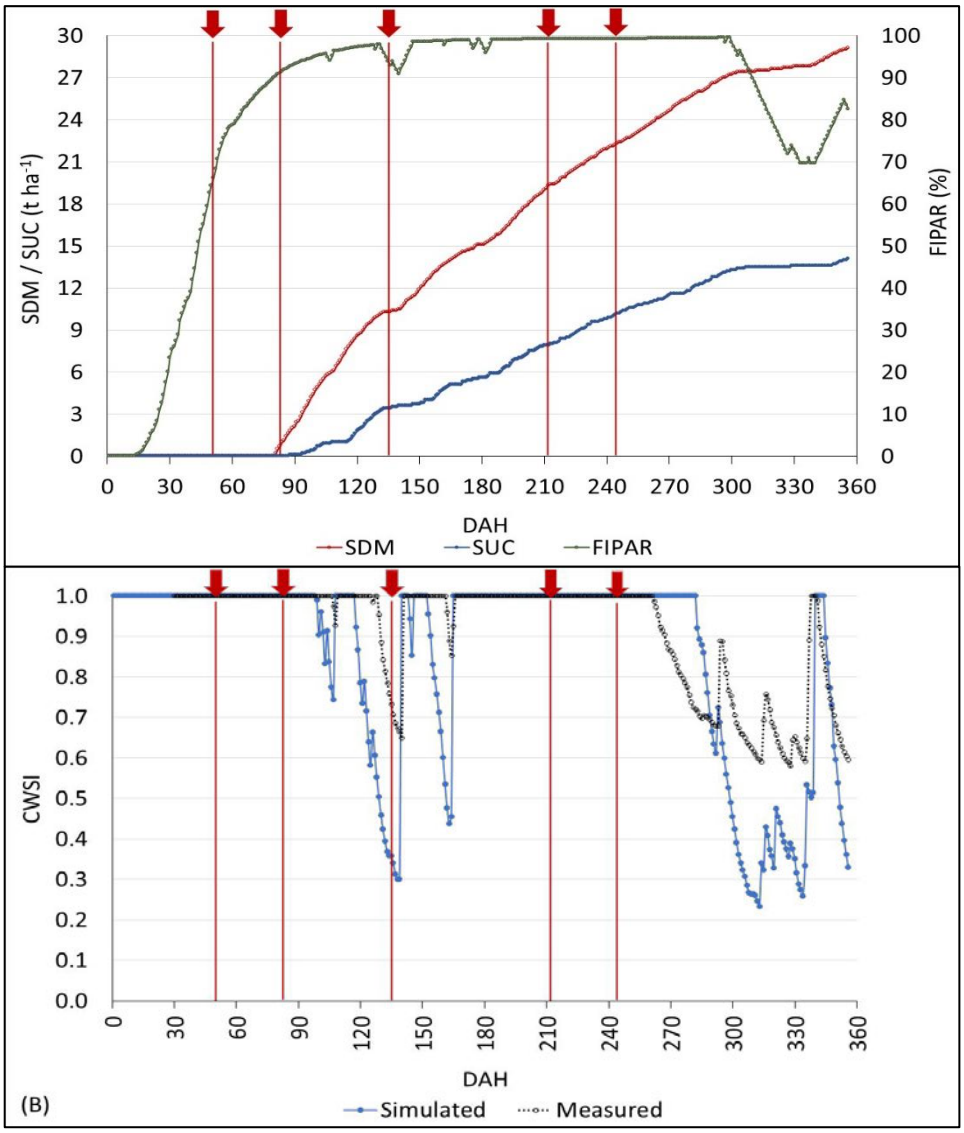

Figure 5.9. (A) Fractional interception of photosynthetic active radiation (FIPAR) and yield (stalk dry mass, SDM and sucrose yield, SUC), and (B) crop water satisfaction index (CWSI) as calculated from simulated and measured soil water status over time (days after harvest, DAH) for the SR 21-22 breeding trial. Vertical red lines and arrows indicate five occasions on which aerial imagery was captured.

Crop growth

Ground measurements

Statistical analysis of ground measured traits at harvest is shown in Table 5.9. SDM differed significantly between genotypes and showed moderate to high broad-sense heritability estimates (0.46 - 0.78) in all trial parts. SH, SD and SPOP also differed significantly between genotypes in all trial parts except for part K and showed moderate to high heritability estimates (0.42 – 0.85).

Table 5.9. Statistical analysis of stalk dry mass yield (SDM, kg m^{-1}), stalk height (SH, m), diameter (SD, mm) and population (SPOP, stalks per plot) measured at harvest within each part of the SR 21-22 trial. Standard deviation values are shown in brackets. F. probabilities (F.pr.) due to genotypic differences (indicated as significant at p = 0.05 with an asterisk) are shown along with corresponding genetic (G) and error (E) variances, genetic coefficient of variation (GCV, %) and broad-sense heritability (HSB) values. The number of datapoints analysed (n) is also shown.

Variable	SDM						SH						SD						SPOP						
Trial part	Mean	F.pr.	G	E	GCV	HSB	Mean	F.pr.	G	E	GCV	HSB	Mean	F.pr.	G	E	GCV	HSB	Mean	F.pr.	G	E	GCV	HSB	n
A	3.19 (0.90)	**0.0021***	0.23	0.56	15.2	0.46	1.81 (0.22)	**0.0001***	1.91	2.69	7.65	0.59	25.2 (2.76)	**<0.0001***	4.75	2.92	8.65	0.77	81.7 (17.6)	**<0.0001***	124.3	174.2	13.6	0.59	232
B	2.91 (0.83)	**<0.0001***	0.27	0.38	17.9	0.59	1.75 (0.22)	**<0.0001***	2.04	2.54	8.14	0.62	25.2 (3.05)	**<0.0001***	5.86	3.47	9.61	0.77	77.4 (17.0)	**<0.0001***	115.4	164.2	13.9	0.58	292
C	2.78 (0.84)	**0.0002***	0.26	0.44	18.5	0.54	1.67 (0.22)	**0.0031***	1.14	2.87	6.41	0.44	24.7 (3.04)	**<0.0001***	6.39	2.89	10.2	0.82	82.9 (19.3)	**<0.0001***	190.2	170.5	16.6	0.69	242
D	2.89 (0.88)	**<0.0001***	0.28	0.44	18.3	0.56	1.79 (0.24)	**0.0006***	1.81	3.52	7.50	0.51	24.9 (2.69)	**<0.0001***	4.45	2.54	8.49	0.78	81.8 (19.1)	**<0.0001***	176.1	189.3	16.2	0.65	252
E	3.02 (0.82)	**<0.0001***	0.23	0.42	15.8	0.52	1.65 (0.22)	**<0.0001***	1.66	2.21	7.82	0.60	23.8 (2.81)	**<0.0001***	4.44	2.93	8.84	0.75	91.7 (19.7)	**<0.0001***	189.5	189.1	15.0	0.67	234
F	3.20 (0.95)	**<0.0001***	0.32	0.46	17.7	0.58	1.82 (0.24)	**0.0043***	1.46	4.07	6.63	0.42	23.5 (2.78)	**<0.0001***	4.73	2.97	9.28	0.76	93.5 (21.8)	**<0.0001***	259.9	203.8	17.2	0.72	236
G	3.50 (1.05)	**<0.0001***	0.52	0.49	20.6	0.68	1.86 (0.21)	**<0.0001***	1.93	2.54	7.48	0.60	23.8 (2.93)	**<0.0001***	3.30	3.64	7.64	0.64	92.8 (22.9)	**<0.0001***	274.0	210.3	17.8	0.72	236
H	3.20 (0.95)	**<0.0001***	0.34	0.55	18.2	0.55	1.78 (0.23)	**<0.0001***	2.05	2.99	8.04	0.58	23.6 (2.68)	**<0.0001***	4.31	2.83	8.80	0.75	93.9 (21.6)	**<0.0001***	284.7	180.9	18.0	0.76	294
I	3.28 (0.87)	**<0.0001***	0.33	0.43	17.6	0.61	1.76 (0.24)	**<0.0001***	2.22	2.79	8.47	0.61	23.7 (2.73)	**<0.0001***	4.99	2.11	9.42	0.83	97.5 (21.4)	**<0.0001***	292.0	167.0	17.5	0.78	256
J	3.14 (0.93)	**0.007***	0.28	0.57	17.0	0.50	1.69 (0.19)	**0.013***	9.29	25.5	5.69	0.42	24.0 (3.06)	**<0.0001***	6.78	2.44	10.8	0.85	86.3 (19.0)	**0.0004***	169.9	193.0	15.1	0.64	146
K	3.85 (1.17)	**0.004***	0.88	0.50	24.4	0.78	1.84 (0.19)	0.16	1.05	2.60	5.43	0.44	22.4 (3.95)	0.33	2.73	5.17	7.37	0.51	88.9 (18.0)	**0.0013***	216.1	109.6	16.5	0.80	56

Aerial imaging

Statistical analysis of aerially measured trait data per flight is shown in Table 5.10. Variation in Tc across the different flights could be attributed to a combination of weather variables (shown in the Appendix in Table 8.20) and CWSI. Higher air temperatures (Tmean) and solar radiation (SRAD) generally led to increased Tc, and higher relative humidity (RH) and windspeed could be associated with lower Tc as a result of cooling by increased evapotranspiration. Of all the flights, average Tc was lowest (18.5 °C) in flight 5, presumably due to the combination of the lowest Tmean (22.5 °C), lowest SRAD (547.2 W m^{-2}) and highest RH (65%), and well-watered conditions. By comparison, flight 3 showed the highest Tc (37.6 °C) of all the flights presumably because of the higher Tmean (31.6 °C), relatively high SRAD (944.4 W m^{-2}), moderate RH (56%), and moderate water stress conditions, which appeared to reduce the cooling effect through transpiration.

Significant genotypic differences in Tc data were observed in the first flight for all trial parts except Part E, with moderate heritability (0.29 - 0.43). Tc data were not available for the second flight. Tc data captured in flight 3, under full canopy and mild water stress conditions, showed significant genotypic variation and moderate to high heritability (0.33 - 0.67). Trait data captured in flights 4 and 5, carried out under full canopy and well-watered conditions, showed mostly statistically non-significant genotypic differences and generally low heritability.

NDVI consistently showed significant genotypic variation, with moderate to high heritability (0.29-0.77), for all trial parts captured in the first two flights, which were carried out under partial canopy and well-watered conditions.

The analyses of NDVI and Tc for categories of CWSI (shown in the Appendix, Table 8.22) showed mostly statistically non-significant genotypic differences in both traits when CWSI was high (flights 1, 2, 4 and 5), and for the pooled dataset across all flights. This was due to significant flight x genotype interactions in both traits.

Table 5.10. Statistical analysis of normalised difference vegetation index (NDVI) and canopy temperature (Tc, °C) estimated from aerial imagery, captured during five drone flights per trial part in the SR 21-22 experiment. Standard deviation values are indicated in brackets. F. probabilities (F.pr.) due to genotypic differences (indicated as significant at p = 0.05 with an asterisk) are shown along with corresponding genetic (G) and error (E) variances, genetic coefficient of variation (GCV, %) and broad-sense heritability (HSB).

	Variable	NDVI							Tc						
Flight	Trial part	Mean	F.pr.	G	E	GCV	HSB	n	Mean	F.pr.	G	E	GCV	HSB	n
1	A	0.70 (0.07)	**0.008***	0.00093	0.0029	4.33	0.39	314	30.9 (2.48)	**0.041***	0.33	1.20	1.85	0.35	314
	B	0.72 (0.07)	**<0.0001***	0.0014	0.0023	5.13	0.54	292	30.5 (1.87)	**0.001***	0.87	2.47	3.05	0.41	292
	C	0.71 (0.06)	**<0.0001***	0.0016	0.0022	5.69	0.60	242	30.8 (1.62)	**0.0004***	0.60	1.62	2.52	0.43	242
	D	0.74 (0.06)	**<0.0001***	0.0014	0.0022	5.02	0.56	252	29.3 (1.64)	**0.039***	0.20	0.82	1.52	0.33	252
	E	0.74 (0.08)	**0.013***	0.00092	0.0046	4.09	0.29	234	30.3 (1.59)	**0.032***	0.03	0.16	0.60	0.29	234
	F	0.79 (0.05)	**0.035***	0.00026	0.0018	2.05	0.23	236	33.0 (3.26)	0.63	0.02	2.90	0.43	0.01	236
2	A	0.76 (0.05)	**0.002***	0.0007	0.0013	3.48	0.52	232	NA	NA	NA	NA	NA	NA	NA
	B	0.78 (0.04)	**<0.0001***	0.0009	0.0007	3.96	0.72	292	NA	NA	NA	NA	NA	NA	NA
	C	0.79 (0.04)	**<0.0001***	0.0006	0.0008	3.01	0.58	242	NA	NA	NA	NA	NA	NA	NA
	D	0.81 (0.03)	**<0.0001***	0.0006	0.0004	3.10	0.74	252	NA	NA	NA	NA	NA	NA	NA
	E	0.80 (0.04)	**0.0004***	0.0005	0.0012	2.88	0.47	234	NA	NA	NA	NA	NA	NA	NA
	F	0.82 (0.03)	**0.03***	0.0002	0.0007	1.64	0.34	236	NA	NA	NA	NA	NA	NA	NA
2	G	0.80 (0.04)	**0.0008***	0.0004	0.0007	2.34	0.48	236	NA	NA	NA	NA	NA	NA	NA
	I	0.81 (0.03)	**<0.0001***	0.0005	0.0003	2.82	0.77	256	NA	NA	NA	NA	NA	NA	NA
	J	0.80 (0.03)	**<0.0001***	0.0005	0.0003	2.68	0.76	146	NA	NA	NA	NA	NA	NA	NA
3	A	NA	NA	NA	NA	NA	NA	NA	37.1 (2.10)	**<0.0001***	1.63	1.57	3.44	0.67	314
	B	NA	NA	NA	NA	NA	NA	NA	35.6 (1.69)	**<0.0001***	1.20	1.49	3.08	0.62	292
	C	NA	NA	NA	NA	NA	NA	NA	34.9 (1.73)	**<0.0001***	1.38	1.48	3.36	0.65	242
	D	NA	NA	NA	NA	NA	NA	NA	34.9 (1.30)	**0.0003***	0.54	0.97	2.12	0.53	252
	E	NA	NA	NA	NA	NA	NA	NA	37.8 (1.62)	0.068	0.20	1.84	1.19	0.18	234
	F	NA	NA	NA	NA	NA	NA	NA	39.9 (1.63)	**0.049***	0.23	0.93	1.20	0.33	234
	G	NA	NA	NA	NA	NA	NA	NA	40.2 (2.06)	0.06	0.17	1.57	1.02	0.18	234
	I	NA	NA	NA	NA	NA	NA	NA	36.9 (1.83)	**<0.0001***	0.78	0.80	2.39	0.66	256
	J	NA	NA	NA	NA	NA	NA	NA	37.1 (2.35)	**<0.0001***	0.60	0.58	2.08	0.67	147
4	A	0.82 (0.03)	**0.03***	0.00007	0.0003	0.99	0.29	314	23.6 (0.97)	0.54	NS	0.53	NS	NS	314
	B	0.81 (0.03)	0.68	NS	0.0006	NS	NS	292	23.3 (0.93)	0.11	0.05	0.42	1.00	0.21	292
	C	0.82 (0.02)	0.71	NS	0.0003	NS	NS	242	22.2 (1.57)	0.26	0.05	0.46	1.00	0.18	242
	D	0.82 (0.03)	0.39	0.00003	0.0005	0.62	0.09	252	21.9 (1.12)	0.66	NS	0.50	NS	NS	252

	Variable	NDVI							Tc						
	Trial part	Mean	F.pr.	G	E	GCV	HSB	n	Mean	F.pr.	G	E	GCV	HSB	n
	E	0.82 (0.02)	0.11	0.00004	0.0005	0.72	0.12	234	21.0 (0.84)	0.14	0.03	0.27	0.78	0.17	234
	F	0.83 (0.02)	0.16	0.00004	0.0002	0.76	0.25	236	22.6 (2.76)	0.66	NS	1.26	NS	NS	236
	G	0.82 (0.02)	0.34	0.00002	0.0004	0.47	0.08	61	25.4 (3.41)	0.52	0.04	0.36	0.80	0.18	61
	I	0.82 (0.03)	**0.02***	0.0005	0.0003	2.61	0.74	58	24.0 (0.51)	0.42	0.03	0.14	0.77	0.32	58
	J	0.82 (0.02)	**<0.0001***	0.0002	0.0002	1.64	0.68	146	24.6 (0.45)	**0.01***	0.03	0.05	0.65	0.49	146
5	A	0.78 (0.04)	**<0.0001***	0.0004	0.0007	2.69	0.55	314	19.6 (0.94)	0.26	0.01	0.45	0.50	0.04	314
	B	0.77 (0.04)	0.14	0.0001	0.001	1.53	0.18	292	19.6 (1.36)	**0.02***	0.14	0.70	1.89	0.28	292
	C	0.80 (0.03)	0.58	NS	0.0008	NS	NS	242	18.1 (1.38)	0.61	NS	0.89	NS	NS	242
	D	0.80 (0.04)	**<0.001***	0.0004	0.0008	2.42	0.50	252	16.7 (1.35)	0.63	NS	1.11	NS	NS	252
	E	0.81 (0.04)	0.09	0.0001	0.0007	1.36	0.25	234	16.8 (1.27)	0.16	0.03	0.77	1.03	0.07	234
	F	0.84 (0.03)	0.23	0.00006	0.0004	0.94	0.22	210	18.2 (1.29)	0.15	0.07	0.39	1.41	0.25	210
	G	0.83 (0.04)	**0.002***	0.0004	0.0007	2.47	0.53	216	19.6 (1.53)	0.53	NS	0.71	NS	NS	216
	I	0.83 (0.03)	**<0.0001***	0.0003	0.0005	1.98	0.53	256	20.0 (1.74)	0.28	0.04	0.59	1.05	0.13	256
	J	0.82 (0.04)	**0.03***	0.0006	0.0006	3.06	0.67	96	20.3 (1.31)	0.50	NS	0.32	NS	NS	96

NA Data not available, as a result of drone image blurring (Flight 1) or instrument failure (flights 2-3).
NS HSB could not be calculated due to statistically non-significant genotypic differences.

Trait correlations

The correlations between SDM and aerially measured traits are shown per flight in Table 5.11. SDM and NDVI consistently showed the strongest phenotypic correlations (0.63* - 0.92*) for all trial parts captured in flights 1 and 2, under partial canopy and well-watered conditions. Thereafter, the correlations were mostly statistically non-significant in flights 4 and 5 when the canopy had fully developed. Similarly, the genetic correlations were also highest in flights 1 and 2 (0.16 - 0.37), declining thereafter in the later flights (0.02 - 0.22). There was no consistent improvement in the strength of correlations when the values of both traits were expressed relative to that of NCo376 (shown in the Appendix, Table 8.23).

SDM and Tc showed significant phenotypic correlations for Parts A-C of flight 1 (-0.69* to -0.86*), and for most trial parts of flight 3 (-0.33 to -0.98*), with generally low to moderate genetic correlations (-0.10 to -0.34). The relationships were mostly poor and statistically non-significant thereafter in flights 4 and 5.

Table 5.11. Phenotypic (r) and genetic correlations (r_g) between stalk dry mass (SDM) yield measured at harvest, with normalized difference vegetation index (NDVI) and canopy temperature (Tc), for each trial part of the SR 21-22 experiment. NDVI and Tc were estimated from aerial imagery, captured in five flights. The number of datapoints (n) is shown, and statistical significance at p = 0.05 is indicated with an asterisk.

	Variable	SDM vs. NDVI				SDM vs. Tc			
Flight	Trial part	r	n	r_g	n	r	n	r_g	n
1	A	**0.92***	10	0.28	314	**-0.86**	10	-0.24	314
	B	**0.63***	10	0.21	292	**-0.69**	10	-0.22	292
	C	**0.71***	10	0.27	242	**-0.66**	10	-0.23	242
	D	**0.69***	10	0.16	252	-0.13	10	-0.12	252
	E	**0.63***	10	0.20	234	0.00	10	-0.10	234
	F	**0.77***	10	0.23	236	0.00	10	-0.14	236
2	A	**0.89***	10	0.34	232	NA	NA	NA	NA
	B	**0.74***	10	0.30	292	NA	NA	NA	NA
	C	**0.85***	10	0.31	242	NA	NA	NA	NA
	D	**0.66***	10	0.27	252	NA	NA	NA	NA
	E	**0.65***	10	0.22	234	NA	NA	NA	NA
	F	**0.64***	10	0.23	236	NA	NA	NA	NA
	G	**0.84***	10	0.30	236	NA	NA	NA	NA
	I	**0.92***	10	0.37	256	NA	NA	NA	NA
	J	**0.75***	10	0.32	146	NA	NA	NA	NA
3	A	NA	NA	NA	NA	**-0.98***	10	-0.34	314
	B	NA	NA	NA	NA	**-0.74***	10	-0.33	292
	C	NA	NA	NA	NA	**-0.76***	10	-0.31	242
	D	NA	NA	NA	NA	**-0.78***	10	-0.27	252
	E	NA	NA	NA	NA	-0.33	10	-0.10	234
	F	NA	NA	NA	NA	**-0.91***	10	-0.18	234
	G	NA	NA	NA	NA	-0.50	10	-0.20	234
3	I	NA	NA	NA	NA	**-0.81***	10	-0.12	256
	J	NA	NA	NA	NA	-0.52	10	-0.14	147
4	A	0.14	10	0.17	314	-0.19	10	-0.14	314
	B	**0.72***	10	0.10	292	-0.06	10	-0.16	292
	C	0.04	10	0.04	242	-0.06	10	-0.04	242
	D	0.00	10	0.04	252	-0.61	10	-0.16	252
	E	0.17	10	0.03	234	-0.03	10	-0.12	234
	F	**0.67***	10	0.22	236	-0.24	10	-0.22	236
	G	0.03	10	0.04	61	-0.05	10	-0.07	61
	I	0.09	10	0.10	58	-0.08	10	-0.05	58
	J	0.06	10	0.14	146	-0.10	10	-0.04	146
5	A	0.06	10	0.10	314	-0.14	10	-0.09	314
	B	0.27	10	0.14	292	0.00	10	-0.07	292
	C	0.01	10	0.06	242	-0.19	10	-0.04	242
	D	0.05	10	0.02	252	**-0.71***	10	-0.19	252
	E	0.01	10	0.04	234	-0.18	10	-0.02	234
	F	0.37	10	0.10	210	-0.01	10	-0.24	210
	G	0.27	10	0.02	216	**-0.63***	10	-0.08	216
	I	0.03	10	0.02	256	-0.39	10	-0.12	256
	J	0.20	10	0.15	96	-0.02	10	-0.10	96

[NA] Trait correlations could not be assessed as data were not available due to instrument failure (flights 2-3).

Genotype selection

Selection accuracy

Direct and indirect genotype selection methods were compared for individual flights to evaluate the efficacy of AP to discern clonal performance for different crop development conditions. The data for each flight were considered within trial parts (shown in the Appendix, Table 8.24), as well as across the entire trial (Table 5.12). The results showed limited instances of success where AP could be used to accurately select for high-yielding genotypes. Notably, in part C of flight 1 and in parts C, G, I and J of flight 3, positive matches (62 – 100%) outnumbered misses (0 – 38%) and false positives (27 – 48%) (Table 8.24). Similarly, flights 1 and 3 showed a higher number of positive matches (76 – 95%) compared to misses (5 – 24%) or false positives (62 – 78%) across the entire trial (Table 5.12). However, despite these occasional successes, the accuracy of indirect selection using NDVI, Tc and combinations thereof, was generally insufficient for breeding, as AP lacked consistent identification of high-yielding genotypes, with positive matches most often offset by a larger number of false positives or misses.

Table 5.12. Comparison of direct (SDM-based) and indirect (based on aerially measured traits, i.e. NDVI, Tc, VPI and SDM_{MLR}) genotype selection methods in the SR 21-22 breeding trial. The analysis included a subset of genotypes after exclusion criteria were applied. Direct and indirect selection methods were considered for each flight, across all trial parts. Selection methods were compared by considering: (1) the number of genotypes that were selected with the respective traits; (2) the number of positive matches (genotypes selected by both SDM and the respective aerially measured trait); (3) misses (genotypes selected with SDM but not with the respective aerially measured trait) and false positives (genotypes selected with aerially measured trait but not with SDM). The green highlighted blocks indicate instances where the number of positive matches exceed the number of misses and false positives.

Flight	Genotypes planted	Genotypes considered after exclusion criteria applied	Genotypes selected					Positive Matches				Misses				False positives			
		Selection trait	SDM	NDVI	Tc	VPI	SDM_{MLR}	NDVI	Tc	VPI	SDM_{MLR}	NDVI	Tc	VPI	SDM_{MLR}	NDVI	Tc	VPI	SDM_{MLR}
1	1200	785 (65%)	131 (17%)	418 (53%)	509 (65%)	456 (58%)	40 (52%)	100 (84%)	114 (87%)	124 (95%)	121 (92%)	21 (16%)	17 (13%)	7 (5%)	10 (8%)	308 (74%)	395 (78%)	332 (73%)	285 (70%)
2	1930	1235 (64%)	351 (28%)	403 (33%)	-	-	-	137 (39%)	-	-	-	214 (61%)	-	-	-	266 (66%)	-	-	-
3	1930	1276 (66%)	353 (28%)	-	707 (55%)	-	-	-	268 (76%)	-	-	-	85 (24%)	-	-	-	439 (62%)	-	-
4	1400	816 (58%)	157 (19%)	329 (40%)	373 (46%)	302 (37%)	354 (43%)	57 (36%)	74 (47%)	42 (27%)	43 (27%)	100 (64%)	83 (53%)	115 (73%)	114 (73%)	272 (83%)	299 (80%)	260 (86%)	311 (88%)
5	1890	1226 (65%)	338 (28%)	445 (36%)	481 (39%)	355 (29%)	372 (30%)	112 (33%)	134 (40%)	87 (26%)	82 (24%)	226 (67%)	204 (60%)	251 (74%)	256 (76%)	333 (75%)	347 (72%)	268 (75%)	290 (78%)

Note: The percentages indicate: (1) The number of genotypes selected with the respective trait, were expressed relative to the number of genotypes considered after exclusion criteria were applied; (2) Positive matches were expressed relative to the number of genotypes selected, with the respective trait; (3) Misses were expressed relative to the number of genotypes selected with SDM; (4) False positives were expressed relative to the number of genotypes selected with the respective trait.

Selection response

The relative efficiency of indirect selection within each flight is shown in Table 5.13. Indirect selection showed on average, higher relative efficiencies in flights 1-3 as compared to flights 4-5, presumably due to significant genotypic variation and higher heritability of traits in the earlier flights. In flight 1, NDVI consistently showed the highest correlated response to selection, and higher relative efficiencies, as compared to the other traits. The relative efficiency of NDVI varied from 14 - 28%, indicating that indirect selection using NDVI is at best, 28% as effective as selection for stalk yield directly. In flight 2, these values varied from 18-42%. Furthermore, combining both traits using VPI and SDM_{MLR} did not result in higher correlated responses to yield, or increased relative efficiencies, for any of the trial parts or flights.

Table 5.13. Metrics of direct response to selection (R_x) for stalk dry mass yield (SDM); the correlated selection response (CR_x) using indirect selection (with aerially measured traits, normalized difference vegetation index, NDVI; canopy temperature, Tc; vegetation productivity index, VPI; SDM estimated from multiple linear regression, SDM_{MLR}); and the relative efficiency of indirect selection (CR_x/R_x), for different trial parts and flights.

		Flight	1		2		3		4		5	
Trial part	Trait	R_x	CR_x	CR_x/R_x	CR_x	CR_x/R_x	CR_x	CR_x/R_x	CR_x	CR_x/R_x	CR_x	CR_x/R_x
A	SDM	0.41										
	NDVI	-	0.11	0.26	0.15	0.36	NA	NA	0.06	0.13	0.05	0.11
	Tc	-	0.06	0.14	NA	NA	0.17	0.41	NS	NS	0.01	0.03
	VPI	-	0.08	0.19	NA	NA	NA	NA	0.03	0.07	0.03	0.07
	SDM_{MLR}	-	0.07	0.17	NA	NA	NA	NA	0.05	0.12	0.05	0.12
B	SDM	0.49										
	NDVI	-	0.10	0.20	0.16	0.33	NA	NA	NS	NS	0.04	0.08
	Tc	-	0.09	0.18	NA	NA	0.17	0.34	0.05	0.10	0.02	0.05
	VPI	-	0.09	0.18	NA	NA	NA	NA	0.02	0.04	0.03	0.06
	SDM_{MLR}	-	0.08	0.16	NA	NA	NA	NA	0.04	0.08	0.04	0.08
C	SDM	0.45										
	NDVI	-	0.13	0.28	0.15	0.32	NA	NA	NS	NS	NS	NS
	Tc	-	0.09	0.21	NA	NA	0.15	0.34	0.01	0.02	NS	NS
	VPI	-	0.11	0.24	NA	NA	NA	NA	0.01	0.02	0.01	0.02
	SDM_{MLR}	-	0.10	0.22	NA	NA	NA	NA	0.02	0.04	0.01	0.02
D	SDM	0.49										
	NDVI	-	0.08	0.16	0.15	0.31	NA	NA	0.01	0.02	0.01	0.02
	Tc	-	0.03	0.07	NA	NA	0.13	0.26	NS	NS	NS	NS
	VPI	-	0.07	0.14	NA	NA	NA	NA	0.02	0.04	0.01	0.02
	SDM_{MLR}	-	0.05	0.10	NA	NA	NA	NA	0.03	0.06	0.02	0.04
E	SDM	0.43										
	NDVI	-	0.06	0.15	0.09	0.21	NA	NA	0.01	0.01	0.01	0.03
	Tc	-	0.01	0.01	NA	NA	0.05	0.11	0.03	0.07	0.00	0.01
	VPI	-	0.01	0.02	NA	NA	NA	NA	0.02	0.05	0.03	0.07
	SDM_{MLR}	-	0.04	0.09	NA	NA	NA	NA	0.01	0.02	0.01	0.02
F	SDM	0.55										
	NDVI	-	0.08	0.14	0.10	0.18	NA	NA	0.08	0.14	0.03	0.06
	Tc	-	0.01	0.02	NA	NA	0.01	0.02	NS	NS	0.09	0.16
	VPI	-	0.03	0.05	NA	NA	NA	NA	0.06	0.11	0.02	0.04
	SDM_{MLR}	-	0.07	0.13	NA	NA	NA	NA	0.05	0.09	0.08	0.15
G	SDM	0.71										
	NDVI	-	NA	NA	0.18	0.25	NA	NA	0.01	0.01	0.01	0.02
	Tc	-	NA	NA	NA	NA	0.03	0.04	0.03	0.04	NS	NS
	VPI	-	NA	NA	NA	NA	NA	NA	0.01	0.01	0.01	0.01
	SDM_{MLR}	-	NA	NA	NA	NA	NA	NA	0.02	0.03	0.01	0.01
I	SDM	0.53										
	NDVI	-	NA	NA	0.22	0.42	NA	NA	0.06	0.11	0.01	0.02
	Tc	-	NA	NA	NA	NA	0.11	0.21	0.02	0.04	0.03	0.06
	VPI	-	NA	NA	NA	NA	NA	NA	0.03	0.06	0.04	0.08
	SDM_{MLR}	-	NA	NA	NA	NA	NA	NA	0.02	0.04	0.02	0.04
J	SDM	0.47										
	NDVI	-	NA	NA	0.18	0.39	NA	NA	0.08	0.16	0.08	0.17
	Tc	-	NA	NA	NA	NA	0.08	0.16	0.02	0.04	NS	NS
	VPI	-	NA	NA	NA	NA	NA	NA	0.04	0.09	0.07	0.15
	SDM_{MLR}	-	NA	NA	NA	NA	NA	NA	0.05	0.11	0.05	0.11

[NA] Data not available, as a result of drone image blurring (Flight 1) or instrument failure (flights 2-3)

[NS] Response metrics could not be calculated due to statistically non-significant genotypic differences, and low heritability.

5.4 Concluding discussion

The study aimed to address the following research questions:

Question 1: *What is the extent of genotypic variation and broad-sense heritability in stalk yield and aerially measured traits, and how are these traits correlated with yield in the breeding population?*

SDM showed significant genotypic variation, and moderate to high broad-sense heritability, in both breeding trials, as was expected. Results from the first trial showed mostly statistically non-significant genotypic differences and low to moderate heritability for both NDVI and Tc, with both traits showing poor correlations with SDM. These weak correlations may be attributed to limitations in the AP methodology. The limited number of flights prevented adequate capture of temporal variations in crop status and their impacts on yield due to crop development and environmental factors. In addition, flights were performed too late to detect genotypic differences in early canopy development as reflected by NDVI, or in photosynthetic activity, as reflected by Tc.

Furthermore, results from the second trial showed significant genotypic variation and moderate to high broad-sense heritability in NDVI and Tc. Genotypic variation in NDVI was reliably detected with earlier flights, conducted between 1.5 – 3 months after crop start, under partial canopy and well-watered conditions. Significant genotypic differences in Tc were also detected with early flights under partial canopy and well-watered conditions, as well as shortly after canopy closure, but before row overlap due to crop growth, under mild water stress conditions. These observations covered a period of 4.5 months after crop start.

NDVI correlated well with SDM in these early flights under partial canopy and well-watered conditions. The strength of correlations decreased with crop age and water stress in later flights. This aligns with the expectation that early estimates of NDVI, reflecting genotypic differences in crop vigour, predict yield differences. Weaker correlations in later flights are likely due to spectral reflectance saturation and the impacts of water stress on yield.

Tc also correlated significantly with SDM under partial canopy and well-watered conditions, supporting the expectation that Tc measurements reflect genotypic differences in g_s and the crop's capacity for transpiration and photosynthesis, thus predicting yield differences.

Additionally, Tc correlated significantly with SDM shortly after canopy closure under mild water stress conditions. This suggests that Tc can predict yield, provided there is no overlapping leaf material from adjacent plots, as this may obscure genotypic differences in Tc. Under mild water stress, genotypes likely maintain open stomata, allowing for the detection of differences in g_s.

These findings underscore the importance of early crop assessments using AP. Early NDVI measurements reflect genotypic variation in vigour and canopy biomass, providing insights into potential yield through radiation interception and conversion efficiency. Early Tc measurements reveal genotypic differences in photosynthetic activity, offering insights into carbon assimilation and biomass accumulation. Early assessments are also crucial as they avoid issues with row overlap and confounding factors such as water stress that can affect later measurements. Therefore, assessing these traits early in the growth cycle under optimal conditions could reliably indicate the crop's yield potential.

Overall, these results are novel as they represent the first application of AP to single-row breeding plots, and to South African breeding populations. Previous studies aimed at assessing AP for enhancing sugarcane breeding have mostly focused on multi-row plot experiments with small population sizes and limited flight assessments. Khuimphukhieo et al. (2023) reported phenotypic correlations between NDVI and stalk yield, measured for seven genotypes grown in large plots, without considering important breeding metrics such as trait heritability or genetic correlations with yield. Basnayake, (2016) reported significant genotypic variation in Tc amongst 40 genotypes evaluated in a single flight, where Tc showed moderate heritability and correlation with stalk yield under rainfed conditions. By contrast, Chapman et al. (2014) observed statistically non-significant genotypic variation in Tc amongst 40 clones, across drought and irrigated treatments within a multi-row plot experiment, assessed during a single flight. These studies highlight the potential use of AP in breeding, but without consideration of early-stage trial conditions. More promising results for the use of NDVI as a screening trait for yield were reported by Natarajan et al. (2019), which found significant genotypic variation and moderate heritability for a large population of 2134 genotypes, planted in a single-row trial.

Question 2: *How does the accuracy of selecting high-yielding genotypes differ when employing direct (SDM-based) compared to indirect (based on aerially measured traits) approaches?*

Results from both breeding trials showed that indirect selection using NDVI, Tc, and combinations of the two traits, could not be used to accurately identify high-yielding genotypes in most cases, as the number of positive matches was most often offset by a larger number of false positives or misses. This suggests that AP as performed in this study lacks the precision to reliably differentiate between individual genotypes under these trial conditions.

Question 3: *Could the integration of AP in the breeding program enhance yield improvement and overall breeding efficiency?*

In assessing the relative efficiency of indirect selection, results from both trials showed generally moderate to low efficiencies which varied across trial parts, suggesting limited effectiveness of aerially measured traits in predicting yield under these trial conditions and for AP as performed in this study.

Overall, the results presented here show promise for AP in identifying genotypic variation in breeding trials early in the growing cycle. However, to fully realize this potential, refinements in trial procedures and AP methodologies are needed. For example, soil variability within large breeding trials is not well characterized, which directly affects the quality of yield data. Additionally, breeding trial operations, such as extended planting times, further impact the quality of ground measured data. Breeding trial designs with constrained land availability for trials also pose difficulties for aerial image processing, notably in extracting crop reflectance information from short overlapping rows. Factors such as water stress and lodging further impact the quality of ground and aerial measurements. These challenges collectively impact the effectiveness of AP to contribute to yield improvement and increase breeding efficiency. Importantly, it should be noted that these challenges and limitations are specific to the AP as performed in this study, under these trial conditions. Overall, these insights are valuable for future research, as they have not been reported previously.

6. CONCLUSIONS

The integration of aerial phenotyping (AP) holds potential for improving sugarcane breeding efficiency. Aerial screening of important physiological traits such as stomatal conductance (g_s) and green canopy cover (GCC) could contribute to yield improvement in sugarcane. These traits could theoretically be estimated aerially through canopy temperature (Tc) and normalized difference vegetation index (NDVI), respectively. However, further research is required to evaluate the efficacy of AP of these traits to enhance breeding.

Research to develop and test an AP procedure for identifying superior genotypes in sugarcane breeding was conducted in three phases. First, a pilot experiment evaluated the potential of AP to estimate treatment differences in FIPAR and g_s in a small, unreplicated trial with two genotypes grown under well-watered (WW) and water deficit (WD) conditions. In the second phase a large, replicated field experiment with 54 genotypes and two water treatments in multi-row plots was used to determine genetic variation and heritability of these traits and their impact on yield, and to further evaluate the reliability of AP to estimate these traits. Finally, the AP procedure was validated in two rainfed early-stage breeding trials, with approximately 2000 genotypes in replicated single-row plots, to assess the reliability of AP for estimating final yield and to determine the feasibility of AP to enhance genotype selection in the early stages of breeding programs.

6.1 Main findings

6.1.1 Physiological traits

The study confirmed that FIPAR and g_s are influential traits for determining stalk dry mass yield (SDM). FIPAR, measured at approximately 2-3 months after crop start, serves as a reliable indicator of early vigour and is strongly associated with high stalk yields in well-watered sugarcane. This could aid in identifying high- and low-yielding genotypes under water stress-free conditions. Breeding programs for irrigated environments could benefit from the early identification of superior genotypes, which could speed up the selection cycle and increase selection pressure. By contrast, the desirability of high or low values of g_s depends on water availability. Selecting for high g_s in sugarcane is beneficial in water stress-free environments, whereas lower g_s may be advantageous under water deficit conditions. However, the limited genotypic variation and low heritability of g_s observed in this study suggest that its practical application in breeding programs requires further evaluation.

6.1.2 Trait phenotyping

The study confirmed that FIPAR could be reliably estimated from NDVI in young, partially canopied crops under well-watered conditions. The relationship weakened with crop age and with water stress, aligning well with previous research. Phenotyping of g_s from Tc was mostly unreliable, and the strength of correlations are considered too weak for effective enhancement of breeding. This highlighted the complexities in measuring both g_s and Tc, which possess an inherently complex relationship, that is further confounded by the variability in trait estimates due to environmental conditions. Further work to improve this relationship for effective use in breeding will require extensive measurements of g_s carried out on a genetically diverse population, with improved data acquisition and image processing procedures which account for spatial variation in Tc.

6.1.3 Yield phenotyping

Encouragingly, early NDVI and Tc, which both showed significant genotypic variation and moderate to high broad-sense heritability, could be used to predict SDM of young well-watered, partially canopied crops planted in multi-row plots.

In large breeding populations planted in single-row plots, early estimates of NDVI and Tc, measured approximately 1.5 to 3 months after crop start, showed significant genotypic variation and moderate to high heritability for partially canopied, well-watered crops. In addition, Tc measured shortly after canopy closure but before row overlap due to crop growth also correlated significantly with SDM. Overall, these findings highlight the importance of early crop assessments using AP, and the potential for improving yield prediction accuracy in multi-row and single-row plot trials.

Furthermore, the study also brought new insights into the use of water treatment differences in Tc, measured in multi-row plots, as a tool for identifying drought tolerant genotypes, a finding which has not been reported for sugarcane previously.

6.1.4 AP-based selection

The AP procedure, while implemented successfully in early-stage breeding trials, did not achieve the precision required for genotype selection. A comparison of direct (SDM-based) and indirect (based on aerially measured traits) selection methods showed that AP, as applied

in this study, could not accurately identify high-yielding genotypes as the number of positive matches (i.e. genotypes commonly identified with both methods) was offset by a larger number of false positives or misses in most cases. It was concluded that the potential benefits of AP in breeding will only be realized if the precision of aerial measurements is improved and breeding trial procedures are refined.

6.1.5 Overall conclusions

Overall, this study represents a novel application of AP for evaluating the genetic potential of diverse sugarcane populations, tested in both multi- and single-row plots within South Africa, a research area that has not been previously investigated. The research findings highlight the potential and limitations of AP for breeding. AP holds great promise for identifying genotypic variation in yield-promoting traits, however further research is required to fully realize this potential. The insights gained from this study provide an important foundation for future research and technological development in physiological breeding. It underscores the need for continued refinement of ground and aerial methodologies, and improvements in breeding trial design and execution.

6.1.6 Recommendations for breeding and future research

It is recommended that the AP procedure be validated in early-stage breeding trials with improved designs, and further tested in advanced multi-row variety trials. Enhancing trial designs by increasing plot length, row numbers, and row-spacing could improve the accuracy of aerially captured data using the AP procedure developed in this study. Currently, ongoing efforts involve validating the AP procedure in an intermediate stage between single-row plots (stage 2) and multi-row plots (stage 3) of the breeding program, utilizing plots consisting of two rows, each 8 m in length. It is recommended that this investigation serves as a basis for establishing the minimum spatial resolution required for accurate aerial data capture. Furthermore, it is crucial to address challenges in breeding trial execution, including biases from lengthy planting periods and variability in soil composition, to improve the accuracy of ground and aerially captured data.

Further research is also recommended to investigate the potential of AP to assist breeding in water limited environments. This includes exploring the role of low g_s in water deficit environments through crop modelling approaches. Additionally, the potential of Tc for

identifying drought tolerant genotypes should be investigated, and a better understanding of the genetic basis of drought tolerance requires further study in physiological research. This could potentially offer opportunities for parental selection in breeding for rainfed production areas.

Lastly, this study has directly and indirectly laid the foundation for other research projects at SASRI focused on advancing aerial screening technologies for precision agriculture. This includes investigating the use of multi-spectral drone imagery for estimating cane quality and detecting pest and disease outbreaks early. Research is also underway to test the utility of multi- and hyperspectral aerial data for modelling crop nutrition, and drone-mounted LiDAR scanning for assisting breeding. Future efforts will include more automated image processing procedures, and advanced computational algorithms for data interpretation such as Machine and Deep Learning.

In conclusion, this study demonstrates the potential of AP to enhance sugarcane breeding by facilitating the early detection of important yield-promoting traits, particularly in well-watered crops. While AP shows promise, further work in refining its application is essential to fully realize its benefits. These research findings provide a strong foundation for future efforts to develop novel breeding strategies and precision agriculture technologies.

7. REFERENCES

Acreche, M.M., 2017. Nitrogen-, water- and radiation-use efficiencies affected by sugarcane breeding in Argentina. *Plant Breeding* 136(2), 174–181. https://doi.org/10.1111/pbr.12440

Afghan, S., Arshad, W.R., Khan, M.E., Malik, K.B., 2022. Sugarcane breeding in Pakistan. *Sugar Tech* 24(9), 232–242. https://doi.org/10.1007/s12355-021-01052-9

Aitken, K.S., 2022. History and development of molecular markers for sugarcane breeding. *Sugar Tech* 24(6), 341–353. https://doi.org/10.1007/s12355-021-01000-7

Akbarian, S., Xu, C., Wang, W., Ginns, S., Lim, S., 2022. Sugarcane yields prediction at the row level using a novel cross-validation approach to multi-year multispectral images. *Computers and Electronics in Agriculture* 198(2), 107024. https://doi.org/10.1016/j.compag.2022.107024

Akbarian, S., Xu, C.-Y., Lim, S., 2020. Analysis on the effect of spatial and spectral resolution of different remote sensing data in sugarcane crop yield study. *ISPRS Annals of the Photogrammetry, Remote Sensing and Spatial Information Sciences* V-3–2020, 655–661. https://doi.org/10.5194/isprs-annals-V-3-2020-655-2020

Aktas, Y.O., Ozdemir, U., Dereli, Y., Tarhan, A.F., Cetin, A., Vuruskan, A., Yuksek, B., Cengiz, H., Basdemir, S., Ucar, M., Genctav, M., Yukselen, A., Ozkol, I., Kaya, M.O., Inalhan, G., 2016. Rapid prototyping of a fixed-wing VTOL UAV for design testing. *Journal of Intelligent and Robotic Systems* 84(1), 639–664. https://doi.org/10.1007/s10846-015-0328-6

Alemán-Montes, B., Zabala, A., Henríquez, C., Serra, P., 2023. Modelling two sugarcane agro-industrial yields using Sentinel/Landsat time-series data and their spatial validation at different scales in Costa Rica. *Remote Sensing* 15(23), 5476. https://doi.org/10.3390/rs15235476

Almeida, T.I.R., De Souza Filho, C.R., Rossetto, R., 2006. ASTER and Landsat ETM+ images applied to sugarcane yield forecast. *International Journal of Remote Sensing* 27(19), 4057–4069. https://doi.org/10.1080/01431160600857451

Amarasingam, N., Ashan Salgadoe, A.S., Powell, K., Gonzalez, L.F., Natarajan, S., 2022. A review of UAV platforms, sensors, and applications for monitoring of sugarcane crops. *Remote Sensing Applications* 26(7), 100712. https://doi.org/10.1016/j.rsase.2022.100712

Araus, J.L., Cairns, J.E., 2014. Field high-throughput phenotyping: The new crop breeding frontier. *Trends in Plant Science* 19(1), 52-61. https://doi.org/10.1016/j.tplants.2013.09.008

Araus, J.L., Kefauver, S.C., Zaman-Allah, M., Olsen, M.S., Cairns, J.E., 2018. Translating high-throughput phenotyping into genetic gain. *Trends in Plant Science* 23(5), 451–466. https://doi.org/10.1016/j.tplants.2018.02.001

Araus, J.L., Slafer, G.A., Royo, C., Serret, M.D., 2008. Breeding for yield potential and stress adaptation in cereals. *Critical reviews in Plant Sciences* 27(6), 377–412. https://doi.org/10.1080/07352680802467736

Aung, N.N., Khaing, E.E., Mon, Y.Y., 2022. History of sugarcane breeding, germplasm development and related research in Myanmar. *Sugar Tech* 24(1), 243–253. https://doi.org/10.1007/s12355-021-01079-y

Barbedo, J.G.A., 2019. A review on the use of unmanned aerial vehicles and imaging sensors for monitoring and assessing plant stresses. *Drones* 3(2), 40. https://doi.org/10.3390/drones3020040

Barbosa Júnior, M.R., Moreira, B.R. de A., de Brito Filho, A.L., Tedesco, D., Shiratsuchi, L.S., da Silva, R.P., 2022. UAVs to monitor and manage sugarcane: Integrative review. *Agronomy* 12(13), 661. https://doi.org/10.3390/agronomy12030661

Barbosa Júnior, M.R., Moreira, B.R. de A., de Oliveira, R.P., Shiratsuchi, L.S., da Silva, R.P., 2023. UAV imagery data and machine learning: A driving merger for predictive analysis of qualitative yield in sugarcane. *Frontiers in Plant Science* 14, 1114852. https://doi.org/10.3389/fpls.2023.1114852

Basnayake, J., 2016. Canopy temperature: a predictor of sugarcane yield for irrigated and rainfed conditions. *Proceedings of the International Society of Sugar Cane Technologists*, 50-57. Available at: https://www.researchgate.net/publication/299820903_Canopy_temperature_a_predictor_of_sugarcane_yield_for_irrigated_and_rainfed_conditions (Accessed: 23 August 2024).

Basnayake, J., Jackson, P.A., Inman-Bamber, N.G., Lakshmanan, P., 2012. Sugarcane for water-limited environments. Genetic variation in cane yield and sugar content in response to water stress. *Journal of Experimental Botany* 63(16), 6023–6033. https://doi.org/10.1093/jxb/ers251

Basnayake, J., Jackson, P.A., Inman-Bamber, N.G., Lakshmanan, P., 2015. Sugarcane for water-limited environments. Variation in stomatal conductance and its genetic correlation with crop productivity. *Journal of Experimental Botany* 66(13), 3945–3958. https://doi.org/10.1093/jxb/erv194

Bauer, M.E., Cipra, J.E., Anuta, P.E., Etheridge, J.B., 1979. Identification and area estimation of agricultural crops by computer classification of LANDSAT MSS data. *Remote Sensing of Environment* 8(1), 77–92. https://doi.org/10.1016/0034-4257(79)90025-7

Begue, A., Lebourgeois, Valentine, Bappel, Eric, Todoroff, Pierre, Pellegrino, Anne, Baillarin, Florence, Siegmund, Bernard, Bèguè, A., Lebourgeois, V, Bappel, E, Todoroff, P, Pellegrino, A, Baillarin, F, Siegmund, B, 2010. Spatio-temporal variability of sugarcane fields and recommendations for yield forecast using NDVI. *International Journal of Remote Sensing* 31(20), 5391–5407. https://doi.org/10.1080/01431160903349057

Belko, N., Zaman-Allah, M., Diop, N.N., Cisse, N., Zombre, G., Ehlers, J.D., Vadez, V., 2013. Restriction of transpiration rate under high vapour pressure deficit and non-limiting water conditions is important for terminal drought tolerance in cowpea. *Plant Biology* 15(2), 304–316. https://doi.org/10.1111/j.1438-8677.2012.00642.x

Birth, G.S., McVey, G.R., 1968. Measuring the color of growing turf with a reflectance spectrophotometer. *Agronomy Journal* 60(6), 640–643. https://doi.org/10.2134/agronj1968.00021962006000060016x

Blatchford, M.L., Mannaerts, C.M., Zeng, Y., Nouri, H., Karimi, P., 2019. Status of accuracy in remotely sensed and in-situ agricultural water productivity estimates: A review. *Remote Sensing of Environment* 234, 111413. https://doi.org/10.1016/j.rse.2019.111413

Blum, A., 2009. Effective use of water (EUW) and not water-use efficiency (WUE) is the target of crop yield improvement under drought stress. *Field Crops Research* 112(2-3), 119–123. https://doi.org/10.1016/j.fcr.2009.03.009

Blum, A., Mayer, J., Gozlan, G., 1982. Infrared thermal sensing of plant canopies as a screening technique for dehydration avoidance in wheat. *Field Crops Research* 5, 137–146. https://doi.org/10.1016/0378-4290(82)90014-4

Bonhomme, R., 2000. Beware of comparing RUE values calculated from PAR vs solar radiation or absorbed vs intercepted radiation. *Field Crops Research* 68(3), 247–252. https://doi.org/10.1016/S0378-4290(00)00120-9

Bonnett, G.D., 1998. Rate of leaf appearance in sugarcane, including a comparison of a range of varieties. *Functional Plant Biology* 25(7), 829-834. https://doi.org/10.1071/PP98041

Bouyoucos, G.J., 1962. Hydrometer method improved for making particle size analyses of soils. *Agronomy Journal* 54(5), 464–465. https://doi.org/10.2134/agronj1962.00021962005400050028x

Caine, R.S., Yin, X., Sloan, J., Harrison, E.L., Mohammed, U., Fulton, T., Biswal, A.K., Dionora, J., Chater, C.C., Coe, R.A., Bandyopadhyay, A., Murchie, E.H., Swarup, R., Quick, W.P., Gray, J.E., 2019. Rice with reduced stomatal density conserves water and has improved drought tolerance under future climate conditions. *New Phytologist* 221(1), 371–384. https://doi.org/10.1111/nph.15344

Campbell, J.A., Robertson, M.J., Grof, C.P.L., 1998. Temperature effects on node appearance in sugarcane. *Australian Journal of Plant Physiology* 25(7), 815-818. https://doi.org/10.1071/PP98040

Cao, A.D., Doan, L.T., 2022. Sugarcane breeding, germplasm development and supporting genetics research in Vietnam. *Sugar Tech* 24(68), 272–278. https://doi.org/10.1007/s12355-021-01068-1

Cardoso, L.A.S., Farias, P.R.S., Soares, J.A.C., 2022. Use of unmanned aerial vehicle in sugarcane cultivation in Brazil: A review. *Sugar Tech* 24(6), 1636–1648. https://doi.org/10.1007/s12355-022-01149-9

Carr, M.K. V., Knox, J.W., 2011. The water relations and irrigation requirements of sugar cane (*Saccharum officinarum*): A review. *Experimental Agriculture* 47(1), 1–25. https://doi.org/10.1017/S0014479710000645

Castillo, R.O., Silva Cifuentes, E., 2022. Sugarcane breeding and supporting genetics research in Ecuador. *Sugar Tech* 24(22), 222–231. https://doi.org/10.1007/s12355-021-01057-4

Chapman, S., Merz, T., Chan, A., Jackway, P., Hrabar, S., Dreccer, M., Holland, E., Zheng, B., Ling, T., Jimenez-Berni, J., 2014. Pheno-Copter: A low-altitude, autonomous remote-sensing robotic helicopter for high-throughput field-based phenotyping. *Agronomy* 4(2), 279–301. https://doi.org/10.3390/agronomy4020279

Chaudhuri, U.N., Deaton, M.L., Kanemasu, E.T., Wall, G.W., Marcarian, V., Dobrenz, A.K., 1986. A procedure to select drought-tolerant sorghum and millet genotypes using canopy temperature and vapor pressure deficit. *Agronomy Journal* 78(3), 490–494. https://doi.org/10.2134/agronj1986.00021962007800030020x

Chea, C., Saengprachatanarug, K., Posom, J., Wongphati, M., Taira, E., 2020. Sugar Yield Parameters and Fiber Prediction in Sugarcane Fields Using a Multispectral Camera Mounted on a Small Unmanned Aerial System (UAS). Sugar Tech 22(4), 605–621. https://doi.org/10.1007/s12355-020-00802-5

Chea, C., Saengprachathanarug, K., Wongphati, M., Posom, J., Nodthaisong, C., Taira, E., 2018. Feasibility study of evaluation brix of sugarcane using multispectral camera mounted on unmanned aerial vehicle. The 11th TASE International conference, April, 148-159.

Cholula, U., da Silva, J.A., Marconi, T., Thomasson, J.A., Solorzano, J., Enciso, J., 2020. Forecasting yield and lignocellulosic composition of energy cane using unmanned aerial systems. *Agronomy* 10(5), 718. https://doi.org/10.3390/agronomy10050718

Christina, M., Jones, M.-R., Versini, A., Mézino, M., Le Mézo, L., Auzoux, S., Soulié, J.C., Poser, C., Gérardeaux, E., 2021. Impact of climate variability and extreme rainfall events on sugarcane yield gap in a tropical island. *Field Crops Research* 274(2), 108326. https://doi.org/10.1016/j.fcr.2021.108326

Coelho, A., Dalri, A.B., Filho, J., Faria, R., Silva, L., Pimenta Gomes, R., 2019. Calibration and evaluation of the DSSAT/Canegro model for sugarcane cultivars under irrigation managements. *Revista Brasileira de Engenharia Agrícola e Ambiental* 24(1), 52-58. http://doi.org/10.1590/1807-1929/agriambi.v24n1p52-58

Condon, A.G., Richards, R.A., 1993. Exploiting genetic variation in transpiration efficiency in eheat: An agronomic view. In: J.R. Ehleringer, A.E. Hall, & G.D. Farquhar, eds. *Stable Isotopes and Plant Carbon-Water Relations*. San Diego, CA: Academic Press, pp. 435–450.

Condon, A.G., Richards, R.A., Rebetzke, G.J., Farquhar, G.D., 2002. Improving intrinsic water-use efficiency and crop yield. *Crop Science* 42(1), 122–131. https://doi.org/10.2135/cropsci2002.1220

Condon, A.G., Richards, R.A., Rebetzke, G.J., Farquhar, G.D., 2004. Breeding for high water-use efficiency. *Journal of Experimental Botany* 55(407), 2447–2460. https://doi.org/10.1093/jxb/erh277

Cursi, D.E., Hoffmann, H.P., Barbosa, G.V.S., Bressiani, J.A., Gazaffi, R., Chapola, R.G., Fernandes Junior, A.R., Balsalobre, T.W.A., Diniz, C.A., Santos, J.M., Carneiro, M.S., 2022. History and current status of sugarcane breeding, germplasm development and molecular genetics in Brazil. *Sugar Tech* 24(1), 112–133. https://doi.org/10.1007/s12355-021-00951-1

de Oliveira, M.P., Cardoso, P.H., Oliveira, R.P. de, Barbosa Júnior, M.R., da Silva, R.P., 2023. Mapping gaps in sugarcane fields using UAV-RTK platform. *Agriculture* 13(6), 1241. https://doi.org/10.3390/agriculture13061241

de Oliveira, R.P., Barbosa Júnior, M.R., Pinto, A.A., Oliveira, J.L.P., Zerbato, C., Furlani, C.E.A., 2022. Predicting sugarcane biometric parameters by UAV multispectral images and machine learning. *Agronomy* 12(9), 1992. https://doi.org/10.3390/agronomy12091992

De Rango, F, Potrino, G., Tropea, M., Santamaria, A.F., Palmieri, N., 2019. Simulation, modeling and technologies for drones coordination techniques in precision agriculture. In: M.S. Obaidat, T. Ören, & F. De Rango eds. *Simulation and Modeling Methodologies, Technologies and Applications: SIMULTECH 2017*. Advances in Intelligent Systems and Computing, vol. 873. Cham: Springer International Publishing, pp. 77–101. https://doi.org/10.1007/978-3-030-01470-4_5

De Silva, A., De Costa, W., 2009. Varietal variation in stomatal conductance, transpiration and photosynthesis of commercial sugarcane varieties under two contrasting water regimes. *Tropical Agricultural Research*. 12(2), 97–102. http://dx.doi.org/10.4038/tare.v12i2.2798

De Silva, A.L., 2004. Varietal variation in growth, physiology and yield of sugarcane under two contrasting water regimes. *Tropical Agricultural Research* 16, 1-12. Available at: https://sugarres.lk/wp-content/uploads/2020/07/CRM-39.-Varietal-variation-in-growth-physiology-and-yield-of-sugarcane-under-two-contrasting-water-regimes.pdf (Accessed: 24 August 2024).

De Silva, A. L.C., De Costa, W.A.J.M., 2012. Growth and radiation use efficiency of sugarcane under irrigated and rain-fed conditions in Sri Lanka. *Sugar Tech* 14(3), 247–254. http://dx.doi.org/10.1007/s12355-012-0148-y

De Sousa-Vieira, O., Milligan, S.B., 1999. Intrarow plant spacing and Family × Environment interaction effects on sugarcane family evaluation. *Crop Science* 39(2), 358–364. https://doi.org/10.2135/cropsci1999.0011183X003900020009xa

De Souza, A.P., Massenburg, L.N., Jaiswal, D., Cheng, S., Shekar, R., Long, S.P., 2017. Rooting for cassava: insights into photosynthesis and associated physiology as a route to improve yield potential. *New Phytologist* 213(1), 50–65. https://doi.org/10.1111/nph.14250

de Souza, C., Lamparelli, R., Rocha, J., Graziano Magalhães, P., 2017. Height estimation of sugarcane using an unmanned aerial system (UAS) based on structure from motion (SfM) point clouds. *International Journal of Remote Sensing* 38(8-10), 2218-2230. https://doi.org/10.1080/01431161.2017.1285082

Dengia, A., Dechassa, N., Wogi, L., Amsalu, B., 2023. A simplified approach to satellite-based monitoring system of sugarcane plantation to manage yield decline at Wonji-Shoa Sugar Estate, central Ethiopia. *Heliyon* 9(8), e18982. https://doi.org/10.1016/j.heliyon.2023.e18982

Dias, H.B., Inman-Bamber, G., Bermejo, R., Sentelhas, P.C., Christodoulou, D., 2019. New APSIM-Sugar features and parameters required to account for high sugarcane yields in tropical environments. *Field Crops Research* 235, 38–53. https://doi.org/10.1016/j.fcr.2019.02.002

Dias, H.B., Inman-Bamber, G., Everingham, Y., Sentelhas, P.C., Bermejo, R., Christodoulou, D., 2020. Traits for canopy development and light interception by twenty-seven Brazilian sugarcane varieties. *Field Crops Research* 249, 107716. https://doi.org/10.1016/j.fcr.2020.107716

Dixon, H.H., Joly, J., 1895. XII. On the ascent of sap. *Philosophical Transactions of the Royal Society of London. Series B, Biological Sciences*, 186, 563–576. https://doi.org/10.1098/rstb.1895.0012

Donaldson, R., Redshaw, K., Rhodes, R., van Antwerpen, R., 2008. Season effects on productivity of some commercial South African sugarcane cultivars. II: Trash production. *Proceedings of the South African Sugar Technologists' Association* 81, 528–538.

Duan, T., Zheng, B., Guo, W., Ninomiya, S., Guo, Y., Chapman, S.C., 2017. Comparison of ground cover estimates from experiment plots in cotton, sorghum and sugarcane based on images and ortho-mosaics captured by UAV. *Functional Plant Biology* 44(1), 169-183. https://doi.org/10.1071/fp16123

Dumont, T., Barau, L., Thong-Chane, A., Dijoux, J., Mellin, M., Daugrois, J., Hoarau, J.Y., 2022. Sugarcane breeding in Reunion: Challenges, achievements and future prospects. *Sugar Tech* 24(4), 181–192. https://doi.org/10.1007/s12355-021-00998-0

Eksteen, A., Singels, A., Ngxaliwe, S., 2014. Water relations of two contrasting sugarcane genotypes. *Field Crops Research* 168, 86–100. https://doi.org/10.1016/j.fcr.2014.08.008

Evensen, C., Muchow, R., El-Swaify, S.A., Osgood, R., 1997. Yield accumulation in irrigated sugarcane: I. Effect of crop age and cultivar. *Agronomy Journal* 89(4), 638-646. http://dx.doi.org/10.2134/agronj1997.00021962008900040016x

Falconer, D.S., Mackay, T.F.C., 1996. Introduction to quantitative genetics, Fourth ed., Longman: Burnt Mill, UK.

FAOSTAT, 2023. FAOSTAT Statistical database. Available at: https://www.fao.org/faostat/en/#home (Accessed: 30 December 2023).

Farquhar, G.D., Ehleringer, J.R., Hubick, K.T., 1989. Carbon isotope discrimination and photosynthesis. *Annual Review of Plant Physiology and Plant Molecular Biology* 40, 503–537. https://doi.org/10.1146/annurev.pp.40.060189.002443

Fehr, W.R., 1987. *Principles of cultivar development*. Macmillan, New York. Available at: https://lib.dr.iastate.edu/agron_books/1 (Accessed: 24 August 2024).

Ferreira, T.H.S., Tsunada, M.S., Bassi, D., Araújo, P., Mattiello, L., Guidelli, G. V., Righetto, G.L., Gonçalves, V.R., Lakshmanan, P., Menossi, M., 2017. Sugarcane water stress tolerance mechanisms and its implications on developing biotechnology solutions. *Frontiers in Plant Science* 8, 1077. https://doi.org/10.3389/fpls.2017.01077

Fischer, R.A., Rees, D., Sayre, K.D., Lu, Z.M., Condon, A.G., Larque Saavedra, A., 1998. Wheat yield progress associated with higher stomatal conductance and photosynthetic rate, and cooler canopies. *Crop Science* 38(6), 1467–1475. https://doi.org/10.2135/cropsci1998.0011183X003800060011x

Furbank, R.T., Tester, M., 2011. Phenomics – technologies to relieve the phenotyping bottleneck. *Trends in Plant Science* 16(12), 635–644. https://doi.org/10.1016/j.tplants.2011.09.005

Gazaffi, R., Oliveira, K.M., Souza, A.P. de, Garcia, A.A.F., 2014. Sugarcane: breeding methods and genetic mapping. In: Cortez, L.A.B., ed. *Sugarcane Bioethanol- R&D for Productivity and Sustainability*. São Paulo: Editora Edgard Blücher, pp. 333–344.

Ghannoum, O., 2016. How can we breed for more water use-efficient sugarcane? *Journal of Experimental Botany* 67(3), 557–559. https://doi.org/10.1093/jxb/erw009

Ghebrezgabher, M.G., Yang, T., Yang, X., Wang, X., Khan, M., 2016. Extracting and analyzing forest and woodland cover change in Eritrea based on landsat data using supervised classification. *The Egyptian Journal of Remote Sensing and Space Science* 19(1), 37–47. https://doi.org/10.1016/j.ejrs.2015.09.002

Gilbert, M.E., Zwieniecki, M.A., Holbrook, N.M., 2011. Independent variation in photosynthetic capacity and stomatal conductance leads to differences in intrinsic water use efficiency in 11 soybean genotypes before and during mild drought. *Journal of Experimental Botany* 62(8), 2875–2887. https://doi.org/10.1093/jxb/erq461

Gilbert, R.A., Rainbolt, C.R., Morris, D.R., McCray, J.M., 2008. Sugarcane growth and yield responses to a 3-month summer flood. *Agricultural Water Management* 95(3), 283–291. https://doi.org/10.1016/j.agwat.2007.10.009

Gill, T., Gill, S.K., Saini, D.K., Chopra, Y., de Koff, J.P., Sandhu, K.S., 2022. A comprehensive review of high throughput phenotyping and machine learning for plant stress phenotyping. *Phenomics* 2(3), 156–183. https://doi.org/10.1007/s43657-022-00048-z

Gitelson, A.A., Kaufman, Y.J., Merzlyak, M.N., 1996. Use of a green channel in remote sensing of global vegetation from EOS-MODIS. *Remote Sensing of Environment* 58(3), 289–298. https://doi.org/10.1016/S0034-4257(96)00072-7

Gitelson, A.A., Viña, A., Arkebauer, T.J., Rundquist, D.C., Keydan, G., Leavitt, B., 2003. Remote estimation of leaf area index and green leaf biomass in maize canopies. *Geophysical Research Letters* 30(5). https://doi.org/10.1029/2002GL016450

Goldemberg, J., Mello, F.C., Cerri, C.E.P., Davies, C.A., Cerri, C.C., 2014. Meeting the global demand for biofuels in 2021 through sustainable land use change policy. *Energy Policy* 69, 14-18. https://doi.org/10.1016/j.enpol.2014.02.008

Gonzalez-de-Santos, P., Fernandez, R., Sepúlveda, D., Navas, E., Armada, M., 2020. Unmanned Ground Vehicles for Smart Farms. In: *Agronomy- Climate Change and Food Security*, ch. 6, pp. 73-95. IntechOpen. http://dx.doi.org/10.5772/intechopen.90683

Gonzalez-Dugo, V., Zarco-Tejada, P., Berni, J.A.J., Suárez, L., Goldhamer, D., Fereres, E., 2012. Almond tree canopy temperature reveals intra-crown variability that is water stress-dependent. *Agricultural and Forest Meteorology* 154–155, 156–165. https://doi.org/10.1016/j.agrformet.2011.11.004

Gravois, K.A., Milligan, S.B., Martin, F.A., 1991. Indirect selection for increased sucrose yield in early sugarcane testing stages. *Field Crops Research* 26(1), 67–73. https://doi.org/10.1016/0378-4290(91)90058-4

Guo, W., Carroll, M.E., Singh, A., Swetnam, T.L., Merchant, N., Sarkar, S., Singh, A.K., Ganapathysubramanian, B., 2021. UAS-based plant phenotyping for research and breeding applications. *Plant Phenomics* 2, 1-21. https://doi.org/10.34133/2021/9840192

Haghighattalab, A., González Pérez, L., Mondal, S., Singh, D., Schinstock, D., Rutkoski, J., Ortiz-Monasterio, I., Singh, R.P., Goodin, D., Poland, J., 2016. Application of unmanned aerial systems for high throughput phenotyping of large wheat breeding nurseries. *Plant Methods* 12(35). https://doi.org/10.1186/s13007-016-0134-6 Hale, A.L., Todd, J.R., Gravois, K.A., Mollov, D., Malapi-Wight, M., Momotaz, A., Laborde, C., Goenaga, R., Kimbeng, C., Solis, A., Waguespack, H., 2022. Sugarcane breeding programs in the USA. *Sugar Tech* 24(10), 97–111. http://dx.doi.org/10.1007/s12355-021-01018-x

Henry, F., Herwindiati, D.E., Mulyono, S., Hendryli, J., 2017. Sugarcane Land Classification with Satellite Imagery using Logistic Regression Model. In: IOP Conference Series: *Materials Science and Engineering*. Institute of Physics Publishing, pp. 012024. Available at: https://iopscience.iop.org/article/10.1088/1757-899X/185/1/012024/meta (Accessed: 24 August 2024).

Hoarau, J.-Y., Dumont, T., Wei, X., Jackson, P., D'Hont, A., 2022. Applications of quantitative genetics and statistical analyses in sugarcane breeding. *Sugar Tech* 24, 320–340. https://doi.org/10.1007/s12355-021-01012-3

Hoffman, N., 2016. Pot trial phenotyping to predict sugarcane genotype field performance with the Canegro model. M.Sc. Thesis. University of KwaZulu-Natal, Pietermaritzburg. Available at: https://researchspace.ukzn.ac.za/items/1b523ad1-c30c-4ec0-9a79-c970499ae851 (Accessed: 24 August 2024).

Hoffman, N., Singels, A., 2019. Evaluating the use of aerially captured spectral data for characterising drought-tolerance traits in sugarcane. *Proceedings of the Australian Society of Sugar Cane Technology* 41.

Hoffman, N., Singels, A., Joshi, S., 2024. Aerial phenotyping for sugarcane yield and drought tolerance. *Field Crops Research* 308, 109275. https://doi.org/10.1016/j.fcr.2024.109275

Hoffman, N., Singels, A., Patton, A., Ramburan, S., 2018. Predicting genotypic differences in irrigated sugarcane yield using the Canegro model and independent trait parameter estimates. *European Journal of Agronomy* 96, 13–21. https://doi.org/10.1016/j.eja.2018.01.005

Huang, Q., Feng, J., Gao, M., Lai, S., Han, G., Qin, Z., Fan, J., Huang, Y., 2024. Precise estimation of sugarcane yield at field scale with allometric variables retrieved from UAV Phantom 4 RTK images. *Agronomy* 14(3), 476. https://doi.org/10.3390/agronomy14030476

Huete, A., Didan, K., Miura, T., Rodriguez, E.P., Gao, X., Ferreira, L.G., 2002. Overview of the radiometric and biophysical performance of the MODIS vegetation indices. *Remote Sensing of Environment* 83(1-2), 195–213. https://doi.org/10.1016/S0034-4257(02)00096-2

Huete, A.R., 1988. A soil-adjusted vegetation index (SAVI). *Remote Sensing of Environment* 25(3), 295–309. https://doi.org/10.1016/0034-4257(88)90106-X

Inman-Bamber, N.G., 1991. A growth model for sugar-cane based on a simple carbon balance and the CERES-Maize water balance. *South African Journal of Plant and Soil* 8(2), 93–99. https://doi.org/10.1080/02571862.1991.10634587

Inman-Bamber, N.G., 1994. Temperature and seasonal effects on canopy development and light interception of sugarcane. *Field Crops Research* 36(1), 41–51. https://doi.org/10.1016/0378-4290(94)90051-5

Inman-Bamber, N.G., Bonnett, G.D., Spillman, M.F., Hewitt, M.L., Xu, J., 2009. Source - sink differences in genotypes and water regimes influencing sucrose accumulation in sugarcane stalks. *Crop Pasture Science* 60(4), 316-327. https://doi.org/10.1071/CP08272

Inman-Bamber, N.G., De Jager, J.M., 1986. The reaction of two varieties of sugarcane to water stress. *Field Crops Research* 14, 15–28. https://doi.org/10.1016/0378-4290(86)90043-2

Inman-Bamber, N.G., Jackson, P.A., Hewitt, M., 2011. Sucrose accumulation in sugarcane stalks does not limit photosynthesis and biomass production. *Crop Pasture Science* 62(10), 848-858. http://dx.doi.org/10.1071/CP11128

Inman-Bamber, N.G., Lakshmanan, P., Park, S., 2012. Sugarcane for water-limited environments: Theoretical assessment of suitable traits. *Field Crops Research* 134, 95–104. https://doi.org/10.1016/j.fcr.2012.05.004

Inman-Bamber, N.G., Smith, D.M., 2005. Water relations in sugarcane and response to water deficits. *Field Crops Research* 92(2-3), 185–202. https://doi.org/10.1016/j.fcr.2005.01.023

Irvine, J.E., 1975. Relations of photosynthetic rates and leaf and canopy characters to sugarcane yield. *Crop Science* 15(5), 671–676. https://doi.org/10.2135/cropsci1975.0011183X001500050017x

Jackson, P., 2019. Why are yields of sugarcane not increasing as much as sugar beet (or other crops)? *Proceedings of the International Society of Sugar Cane Technologists (ISSCT)* 30, 128–137. Available at: https://issct.org/wp-content/uploads/proceedings/2019/Plenary%20papers/Jackson.pdf (Accessed: 24 August 2024).

Jackson, P., Basnayake, J., Inman-Bamber, G., Lakshmanan, P., Natarajan, S., Stokes, C., 2016. Genetic variation in transpiration efficiency and relationships between whole plant and leaf gas exchange measurements in Saccharum spp. and related germplasm. *Journal of Experimental Botany* 67(3), 861–871. https://doi.org/10.1093/jxb/erv505

Jackson, P., Robertson, M., Cooper, M., Hammer, G., 1996. The role of physiological understanding in plant breeding; from a breeding perspective. *Field Crops Research* 49(1), 11–37. https://doi.org/10.1016/S0378-4290(96)01012-X

Jackson, P.A., 2005. Breeding for improved sugar content in sugarcane. *Field Crops Research* 92(2-3), 277–290. https://doi.org/10.1016/j.fcr.2005.01.024Jackson, R.D., Idso, S.B., Reginato, R.J., Pinter, P.J., 1981. Canopy temperature as a crop water stress indicator. *Water Resources Research* 17(4), 1133–1138. https://doi.org/10.1029/WR017i004p01133

Jarvis, P.G., Mcnaughton, K.G., 1986. Stomatal control of transpiration: Scaling up from leaf' to region. *Advances in Ecological Research* 15, 1-49. https://doi.org/10.1016/S0065-2504(08)60119-1

Jones, C.A., Kiniry, J., 1986. CERES-Maize: A simulation model of maize growth and development. Texas A & M University Press, College Station, Texas. Available at: https://www.ars.usda.gov/ARSUserFiles/30980500/CERES-Maize%20Book.pdf (Accessed: 24 August 2024)

Jones, H., Sirault, X., 2014. Scaling of thermal images at different spatial resolution: The mixed pixel problem. *Agronomy* 4(3), 380–396. https://doi.org/10.3390/agronomy4030380

Jones, H.G., 2002. Use of infrared thermography for monitoring stomatal closure in the field: application to grapevine. *Journal of Experimental Botany* 53(378), 2249–2260. https://doi.org/10.1093/jxb/erf083

Jones, H.G., Vaughan, R.A., 2010. Remote sensing of vegetation: principles, techniques, and applications. Oxford university press.

Jones, M.R., Singels, A., Chinorumba, S., Patton, A., Poser, C., Singh, M., Martiné, J.F., Christina, M., Shine, J., Annandale, J., Hammer, G., 2019. Exploring process-level genotypic and environmental effects on sugarcane yield using an international experimental dataset. *Field Crops Research* 244, 107622. https://doi.org/10.1016/j.fcr.2019.107622

Jordan, C.F., 1969. Derivation of leaf-area index from quality of light on the forest floor. *Ecology* 50(4), 663–666. https://doi.org/10.2307/1936256

Jung, J., Maeda, M., Chang, A., Landivar, J., Yeom, J., McGinty, J., 2018. Unmanned aerial system assisted framework for the selection of high yielding cotton genotypes. *Computers and Electronics in Agriculture* 152, 74–81. https://doi.org/10.1016/j.compag.2018.06.051

Karno, 2007. Physiology of bud outgrowth in sugarcane.Ph.D. Thesis. University of Queensland.

Kelly, J., Kljun, N., Olsson, P.O., Mihai, L., Liljeblad, B., Weslien, P., Klemedtsson, L., Eklundh, L., 2019. Challenges and best practices for deriving temperature data from an uncalibrated UAV thermal infrared camera. *Remote Sensing* 11(5), 567. https://doi.org/10.3390/rs11050567

Kempthorne, O., 1957. An introduction to genetic statistics. John Wiley and Sons, Inc., New York.

Kennedy, A.J., 2022. Sugarcane variety development in the Caribbean. *Sugar Tech* 24(4), 64–72. https://doi.org/10.1007/s12355-020-00936-6

Khera, K., Sandhu, B., 1986. Canopy temperature of sugarcane as influenced by irrigation regime. *Agricultural and Forest Meteorology* 37(3), 245–258. https://doi.org/10.1016/0168-1923(86)90034-1

Khuimphukhieo, I., Marconi, T., Enciso, J., da Silva, J.A., 2023. The use of UAS-based high throughput phenotyping (HTP) to assess sugarcane yield. *Journal of Agriculture and Food Research* 11, 100501. https://doi.org/10.1016/j.jafr.2023.100501

Khumla, N., Sakuanrungsirikul, S., Punpee, P., Hamarn, T., Chaisan, T., Soulard, L., Songsri, P., 2022. Sugarcane breeding, germplasm development and supporting genetics research in Thailand. *Sugar Tech* 24, 193–209. https://doi.org/10.1007/s12355-021-00996-2

Kim, J., Kim, S., Ju, C., Son, H. Il, 2019. Unmanned aerial vehicles in agriculture: A review of perspective of platform, control, and applications. *IEEE Access* 7, 105100-105115. https://doi.org/10.1109/ACCESS.2019.2932119

Kumar, U., Priyanka, Kumar, S., 2016. Genetic Improvement of Sugarcane Through Conventional and Molecular Approaches. In: Rajpal, V.R., Rao, S.R., Raina, S.N., eds. *Molecular Breeding for Sustainable Crop Improvement: Volume 2*. Cham: Springer International Publishing, pp. 325–342.

Leanasawat, N., Kosittrakun, M., Lontom, W., Songsri, P., 2021. Physiological and agronomic traits of certain sugarcane genotypes grown under field conditions as influenced by early drought stress. *Agronomy* 11(11), 2319. https://doi.org/10.3390/agronomy11112319

Li, C., Jackson, P., Lu, X., Xu, C., Cai, Q., Basnayake, J., Lakshmanan, P., Ghannoum, O., Fan, Y., 2017. Genotypic variation in transpiration efficiency due to differences in photosynthetic capacity among sugarcane-related clones. *Journal of Experimental Botany* 68(9), 2377–2385. https://doi.org/10.1093/jxb/erx107

Li, X., Ba, Y., Zhang, M., Nong, M., Yang, C., Zhang, S., 2022. Sugarcane nitrogen concentration and irrigation level prediction based on UAV multispectral imagery. *Sensors* 22(7), 2711. https://doi.org/10.3390/s22072711

Li, Xiaohan, Li, Xuezhang, Liu, W., Wei, B., Xu, X., 2021. A UAV-based framework for crop lodging assessment. *European Journal of Agronomy* 123, 126201. https://doi.org/10.1016/j.eja.2020.126201

Liu, D.L., Kingston, G., Bull, T.A., 1998. A new technique for determining the thermal parameters of phenological development in sugarcane, including suboptimum and supra-optimum temperature regimes. *Agricultural and Forest Meteorology* 90(1-2), 119–139. https://doi.org/10.1016/S0168-1923(97)00087-7

Lobell, D.B., Burke, M.B., Tebaldi, C., Mastrandrea, M.D., Falcon, W.P., Naylor, R.L., 2008. Prioritizing climate change adaptation needs for food security in 2030. *Science* 319(5863), 607–610. https://doi.org/10.1126/science.1152339

Lobell, D.B., Hammer, G.L., McLean, G., Messina, C., Roberts, M.J., Schlenker, W., 2013. The critical role of extreme heat for maize production in the United States. *Nature Climate Change* 3, 497–501. https://doi.org/10.1038/nclimate1832

Luna, I., Lobo, A., 2016. Mapping crop planting quality in sugarcane from UAV Imagery: A pilot study in Nicaragua. *Remote Sensing* 8(6), 500. https://doi.org/10.3390/rs8060500

Luo, T., Liu, X., Lakshmanan, P., 2023. A combined genomics and phenomics approach is needed to boost breeding in sugarcane. *Plant Phenomics* 5, 0074. https://doi.org/10.34133/plantphenomics.0074

Luzaran, R.T., Engle, L.M., Villariez, H.P., Oquias, G.B., 2022. Sugarcane breeding and germplasm development in the Philippines. *Sugar Tech* 24, 210–221. https://doi.org/10.1007/s12355-021-00979-3

Maes, W.H., Steppe, K., 2019. Perspectives for remote sensing with unmanned aerial vehicles in precision agriculture. *Trends in Plant Science* 24(2), 154–162. https://doi.org/10.1016/j.tplants.2018.11.007

Mahachi, A., Aloni, T., Mashevedze, L., 2022. Unmanned aerial vehicle for agriculture surveillance. In: Ali, Z.A., Cvetković, D., eds. *Aeronautics*. Rijeka: IntechOpen. http://dx.doi.org/10.5772/intechopen.104476

Mall, A.K., Misra, V., Singh, B.D., Kumar, M., Pathak, A.D., 2020. Drought tolerance: Breeding efforts in sugarcane. In: Hasanuzzaman, M., ed. *Agronomic crops*. Singapore: Springer. https://doi.org/10.1007/978-981-15-0025-1_10.

Mangelsdorf, A., 1953. Sugarcane breeding in Hawaii. Part II- 1921 - 1952. *Hawaiian Planters Record* 54, 101-137.

Marin, F.R., Jones, J.W., Royce, F., Suguitani, C., Donzeli, J.L., Filho, W.J.P., Nassif, D.S.P., 2011. Parameterization and evaluation of predictions of DSSAT/CANEGRO for Brazilian sugarcane. *Agronomy Journal* 103(2), 304–315. https://doi.org/10.2134/agronj2010.0302

McGlinchey, M.G., Inman-Bamber, N., 1996. Effect of irrigation scheduling on water use efficiency and yield. *Proceedings of the South African Sugar Technologists' Association* 70, 55-56. Available at: https://citeseerx.ist.psu.edu/document?repid=rep1&type=pdf&doi=3c200648e2e8a3bc0689475aec1b8f6e782a01e6 (Accessed: 24 August 2024).

Meehl, G.A., Stocker, T.F., Collins, W.D., Friedlingstein France, P., Gaye, A.T., Gregory, J.M., Kitoh, Akio, Knutti, Reto, Murphy, J.M., Noda, Akira, Raper, S.C., Allen, M., Stocker, T., Collins, W., Friedlingstein, P., Gaye, A., Gregory, J., Kitoh, A, Knutti, R, Murphy, J., Noda, A, Raper, S., Watterson, I., Weaver, A., Zhao, Z., Qin, D., Manning, M., Chen, Z., Marquis, M., Averyt, K., Tignor, M., 2007. Global climate projections. In: *Climate Change 2007: The physical science basis. Contribution of Working Group I to the fourth assessment report of the intergovernmental panel on climate change*, Cambridge University Press, Cambridge, 976.

Meena, M.R., Appunu, C., Arun Kumar, R., Manimekalai, R., Vasantha, S., Krishnappa, G., Kumar, R., Pandey, S.K., Hemaprabha, G., 2022. Recent advances in sugarcane genomics, physiology, and phenomics for superior agronomic traits. *Frontiers in Genetics* 13, 854936. https://doi.org/10.3389/fgene.2022.854936

Mehareb, E.M., El-Shafai, A.M.A., Fouz, F.M.A.E., 2022. History and current status of sugarcane breeding in Egypt. *Sugar Tech* 24, 267–271. https://doi.org/10.1007/s12355-021-01010-5

Meinzer, F.C., Grantz, D.A., 1990. Stomatal and hydraulic conductance in growing sugarcane: stomatal adjustment to water transport capacity. *Plant, Cell and Environment* 13(4), 383–388. http://dx.doi.org/10.1111/j.1365-3040.1990.tb02142.x

Meki, M.N., Kiniry, J.R., Youkhana, A.H., Crow, S.E., Ogoshi, R.M., Nakahata, M.H., Tirado-Corbalá, R., Anderson, R.G., Osorio, J., Jeong, J., 2015. Two-year growth cycle sugarcane crop parameter attributes and their application in modeling. *Agronomy Journal* 107(4), 1310–1320. https://doi.org/10.2134/agronj14.0588

Meron, M., Sprintsin, M., Tsipris, J., Alchanatis, V., Cohen, Y., 2013. Foliage temperature extraction from thermal imagery for crop water stress determination. *Precision Agriculture* 14, 467–477. https://doi.org/10.1007/s11119-013-9310-0

Mesas-Carrascosa, F.J., Pérez-Porras, F., de Larriva, J.E.M., Frau, C.M., Agüera-Vega, F., Carvajal-Ramírez, F., Martínez-Carricondo, P., García-Ferrer, A., 2018. Drift correction of lightweight microbolometer thermal sensors on-board unmanned aerial vehicles. *Remote Sensing* 10(4), 615. https://doi.org/10.3390/rs10040615

Messina, C.D., Podlich, D., Dong, Z., Samples, M., Cooper, M., 2011. Yield-trait performance landscapes: From theory to application in breeding maize for drought tolerance. *Journal of Experimental Botany* 62(3), 855-868. https://doi.org/10.1093/jxb/erq329

Messina, C.D., Sinclair, T.R., Hammer, G.L., Curan, D., Thompson, J., Oler, Z., Gho, C., Cooper, M., 2015. Limited-transpiration trait may increase maize drought tolerance in the US corn belt. *Agronomy Journal* 107(6), 1978–1986. https://doi.org/10.2134/agronj15.0016

Micheli, E., Schád, P., Spaargaren, O., Dent, D., Nachtergaele, F., WRB, I., 2006. World reference base for soil resources: 2006: a framework for international classification, correlation and communication. Rome: FAO. Available at: https://openknowledge.fao.org/server/api/core/bitstreams/1bd0747c-e9d8-4b28-99bf-55684d121e38/content (Accessed: 24 August 2024).

Mirajkar, S.J., Devarumath, R.M., Nikam, A.A., Sushir, K. V., Babu, H., Suprasanna, P., 2019. Sugarcane (Saccharum spp.): Breeding and genomics. In: Al-Khayri, J., Jain, S., Johnson, D., eds. *Advances in Plant Breeding Strategies: Industrial and Food Crops*. Cham: Springer. https://doi.org/10.1007/978-3-030-23265-8_11

Monteith, J.L., Moss, C.J., 1977. Climate and the efficiency of crop production in Britain. *Philosophical Transactions of the Royal Society of London. Series B, Biological Sciences* 281(980), 277–294.

Morel, J., Bégué, A., Todoroff, P., Martiné, J.F., Lebourgeois, V., Petit, M., 2014. Coupling a sugarcane crop model with the remotely sensed time series of fIPAR to optimise the yield estimation. *European Journal of Agronomy* 61, 60–68. https://doi.org/10.1016/j.eja.2014.08.004

Moriya, E., Imai, N., Tommaselli, A., Miyoshi, G., 2017. Mapping mosaic virus in sugarcane based on hyperspectral images. *IEEE Journal of Selected Topics in Applied Earth Observations and Remote Sensing* 10(2), 740-748. http://dx.doi.org/10.1109/JSTARS.2016.2635482

Muchow, R., Spillman, M., Wood, A., Thomas, M., 1994. Radiation interception and biomass accumulation in a sugarcane crop grown under irrigated tropical conditions. *Australian Journal of Agricultural Research* 45(1), 37-49. https://doi.org/10.1071/AR9940037

Muller, S.J., Sithole, P., Singels, A., Van Niekerk, A., 2020. Assessing the fidelity of Landsat-based fAPAR models in two diverse sugarcane growing regions. *Computers and Electronics in Agriculture* 170, 105248. https://doi.org/10.1016/j.compag.2020.105248

Nakalembe, C., Becker-Reshef, I., Bonifacio, R., Hu, G., Humber, M.L., Justice, C.J., Keniston, J., Mwangi, K., Rembold, F., Shukla, S., Urbano, F., Whitcraft, A.K., Li, Y., Zappacosta, M., Jarvis, I., Sanchez, A., 2021. A review of satellite-based global agricultural monitoring systems available for Africa. *Global Food Security* 29(9), 100543. http://dx.doi.org/10.1016/j.gfs.2021.100543

Narmilan, A., Gonzalez, F., Salgadoe, A.S.A., Powell, K., 2022. Detection of white leaf disease in sugarcane using machine learning techniques over UAV multispectral images. *Drones* 6(9), 230. https://doi.org/10.3390/drones6090230

Natarajan, S., Basnayake, J., Lakshmanan, P., Fukai, S., 2020. Limited contribution of water availability in genotype-by-environment interaction in sugarcane yield and yield components. *Journal of Agronomy and Crop Science* 206(6), 665–678. https://doi.org/10.1111/jac.12407

Natarajan, S., Basnayake, J., Lakshmanan, P., Fukai, S., 2021. Genotypic variation in intrinsic transpiration efficiency correlates with sugarcane yield under rainfed and irrigated field conditions. *Physiologia Plantarum* 172(2), 976–989. https://doi.org/10.1111/ppl.13221

Natarajan, S., Basnayake, J., Wei, X., Lakshmanan, P., 2019. High-throughput phenotyping of indirect traits for early-stage selection in sugarcane breeding. *Remote Sensing* 11(24), 2952. https://doi.org/10.3390/rs11242952

Ngxaliwe, S., 2014. Water stress effects on growth, development, resource capture and resource use efficiency of two contrasting sugarcane genotypes. M.Sc Thesis. University of KwaZulu-Natal, Pietermaritzburg.

Nijland, W., de Jong, R., de Jong, S.M., Wulder, M.A., Bater, C.W., Coops, N.C., 2014. Monitoring plant condition and phenology using infrared sensitive consumer grade digital cameras. *Agricultural and Forest Meteorology* 184, 98–106. https://doi.org/10.1016/j.agrformet.2013.09.007

Olivares-Villegas, J.J., Reynolds, M.P., McDonald, G.K., 2007. Drought-adaptive attributes in the Seri/Babax hexaploid wheat population. *Functional Plant Biology* 34(3), 189–203. https://doi.org/10.1071/fp06148

Olivier, F., Singels, A., 2003. Water use efficiency of irrigated sugarcane as affected by row spacing and variety. *Proceedings of the South African Society of Sugar Technologists* 77, 347-351.

Olivier, F.C., Singels, A., 2015. Increasing water use efficiency of irrigated sugarcane production in South Africa through better agronomic practices. *Field Crops Research* 176, 87–98. https://doi.org/10.1016/j.fcr.2015.02.010

Olivier, F.C., Singels, A., Eksteen, A.B., 2016. Water and radiation use efficiency of sugarcane for bioethanol production in South Africa, benchmarked against other selected crops. *South African Journal of Plant and Soil* 33(1), 1–11. https://doi.org/10.1080/02571862.2015.1075231

Orozco, H., Queme, J., 2022. Sugarcane improvement in Central America and México with special focus on Guatemala. *Sugar Tech* 24, 254–266. https://doi.org/10.1007/s12355-021-01072-5

Ostengo, S., Serino, G., Perera, M.F., Racedo, J., Mamaní González, S.Y., Yáñez Cornejo, F., Cuenya, M.I., 2022. Sugarcane breeding, germplasm development and supporting genetic research in Argentina. *Sugar Tech* 24, 166–180. https://doi.org/10.1007/s12355-021-00999-z

Passioura, J.B., 1977. Grain yield, harvest index, and water use of wheat. *Journal of the Australian Institute of Agricultural Science* 43(3-4), 117–120.

Passioura, J.B., Angus, J.F., 2010. Improving productivity of crops in water-limited environments. *Advances in Agronomy* 106, 37–75. https://doi.org/10.1016/S0065-2113(10)06002-5

Pauli, D., Chapman, S.C., Bart, R., Topp, C.N., Lawrence-Dill, C.J., Poland, J., Gore, M.A., 2016. The quest for understanding phenotypic variation via integrated approaches in the field environment. *Plant Physiology* 172(2), 622-634. https://doi.org/10.1104/pp.16.00592

Pereira, R.M., Casaroli, D., Vellame, L.M., Júnior, J.A., Evangelista, A.W.P., Battisti, R., 2020. Water deficit detection in sugarcane using canopy temperature from satellite images. *Australian Journal of Crop Science* 14(3), 1835-2707. http://dx.doi.org/10.21475/ajcs.20.14.03.p1647

Pircher, M., Geipel, J., Kusnierek, K., Korsaeth, A., 2017. Development of a hybrid UAV sensor platform suitable for farm-scale applications in precision agriculture. *The International Archives of the Photogrammetry, Remote Sensing and Spatial Information Sciences* XLII-2/W6, 297–302. https://doi.org/10.5194/isprs-archives-XLII-2-W6-297-2017, 2017

Potgieter, A.B., George-Jaeggli, B., Chapman, S.C., Laws, K., Cadavid, L.A.S., Wixted, J., Watson, J., Eldridge, M., Jordan, D.R., Hammer, G.L., 2017. Multi-spectral imaging from an unmanned aerial vehicle enables the assessment of seasonal leaf area dynamics of sorghum breeding lines. *Frontiers in Plant Science* 8(8), 1532. https://doi.org/10.3389/fpls.2017.01532

Poudyal, C., Costa, L.F., Sandhu, H., Ampatzidis, Y., Odero, D.C., Arbelo, O.C., Cherry, R.H., 2022. Sugarcane yield prediction and genotype selection using unmanned aerial vehicle-based hyperspectral imaging and machine learning. *Agronomy Journal* 114(4), 2320–2333. https://doi.org/10.1002/agj2.21133

Qi, Y., Gao, X., Zeng, Q., Zheng, Z., Wu, C., Yang, R., Feng, X., Wu, Z., Fan, L., Huang, Z., 2022. Sugarcane breeding, germplasm development and related molecular research in China. *Sugar Tech* 24, 73–85. https://doi.org/10.1007/s12355-021-01055-6

Ram, B., Hemaprabha, G., Singh, B.D., Appunu, C., 2022. History and current status of sugarcane breeding, germplasm development and molecular biology in India. *Sugar Tech* 24, 4–29. https://doi.org/10.1007/s12355-021-01015-0

Rebetzke, G.J., Botwright, T.L., Moore, C.S., Richards, R.A., Condon, A.G., 2004. Genotypic variation in specific leaf area for genetic improvement of early vigour in wheat. *Field Crops Research* 88(2-3), 179–189. https://doi.org/10.1016/j.fcr.2004.01.007

Reyes-Trujillo, A., Daza-Torres, M.C., Galindez-Jamioy, C.A., Rosero-García, E.E., Muñoz-Arboleda, F., Solarte-Rodriguez, E., 2021. Estimating canopy nitrogen concentration of sugarcane crop using in situ spectroscopy. *Heliyon* 7(3), e06566. https://doi.org/10.1016/j.heliyon.2021.e06566

Reynolds, M., Langridge, P., 2016. Physiological breeding. *Current Opinion in Plant Biology* 31, 162 - 71. https://doi.org/10.1016/j.pbi.2016.04.005

Richards, R.A., 2006. Physiological traits used in the breeding of new cultivars for water-scarce environments. *Agricultural Water Management* 80(1-3), 197–211. https://doi.org/10.1016/j.agwat.2005.07.013

Richards, R.A., Rebetzke, G.J., Condon, A.G., van Herwaarden, A.F., 2002. Breeding opportunities for increasing the efficiency of water use and crop yield in temperate cereals. *Crop Science* 42(1), 111–121. https://doi.org/10.2135/cropsci2002.1110

Robertson, M.J., Inman-Bamber, N.G., Muchow, R.C., Wood, A.W., 1999. Physiology and productivity of sugarcane with early and mid-season water deficit. *Field Crops Research* 64(3), 211–227. https://doi.org/10.1016/S0378-4290(99)00042-8

Robertson, M.J., Wood, A.W., Muchow, R.C., 1996. Growth of sugarcane under high input conditions in tropical Australia. I. Radiation use, biomass accumulation and partitioning. *Field Crops Research* 48(1), 11–25. https://doi.org/10.1016/0378-4290(96)00041-X

Rossler, R., 2013. Water stress effects on the growth, development and yield of sugarcane. M.Sc Thesis. University of Pretoria.

Rouse Jr, J.W., Haas, R.H., Deering, D.W., Schell, J.A., Harlan, J.C., 1974. Monitoring the vernal advancement and retrogradation (green wave effect) of natural vegetation [Great Plains Corridor]. *NASA/GSFC Type III final report.* Greenbelt, MD.

Sadras, V., KGG, C., Grassini, P., AJ, H., Bastiaanssen, W.G.M., Laborte, A., AE, M., Sileshi, G., Steduto, P., 2015. Yield gap analysis of field crops: Methods and case studies. *FAO Water Reports No.41*. Rome, Italy.

Sanseechan, P., Saengprachathanarug, K., Posom, J., Wongpichet, S., Chea, C., Wongphati, M., 2019. Use of vegetation indices in monitoring sugarcane white leaf disease symptoms in sugarcane field using multispectral UAV aerial imagery. *IOP Conference Series Earth and Environmental Science* 301(1), 012025. http://dx.doi.org/10.1088/1755-1315/301/1/012025

Santchurn, D., Badaloo, M.G.H., Koonjah, S., Dookun-Saumtally, A., 2022. Sugarcane breeding and supporting genetics research in Mauritius. *Sugar Tech* 24, 48–63. http://dx.doi.org/10.1007/s12355-021-00960-0

Schoonees-Muir BM, Ronaldson MA, Naidoo G, Schorn PM, 2009. SASTA laboratory manual including the official methods. South African Sugar Technologists' Association, Mount Edgecombe, South Africa.

Schulze, R., Kunz, R., 2010. Climate change 2010 and heat waves. In: R.E. Schulze, ed. *Atlas of Climate Change and the South African Agricultural Sector: A 2010 Perspective*. Pretoria: Department of Agriculture, Forestry and Fisheries, pp. 73-78.

Sentera Documentation, 2017. Available at: https://www.cybernetech.co.jp/wp-content/uploads/2023/05/precision_ndvi_single_sensor.pdf (Accessed: 24 August 2024).

Sexton, J., Everingham, Y.L., Inman-Bamber, G., 2017. A global sensitivity analysis of cultivar trait parameters in a sugarcane growth model for contrasting production environments in Queensland, Australia. *European Journal of Agronomy* 88, 96–105. https://doi.org/10.1016/j.eja.2015.11.009

Shahab, H., Iqbal, M., Sohaib, A., Ullah Khan, F., Waqas, M., 2024. IoT-based agriculture management techniques for sustainable farming: A comprehensive review. *Computers and Electronics in Agriculture* 220, 108851. https://doi.org/10.1016/j.compag.2024.108851

Shendryk, Y., Sofonia, J., Garrard, R., Rist, Y., Skocaj, D., Thorburn, P., 2020. Fine-scale prediction of biomass and leaf nitrogen content in sugarcane using UAV LiDAR and multispectral imaging. *International Journal of Applied Earth Observation and Geoinformation* 92, 102177. https://doi.org/10.1016/j.jag.2020.102177

Simões, I.O.P.S., Rios do Amaral, L., 2023. UAV-based multispectral data for sugarcane resistance phenotyping of orange and brown rust. *Smart Agricultural Technology* 4, 100144. https://doi.org/10.1016/j.atech.2022.100144

Simões, M. dos S., Rocha, J.V., Lamparelli, R.A.C., 2005. Spectral variables, growth analysis and yield of sugarcane. *Scientia Agricola* 62(3), 199–207. http://dx.doi.org/10.1590/S0103-90162005000300001

Sinclair, T.R., 2012. Is transpiration efficiency a viable plant trait in breeding for crop improvement? *Functional Plant Biology* 39(5), 359–365. https://doi.org/10.1071/fp11198

Sinclair, T.R., Gilbert, R.A., Perdomo, R.E., Shine, J.M., Powell, G., Montes, G., 2004. Sugarcane leaf area development under field conditions in Florida, USA. *Field Crops Research* 88(2-3), 171–178. https://doi.org/10.1016/j.fcr.2003.12.005

Singels, A., 2008. DSSAT v4.5 - Canegro sugarcane plant module: Scientific documentation. Available at: https://sasri.sasa.org.za/agronomy/icsm/documents/DSSAT%20Canegro%20SCIENTIFIC%20documentation_20081215.pdf (Accessed: 24 August 2024).

Singels, A., Donaldson, R., 2000. A simple model of unstressed sugarcane canopy development. *Proceedings of the South African Sugar Technologists' Association* 74, 151–154.

Singels, A., Inman-Bamber, N.G., 2011. Modelling genetic and environmental control of biomass partitioning at plant and phytomer level of sugarcane grown in controlled environments. *Crop and Pasture Science* 62(1), 66-81. https://doi.org/10.1071/CP10182

Singels, A., Jackson, P., Inman-Bamber, G., 2021. Sugarcane. In: V.O. Sadras, D.F. Calderini, eds. *Crop Physiology Case Histories for Major Crops*. Academic Press, pp. 674-713. https://doi.org/10.1016/B978-0-12-819194-1.00021-9

Singels, A., Jarmain, C., Bastidas-Obando, E., Olivier, F.C., Paraskevopoulos, A.L., 2018. Monitoring water use efficiency of irrigated sugarcane production in Mpumalanga, South Africa, using SEBAL. *Water SA* 44(4), 636–646. http://dx.doi.org/10.4314/wsa.v44i4.12

Singels, A., Jones, M.R., van der Laan, M., 2016. Modelling impacts of stomatal drought sensitivity and root growth rate on sugarcane yield. *ICROPM2016 International Crop Modelling Symposium*, Berlin, Germany.

Singels, A., Smit, M., 2002. The effect of row spacing on an irrigated plant crop of sugarcane variety NCo376. *Proceedings of the South African Society of Sugar Technologists* 76.

Singels, A., Smit, M.A., Redshaw, K.A., Donaldson, R.A., 2005. The effect of crop start date, crop class and cultivar on sugarcane canopy development and radiation interception. *Field Crops Research* 92(2-3), 249–260. https://doi.org/10.1016/j.fcr.2005.01.028

Singels, A., van den Berg, M., Smit, M.A., Jones, M.R., van Antwerpen, R., 2010. Modelling water uptake, growth and sucrose accumulation of sugarcane subjected to water stress. *Field Crops Research* 117(1), 59–69. https://doi.org/10.1016/j.fcr.2010.02.003

Sithole P, Rj, N., Ra, S., 2023. A review of South African sugarcane production in the 2022/23 season: climate, production and economics. *Proceedings of the South African Society of Sugar Technologists Association* 95, 1-16.

Smit, M.A., Singels, A., 2006. The response of sugarcane canopy development to water stress. *Field Crops Research* 98(2-3), 91–97. https://doi.org/10.1016/j.fcr.2005.12.009

Smith, J.P., Lawn, R., Nable, R.O., 1999. Investigations into the root:shoot relationship of sugarcane, and some implications for crop productivity in the presence of sub-optimal soil conditions. *Proceedings of the South African Society of Sugar Technologists Association* 21, 108–113.

Sofonia, J., Shendryk, Y., Phinn, S., Roelfsema, C., Kendoul, F., Skocaj, D., 2019. Monitoring sugarcane growth response to varying nitrogen application rates: A comparison of UAV SLAM LiDAR and photogrammetry. *International Journal of Applied Earth Observation and Geoinformation* 82, 101878. https://doi.org/10.1016/j.jag.2019.05.011

Soil Classification Working Group, 1991. Soil classification- a taxonomic system for South Africa. *Memoirs on the Agricultural Natural Resources of South Africa No. 15*. Department of Agricultural Development, Pretoria.

Soil Survey Staff, 1999. Soil survey manual. USDA Handbook No. 18. Government Printing Office, Washington DC.

Som-ard, J., Hossain, M., Ninsawat, S., Veerachitt, V., 2018. Pre-harvest sugarcane yield estimation using UAV-based RGB images and ground observation. *Sugar Tech* 20(1), 645-657. https://doi.org/10.1007/s12355-018-0601-7

Som-ard, J., Immitzer, M., Vuolo, F., Atzberger, C., 2024. Sugarcane yield estimation in Thailand at multiple scales using the integration of UAV and Sentinel-2 imagery. *Precision Agriculture* 25(3), 1581-1608. https://doi.org/10.1007/s11119-024-10124-1

Song, P., Wang, J., Guo, X., Yang, W., Zhao, C., 2021. High-throughput phenotyping: Breaking through the bottleneck in future crop breeding. *Crop Journal* 9(3), 633-645. https://doi.org/10.1016/j.cj.2021.03.015

Stevenson, G., 1966. Genetics and Breeding of Sugar Cane. *Experimental Agriculture* 2(4), 264–264. https://doi.org/10.1017/S0014479700021682

Sumesh, K.C., Ninsawat, S., Som-ard, J., 2021. Integration of RGB-based vegetation index, crop surface model and object-based image analysis approach for sugarcane yield estimation using unmanned aerial vehicle. *Computers and Electronics in Agriculture* 180, 105903. https://doi.org/10.1016/j.compag.2020.105903

Tanner, C.B., Sinclair, T.R., 2015. Efficient water use in crop production: Research or re-search? In: H.M. Taylor, W.R. Jordan, T.R. Sinclair, eds. *Limitations to Efficient Water Use in Crop Production*. American Society of Agronomy. https://doi.org/10.2134/1983.limitationstoefficientwateruse.c1

Terajima, Y., Hattori, T., Shimatani, M., Sato, M., Takaragawa, H., Sakaigaichi, T., Umeda, M., Naito, T., Irei, S., 2022. Sugarcane breeding and supporting genetics research in Japan. *Sugar Tech* 24(1), 134–150. https://doi.org/10.1007/s12355-020-00930-y

Tilman, D., Balzer, C., Hill, J., Befort, B.L., 2011. Global food demand and the sustainable intensification of agriculture. *Proceedings of the National Academy of Sciences* 108(50), 20260–20264. https://doi.org/10.1073/pnas.1116437108

Tippayawat, A., Jogloy, S., Vorasoot, N., Songsri, P., Kimbeng, C.A., Jifon, J.L., Janket, A., Thangthong, N., Jongrungklang, N., 2023. Differential physiological responses to different drought durations among a diverse set of sugarcane genotypes. *Agronomy* 13(10), 2594. https://doi.org/10.3390/agronomy13102594.Tucker, C.J., 1979. Red and photographic infrared linear combinations for monitoring vegetation. *Remote Sensing of Environment* 8(2), 127–150. https://doi.org/10.1016/0034-4257(79)90013-0

Ueno, M., Kawamitsu, Y., Sun, L., Taira, E., Maeda, K., 2005. Combined applications of NIR, RS, and GIS for sustainable sugarcane production. *Proceedings of the International Society of Sugar Cane Technologists (ISSCT)* 25, 204-210. Guatemala.

Vadez, V., Kholova, J., Medina, S., Kakkera, A., Anderberg, H., 2014. Transpiration efficiency: new insights into an old story. *Journal of Experimental Botany* 65(21), 6141–6153. https://doi.org/10.1093/jxb/eru040

Van Antwerpen, R., Meyer, J., Johnston, M., 1994. Estimating water retention of some Natal sugar belt soils in relation to clay content. *Proceedings of the South African Society of Sugar Technologists Association* 68, 75-79.

van Dijk, M., Morley, T., Rau, M.L., Saghai, Y., 2021. A meta-analysis of projected global food demand and population at risk of hunger for the period 2010–2050. *Nature Food* 2(7), 494–501. https://doi.org/10.1038/s43016-021-00322-9

Vasconcelos, J.C.S., Speranza, E.A., Antunes, J.F.G., Barbosa, L.A.F., Christofoletti, D., Severino, F.J., de Almeida Cançado, G.M., 2023. Development and validation of a model based on vegetation indices for the prediction of sugarcane yield. *AgriEngineering* 5(2), 698–719. https://doi.org/10.3390/agriengineering5020044

Villareal, M., Tongco, A., 2020. Remote sensing techniques for classification and mapping of sugarcane growth. *Engineering, Technology & Applied Science Research* 10(4), 6041–6046.

Walsh B, Lynch M, 1998. *Evolution and selection of quantitative traits*. Oxford: Oxford University Press. https://doi.org/10.1093/oso/9780198830870.001.0001

Wang, T., Fang, J., Zhang, J., 2022. Advances in sugarcane genomics and genetics. *Sugar Tech* 24(1), 3548–368. https://doi.org/10.1007/s12355-021-01065-4

Wang, M., Liu, Z., Ali Baig, M.H., Wang, Y., Li, Y., Chen, Y., 2019. Mapping sugarcane in complex landscapes by integrating multi-temporal Sentinel-2 images and machine learning algorithms. *Land Use Policy* 88, 104190. https://doi.org/10.1016/j.landusepol.2019.104190

Wanjura, D.F., Kelly, C.A., Wendt, C.W., Hatfield, J.L., 1984. Canopy temperature and water stress of cotton crops with complete and partial ground cover. *Irrigation Science* 5, 37–46. https://doi.org/10.1007/BF00275036

Wei, X., Eglinton, J., Piperidis, G., Atkin, F., Morgan, T., Parfitt, R., Hu, F., 2022. Sugarcane breeding in Australia. *Sugar Tech* 24, 151–165. https://doi.org/10.1007/s12355-021-00969-5

Wei, X., Jackson, P., 2017. Addressing slow rates of long-term genetic gain in sugarcane. *Pakistan Sugar Journal* 32(4), 23.

Weiss, M., Jacob, F., Duveiller, G., 2020. Remote sensing for agricultural applications: A meta-review. *Remote Sensing of Environment* 236, 111402. https://doi.org/10.1016/j.rse.2019.111402

White, J.W., Andrade-Sanchez, P., Gore, M.A., Bronson, K.F., Coffelt, T.A., Conley, M.M., Feldmann, K.A., French, A.N., Heun, J.T., Hunsaker, D.J., Jenks, M.A., Kimball, B.A., Roth, R.L., Strand, R.J., Thorp, K.R., Wall, G.W., Wang, G., 2012. Field-based phenomics for plant genetics research. *Field Crops Research* 133, 101–112. https://doi.org/10.1016/j.fcr.2012.04.003

Widyasari, W.B., Putra, L.K., Ranomahera, M.R.R., Puspitasari, A.R., 2022. Historical notes, germplasm development, and molecular approaches to support sugarcane breeding program in Indonesia. *Sugar Tech* 24(2), 30–47. https://doi.org/10.1007/s12355-021-01069-0

Xu, Y., Li, P., Zou, C., Lu, Y., Xie, C., Zhang, X., Prasanna, B.M., Olsen, M.S., 2017. Enhancing genetic gain in the era of molecular breeding. *Journal of Experimental Botany* 68(11), 2641–2666. https://doi.org/10.1093/jxb/erx135

Xu, Y., Liu, X., Fu, J., Wang, H., Wang, J., Huang, C., Prasanna, B.M., Olsen, M.S., Wang, G., Zhang, A., 2020. Enhancing genetic gain through genomic selection: from livestock to plants. *Plant Communications* 1(1), 100005. https://doi.org/10.1016/j.xplc.2019.100005

Yadav, S., Jackson, P., Wei, X., Ross, E.M., Aitken, K., Deomano, E., Atkin, F., Hayes, B.J., Voss-Fels, K.P., 2020. Accelerating genetic gain in sugarcane breeding using genomic selection. *Agronomy* 10(4), 585. https://doi.org/10.3390/agronomy10040585

Yadav, S., Wei, X., Joyce, P., Atkin, F., Deomano, E., Sun, Y., Nguyen, L.T., Ross, E.M., Cavallaro, T., Aitken, K.S., Hayes, B.J., Voss-Fels, K.P., 2021. Improved genomic prediction of clonal performance in sugarcane by exploiting non-additive genetic effects. *Theoretical and Applied Genetics* 134(7), 2235–2252. https://doi.org/10.1007/s00122-021-03822-1

Yang, G., Liu, J., Zhao, C., Li, Zhenhong, Huang, Y., Yu, H., Xu, B., Yang, X., Zhu, D., Zhang, X., Zhang, R., Feng, H., Zhao, X., Li, Zhenhai, Li, H., Yang, H., 2017. Unmanned aerial vehicle remote sensing for field-based crop phenotyping: Current status and perspectives. *Frontiers in Plant Science* 8: 1111. https://doi.org/10.3389/fpls.2017.01111

Yao, H., Qin, R., Chen, X., 2019. Unmanned aerial vehicle for remote sensing applications—A review. *Remote Sensing* 11(12), 1443. https://doi.org/10.3390/rs11121443

Yu, D., Zha, Y., Shi, L., Jin, X., Hu, S., Yang, Q., Huang, K., Zeng, W., 2020. Improvement of sugarcane yield estimation by assimilating UAV-derived plant height observations. *European Journal of Agronomy* 121, 126159. https://doi.org/10.1016/j.eja.2020.126159

Zhao, D., Glaz, B., Irey, M.S., Hu, C., 2015. Sugarcane genotype variation in leaf photosynthesis properties and yield as affected by mill mud application. *Agronomy Journal* 107(2), 506–514. https://doi.org/10.2134/agronj14.0401

Zhao, D., Gordon, V.S., Comstock, J.C., Glynn, N.C., Johnson, R.M., 2016. Assessment of sugarcane yield potential across large numbers of genotypes using canopy reflectance measurements. *Crop Science* 56(4), 1747–1759. https://doi.org/10.2135/cropsci2015.12.0747

Zhao, D., Irey, M., LaBorde, C., Hu, C., 2017. Identifying physiological and yield-related traits in sugarcane and energy cane. *Agronomy Journal* 109(3), 927–937. https://doi.org/10.2134/agronj2016.10.0585

Zhao, D., Irey, M., LaBorde, C., Hu, C., 2019. Sugarcane genotypic variation in physiological and yield traits and their relationships. *Proceedings of the International Society of Sugar Cane Technologist*s (ISSCT) 30, 476–481.

Zhao, D., Li, Y.-R., 2015. Climate change and sugarcane production: Potential impact and mitigation strategies. *International Journal of Agronomy* 2015(1), 1–10. https://doi.org/10.1155/2015/547386

Zhao, P., Jackson, P.A., Basnayake, J., Liu, J., Chen, X., Zhao, J., Zhao, X., Bai, Y., Yang, L., Zan, F., Yang, K., Xia, H., Qin, W., Zhao, L., Yao, L., Lakshmanan, P., Fan, Y., 2017. Genetic variation in sugarcane for leaf functional traits and relationships with cane yield, in environments with varying water stress. *Field Crops Research* 213(2), 143–153. https://doi.org/10.1016/j.fcr.2017.08.004

Zhou, M., 2013. Conventional sugarcane breeding in South Africa: Progress and future prospects. *American Journal of Plant Sciences* 4(2), 189–197. http://dx.doi.org/10.4236/ajps.2013.42025

Zhou, M., 2022. History and current status of sugarcane breeding, germplasm development and supporting molecular research in South Africa. *Sugar Tech* 24, 86–96. https://doi.org/10.1007/s12355-021-00961-z

Zhou, M.M., Singels, A., Savage, M., 2003. Physiological parameters for modelling differences in canopy development between sugarcane cultivars. *Proceedings of the South African Sugar Technologists' Association* 77, 610-621.

8. APPENDIX

8.1 Pilot study

8.1.1 Methodology

8.1.2 Results

Weather data

Table 8.1. Half-hourly average weather data recorded at the time of the thermal flight for seven measurement days (RH - relative humidity, SRAD - solar radiation, also expressed as a fraction of clear-sky radiation estimated for the given hour, and wind speed).

Flight	Temperature (°C)	RH (%)	SRAD (W m^{-2} / %)	Wind speed (m s^{-1})
1	27.0	72.6	921	3.11
2	25.4	49.1	744	3.11
3	26.1	65.0	817	4.76
4	23.5	68.3	576	2.75
5	27.1	49.4	517	2.60
6	26.0	51.0	451	1.23

Table 8.2. Daily weather data for seven measurement days (Tmax, Tmin and Tmean – maximum, minimum and mean temperature; RH – relative humidity; SRAD – solar radiation, also expressed as a fraction of daily average clear-sky radiation; windspeed and Ecref – reference evapotranspiration for sugarcane).

Flight	Tmax (°C)	Tmin (°C)	Tmean (°C)	RHmax (%)	RHmin (%)	RHmean (%)	SRAD (MJ m^{-2} d^{-1} / %)	Wind speed (km d^{-1})	Ecref (mm d^{-1})
1	27.7	20.3	23.7	87	70	86	21.8	107	4.6
2	26.6	18.7	22.3	50	47	63	22.3	132.9	6.3
3	28.8	16.5	22.8	72	54	74	21.4	123.2	4.9
4	24.3	16.5	20	94	63	81	14.3	151	2.7
5	27.4	9.6	18.7	61	49	68	14.5	73.4	3.6
6	28.1	12.5	20.1	61	59	65	12.4	55.6	1.8

Crop growth

Ground measurements

Phenology

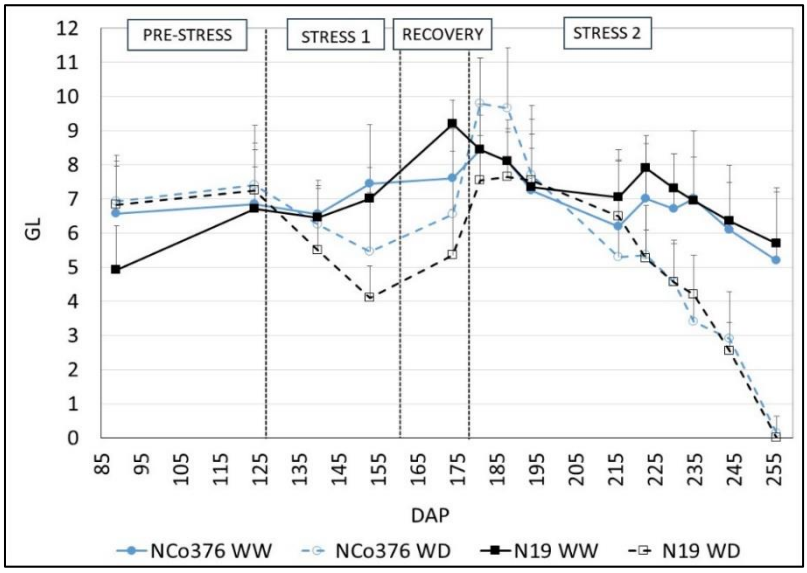

Figure 8.1. Green leaf number (GL) over time (days after planting, DAP) for two varieties (NCo376 and N19) grown under well-watered (WW) and water deficit (WD) conditions. Stress and recovery events indicate periods during which irrigation was withheld and re-applied in WD plots, respectively.

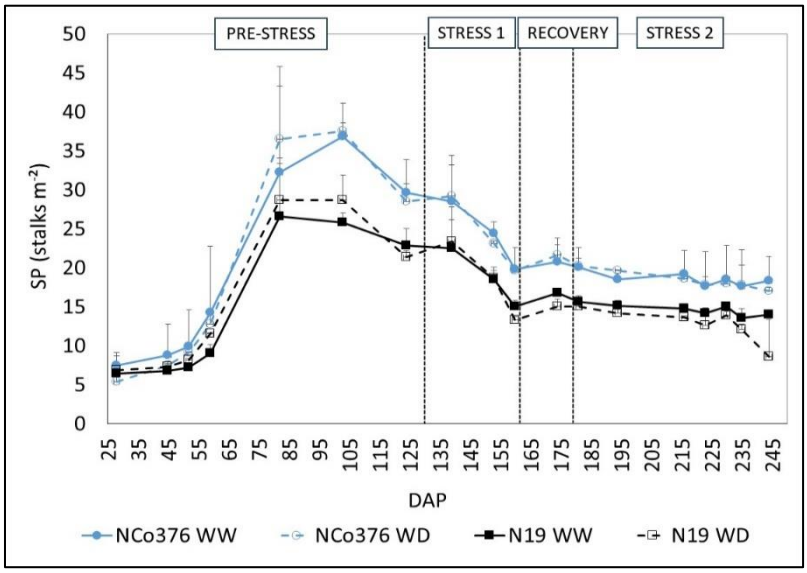

Figure 8.2. Stalk population (SPOP) over time (days after planting, DAP) for two varieties (NCo376 and N19) grown under well-watered (WW) and water deficit (WD) conditions. Stress and recovery events indicate periods during which irrigation was withheld and re-applied in WD plots, respectively.

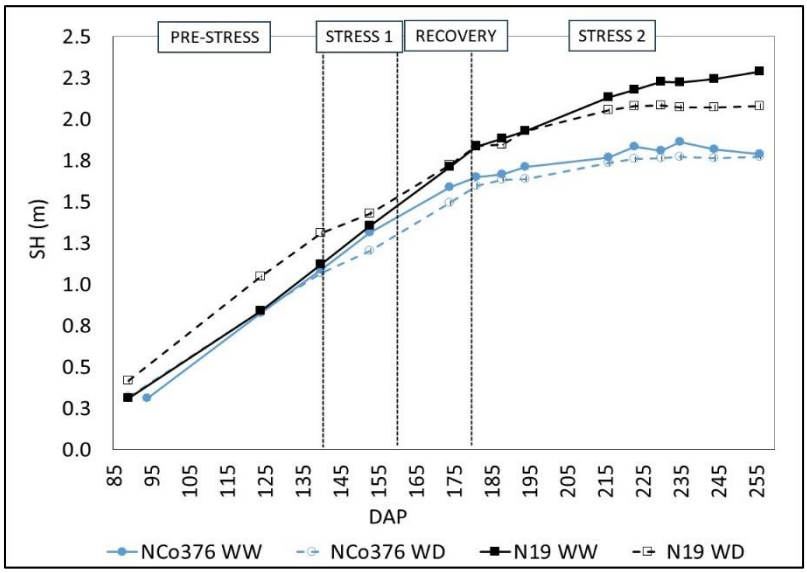

Figure 8.3. Stalk height (SH) over time (days after planting, DAP) for two varieties (NCo376 and N19) grown under well-watered (WW) and water deficit (WD) conditions. Stress and recovery events indicate periods during which irrigation was withheld and re-applied in WD plots, respectively.

Yield components

Table 8.3. Above-ground dry biomass (ADM, kg m^{-2}), stalk dry mass (SDM, kg m^{-2}), sucrose yield (SY, kg m^{-2}), green leaf area index (GLAI, m^{-2} m^{-2}), green leaf number (GL), stalk population (SPOP, stalks m^{-2}), stalk height (H, m), and biomass and stalk fractions measured destructively at harvest. Varieties NCo376 and N19 were grown under well-watered (WW) and water deficit (WD) conditions. Standard deviation of the mean value is indicated in brackets.

Treatment	ADM	SDM	SY	GLAI	Phenology			Biomass fractions				Stalk fractions		
					GL	SPOP	SH (m)	Senesced leaf	Stalk	Meristem	Green leaf	Fibre	Sucrose	Non-sucrose
NCo376 WW	2.77 (0.37)	1.48 (0.34)	0.66 (0.08)	7.38 (0.84)	5.20 (2.02)	18.33 (3.11)	1.79 (0.27)	0.19 (0.03)	0.53 (0.05)	0.034 (0.006)	0.25 (0.05)	0.45 (0.03)	0.42 (0.02)	0.053 (0.002)
N19 WW	3.47 (1.01)	1.94 (0.72)	0.81 (0.24)	5.03 (0.95)	5.70 (1.63)	14.00 (0.38)	2.29 (0.15)	0.17 (0.02)	0.55 (0.05)	0.03 (0.008)	0.25 (0.06)	0.42 (0.03)	0.43 (0.03)	0.058 (0.009)
NCo376 WD	2.99 (0.40)	1.81 (0.55)	0.68 (0.26)	1.77 (0.61)	0.15 (0.49)	17.07 (0.38)	1.77 (0.16)	0.25 (0.03)	0.60 (0.04)	0.039 (0.008)	0.11 (0.02)	0.39 (0.02)	0.38 (0.03)	0.091 (0.013)
N19 WD	2.05 (0.18)	1.26 (0.48)	0.70 (0.16)	1.24 (0.99)	0.00 (0.00)	8.60 (4.81)	2.08 (0.17)	0.24 (0.03)	0.61 (0.02)	0.042 (0.008)	0.11 (0.02)	0.41 (0.03)	0.35 (0.03)	0.094 (0.009)

8.2 Phenotyping trials

8.2.1 Methodology

Trial design and operations

Rep 1	1 10F1110	2 10F2397	3 10F3334	4 03S0767	5 07F4070	6 N41	7 08U0279	8 Q138	9 N39	163 10F1110	164 10F2397	165 03B0158	166 06U0999	167 Q138	168 N32	169 N37	170 06G1483	171 N41
	18 N14	17 N12	16 N32	15 08T3713	14 NCo310	13 R570	12 HoCP96	11 N51	10 08F3864	180 CP88	179 08T3713	178 08U0279	177 NCo310	176 04S0063	175 N36	174 CP66	173 04B1836	172 07T2881
	19 08F2857	20 N16	21 CP66	22 N31	23 N37	24 N33	25 CP88	26 N46	27 08T0593	181 R570	182 06K2979	183 N14	184 N46	185 03S2040	186 08F3864	187 08F2857	188 03S0767	189 N12
	36 04S0063	35 03S2040	34 N36	33 N61	32 N24	31 D141	30 06G1483	29 R579	28 Red cane	198 N35	197 08T0593	196 HoCP96	195 N22	194 Red cane	193 N16	192 N51	191 CP65	190 N39
	37 N57	38 N55	39 06U0999	40 N22	41 03B0158	42 N49	43 N30	44 N19	45 06K2979	199 N55	200 N24	201 N57	202 N49	203 N19	204 D141	205 N33	206 R579	207 NCo376
	54 NCo376	53 04B1836	52 N40	51 CP65	50 07T2881	49 N35	48 N28	47 10F0844	46 10F2307	216 N40	215 N30	214 N61	213 07F4070	212 N31	211 N28	210 10F0844	209 10F2307	208 10F3334
Rep 2	55 10F0844	56 10F2307	57 10F3334	58 N30	59 03S2040	60 N32	61 08F2857	62 08F3864	63 N35	217 10F0844	218 10F3334	219 10F1110	220 08F3864	221 N32	222 N55	223 N49	224 N36	225 06K2979
	72 08U0279	71 N51	70 N31	69 N46	68 N61	67 N40	66 03B0158	65 Q138	64 08T0593	234 N61	233 R579	232 N28	231 N16	230 N37	229 04B1836	228 CP88	227 N51	226 N31
	73 06K2979	74 N55	75 CP66	76 NCo310	77 Red cane	78 NCo376	79 N37	80 N57	81 N28	235 N35	236 CP65	237 R570	238 N33	239 N41	240 07T2881	241 N57	242 N14	243 N30
	90 N22	89 03S0767	88 04B1836	87 N14	86 06G1483	85 HoCP96	84 N41	83 N49	82 D141	252 07F4070	251 N19	250 06G1483	249 HoCP96	248 CP66	247 NCo310	246 Red cane	245 N39	244 Q138
	91 N12	92 04S0063	93 N19	94 07F4070	95 R570	96 N36	97 N33	98 CP65	99 R579	253 03S2040	254 N12	255 04S0063	256 D141	257 NCo376	258 08T3713	259 08T0593	260 03B0158	261 03S0767
	108 N39	107 08T3713	106 06U0999	105 N24	104 07T2881	103 CP88	102 N16	101 10F1110	100 10F2397	270 08F2857	269 08U0279	268 N46	267 N40	266 N22	265 06U0999	264 N24	263 10F2307	262 10F2397
Rep 3	109 10F1110	110 10F2397	111 10F0844	112 08F2857	113 CP66	114 N16	115 N57	116 N32	117 NCo376	271 10F2307	272 10F0844	273 10F1110	274 N39	275 06K2979	276 N32	277 04B1836	278 N46	279 N36
	126 R579	125 D141	124 Red cane	123 06U0999	122 06K2979	121 04B1836	120 N12	119 N61	118 R570	288 N33	287 08T0593	286 03S0767	285 N49	284 N61	283 NCo310	282 CP65	281 N16	280 N37
	127 08T3713	128 08F3864	129 08U0279	130 N41	131 HoCP96	132 N30	133 N35	134 N40	135 04S0063	289 08T3713	290 N22	291 N35	292 N55	293 D141	294 Q138	295 R570	296 N28	297 03B0158
	144 03B0158	143 N14	142 N28	141 N19	140 CP65	139 03S2040	138 N49	137 N37	136 N39	306 07T2881	305 N30	304 N51	303 R579	302 N41	301 08F2857	300 06G1483	299 N24	298 08U0279
	145 N22	146 N36	147 N46	148 08T0593	149 NCo310	150 N33	151 N31	152 06G1483	153 N51	307 04S0063	308 CP66	309 06U0999	310 03S2040	311 07F4070	312 N40	313 N14	314 HoCP96	315 Red cane
	162 03S0767	161 N24	160 07T2881	159 07F4070	158 Q138	157 CP88	156 N55	155 10F2307	154 10F3334	324 N31	323 NCo376	322 N19	321 08F3864	320 N12	319 N57	318 CP88	317 10F2397	316 10F3334

Figure 8.4. Komati field trial randomisation. Genotypes grown under well-watered (WW) and water deficit (WD) conditions are labelled in green and red, respectively. Grey highlighted plots indicate selected genotypes for which measurements of crop growth and physiology were carried out.

Table 8.4. Details of genotypes used in the Komati phenotyping trial. The status of the genotypes at the time of the study (unreleased / released commercially) is indicated.

Genotype	Country of origin	Status
NCo310	South Africa	Released
NCo376		
N12		
N14		
N16		
N19		
N22		
N24		
N28		
N30		
N31		
N32		
N33		
N35		
N36		
N37		
N39		
N40		
N41		
N46		
N49		
N51		
N55		
N57		
N61		
Q138	Australia	
HoCP96-540	USA	
D141/46	Mauritius	
CP88-1762	USA	
CP66/1043		
CP65/357		
R570	Reunion Island	
R579	Reunion Island	
03B0158	South Africa	Unreleased
10F0844		
10F1110		
08F2857		
03S2040		
08U0279		
10F2397		
08T3713		
10F3334		
08T0593		
03S0767		
06U0999		
06K2979		
08F3453		
07F4070		
04B1836		
08F3864		
07T2881		
08F3426		
10F2307		
06G1483		
04S0063		
Red cane		Unreleased- used as experimental benchmark

Soil characterisation

Figure 8.5. Soil parameters (clay content, estimated rooting depth, ERD and plant available water content, ASWCmax) measured in the Komati field trial. Plot boundaries are outlined with solid black lines.

Table 8.5. Properties of soil samples from selected plots in the Komati field trial. Values of soil textural (clay and silt %), structural (bulk density, BD), and water retention properties (field capacity, FC; permanent wilting point, PWP; and plant available soil water capacity, ASWCmax, calculated as the product of the average difference between FC and PWP and estimated rooting depth) are given. Retention properties were estimated from clay content (as in Antwerpen et al., 1994).

Plot	Rep	Water treatment	Depth (cm)	Clay (%)	Silt (%)	BD (g cm-^{3})	FC (mm m^{-1})	PWP (mm m^{-1})	ASWCmax (mm)
8	1	WW	30	54	9	0.88	376.1	261.9	113.4
			60	40	6	0.96	339.1	209.5	
			90	28	6	0.94	291.6	157.4	
			Average	41	7	0.93	335.6	209.6	
35	1	WW	30	52	8	1.03	371.7	254.9	112.4
			60	46	4	0.97	356.8	233.0	
			90	28	6	1.03	291.6	157.4	
			Average	42	6	1.01	340.0	215.1	
173	1	WD	30	46	8	1.05	356.8	233.0	76.9
			60	36	10	0.99	325.3	192.9	
			Average	41	9	1.02	341.0	213.0	
203	1	WD	30	46	10	0.96	356.8	233.0	76.5
			60	38	2	0.95	332.4	201.3	
			Average	42	6	0.96	344.6	217.1	
207	1	WD	30	54	6	1.01	376.1	261.9	73.6
			60	38	8	1.17	332.4	201.3	
			Average	46	7	1.09	354.3	231.6	
			Rep average	42.4	7.0	1.00	343.1	217.3	90.6
95	2	WW	30	48	8	0.97	362.0	240.4	104.1
			60	60	6	1.00	388.3	282.1	
			90	50	6	0.97	367.0	247.8	
			Average	53	7	0.98	372.4	256.8	
223	2	WD	30	48	12	1.01	362.0	240.4	107.4
			60	58	6	0.84	384.4	275.5	
			90	20	4	1.17	245.7	118.2	
			Average	42	8	1.00	330.7	211.4	
239	2	WD	30	42	4	1.06	345.3	217.5	109.4
			60	62	8	0.99	391.9	288.6	
			90	34	10	0.91	317.8	184.4	
			Average	46	7	0.99	351.7	230.1	
257	2	WD	30	52	2	0.92	371.7	254.9	72.2
			60	46	4	0.94	356.8	233.0	
			Average	49	3	0.93	364.2	243.9	
			Rep average	47.5	6.3	0.98	354.8	235.6	98.3
296	3	WW	30	38	8	1.03	332.4	201.3	79.0
			60	24	10	0.88	270.5	138.3	
			Average	31	9	0.96	301.5	169.8	
308	3	WW	30	44	6	0.99	351.2	225.3	155.7
			60	26	8	1.08	281.5	148.0	
			90	24	4	1.24	270.5	138.3	
			120	20	8	1.03	245.7	118.2	
			Average	29	7	1.09	287.2	157.5	
117	3	WD	30	50	4	1.06	367.0	247.8	74.6
			60	40	10	0.98	339.1	209.5	
			Average	45	7	1.02	353.0	228.6	
120	3	WD	30	36	10	0.94	325.3	192.9	66.6
			50	28	8	1.14	291.6	157.4	
			Average	32	9	1.04	308.4	175.2	
141	3	WD	30	46	16	0.96	356.8	233.0	77.1
			60	34	10	1.01	317.8	184.4	
			Average	40	13	0.99	337.3	208.7	
146	3	WD	30	44	10	0.99	351.2	225.3	78.0
			60	28	6	1.02	291.6	157.4	
			Average	36	8	1.0	321.4	191.4	
			Rep average	35.5	8.8	1.02	318.1	188.5	88.5

Aerial imaging

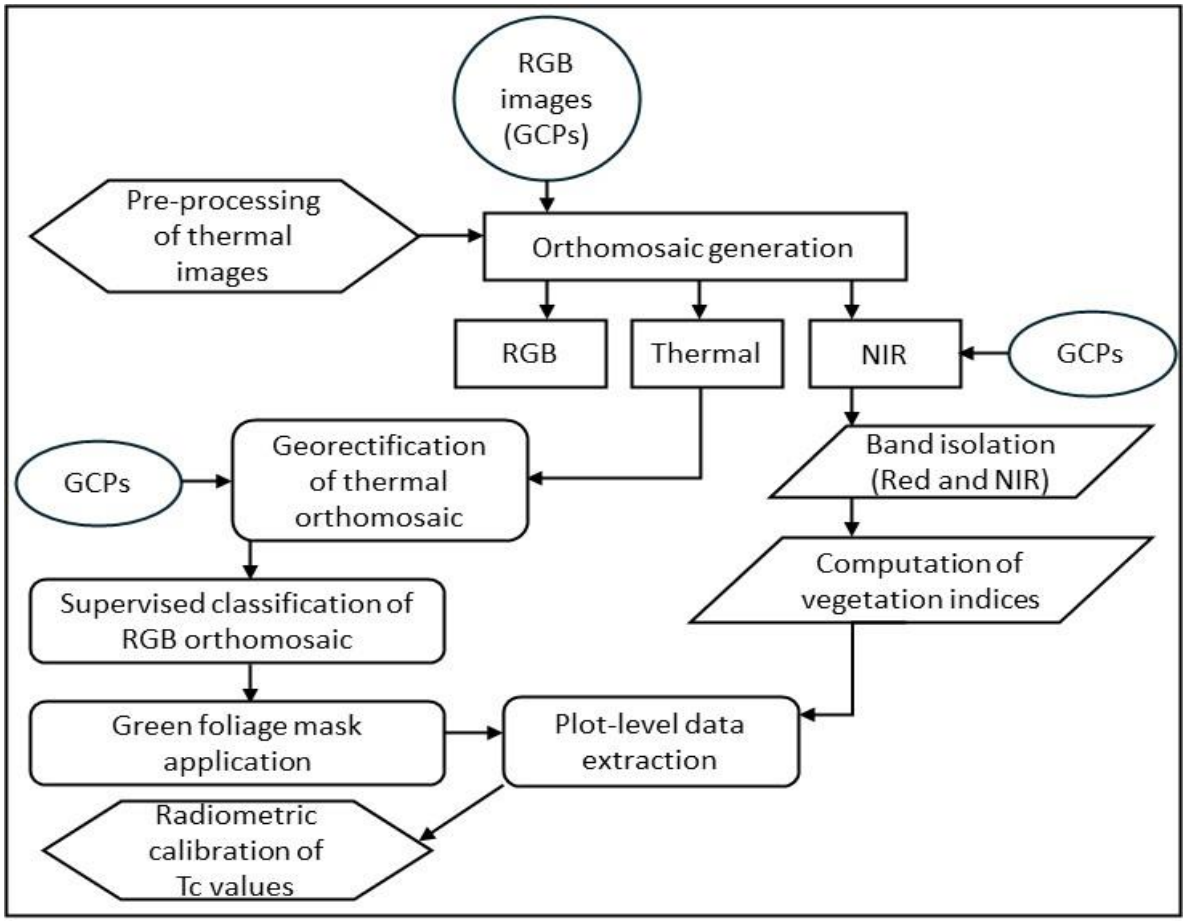

Figure 8.6. Image processing workflow for aerially captured visual (RGB), thermal and near infrared (NIR) images. The processing stages are as follows: pre-processing of thermal images in FLIR thermal studio, and post-processing radiometric calibration of canopy temperature (Tc) values using ground targets (indicated with hexagons); orthomosaic generation in Pix4D (rectangles); georectification of images with ground control points (GCPs, indicated with circles) and computation of vegetation indices in ArcGIS (slanted rectangle); thermal image filtering in ArcGIS (rounded edge rectangles).

Table 8.6. Regression equations fitted to canopy temperature data (y-axis) with column number (x-axis). Equations were fitted for each flight, replicate and water treatment (well-watered, WW and water deficit, WD) of the plant crop only. Significance at p = 0.05 is indicated in bold with an asterisk.

Flight	Rep	Water treatment	Regression	R^2	n
1	1	WW	$y = -0.11x^2 + 0.75x + 28.7$	**0.17***	53
		WD	$y = -0.11x^2 + 3.16x + 4.12$	**0.12***	53
	2	WW	$y = 0.06x^2 - 0.83x + 31.30$	**0.07***	53
		WD	$y = -0.16x^2 + 4.63x - 4.47$	**0.18***	53
	3	WW	$y = 0.09x + 27.48$	0.03	53
		WD	$y = -0.03x^2 + 1.03x + 21.24$	0.03	53
2	1	WW	$y = -0.16x + 21.20$	**0.10***	53
		WD	$y = -0.02x^2 + 0.59x + 16.48$	0.05	53
	2	WW	$y = 0.15x + 19.21$	**0.11***	53
		WD	$y = 0.16x + 20.04$	**0.17***	53
	3	WW	$y = 0.22x + 18.12$	**0.13***	53
		WD	$y = -0.23x + 23.62$	**0.27***	53
3	1	WW	$y = 0.01x^2 + 0.07x + 21.40$	**0.33***	53
		WD	$y = -0.04x^3 + 1.86x^2 - 25.71x + 136.50$	**0.94***	53
	2	WW	$y = -0.03x^3 + 0.45x^2 - 1.65x + 23.86$	**0.61***	53
		WD	$y = -0.08x^2 + 3.02x + 0.68$	**0.89***	53
	3	WW	$y = 0.00x^2 - 0.03x + 23.73$	0.05	53
		WD	$y = 0.01x^2 - 0.12x + 24.63$	0.04	53
4	1	WW	$y = 0.39x + 18.12$	**0.73***	53
		WD	$y = -0.07x^3 + 2.58x^2 - 31.97x + 153.98$	**0.81***	53
	2	WW	$y = 0.02x^3 - 0.31x^2 - 1.38x + 16.75$	**0.79***	53
		WD	$y = -0.06x^3 + 2.43x^2 - 30.58x + 148.92$	**0.91***	53
	3	WW	$y = 0.02x^2 - 0.55x + 28.02$	0.04	53
		WD	$y = 0.02x^2 - 0.27x + 29.59$	**0.14***	53
5	1	WW	$y = 0.01x^3 + 0.01x^2 - 2.13x + 26.54$	**0.96***	53
		WD	$y = 0.00x^3 - 0.26x^2 - 4.73x + 5.25$	**0.67***	53
	2	WW	$y = 0.03x^3 - 0.31x^2 - 0.20x + 21.73$	**0.97***	53
		WD	$y = 0.76x + 7.60$	**0.91***	53
	3	WW	$y = 0.05x^2 - 1.45x + 28.47$	**0.57***	53
		WD	$y = 0.00x^3 + 0.15x^2 - 2.39x + 28.60$	**0.90***	53
6	1	WW	$y = 0.02x^3 - 0.31x^2 + 1.38x + 15.64$	**0.66***	53
		WD	$y = -0.04x^2 + 0.70x + 19.00$	**0.88***	53
	2	WW	$y = 0.05x^2 - 0.26x + 17.43$	**0.65***	53
		WD	$y = 0.02x^3 - 0.93x^2 + 11.96x - 27.97$	**0.91***	53
	3	WW	$y = 0.03x^2 - 0.56x + 18.84$	**0.71***	53
		WD	$y = 0.03x^2 - 1.08x + 25.67$	**0.87***	53
7	1	WW	$y = 0.07x^2 - 1.37x + 18.42$	**0.81***	53
		WD	$y = 0.02x^3 - 0.71x^2 + 10.58x - 34.47$	**0.67***	53
	2	WW	$y = 0.02x^3 - 0.26x^2 + 1.07x - 11.24$	**0.22***	53
		WD	$y = -0.06x^2 + 2.52x - 4.31$	**0.89***	53
	3	WW	$y = 0.02x^2 + 0.35x + 17.39$	**0.24***	53
		WD	$y = 0.02x^3 - 0.49x^2 + 3.77x + 10.09$	**0.85***	53

8.2.2 Results

Weather data

Table 8.7. Hourly average weather data recorded at the time of the thermal flight for flight measurement days in the plant and ratoon crops (RH - relative humidity, SRAD - solar radiation, also expressed as a fraction of clear-sky radiation estimated for the given hour, and wind speed).

Crop	Flight	Temperature (°C)	RH (%)	SRAD (W m^{-2} / %)	Wind speed (m s^{-1})
Plant	1	27.8	62.3	721 / 90	2.4
	2	26.4	76.8	485 / 59	2.1
	3	27.7	64.3	809 / 97	3.6
	4	26.4	64.8	571 / 88	1.6
	5	22.9	51.5	526 / 87	2.9
	6	27.8	29.9	648 / 98	3.8
	7	20.8	45.5	499 / 78	2.9
Ratoon	1	28.7	67.8	567 / 91	1.0
	2	30.9	43.3	943 / 98	1.1
	3	29.3	54.8	885 / 97	1.8
	4	26.6	45.4	823 / 94	1.0

Table 8.8. Daily average weather data for flight measurement days in the plant and ratoon crops (Tmax, Tmin and Tmean – maximum, minimum and mean temperature; RH – relative humidity; SRAD – solar radiation, also expressed as a fraction of daily average clear-sky radiation; windspeed and Ecref – reference evapotranspiration for sugarcane).

Crop	Flight	Tmax (°C)	Tmin (°C)	Tmean (°C)	RHmax (%)	RHmin (%)	RHmean (%)	SRAD (MJ m^{-2} d^{-1} / %)	Wind speed (km d^{-1})	Ecref (mm d^{-1})
Plant	1	32.6	18.3	25.1	99.0	46.0	75.0	24.5 / 0.84	100.0	6.1
	2	29.6	21.2	25.1	98.0	60.0	83.0	14.7 / 0.55	86.8	3.3
	3	31.0	18.8	23.8	100.0	45.0	80.0	19.9 / 0.85	127.0	4.3
	4	31.0	14.9	21.7	98.0	39.0	76.0	15.6 / 0.81	64.3	3.3
	5	26.6	9.4	17.4	97.0	31.0	71.0	13.6 / 0.82	106.8	3.6
	6	30.5	7.0	17.3	97.0	20.0	61.0	15.2 / 0.90	119.8	4.1
	7	24.6	11.5	17.4	88.0	33.0	57.0	13.9 / 0.53	275.3	6.2
Ratoon	1	37.2	22.2	28.3	98	32	70	28.2 / 97	6.4	8.0
	2	33.0	15.2	23.3	99	36	73	24.8 / 91	7.4	5.8
	3	33.3	16.8	25.0	96	42	70	22.9 / 92	5.3	6.2
	4	29.4	10.4	19.9	99	32	73	21.1 / 93	6.5	4.3

Crop growth

Ground measurements

Phenology

Table 8.9. Final green leaf number (GL), stalk population (SPOP, stalks m^{-2}) and stalk height (SH, m) of ten genotypes, measured in the well-watered (WW) and water deficit (WD) treatments at harvest of plant and ratoon crops. WD values for the respective traits were expressed as a fraction of that of the WW treatment (GL*, SP* and SH*). Standard deviation values are indicated in brackets, and where absent, are due to measurements being recorded in <2 replications due to lodging.

	Plant									Ratoon								
Genotype	GL WW	GL WD	GL*	SPOP WW	SPOP WD	SPOP*	SH WW	SH WD	SH*	GL WW	GL WD	GL*	SPOP WW	SPOP WD	SPOP*	SH WW	SH WD	SH*
N12	12.3 (1.27)	5.3 (1.26)	0.43	12.4 (1.59)	12.1 (0.70)	0.98	2.44 (0.10)	1.97 (0.08)	0.81	7.3 (1.3)	5.9 (1.9)	0.81	11.2 (1.2)	11.8 (0.7)	1.05	2.69 (0.18)	2.25 (0.23)	0.83
N14	11.9 (1.14)	4.6 (0.86)	0.39	12.3 (0.62)	11.9 (0.50)	0.97	2.72 (0.11)	1.98 (0.12)	0.73	8.0 (1.3)	6.4 (1.6)	0.80	10.4 (1.3)	8.4 (1.9)	0.81	3.07 (0.17)	2.61 (0.28)	0.85
N19	10.7 (1.35)	4.5 (0.68)	0.43	9.8 (0.77)	10.8 (0.23)	1.10	2.83 (1.37)	2.08 (0.06)	0.74	8.0 (1.5)	6.5 (1.4)	0.81	10.1 (3.1)	11.0 (1.6)	1.09	-	2.69 (0.12)	-
N31	10.0 (1.43)	4.6 (0.90)	0.46	11.9 (0.41)	11.2 (2.41)	0.95	3.04 (0.05)	2.27 (0.12)	0.75	7.8 (1.2)	6.2 (1.4)	0.79	9.6 (1.5)	8.0 (1.1)	0.83	3.27	2.96 (0.13)	0.91
N36	11.5 (1.33)	4.8 (0.82)	0.42	8.7 (1.04)	8.3 (1.18)	0.96	2.85 (0.05)	2.19 (0.12)	0.77	8.5 (1.2)	6.7 (1.9)	0.79	10.5 (0.6)	6.1 (0.1)	0.58	-	2.57 (0.16)	-
N41	11.8 (1.29)	4.7 (1.11)	0.40	10.0 (1.15)	11.2 (0.40)	1.12	2.74 (0.12)	2.34 (0.15)	0.86	8.7 (1.5)	7.1 (2.1)	0.82	12.6 (0.6)	10.9 (1.5)	0.87	3.03 (0.06)	2.83 (0.16)	0.93
N51	11.1 (1.33)	4.6 (0.81)	0.42	10.5 (1.86)	10.7 (0.97)	1.04	2.77 (1.33)	2.10 (0.14)	0.78	8.3 (1.1)	6.4 (1.6)	0.77	12.0 (0.9)	12.0 (0.9)	0.99	3.14 (0.09)	2.58 (0.05)	0.82
N61	11.1 (1.73)	4.6 (0.72)	0.41	9.2 (0.89)	7.9 (1.43)	0.88	2.90 (1.38)	2.34 (0.08)	0.81	8.4 (1.6)	7.1 (2.2)	0.85	10.8 (1.1)	6.9 (0.6)	0.64	-	-	-
NCo376	11.4 (1.54)	4.6 (0.93)	0.41	13.5 (1.22)	12.9 (0.81)	0.97	2.72 (0.11)	2.00 (0.06)	0.73	8.1 (1.2)	6.5 (1.6)	0.80	11.3 (2.7)	12.3 (1.4)	1.09	2.88 (0.07)	2.46 (0.18)	0.85
R570	11.8 (1.23)	5.0 (0.88)	0.39	7.6 (1.20)	6.7 (0.67)	0.90	2.91 (0.08)	2.25 (0.09)	0.77	8.5 (1.2)	6.6 (1.4)	0.78	6.0 (0.0)	12.1 (1.4)	2.02	3.34 (0.07)	2.66 (0.24)	0.79
Average	11.4 (0.69)	4.7 (0.21)	0.41 (0.02)	10.6 (2.18)	10.4 (2.03)	0.99 (0.16)	2.79 (0.96)	2.15 (0.17)	0.77	8.1 (1.35)	6.5 (1.75)	0.80 (0.02)	10.5 (2.0)	10.0 (2.5)	1.00 (0.40)	2.99 (0.28)	2.61 (0.27)	0.86 (0.05)

Radiation interception

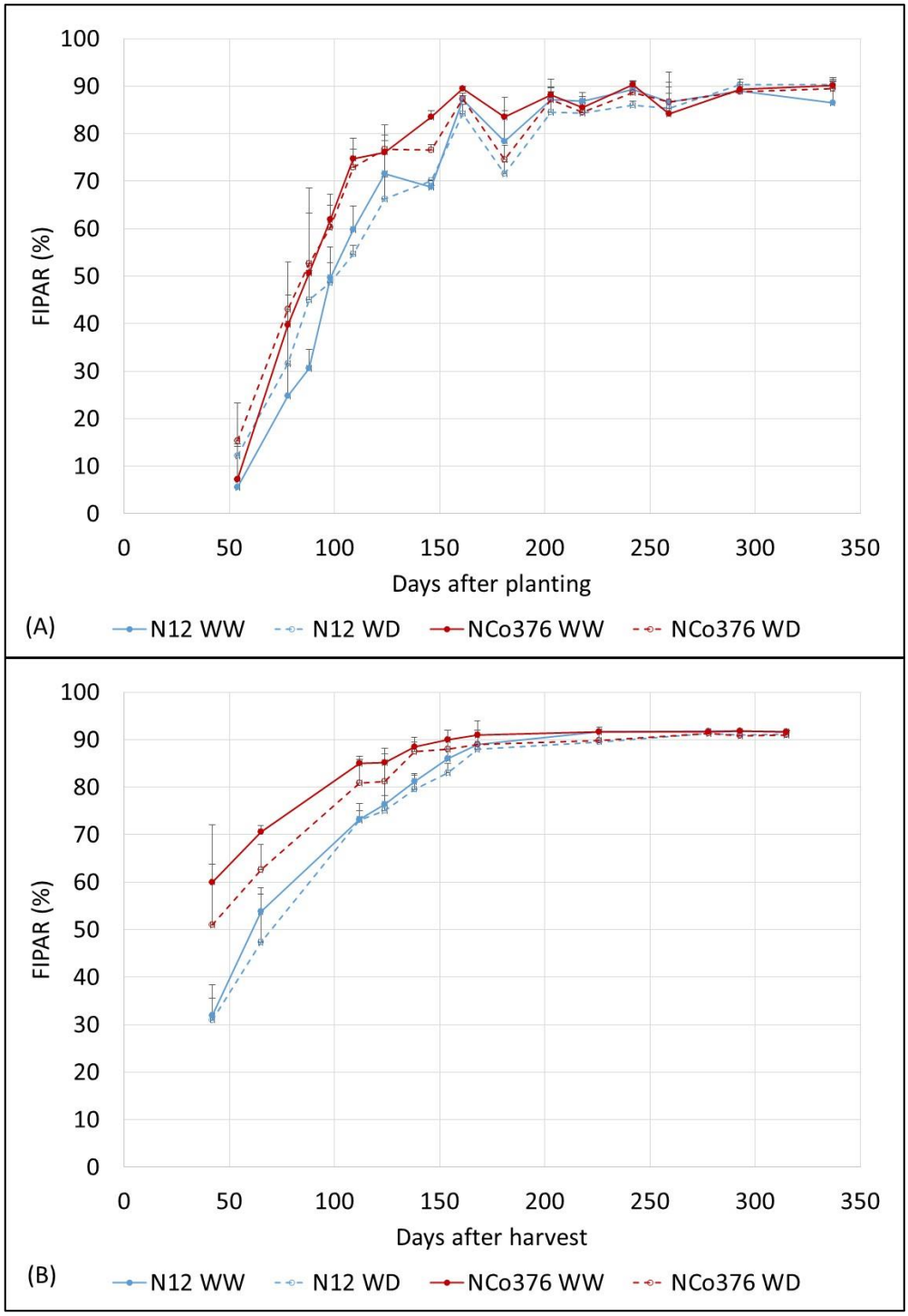

Figure 8.7. Fractional interception of photosynthetic active radiation (PAR) by the canopy (FIPAR) for two contrasting varieties (NCo376 and N12) grown under well-watered (WW) and water deficit (WD) in the plant (A) and ratoon (B) crops.

Stalk yield

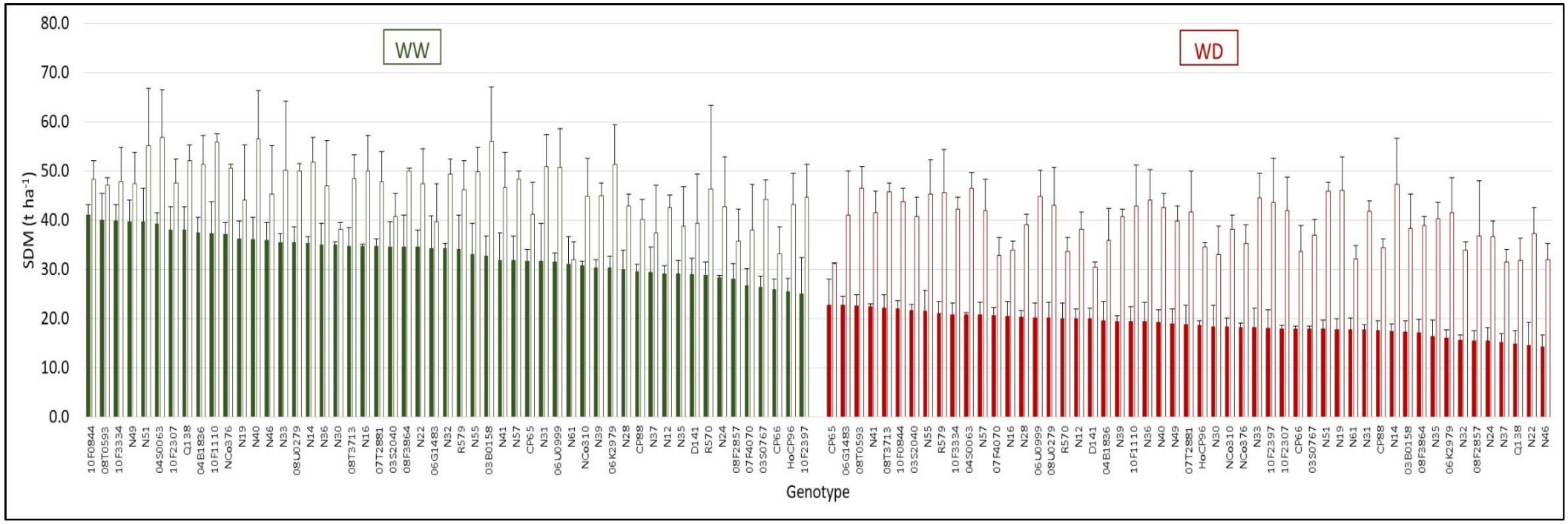

Figure 8.8. Stalk dry mass (SDM) yield at harvest of genotypes, as measured in the well-watered (WW) and water deficit (WD) treatments of the plant (solid bars) and ratoon (hollow bars) crops.

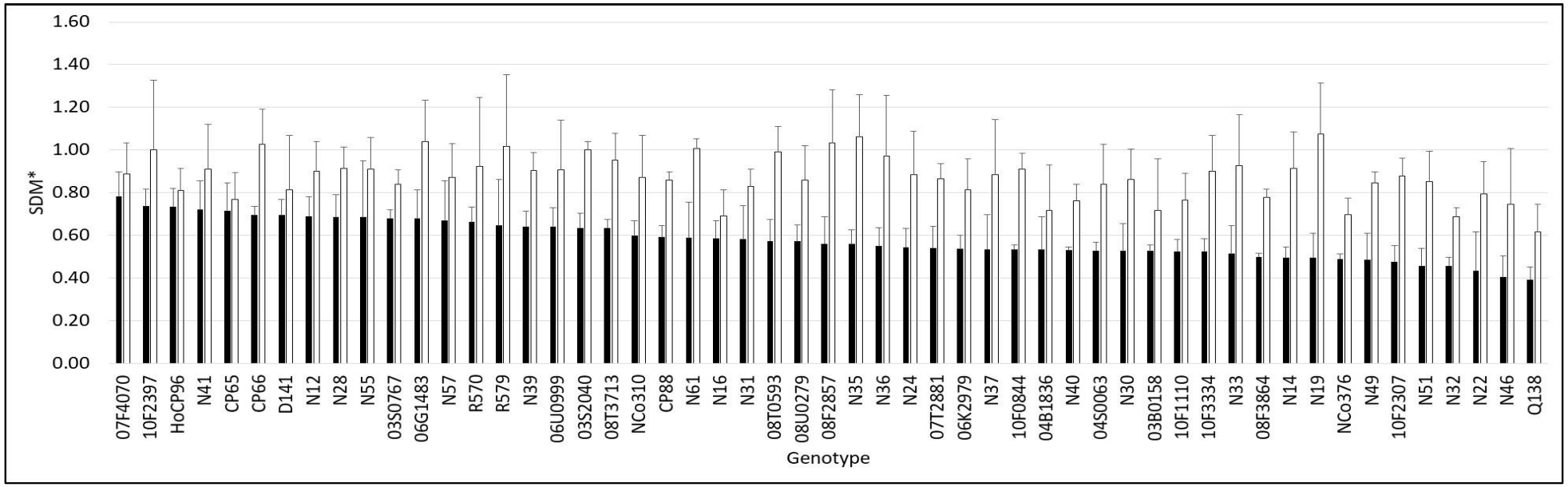

Figure 8.9. Stalk dry mass yield of the water deficit treatment expressed relative to the corresponding well-watered values (SDM*), measured at harvest in the plant (solid bars) and ratoon (hollow bars) crops.

Aerial imaging

Canopy temperature

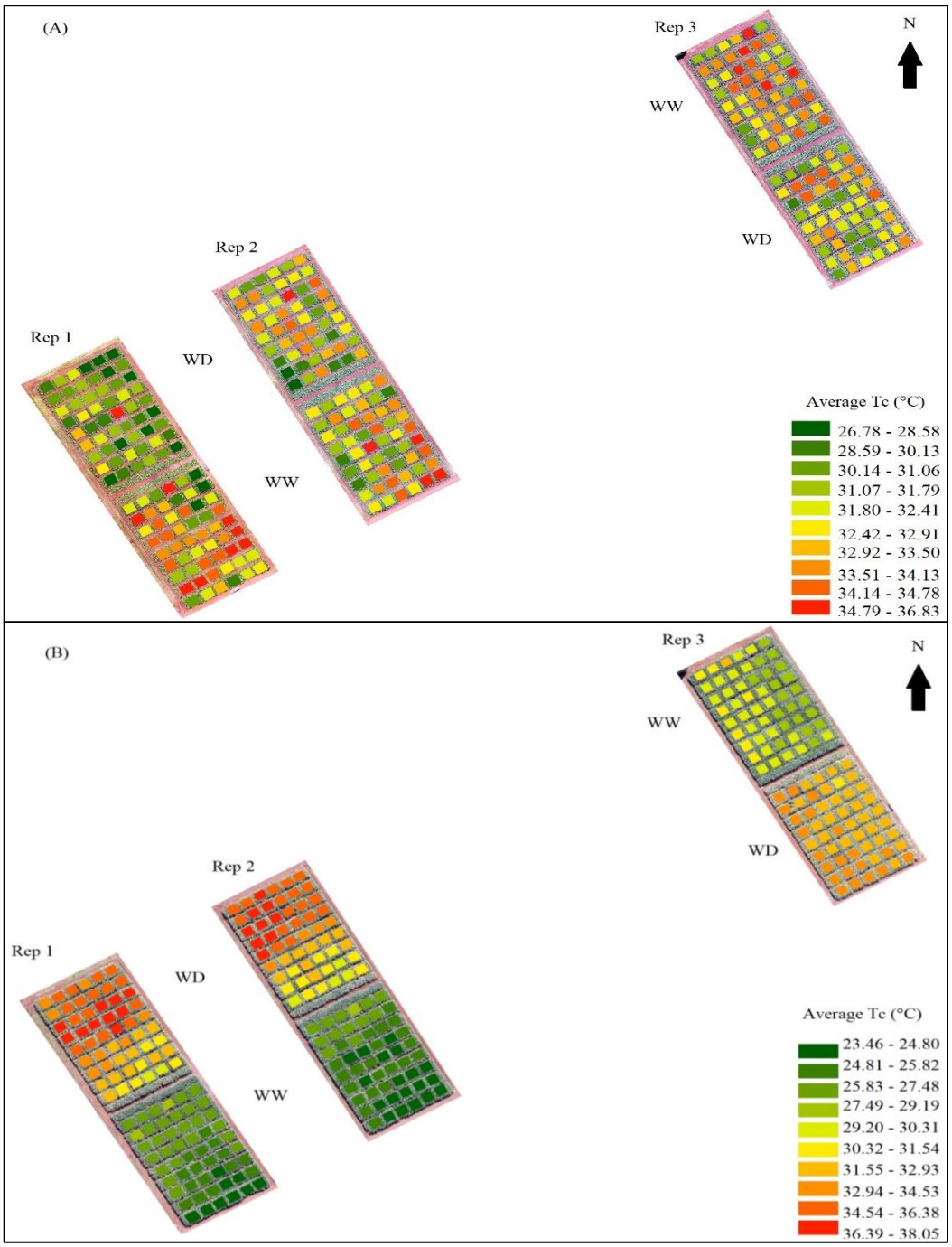

Figure 8.10. Average canopy temperature (Tc, °C) values for each plot captured during drone flights 1 (A) and 4 (B) of the Komati plant crop trial. Flight 1 showed significant genotypic variation in Tc, while flight 4 showed significant spatial variation in relation to column number which obscured genotypic differences.

Table 8.10. Statistical analysis of canopy temperature index (Tc_i, °C) estimated from aerial imagery, captured in the well-watered (WW) and water deficit (WD) treatments of the plant crop. Standard deviation values are indicated in brackets. Values of F. probability (F.pr.) due to genotypic differences, genetic (G) and error (E) variance, genetic coefficient of variation (GCV, %) and broad-sense heritability (HSB) are shown. The number datapoints (n) analysed per flight are also shown.

Water treatment		WW						WD						
Crop	Flight	Mean	F.pr.	G	E	HSB	GCV	Mean	F.pr.	G	E	HSB	GCV	n
Plant	1	-0.083 (2.23)	**<0.0001***	2.11	2.58	0.70	-1760	-1.85 (2.20)	**<0.0001***	1.29	1.54	0.71	-61.2	159
	2	-0.048 (1.23)	**0.018***	0.17	0.58	0.48	-869	1.51 (1.25)	**<0.0001***	0.18	0.29	0.64	27.7	159
	3	-0.029 (0.48)	**0.005***	0.05	0.17	0.47	-764	3.12 (1.84)	0.36	0.01	0.36	0.09	3.50	159
	4	-0.012 (0.66)	**0.002***	0.06	0.16	0.51	-1896	8.48 (3.22)	0.25	0.06	0.77	0.19	2.93	159
	5	-0.014 (0.49)	**0.03***	0.03	0.17	0.37	-1278	3.44 (1.42)	**0.002***	0.11	0.29	0.53	9.61	159
	6	0.015 (0.57)	0.09	0.03	0.25	0.27	1145	2.52 (1.03)	**0.01***	0.04	0.14	0.46	7.76	159
	7	0.009 (1.05)	**0.01***	0.19	0.69	0.46	4643	4.24 (3.11)	**0.01***	0.36	1.40	0.43	14.1	159

Table 8.11. Statistical analysis of canopy temperature index (Tc_i, °C) estimated from aerial imagery, captured in the well-watered (WW) and water deficit (WD) treatments of the plant crop. The data were grouped for different categories of crop water satisfaction (high (H), medium (M) and low (L)), and combinations thereof. Standard deviation values are indicated in brackets. Values of F. probability (F.pr.) due to genotypic differences, genetic (G) and error (E) variance, genetic coefficient of variation (GCV, %) and broad-sense heritability (HSB) are shown. The number datapoints (n) per dataset are also shown.

Crop	Water treatment	Crop water satisfaction category	Mean	F.pr.	G	E	HSB	GCV	n
Plant	WW	H	-0.023 (1.12)	**<0.0001***	0.09	1.12	0.19	-1298	1113
	WD	H	0.93 (2.75)	**0.01***	0.17	2.29	0.18	44.1	477
		M	5.96 (3.54)	0.99	-	4.61	-	-	318
		L	3.38 (2.47)	0.99	-	4.33	-	-	318
		H+M	2.82 (4.35)	0.88	-	3.78	-	-	795
		M+L	4.67 (3.31)	0.99	-	4.75	-	-	636
		H+M+L	3.07 (3.60)	0.96	-	4.00	-	-	1113

Trait and yield phenotyping

Figure 8.11. Phenotypic (r) correlations estimated in plant (up to 337 days after planting, DAP) and ratoon (338 – 685 DAP) crops, between: (A) stalk dry mass yield (SDM) and fractional interception of radiation (FIPAR); (B) FIPAR and normalized difference vegetation index (NDVI); (C) SDM and NDVI; (D) SDM and stomatal conductance (g_s); (E) g_s and canopy temperature (Tc); (F) SDM and Tc. Data for the well-watered (solid bars) and water deficit (striped bars) treatments were categorised according to crop water satisfaction index (CWSI). Values in bold with an asterisk indicate statistical significance at $p = 0.05$.

8.3 Breeding trials

8.3.1 Methodology

Soil characterisation

Table 8.12. Properties of soil samples from selected banks in the Empangeni breeding trials. Values of textural (clay and silt %), and retention properties (field capacity, FC; permanent wilting point, PWP; and plant available soil water capacity, ASWCmax, calculated as the product of the average difference between FC and PWP and estimated rooting depth) are given. Retention properties were estimated from clay content (as invan Antwerpen et al., 1994). The average and standard deviation values (indicated in brackets) for soil properties are given.

Trial	Bank	Trial part	Depth (cm)	Clay (%)	Silt (%)	FC (mm/m)	PWP (mm/m)	ASWCmax (mm)
SR 19-20	1	A	20	44	5.4	351.2	225.3	127.8
			40	40	9.4	339.1	209.5	
			60	44	9.4	351.2	225.3	
			80	40	19.4	339.1	209.5	
	39	F	20	36	7.4	325.3	192.9	132.6
			40	36	7.4	325.3	192.9	
			60	38	7.4	332.4	201.3	
			80	30	15.4	300.9	166.6	
			Average	38.5 (4.63)	10.2 (4.77)	333.1 (16.4)	202.9 (19.3)	130.2 (3.39)
SR 21-22	11	B	20	50	5.4	367.0	247.8	117.8
			40	46	7.4	356.8	233.0	
			60	58	5.4	384.4	275.5	
			80	50	3.4	367.0	247.8	
	65	I	20	38	9.4	332.4	201.3	126.0
			40	46	1.4	356.8	233.0	
			60	46	7.4	356.8	233.0	
			80	44	5.4	351.2	225.3	
			Average	47.3 (5.75)	5.65 (2.49)	359.1 (14.9)	237.1 (21.3)	121.9 (5.80)

Genotype selection

Table 8.13. Multiple linear regression coefficients for traits NDVI and Tc in estimating SDM within trial parts for categories of CWSI (medium, M, high, H and for the pooled dataset) for the SR 19-20 trial.

CWSI	M+H				M			H		
Trial part	Parameter	Coefficient	Standard error	P-value	Coefficient	Standard error	P-value	Coefficient	Standard error	P-value
A	NDVI	94.5	41.5	0.06	12.1	6.31	0.06	0.29	3.36	0.93
	Tc	-2.46	1.52	0.15	-0.12	0.22	0.58	-0.44	0.16	0.01
	Intercept	12.9	73.4	0.87	-0.26	11.38	0.98	12.9	4.83	0.01
	R^2	0.70	-	-	0.07	-	-	0.10	-	-
B	NDVI	-4.61	35.6	0.90	9.90	0.15	0.71	-2.46	3.31	0.46
	Tc	-1.50	0.84	0.12	-0.05	6.94	0.16	-0.24	0.14	0.09
	Intercept	57.6	38.6	0.18	-1.86	8.97	0.84	10.6	4.43	0.02
	R^2	0.32	-	-	0.05	-	-	0.06	-	-
C	NDVI	95.9	51.3	0.10	18.6	8.30	0.03	-7.88	5.67	0.17
	Tc	1.81	1.73	0.33	0.11	0.32	0.72	-0.44	0.22	0.06
	Intercept	-131.2	94.2	0.21	-14.8	17.31	0.40	19.1	7.32	0.01
	R^2	0.38	-	-	0.16	-	-	0.12	-	-
F	NDVI	100.8	39.0	0.04	8.08	4.41	0.07	4.48	3.11	0.15
	Tc	-1.76	1.80	0.36	-0.05	0.13	0.69	-0.09	0.23	0.68
	Intercept	-7.71	57.4	0.90	0.05	6.35	0.99	2.53	6.53	0.70
	R^2	0.49	-	-	0.04	-	-	0.02	-	-
J	NDVI	71.6	88.5	0.45	11.2	9.38	0.24	-0.58	5.50	0.92
	Tc	-0.52	3.14	0.87	0.21	0.34	0.54	-0.50	0.35	0.16
	Intercept	-32.0	154.5	0.84	-12.5	18.50	0.50	20.4	12.95	0.12
	R^2	0.11	-	-	0.02	-	-	0.03		

Table 8.14. Multiple linear regression coefficients for traits NDVI and Tc in estimating SDM within trial parts for individual flights in the SR 21-22 trial.

Flight	Trial part	Parameter	Coefficient	Standard error	P-value
1	A	NDVI	2.69	1.01	0.008
		Tc	-0.033	0.03	0.25
		Intercept	2.30	1.47	0.12
		R^2	0.08	-	-
	B	NDVI	1.48	0.94	0.12
		Tc	-0.06	0.03	0.07
		Intercept	3.73	1.58	0.02
		R^2	0.06	-	-
	C	NDVI	2.93	1.15	0.01
		Tc	-0.04	0.05	0.42
		Intercept	1.82	2.06	0.38
		R^2	0.08	-	-
	D	NDVI	4.63	1.04	0.00
		Tc	0.16	0.04	0.00
		Intercept	-5.27	1.69	0.00
		R^2	0.09	-	-
	E	NDVI	3.34	0.82	0.00
		Tc	0.11	0.04	0.01
		Intercept	-2.66	1.65	0.11
		R^2	0.07	-	-
	F	NDVI	4.85	1.28	0.00
		Tc	0.04	0.02	0.02
		Intercept	-2.10	1.21	0.08
		R^2	0.08	-	-
4	A	NDVI	5.38	1.88	0.00
		Tc	-0.12	0.05	0.02
		Intercept	1.48	2.05	0.47
		R^2	0.05	-	-
	B	NDVI	4.94	1.91	0.01
		Tc	-0.18	0.05	0.00
		Intercept	3.06	1.68	0.07
		R^2	0.05	-	-
	C	NDVI	1.58	2.97	0.60
		Tc	-0.02	0.03	0.58
		Intercept	1.91	2.60	0.46
		R^2	0.01	-	-
	D	NDVI	-1.88	2.06	0.36
		Tc	0.14	0.05	0.01
		Intercept	1.44	1.89	0.45
		R^2	0.03	-	-
	E	NDVI	-0.46	0.06	0.07
		Tc	-0.12	0.06	0.07
		Intercept	5.82	2.13	0.01
		R^2	0.01	-	-
	F	NDVI	11.0	3.29	0.00
		Tc	0.07	0.02	0.00
		Intercept	-7.60	2.74	0.01
		R^2	0.03	-	-
	G	NDVI	-2.45	8.65	0.78
		Tc	-0.10	0.06	0.13
		Intercept	8.56	7.63	0.27
		R^2	0.08	-	-
	J	NDVI	8.34	3.45	0.02

		Parameter	Coefficient	Standard error	P-value
4	J	Tc	0.03	0.17	0.87
		Intercept	-4.35	4.79	0.37
		R^2	0.04	-	-
5	A	NDVI	2.42	1.40	0.09
		Tc	-0.09	0.05	0.11
		Intercept	2.99	1.54	0.05
		R^2	0.02	-	-
	B	NDVI	3.04	1.23	0.01
		Tc	-0.05	0.04	0.17
		Intercept	1.52	1.14	0.18
		R^2	0.03	-	-
	C	NDVI	-1.58	1.83	0.39
		Tc	-0.02	0.04	0.61
		Intercept	4.41	1.56	0.01
		R^2	0.01	-	-
	D	NDVI	-0.20	1.54	0.90
		Tc	0.12	0.04	0.00
		Intercept	0.97	1.34	0.47
		R^2	0.04	-	-
	E	NDVI	0.88	1.69	0.60
		Tc	0.01	0.05	0.91
		Intercept	2.21	1.27	0.08
		R^2	0.00	-	-
	F	NDVI	5.56	2.41	0.02
		Tc	0.20	0.05	0.00
		Intercept	-5.13	2.39	0.03
		R^2	0.08	-	-
	G	NDVI	-0.02	2.16	0.99
		Tc	0.05	0.05	0.28
		Intercept	2.46	2.29	0.29
		R^2	0.01	-	-
	H	NDVI	6.00	1.93	0.00
		Tc	-0.01	0.04	0.09
		Intercept	-0.54	1.95	0.78
		R^2	0.05	-	-
	I	NDVI	1.87	1.89	0.32
		Tc	0.07	0.03	0.03
		Intercept	0.30	1.87	0.87
		R^2	0.02	-	-

8.3.2 Results

SR 19-20

Weather data

Table 8.15. Hourly average weather data recorded at the time of the thermal flight for three measurement days (RH - relative humidity, SRAD - solar radiation, also expressed as a fraction of clear-sky radiation estimated for the given hour, and wind speed) in the SR 19-20 trial.

Flight	Date (DAP)	Temperature (°C)	RH (%)	SRAD SRAD ($W\ m^{-2}\ s^{-1}$ / %)	Wind speed ($m\ s^{-1}$)
1	16 Jan 2020 (317)	27.7	65.7	722.2 / 98	0.6
2	30 Jan 2020 (331)	30.1	60.7	663.9 / 96	3.2
3	24 Mar 2020 (385)	28.0	67.9	810.0 / 96	1.1

Table 8.16. Daily weather data for three measurement days during which drone flights were conducted (Tmax, Tmin and Tmean – maximum, minimum and mean temperature; RH – relative humidity; SRAD – solar radiation, also expressed as a fraction of daily average clear-sky radiation; windspeed and Ecref – reference evapotranspiration for sugarcane).

Flight	Tmax (°C)	Tmin (°C)	Tmean (°C)	RHmax (%)	RHmin (%)	RHmean (%)	SRAD ($MJ\ m^{-2}\ d^{-1}$ / %)	Ecref ($mm\ d^{-1}$)
1	32.9	21.3	28.1	75	54	72	31.3 / 97	6.8
2	38.0	21.6	28.7	99	34	72	31.2 / 97	10.9
3	30.6	19.8	24.2	100	51	86	22.8 / 94	4.6

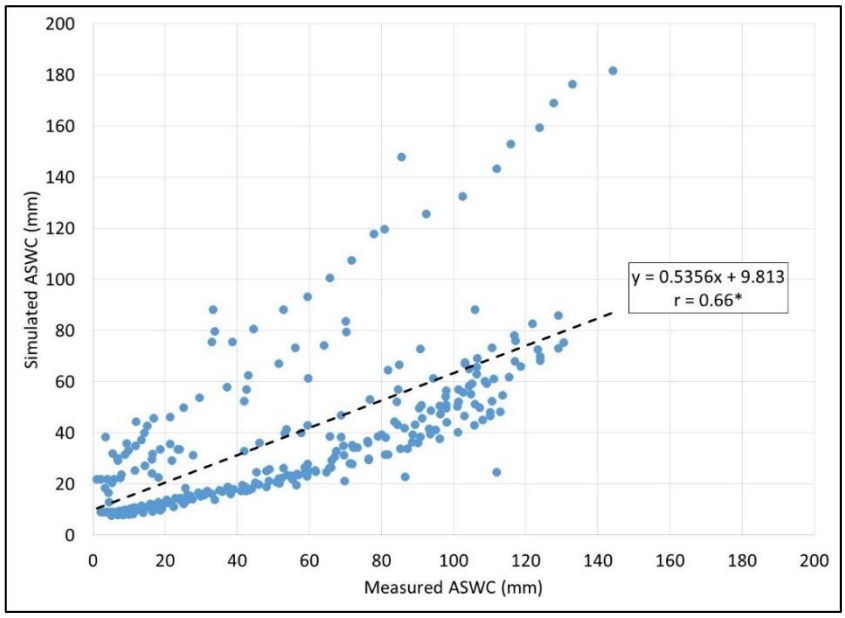

Figure 8.12. Comparison of plant available soil water content (ASWC), measured in the SR 19-20 trial using capacitance probes and simulated using the MyCanesim® model. Statistical significance at p = 0.05 is indicated with an asterisk.

Crop growth

Aerial imaging

Table 8.17. Statistical analysis of normalised difference vegetation index (NDVI) and canopy temperature (Tc, °C) estimated from aerial imagery across multiple flights for each part of the SR 19-20 experiment. Data were grouped by crop water satisfaction (medium or high, M / H, and combinations thereof). Standard deviation values are indicated in brackets. F. probabilities (F.pr.) due to genotypic differences (indicated as significant with an asterisk) are shown along with corresponding genetic (G) and error (E) variances, genetic coefficient of variation (GCV, %) and broad-sense heritability (HSB) values for the respective categories. The number of datapoints analysed (n) is also shown.

Variable		NDVI						Tc						
Trial part	CWSI	Mean	F.pr.	G	E	GCV	HSB	Mean	F.pr.	G	E	GCV	HSB	n
A	M	0.76 (0.039)	0.06	0.000085	0.00091	1.2	0.16	39.9 (3.03)	0.98	NS	8.85	NS	NS	276
	M+H	0.78 (0.051)	0.95	NS	0.0024	NS	NS	33.7 (9.23)	0.99	NS	85.2	NS	NS	414
B	M	0.78 (0.032)	0.11	0.00014	0.00083	1.5	0.25	39.5 (2.42)	0.99	NS	5.80	NS	NS	212
	M+H	0.80 (0.044)	0.61	NS	0.0019	NS	NS	33.2 (9.22)	0.98	NS	84.9	NS	NS	318
C	M	0.75 (0.045)	0.05	0.00032	0.00086	2.4	0.43	40.9 (2.23)	0.97	NS	4.84	NS	NS	148
	M+H	0.77 (0.059)	0.97	NS	0.0032	NS	NS	33.9 (10.06)	0.99	NS	101.2	NS	NS	222
F	M	0.72 (0.037)	0.08	0.00026	0.00097	2.2	0.35	41.5 (2.29)	0.99	NS	4.71	NS	NS	348
	M+H	0.76 (0.066)	0.99	NS	0.0044	NS	NS	36.7 (6.98)	0.97	NS	48.8	NS	NS	522
J	M	0.76 (0.038)	0.07	0.000063	0.00080	1.0	0.14	40.2 (1.52)	0.99	NS	2.06	NS	NS	240
	M+H	0.78 (0.055)	0.99	NS	0.0028	NS	NS	37.2 (4.47)	0.98	NS	19.9	NS	NS	360

NS Variance components and HSB could not be calculated due to statistically non-significant genotypic differences.

Trait correlations

Table 8.18. Phenotypic (r) and genetic correlations (r_g) between stalk dry mass yield (SDM) measured at harvest, with normalized difference vegetation index (NDVI) and canopy temperature (Tc) estimated from aerial imagery. Data were expressed relative to that of NCo376 (SDM_{ref}, $NDVI_{ref}$ and Tc_{ref}), and categorised by crop water satisfaction (medium or high, M / H, and combinations thereof), for all parts of the SR 19-20 trial.

	Variable	SDM_{ref} vs. $NDVI_{ref}$		SDM_{ref} vs. Tc_{ref}	
Trial part	Crop water satisfaction category	r	r_g	r	r_g
A	M	0.42	0.50	**-0.71***	-0.24
	H	0.20	0.10	**-0.72***	-0.50
	M+H	0.39	0.33	**-0.93***	-0.33
B	M	**0.76***	0.13	-0.10	0.13
	H	0.10	0.21	-0.60	-0.09
	M+H	0.53	0.05	-0.48	0.07
C	M	0.62	0.32	-0.20	-0.13
	H	0.17	0.25	-0.14	-0.21
	M+H	0.60	0.19	-0.47	-0.14
F	M	0.62	0.00	-0.42	-0.11
	H	0.57	0.15	-0.45	-0.14
	M+H	0.51	0.05	-0.40	-0.12
J	M	0.14	0.06	-0.30	-0.12
	H	0.36	0.00	-0.47	-0.11
	M+H	0.24	0.06	-0.36	-0.12

Genotype selection

Selection accuracy

Table 8.19. Comparison of direct (SDM-based) and indirect (based on aerially measured traits, i.e. NDVI, Tc, VPI and SDM_{MLR}) genotype selection methods in the SR 19-20 breeding trial. The analysis included a subset of genotypes after exclusion criteria were applied. Selection methods were evaluated for each trial part, as well as across the trial. Data were categorised by crop water satisfaction (high or medium, H / M, and combinations thereof). Selection methods were compared by considering: (1) the number of genotypes that were selected with the respective traits; (2) the number of positive matches (i.e. genotypes selected by both SDM and the respective aerially measured trait); (3) misses (genotypes selected with SDM but not with the respective aerially measured trait) and false positives (genotypes selected with the aerially measured trait but not with SDM). The green highlighted blocks indicate instances where the number of positive matches exceed the number of misses and false positives.

		CWSI	M																
Trial part	Genotypes planted	Genotypes considered	Genotypes selected					Positive Matches				Misses				False positives			
		Selection trait	SDM	NDVI	Tc	VPI	SDM_{MLR}	NDVI	Tc	VPI	SDM_{MLR}	NDVI	Tc	VPI	SDM_{MLR}	NDVI	Tc	VPI	SDM_{MLR}
A	200	69 (35%)	22 (32%)	49 (71%)	24 (35%)	39 (57%)	45 (65%)	19 (39%)	8 (33%)	16 (41%)	17 (38%)	3 (14%)	14 (64%)	6 (27%)	5 (23%)	30 (61%)	16 (67%)	23 (59%)	28 (62%)
B	200	54 (27%)	30 (56%)	1 (2%)	15 (28%)	4 (7%)	1 (2%)	1 (100%)	9 (60%)	4 (100%)	1 (100%)	29 (97%)	21 (70%)	26 (87%)	29 (97%)	0	6 (40%)	0	0
C	150	38 (25%)	2 (5%)	16 (42%)	29 (76%)	23 (61%)	12 (32%)	1 (6%)	2 (7%)	2 (9%)	1 (8%)	1 (50%)	0	0	1 (50%)	15 (94%)	27 (93%)	21 (91%)	11 (92%)
F	200	87 (44%)	37 (43%)	35 (40%)	8 (9%)	8 (9%)	26 (30%)	18 (49%)	4 (50%)	6 (75%)	12 (46%)	19 (51%)	33 (89%)	31 (84%)	25 (68%)	17 (49%)	4 (50%)	2 (25%)	14 (54%)
J	200	61 (31%)	36 (59%)	4 (7%)	4 (7%)	10 (16%)	10 (16%)	2 (50%)	3 (75%)	8 (80%)	9 (90%)	34 (94%)	33 (92%)	28 (78%)	27 (75%)	2 (50%)	1 (25%)	2 (20%)	1 (10%)

Trial part	Genotypes planted	CWSI Genotypes considered	M																
			Genotypes selected					Positive Matches				Misses				False positives			
		Selection trait	SDM	NDVI	Tc	VPI	SDM_{MLR}	NDVI	Tc	VPI	SDM_{MLR}	NDVI	Tc	VPI	SDM_{MLR}	NDVI	Tc	VPI	SDM_{MLR}
Total	950	309 (33%)	127 (41%)	105 (34%)	80 (26%)	84 (27%)	94 (30%)	41 (32%)	26 (33%)	36 (43%)	40 (43%)	86 (68%)	101 (80%)	91 (72%)	87 (69%)	64 (61%)	54 (68%)	48 (57%)	54 (57%)
			H																
A	200	69 (35%)	22 (32%)	0	17 (25%)	10 (14%)	16 (23%)	0	11 (65%)	6 (60%)	11 (69%)	22 (100%)	11 (50%)	16 (73%)	11 (50%)	0	6 (35%)	4 (40%)	5 (31%)
B	200	54 (27%)	30 (56%)	14 (26%)	8 (15%)	7 (13%)	12 (22%)	10 (71%)	6 (75%)	5 (71%)	7 (58%)	20 (67%)	24 (80%)	25 (83%)	23 (77%)	4 (29%)	2 (25%)	2 (29%)	5 (42%)
C	150	38 (25%)	2 (5%)	2 (5%)	8 (21%)	4 (11%)	16 (42%)	0	1 (13%)	1 (25%)	1 (6%)	2 (100%)	1 (50%)	1 (50%)	1 (50%)	2 (100%)	7 (88%)	3 (75%)	15 (94%)
F	200	87 (44%)	37 (43%)	80 (92%)	51 (59%)	75 (86%)	80 (92%)	36 (45%)	25 (49%)	34 (45%)	36 (45%)	1 (3%)	12 (32%)	3 (8%)	1 (3%)	44 (55%)	26 (51%)	41 (55%)	44 (55%)
J	200	61 (31%)	36 (59%)	17 (28%)	29 (48%)	25 (41%)	29 (48%)	11 (65%)	**21 (72%)**	18 (72%)	**21 (72%)**	25 (69%)	**15 (42%)**	18 (50%)	**15 (42%)**	6 (35%)	**8 (28%)**	7 (28%)	**8 (28%)**
Total	950	309 (33%)	127 (41%)	113 (37%)	113 (37%)	121 (39%)	153 (50%)	57 (50%)	64 (57%)	64 (53%)	76 (50%)	70 (55%)	63 (50%)	63 (50%)	51 (40%)	56 (50%)	49 (43%)	57 (47%)	77 (50%)
			M + H																
A	200	69 (35%)	22 (32%)	25 (36%)	20 (29%)	20 (29%)	20 (29%)	11 (50%)	9 (41%)	9 (41%)	8 (36%)	11 (50%)	13 (59%)	13 (59%)	14 (64%)	14 (56%)	11 (55%)	11 (55%)	12 (60%)
B	200	54 (27%)	30 (56%)	3 (6%)	8 (15%)	2 (4%)	12 (22%)	2 (7%)	6 (20%)	2 (7%)	8 (27%)	28 (93%)	24 (80%)	28 (93%)	22 (73%)	1 (33%)	2 (25%)	0	4 (33%)
C	150	38 (25%)	2 (5%)	7 (18%)	19 (50%)	12 (32%)	4 (11%)	1 (50%)	1 (50%)	1 (50%)	1 (50%)	1 (50%)	1 (50%)	1 (50%)	1 (50%)	6 (86%)	18 (95%)	11 (92%)	3 (75%)
F	200	87 (44%)	37 (43%)	72 (83%)	13 (15%)	25 (68%)	57 (66%)	32 (86%)	7 (19%)	14 (38%)	27 (73%)	5 (14%)	30 (81%)	23 (62%)	10 (27%)	40 (56%)	6 (46%)	11 (44%)	30 (53%)
J	200	61 (31%)	36 (59%)	13 (21%)	13 (21%)	15 (25%)	12 (20%)	11 (31%)	8 (22%)	10 (28%)	11 (31%)	25 (69%)	28 (78%)	26 (72%)	25 (69%)	2 (15%)	5 (38%)	5 (33%)	1 (8%)
Total	950	309 (33%)	127 (41%)	120 (39%)	73 (24%)	74 (24%)	105 (34%)	57 (45%)	31 (24%)	36 (28%)	55 (43%)	70 (55%)	96 (76%)	91 (72%)	72 (57%)	63 (53%)	42 (58%)	38 (51%)	50 (48%)

Note: The percentages indicate: (1) The number of genotypes selected with the respective trait, were expressed relative to the number of genotypes considered after exclusion criteria were applied; (2) Positive matches were expressed relative to the number of genotypes selected, with the respective trait; (3) Misses were expressed relative to the number of genotypes selected with SDM; (4) False positives were expressed relative to the number of genotypes selected with the respective trait.

SR 21-22

Weather data

Table 8.20. Hourly average weather data recorded at the time of the thermal flight for five measurement days (RH - relative humidity, SRAD - solar radiation, also expressed as a fraction of clear-sky radiation estimated for the given hour, and wind speed) in the SR 21-22 trial.

Flight	Date (DAP)	Temperature (°C)	RH (%)	SRAD (W m^{-2} s^{-1} / %)	Wind speed (m s^{-1})
1	9 Dec 2021 (51)	33.7	43	1019.4 / 98	3.0
2	10 Jan 2022 (83)	30.5	59	1047.2 / 99	4.6
3	3 Mar 2022 (135)	31.6	56	944.4 / 99	4.3
4	18 May 2022 (211)	26.0	60	611.1 / 99	4.3
5	21 Jun 2022 (245)	22.5	65	547.2 / 98	2.1

Table 8.21. Daily weather data for five measurement days during which drone flights were conducted in the SR 21-22 trial (Tmax, Tmin and Tmean – maximum, minimum and mean temperature; RH – relative humidity; SRAD – solar radiation, also expressed as a fraction of daily average clear-sky radiation; windspeed and Ecref – reference evapotranspiration for sugarcane).

Flight	Tmax (°C)	Tmin (°C)	Tmean (°C)	RHmax (%)	RHmin (%)	RHmean (%)	SRAD (MJ m^{-2} d^{-1} / %)	Ecref (mm d^{-1})
1	36.5	21.7	27.5	98	36	74	25.2 / 77	7.4
2	32.8	20.0	25.6	98	49	79	27.6 / 85	9.2
3	34.0	20.7	26.1	92	48	74	26.5 / 96	9.3
4	27.8	16.7	21.1	99	48	81	14.8 / 92	4.4
5	24.1	12.3	17.6	100	59	88	12.8 / 89	1.6

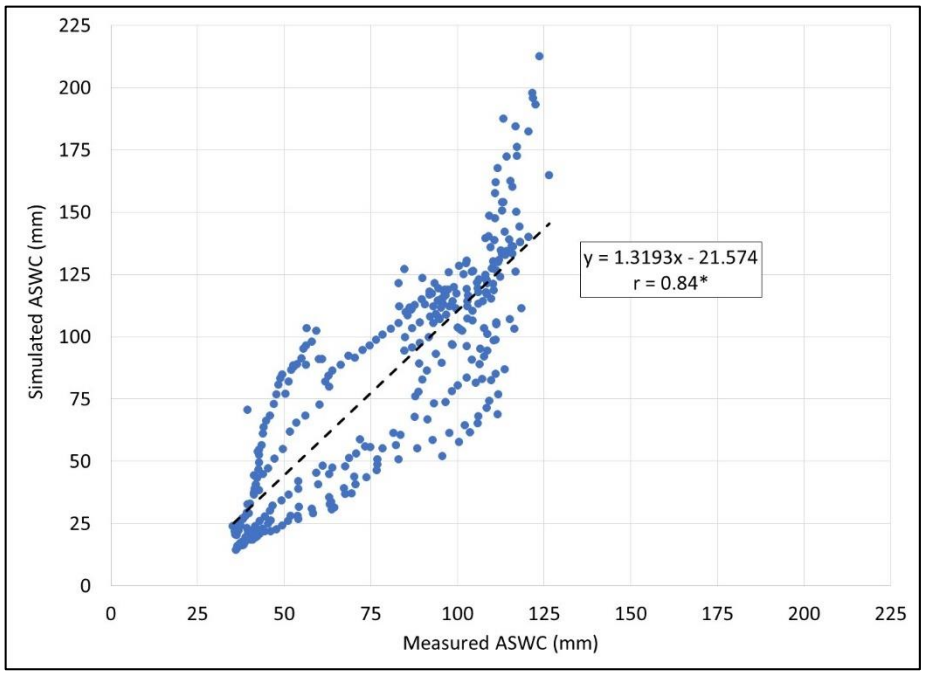

Figure 8.13. Comparison of plant available soil water content (ASWC), measured in the SR 21-22 trial using capacitance probes and simulated using the MyCanesim® model. Statistical significance at p = 0.05 is indicated with an asterisk.

Crop growth

Aerial imaging

Table 8.22. Statistical analysis of normalised difference vegetation index (NDVI) and canopy temperature (Tc, °C) estimated from aerial imagery across multiple flights for each part of the SR 21-22 experiment. Data were grouped by crop water satisfaction (medium or high, M / H, and combinations thereof). Standard deviation values are indicated in brackets. F. probabilities (F.pr.) due to genotypic differences (indicated as significant with an asterisk) are shown along with corresponding genetic (G) and error (E) variances, genetic coefficient of variation (GCV, %) and broad-sense heritability (HSB) values for the respective categories. The number of datapoints analysed (n) is also shown.

Variable		NDVI							Tc						
Trial part	CWSI	Mean	F.pr.	G	E	GCV	HSB	n	Mean	F.pr.	G	E	GCV	HSB	n
A	H	0.77 (0.07)	0.07	0.00085	0.0063	3.79	0.21	1174	24.7 (4.94)	0.34	0.29	1.36	2.18	0.30	942
	M+H	NA	NA	NA	NA	NA	NA	NA	27.8 (6.96)	0.59	NS	2.61	NS	NS	1256
B	H	0.77 (0.06)	0.45	0.0003	0.0098	2.25	0.06	1168	24.5 (4.74)	0.06	0.50	1.86	2.89	0.35	876
	M+H	NA	NA	NA	NA	NA	NA	NA	27.3 (6.40)	0.05	0.78	1.59	3.24	0.50	1168
C	H	0.78 (0.06)	0.41	0.0005	0.006	2.87	0.14	968	23.7 (5.51)	0.48	0.55	1.73	3.13	0.39	726
	M+H	NA	NA	NA	NA	NA	NA	NA	26.5 (6.86)	0.46	0.64	1.48	3.02	0.46	968
D	H	0.79 (0.05)	0.08	0.00009	0.0002	1.20	0.47	1008	22.6 (5.35)	0.55	NS	1.99	NS	NS	756
	M+H	NA	NA	NA	NA	NA	NA	NA	25.7 (7.08)	0.42	0.50	1.30	2.75	0.43	1008
E	H	0.79 (0.06)	0.06	0.0009	0.0008	3.80	0.69	936	22.7 (5.78)	0.49	0.02	1.10	0.62	0.04	702
	M+H	NA	NA	NA	NA	NA	NA	NA	26.5 (8.27)	0.50	0.19	1.67	1.64	0.19	936
F	H	0.82 (0.04)	0.10	0.00006	0.0005	0.94	0.19	918	24.9 (6.73)	0.54	NS	1.40	NS	NS	682
	M+H	NA	NA	NA	NA	NA	NA	NA	28.7 (8.81)	0.52	NS	1.28	NS	NS	916
G	H	0.81 (0.04)	0.07	0.00004	0.007	0.78	0.01	517	21.1 (3.57)	0.08	0.19	1.30	2.07	0.23	281
	M+H	NA	NA	NA	NA	NA	NA	NA	29.8 (10.01)	0.51	NS	0.89	NS	NS	515
I	H	0.82 (0.03)	**0.04***	0.0005	0.0004	2.73	0.71	570	20.7 (2.24)	0.31	0.04	0.40	0.97	0.17	314
	M+H	NA	NA	NA	NA	NA	NA	NA	28.0 (8.32)	0.25	0.61	0.77	2.79	0.61	570
J	H	0.81 (0.03)	**0.04***	0.0005	0.0006	2.76	0.63	388	22.9 (2.26)	0.50	NS	0.12	NS	NS	242
	M+H	NA	NA	NA	NA	NA	NA	NA	28.3 (7.28)	0.53	NS	0.48	NS	NS	389

NA Data not available for flight 3 when CWSI was medium, as a result of instrument failure.

NS HSB could not be calculated due to statistically non-significant genotypic differences.

Trait correlations

Table 8.23. Phenotypic (r) and genetic correlations (r_g) between stalk dry mass yield (SDM) measured at harvest, with normalized difference vegetation index (NDVI) and canopy temperature (Tc), expressed relative to that of NCo376 (SDM_{ref}, $NDVI_{ref}$ and Tc_{ref}) for trial parts measured over five flights in the SR 21-22 experiment.

	Variable	SDM_{ref} vs. $NDVI_{ref}$		SDM_{ref} vs. Tc_{ref}	
Flight	Trial part	r	r_g	r	r_g
1	A	**0.89***	0.29	**-0.90***	-0.23
	B	**0.67***	0.26	**-0.71***	-0.20
	C	**0.69***	0.30	**-0.65***	-0.25
	D	**0.64***	0.18	-0.09	-0.13
	E	0.21	0.19	-0.07	-0.05
	F	**0.68***	0.22	-0.03	-0.16
2	A	**0.85***	0.32	NA	NA
	B	**0.70***	0.29	NA	NA
	C	**0.82***	0.30	NA	NA
	D	**0.64***	0.24	NA	NA
	E	**0.65***	0.21	NA	NA
	F	0.58	0.20	NA	NA
	G	**0.80***	0.29	NA	NA
	I	**0.89***	0.33	NA	NA
	J	**0.77***	0.30	NA	NA
3	A	NA	NA	**-0.95***	-0.31
	B	NA	NA	**-0.72***	-0.30
	C	NA	NA	**-0.74***	-0.28
	D	NA	NA	**-0.76***	-0.23
	E	NA	NA	-0.30	-0.02
	F	NA	NA	**-0.89***	-0.12
	G	NA	NA	-0.44	-0.16
	I	NA	NA	**-0.80***	-0.05
	J	NA	NA	-0.49	-0.11
4	A	0.20	0.10	-0.20	-0.09
	B	**0.78***	0.04	-0.10	-0.15
	C	0.06	0.01	-0.05	-0.01
	D	0.00	0.02	-0.59	0.00
	E	0.19	0.00	-0.11	0.00
	F	**0.71***	0.14	-0.19	-0.13
	G	0.04	0.01	-0.06	-0.02
	I	0.08	0.05	-0.10	-0.04
	J	0.04	0.09	-0.12	-0.02
5	A	0.10	0.03	-0.20	-0.01
	B	0.32	0.07	0.00	-0.03
	C	0.03	0.05	-0.21	-0.01
	D	0.09	0.00	-0.55	-0.10
	E	0.02	0.01	-0.16	0.00
	F	0.11	0.04	0.00	-0.05
	G	0.14	0.00	-0.51	-0.01
	I	0.01	0.00	-0.29	-0.06
	J	0.09	0.09	0.00	-0.07

NA Tc and NDVI data not available for flights 2 and 3 respectively, as a result of instrument failure.

Genotype selection

Selection accuracy

Table 8.24. Comparison of direct (SDM-based) and indirect (based on aerially measured traits, i.e. NDVI, Tc, VPI and SDM_{MLR}) genotype selection methods in the SR 21-22 breeding trial. The analysis considered a subset of genotypes after exclusion criteria were applied. Selection methods were considered for each flight, trial part, and across all trial parts. The table details: (1) the number of genotypes that were selected with the respective traits; (2) the number of positive matches (genotypes selected by both SDM and the respective aerially measured trait); (3) misses (genotypes selected with SDM but not with the respective aerially measured trait) and false positives (genotypes selected with the aerially measured trait but not with SDM). The green highlighted blocks indicate instances where the number of positive matches exceed the number of misses and false positives.

Flight	Trial part	Genotypes planted	Genotypes considered	Genotypes selected					Positive Matches				Misses				False positives			
			Selection trait	SDM	NDVI	Tc	VPI	SDM_{MLR}	NDVI	Tc	VPI	SDM_{MLR}	NDVI	Tc	VPI	SDM_{MLR}	NDVI	Tc	VPI	SDM_{MLR}
1	A	200	157	10 (6%)	127 (81%)	98 (62%)	111 (71%)	101 (64%)	10 (100%)	9 (90%)	10 (100%)	10 (100%)	0	1 (10%)	0	0	117 (92%)	89 (91%)	101 (91%)	91 (90%)
	B	200	146	10 (7%)	10 (7%)	63 (43%)	42 (29%)	15 (10%)	1 (10%)	4 (40%)	7 (70%)	4 (40%)	9 (90%)	6 (60%)	3 (30%)	6 (60%)	9 (90%)	59 (94%)	35 (83%)	11 (73%)
	C	200	121	47 (39%)	85 (70%)	90 (74%)	83 (69%)	87 (72%)	**47 (100%)**	**47 (100%)**	**47 (100%)**	**47 (100%)**	**0**	**0**	**0**	**0**	**38 (45%)**	**43 (48%)**	**36 (43%)**	**40 (46%)**
	D	200	126	9 (7%)	47 (37%)	79 (63%)	64 (51%)	52 (41%)	7 (78%)	6 (67%)	7 (78%)	9 (100%)	2 (22%)	3 (33%)	2 (22%)	0	40 (85%)	73 (92%)	57 (89%)	43 (83%)
	E	200	117	32 (27%)	56 (48%)	85 (73%)	63 (54%)	59 (50%)	22 (69%)	29 (91%)	30 (94%)	28 (88%)	10 (31%)	3 (9%)	2 (6%)	4 (13%)	34 (61%)	56 (66%)	33 (52%)	31 (53%)
	F	200	118	23 (19%)	93 (79%)	94 (80%)	93 (79%)	92 (78%)	23 (100%)	19 (83%)	23 (100%)	23 (100%)	0	4 (17%)	0	0	70 (75%)	75 (80%)	70 (75%)	69 (75%)
	Total	1200	785 (65%)	131 (17%)	418 (53%)	509 (65%)	456 (58%)	40 (52%)	100 (84%)	114 (87%)	124 (95%)	121 (92%)	21 (16%)	17 (13%)	7 (5%)	10 (8%)	308 (74%)	395 (78%)	332 (73%)	285 (70%)
2	A	200	116	8 7%	98 (84%)	-	-	-	8 (100%)	-	-	-	0	-	-	-	90 (92%)	-	-	-
	B	200		10 7%	3 (2%)	-	-	-	1 (10%)	-	-	-	9 (90%)	-	-	-	2 (67%)	-	-	-

	Trial part	Genotypes planted	Genotypes considered	Genoptypes selected					Positive matches				Misses				False positives			
			Selection trait	SDM	NDVI	Tc	VPI	SDM_{MLR}	NDVI	Tc	VPI	SDM_{MLR}	NDVI	Tc	VPI	SDM_{MLR}	NDVI	Tc	VPI	SDM_{MLR}
	C	200	121	66 55%	7 (6%)	-	-	-	5 (8%)	-	-	-	61 (92%)	-	-	-	2 (29%)	-	-	-
	D	200	126	9 7%	41 (33%)	-	-	-	3 (33%)	-	-	-	6 (67%)	-	-	-	38 (93%)	-	-	-
	E	200	117	32 27%	38 (32%)	-	-	-	18 (56%)	-	-	-	14 (44%)	-	-	-	20 (53%)	-	-	-
	F	200	118	23 19%	59 (50%)	-	-	-	16 (70%)	-	-	-	7 (30%)	-	-	-	43 (73%)	-	-	-
	G	200	115	60 (52%)	26 (23%)	-	-	-	22 (37%)	-	-	-	38 (63%)	-	-	-	4 (15%)	-	-	-
	H	200	147	34 (23%)	83 (56%)	-	-	-	30 (88%)	-	-	-	4 (12%)	-	-	-	53 (64%)	-	-	-
	I	200	128	51 (40%)	15 (12%)	-	-	-	10 (20%)	-	-	-	41 (80%)	-	-	-	5 (33%)	-	-	-
	J	90	73	48 (66%)	29 (40%)	-	-	-	23 (48%)	-	-	-	25 (52%)	-	-	-	6 (21%)	-	-	-
	K	40	28	10 (36%)	4 (14%)	-	-	-	1 (10%)	-	-	-	9 (90%)	-	-	-	3 (75%)	-	-	-
	Total	1930	1235	351 (28%)	403 (33%)	-	-	-	137 (39%)	-	-	-	214 (61%)	-	-	-	266 (66%)	-	-	-
3	A	200	157	10 (6%)	-	118 (75%)	-	-	-	10 (100%)	-	-	-	0	-	-	-	108 (92%)	-	-
	B	200	146	10 (7%)	-	44 (30%)	-	-	-	4 (40%)	-	-	-	6 (60%)	-	-	-	40 (91%)	-	-
	C	200	121	66 (55%)	-	62 (51%)	-	-	-	**41 (62%)**	-	-	-	**25 (38%)**	-	-	-	**21 (34%)**	-	-
	D	200	126	9 (7%)	-	58 (46%)	-	-	-	6 (67%)	-	-	-	3 (33%)	-	-	-	52 (90%)	-	-
	E	200	117	32 (27%)	-	68 (58%)	-	-	-	25 (78%)	-	-	-	7 (22%)	-	-	-	43 (63%)	-	-
	F	200	118	23 (19%)	-	57 (48%)	-	-	-	14 (61%)	-	-	-	9 (39%)	-	-	-	43 (75%)	-	-
	G	200	114	60 (53%)	-	70 (61%)	-	-	-	**47 (78%)**	-	-	-	**13 (22%)**	-	-	-	**23 (33%)**	-	-
	H	200	147	34 (23%)	-	83 (56%)	-	-	-	30 (88%)	-	-	-	4 (12%)	-	-	-	53 (64%)	-	-
	I	200	128	51 (40%)	-	68 (53%)	-	-	-	**37 (73%)**	-	-	-	**14 (27%)**	-	-	-	**31 (46%)**	-	-
	J	90	74	48 (65%)	-	64 (86%)	-	-	-	**47 (98%)**	-	-	-	**1 (2%)**	-	-	-	**17 (27%)**	-	-
	K	40	28	10 (36%)	-	15 (54%)	-	-	-	7 (70%)	-	-	-	3 (30%)	-	-	-	8 (53%)	-	-

	Trial part	Genotypes planted	Genotypes considered	Genoptypes selected					Positive matches				Misses				False positives			
			Selection trait	SDM	NDVI	Tc	VPI	SDM_{MLR}	NDVI	Tc	VPI	SDM_{MLR}	NDVI	Tc	VPI	SDM_{MLR}	NDVI	Tc	VPI	SDM_{MLR}
	Total	1930	1276	353 (28%)	-	707 (55%)	-	-	-	268 (76%)	-	-	-	85 (24%)	-	-	-	439 (62%)	-	-
4	A	200	157	10 (6%)	143 (91%)	43 (27%)	95 (61%)	122 (78%)	10 (100%)	5 (50%)	9 (90%)	10 (100%)	0	5 (50%)	1 (10%)	0	133 (93%)	38 (88%)	86 (91%)	112 (92%)
	B	200	146	10 (7%)	19 (13%)	43 (29%)	20 (14%)	22 (15%)	3 (30%)	6 (60%)	3 (30%)	4 (40%)	7 (70%)	4 (40%)	7 (70%)	6 (60%)	16 (84%)	37 (86%)	17 (85%)	18 (82%)
	C	200	121	66 (55%)	29 (24%)	32 (26%)	28 (23%)	30 (25%)	17 (26%)	18 (27%)	10 (15%)	6 (9%)	49 (74%)	48 (73%)	56 (85%)	60 (91%)	12 (41%)	14 (44%)	18 (64%)	24 (80%)
	D	200	126	9 (7%)	53 (42%)	76 (60%)	61 (48%)	54 (43%)	3 (33%)	4 (44%)	4 (44%)	7 (78%)	6 (67%)	5 (56%)	5 (56%)	2 (22%)	50 (94%)	72 (95%)	57 (93%)	47 (87%)
	E	200	117	32 (27%)	17 (15%)	72 (62%)	23 (20%)	46 (39%)	6 (19%)	20 (63%)	5 (16%)	6 (19%)	26 (81%)	12 (38%)	27 (84%)	26 (81%)	11 (65%)	52 (72%)	18 (78%)	40 (87%)
	F	200	118	23 (19%)	60 (51%)	82 (69%)	64 (54%)	70 (59%)	16 (70%)	14 (61%)	9 (39%)	8 (35%)	7 (30%)	9 (39%)	14 (61%)	15 (65%)	44 (73%)	68 (83%)	55 (86%)	62 (89%)
	G	200	31	7 (23%)	8 (26%)	25 (81%)	11 (35%)	10 (32%)	2 (29%)	7 (100%)	2 (29%)	2 (29%)	5 (71%)	0	5 (71%)	5 (71%)	6 (75%)	18 (72%)	9 (82%)	8 (80%)
	Total	1400	816	157 (19%)	329 (40%)	373 (46%)	302 (37%)	354 (43%)	57 (36%)	74 (47%)	42 (27%)	43 (27%)	100 (64%)	83 (53%)	115 (73%)	114 (73%)	272 (83%)	299 (80%)	260 (86%)	311 (88%)
5	A	200	157	10 (6%)	108 (69%)	9 (6%)	21 (13%)	18 (11%)	7 (70%)	1 (10%)	3 (30%)	2 (20%)	3 (30%)	9 (90%)	7 (70%)	8 (80%)	101 (94%)	8 (89%)	18 (86%)	16 (89%)
	B	200	146	10 (7%)	5 (3%)	38 (26%)	7 (5%)	19 (13%)	2 (20%)	5 (50%)	4 (40%)	5 (50%)	8 (80%)	5 (50%)	6 (60%)	5 (50%)	3 (60%)	33 (87%)	3 (43%)	14 (74%)
	C	200	121	66 (55%)	29 (24%)	35 (29%)	30 (25%)	31 (26%)	16 (24%)	18 (27%)	14 (21%)	11 (17%)	50 (76%)	48 (73%)	52 (79%)	55 (83%)	13 (45%)	17 (49%)	16 (53%)	20 (65%)
	D	200	126	9 (7%)	7 (6%)	81 (64%)	14 (11%)	20 (16%)	0	5 (56%)	3 (33%)	2 (22%)	9 (100%)	4 (44%)	6 (67%)	7 (78%)	7 (100%)	76 (94%)	11 (79%)	18 (90%)
	E	200	117	32 (27%)	50 (43%)	41 (35%)	40 (34%)	43 (37%)	15 (47%)	15 (47%)	10 (31%)	12 (38%)	17 (53%)	17 (53%)	22 (69%)	20 (63%)	35 (70%)	26 (63%)	30 (75%)	31 (72%)
	F	200	105	23 (22%)	75 (71%)	81 (77%)	77 (73%)	72 (69%)	15 (65%)	17 (74%)	15 (65%)	15 (65%)	8 (35%)	6 (26%)	8 (35%)	8 (35%)	60 (80%)	64 (79%)	62 (81%)	57 (79%)
	G	200	105	55 (52%)	21 (20%)	29 (28%)	21 (20%)	23 (22%)	13 (24%)	21 (38%)	13 (24%)	8 (15%)	42 (76%)	34 (62%)	42 (76%)	47 (85%)	8 (38%)	8 (28%)	8 (v)	15 (65%)
	H	200	147	34 (23%)	117 (80%)	108 (73%)	110 (75%)	109 (74%)	32 (94%)	29 (85%)	14 (41%)	18 (53%)	2 (6%)	5 (15%)	20 (59%)	16 (47%)	85 (73%)	79 (73%)	96 (87%)	91 (83%)
	I	200	128	51 (40%)	15 (12%)	47 (37%)	20 (16%)	24 (19%)	8 (16%)	19 (37%)	8 (16%)	7 (14%)	43 (84%)	32 (63%)	43 (84%)	44 (86%)	7 (47%)	28 (60%)	12 (60%)	17 (71%)
	J	90	74	48 (65%)	18 (24%)	12 (16%)	15 (20%)	13 (18%)	4 (8%)	4 (8%)	3 (6%)	2 (4%)	44 (92%)	44 (92%)	45 (94%)	46 (96%)	14 (78%)	8 (67%)	12 (80%)	11 (85%)
	Total	1890	1226	338 (28%)	445 (36%)	481 (39%)	355 (29%)	372 (30%)	112 (33%)	134 (40%)	87 (26%)	82 (24%)	226 (67%)	204 (60%)	251 (74%)	256 (76%)	333 (75%)	347 (72%)	268 (75%)	290 (78%)

Note: The percentages indicate: (1) The number of genotypes selected with the respective trait, were expressed relative to the number of genotypes considered after exclusion criteria were applied; (2) Positive matches were expressed relative to the number of genotypes selected, with the respective trait; (3) Misses were expressed relative to the number of genotypes selected with SDM; (4) False positives were expressed relative to the number of genotypes selected with the respective trait.